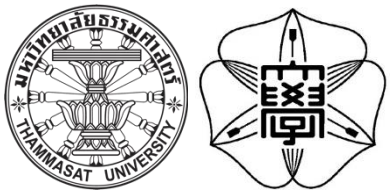

STUDY ON CORROSIVE RESISTANCE OF BARE, PAINTED, AND HOT-DIP GALVANIZED STRUCTURAL STEEL IN THAILAND

BY

BUNYA CHEA

A DISSERTATION SUBMITTED IN PARTIAL FULFILLMENT OF THE REQUIREMENTS FOR THE DEGREE OF DOCTOR OF PHILOSOPHY (ENGINEERING AND TECHNOLOGY)/DOCTOR OF ENGINEER

SIRINDHORN INTERNATIONAL INSTITUTE OF TECHNOLOGY

THAMMASAT UNIVERSITY

AND

GRADUATE SCHOOL OF ENGINEERING

HOKKAIDO UNIVERSITY

ACADEMIC YEAR 2023

THAMMASAT UNIVERSITY
SIRINDHORN INTERNATIONAL INSTITUTE OF TECHNOLOGY
AND
HOKKAIDO UNIVERSITY, GRADUATE SCHOOL OF ENGINEERING

DISSERTATION

BY

BUNYA CHEA

ENTITLED

STUDY ON CORROSIVE RESISTANCE OF BARE, PAINTED, AND HOT-DIP GALVANIZED STRUCTURAL STEEL IN THAILAND

was approved as partial fulfillment of the requirements for the degree of
Doctor of Philosophy (Engineering and Technology)/ Doctor of Engineer

on December 20, 2023

Chairman

(Professor Takashi Matsumoto, Ph.D.)

Member and Advisor

(Professor Kriengsak Panuwatwanich, Ph.D.)

Member and Co-advisor

(Associate Professor Taweep Chaisomphob, D.Eng.)

Member and Co-advisor

(Associate Professor Akira Furukawa, Ph.D.)

Member

(Professor Takafumi Sugiyama, Ph.D.)

Member

(Associate Professor Piya Chotickai, Ph.D.)

Member

(Associate Professor Warangkana Saengsoy, Ph.D.)

Member

(Assistant Professor Pakawat Sancharoen, Ph.D.)

Director

(Professor Pruettha Nanakorn, D.Eng.)

Thesis Title	STUDY ON CORROSIVE RESISTANCE OF BARE, PAINTED, AND HOT-DIP GALVANIZED STRUCTURAL STEEL IN THAILAND
Author	Bunya Chea
Degree	Doctor of Philosophy (Engineering and Technology) and Doctor of Engineer
Faculty/University	Sirindhorn International Institute of Technology/ Thammasat University and Graduate School of Engineering/Hokkaido University
Dissertation Advisor	Prof. Dr. Takashi Matsumoto, Ph.D. Prof. Dr. Kriengsak Panuwatwanich, Ph.D.
Dissertation Co-Advisor	Assoc. Prof. Dr. Taweep Chaisomphob, D.Eng. Assoc. Prof. Dr. Akira Furukawa, Ph.D.
Academic Years	2023

ABSTRACT

Organization or owner has had a lot of trouble lately maintaining steel structures. Many steel structures were built without taking maintenance costs, good coating systems, or sustainable materials with low maintenance costs into account. For this reason, durable materials like hot-dip galvanized steel (HDG) should have been used. The most difficult problem for steel construction is corrosion. The many environmental circumstances in Thailand, such as marine, industrial, urban, or rural zones, influence the corrosion rate at varying rates. Nonetheless, knowledge regarding how various coated structural steel types perform in those varied environments is still limited.

This study examined the effects of atmospheric parameters and environmental pollutants on coated structural steel across Thailand. For this study, two steel grades—SS400 and SM490A—with six different coating types were used. Based on ASTM standards, 19 test sites representing a variety of Thai atmospheric conditions were

selected. Additionally, of those 19 locations, 7 have established environmental parameter-collecting data stations, with the remaining locations utilizing meteorological data collected from meteorological authorities. The exposed specimens were collected for analysis after being exposed for a determined period of time in order to determine the thickness loss of the steel, the changing appearance, and the assessment of the painted steel using ASTM and ISO standards.

To adequately inform consumers or designers, thickness loss data for the test sites alone is insufficient. Since construction might occur anywhere in the country under a variety of environmental circumstances, a corrosion map is required. A large number of test locations are needed to cover the entire nation, which is made up of various zones of atmospheric and environmental behaviors. A significant source of information for predicting corrosion rates and managing atmospheric corrosion risk is the atmospheric corrosivity map. A corrosion map in Thailand that shows the thickness loss value ranges for HDG steel and bare steel with two steel grades, SS400 and SM490A, has never been developed. More sites with data on atmospheric factors and environmental pollutants are needed to improve the accuracy of the corrosion map. In order to produce a corrosivity heat map, additional data points must be added to the map by gathering information at the designated places from the meteorological authority. To obtain more information when the number of on-site test locations is limited, dose response models must be investigated and developed. The dose-response function is an empirical relationship equation that relates contaminants and atmospheric conditions to the steel's rate of corrosion.

Although some researchers have attempted to conduct atmospheric tests over longer time periods, such as three, or five years, the behavior cannot yet be sufficiently understood for longer time periods, such as 20, or 25 years. The majority of atmospheric exposure tests have been conducted over short time periods. The thickness loss amount for the subsequent years can be inferred from the first year. A good prediction model can be used to forecast thickness loss, which helps anticipate corrosive behavior in a given environment. Researchers and designers can estimate the thickness loss of steel without requiring a long-period experiment by using the projection of thickness loss for both bare steel and HDG steel.

The research findings provide a guide for choosing between hot-dip galvanizing and painting for corrosion protection, along with information on the corrosion rate and the effectiveness of hot-dip galvanized, and painted steel in different regions of Thailand. Users and designers can obtain the relevant information regarding the thickness loss of HDG and bare steel throughout the corrosivity map. Users and designers can utilize the corrosivity maps to determine the thickness loss value at the site of their intended building. They have two options: either they can reserve thickness loss for the structure's intended year life, or they can estimate the structure's year life using the permitted thickness loss. The research results demonstrate that the HDG and duplex system (HDG + paint) coatings are the best coatings for preventing steel corrosion, which assist engineers and users in solving steel corrosion problems.

Keywords: Atmospheric exposure test, Hot-dipped galvanized steel, Painted steel, Dose response function, Inverse Distance Weight method, Corrosion map

ACKNOWLEDGEMENT

First and foremost, I would like to express my sincere gratitude to all of my advisers, Prof. Dr. Takashi Matsumoto, Assoc. Prof. Dr. Taweep Chaisomphob, and Prof. Dr. Kriengsak Panuwatwanich, for their insightful advice and helpful recommendations during my doctoral program. Their helpful advice and guidance motivated me to work harder in my studies.

I would like to appreciate to all of my thesis committee members for their constructive comments and recommendations that helped me improve my research and my thesis. Additionally, I would like to thank Mr. Adithep Bunphot, a master degree student at Thammasat University's Sirindhorn International Institute of Technology, for his help during the exposure test.

I would like to deeply thank Sirindhorn International Institute of Technology, Thammasat University, Hokkaido University, and AUN-SEED/Net for their scholarship. I would like to acknowledge the Thai Galvanizing Association (TGA) for financial support and all of the institutions for their test locations. I would also like to thank the School of Civil Engineering and Technology at SIIT and the Graduate School of Engineering at Hokkaido University for their help and support throughout my doctoral degree.

Lastly, I would like to thank to my parents, my relatives, seniors, juniors, and all of my friends for their endless encouragement and support during my doctoral program.

TABLE OF CONTENTS

LIST OF TABLES

LIST OF FIGURES

LIST OF SYMBOLS/ABBREVIATIONS

Symbols/Abbreviations	Terms
HDG	Hot-dip galvanized
IDW	Inversed Distance Weight
TMD	Thai Meteorological Department
PCD	Pollution Control Department

CHAPTER 1
INTRODUCTION

1.1 General

The consumption of steel products is increasing compared to the consumption in 2015, based on data from the World Steel Association (WSA, 2021). The usage of structural steel in construction is 57.1% compared to other sectors, based on data in 2018 from the Iron and Steel Institute of Thailand (ISIT, 2018). However, corrosion is the most challenging issue for steel. In Thailand, carbon steel with two grades (SS400 and SM490A) is commonly used for general steel and welded steel structures. There are several types of materials used for coating to prevent corrosion, such as zinc, aluminum, magnesium, and paint. Hot-dip galvanizing (coating with zinc) is one of the methods of coating. Engineers attempt to make their structural steel more durable with less maintenance. The study of hot-dip galvanized steel (HDG) is one of the most interesting and challenging topics in the steel coating research field. Hot-dip galvanization is the process of coating iron and steel by immersing the metal in a bath of molten zinc at a temperature of around 450 °C (AGA, 2023) as shown in Figure 1.1. Surface preparation, galvanizing, and post-treatment are the three primary processes in the hot-dip galvanizing procedure. The surface preparation aims to prepare the steel surface for cleaning by removing contaminants and oxides. There are three processes in cleaning and surface preparing steel: degreasing, pickling, and fluxing. In galvanizing step, steel is immersed into the molten zinc. The steel product is removed from the zinc bath once the iron and zinc diffusion reaction is finished. A post-treatment to improve the galvanized coating may be applied to the steel after it has been taken from the molten zinc bath. After all the processes, hot-dip galvanized steel is stored and transported to the users.

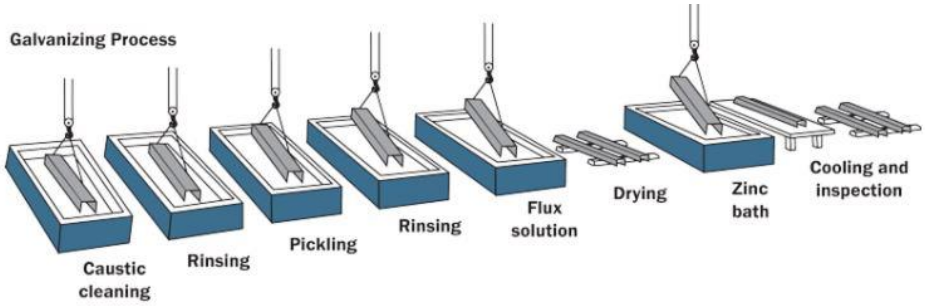

Figure 1.1 Process of hot-dip galvanizing (AGA, 2023)

Due to the protective layer that is applied to hot-dip galvanized steel during the galvanization process, it has a number of benefits. Some of the main benefits are as follows (AGA, 2023):

- Excellent Corrosion Resistance: Steel that has been hot-dip galvanized has a high level of corrosion resistance. The zinc coating serves as a barrier, keeping moisture and other corrosive elements away from the steel underneath. Even in hostile situations where corrosion is common, this protection aids in greatly extending the steel's lifespan.
- Galvanized steel is strong and has a long lifespan, lasting 50 to 100 years or more on average, depending on the environment and maintenance procedures. The steel is continuously protected by the zinc coating, guaranteeing that it lasts a long time without corroding. Due to its longevity, it is a cost-effective option for many applications, which lowers the frequency of replacements and maintenance.
- Maintenance-Free: Once installed, hot-dip galvanized steel requires very little upkeep for the duration of its useful life. Galvanized steel offers long-term protection without the need for further maintenance or the reapplication of protective coatings, in contrast to other coatings or surface treatments that may need periodic reapplication or touch-ups.
- Hot-dip galvanized steel is regarded as being environmentally sustainable. Zinc, an abundant and natural resource, is used in the galvanization process. Galvanized steel's lifespan and durability also lessen the need for regular replacements, which over time reduces material consumption and waste production.

Corrosion protection is an essential part of the economic use of steel. The application of the proper protective coating can result in initial cost savings as well as significant service cost savings owing to the elimination or reduction of maintenance. Hot-dip galvanizing provides a metallurgically bonded zinc coating that protects the steel surface from the surrounding environment. HDG steel can be used in various type of structures. HDG steel is used for the roof structure for the NSW Tennis Center in Australia as an example, as shown in Figure 1.2. HDG steel can account for a variety of atmospheres, including the local climate, the amount of pollutants in the air caused

by industrial or urban activities, and the presence of chlorides in the air because of the area's closeness to the sea.

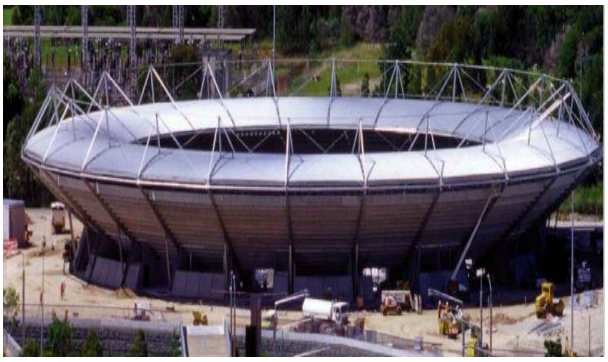

Figure 1.2 NSW Tennis Center with HDG steel roof structure (GAA, 2021)

Atmospheric parameters and environmental pollutants will affect the corrosion rate of the steel. The corrosivity level of steel is based on the level of the contaminant environmental parameters in the atmosphere. According to the ISO 9223 standard (ISO9223, 2012), the main factors for corrosivity estimation are temperature and humidity (relative humidity and rainfall), as well as the pollutants SO_2 and chloride. The smoke from vehicles and industrial activities are the main sources of SO_2 in the air. For chloride, winds bring chloride from the moisture of the ocean, which makes the rate of chloride deposition depend on the distance from the sea.

1.2 Statement of problem

When it comes to steel structures, Thailand, like many other countries, has a number of corrosion-related difficulties. In Thailand, some of the typical corrosion issues include:

- Inland corrosion: With its hot and high humidity, Thailand's tropical climate has a tropical effect that speeds up the atmospheric corrosion of steel structures. Unprotected steel surfaces are susceptible to surface corrosion, pitting, and the production of rust when moisture, oxygen, and airborne contaminants are present.
- Marine zone corrosion: Thailand has a sizable coastline and various initiatives for coastal infrastructure. Corrosion is more likely to occur in

marine areas where steel structures are exposed to near harsh saltwater. The presence of salt air along the coastal areas cause severe corrosion.

- Industrial zone corrosion: Thailand's industrial sector, which consists of petrochemical plants, refineries, power plants, and manufacturing facilities, is expanding. Steel constructions can experience corrosion problems in these locations because of the frequent exposure to corrosive chemicals, high temperatures, and hostile atmospheres. If the right protection measures are not put in place, corrosive gases, acids, and other industrial pollutants can result in serious corrosion.
- Poor Maintenance Techniques: Corrosion issues in steel structures can be made worse by inadequate or inappropriate maintenance techniques. Accelerated corrosion rates and impaired structural integrity can be caused by inadequate cleaning, a lack of protective coatings, and a failure to resolve corrosion-related problems in a timely manner.

In Thailand, common painted steel is currently used widely in the construction industry. Those applications in different locations are affected by different environmental conditions, inducing different corrosion damages. The diversity of characteristics of the climate in Thailand, since the country’s geography consists of inland and seashore regions, causes different environmental impacts. The damaged painted steel provides a lot of rust that will affect the strength and external appearance of the structure. Therefore, hot-dip galvanizing is needed.

From year to year, more research is being carried out about the galvanization for structural steel in order to study and improve its quality. Furthermore, the use of hot-dip galvanized steel in Thailand has recently increased. Since knowledge about hot-dip galvanized performance is still limited, the study of hot-dip galvanized steel is necessary in order to develop or improve the hot-dip galvanizing standard in Thailand.

Industrialization, pollution, and chloride will affect the structural steel, with the corrosion occurring at a different rate compared to the natural atmosphere. As a result, the location chosen becomes one of the most important criteria to consider in the study of the corrosion rate and the performance of each coating method.

Providing thickness loss information only for the test locations is not enough for the users or designers. Because construction can occur anywhere in the country, with varying atmospheric conditions, a corrosion map is required.

1.3 Purpose of study

The main purpose of this research is to gather more knowledge about coated steel for the Thai structural steel industry, and to study the performance of coated steel in Thailand to detect or identify problems in order to develop or improve the hot-dip galvanizing standard in Thailand.

The main objectives of this study include:

- Conduct atmospheric exposure test on bare steel, hot-dip galvanized steel, and four different painted steels.
- Conduct atmospheric exposure test in each different region of Thailand and interested location within each region which have different in environmental corrosion factor.
- Detect or identify problems in order to develop or improve the HDG standard in Thailand.
- Compare the corrosive resistance of bare steel, HDG steel, and painted steel at various locations throughout Thailand.
- Investigate the thickness loss as well as effecting factors.
- Create a correlation equation (dose response function) with environmental parameters to predict the thickness loss of steel at the locations provided by the Thai Meteorological Department.
- Create a corrosion heat map for bare steel and HDG steel.
- Project the thickness loss of bare steel and HDG steel in further year like 10, 20, and 25 years.
- Provide guidance to the user and engineer for choosing a coating system in a particular location for their structure.

1.4 Scope of study

The study has the scope as follows:

- Three criteria for choosing test location: distance from shoreline, natural atmospheric character, and high corrosion tendency area (industrial zone, construction growth area, pollution zone, etc).
- 19 locations were chosen throughout Thailand.
- Two types of steel will be tested: SS400 and SM490A with 6 different kinds of coating method.
- Period of atmospheric exposure 3, 6, and 12 months.
- Standard practices used in the project are as follows:

  -ASTM Series

  ASTM A123, ASTM A385, ASTMD1014, ASTM G-50, ASTM G-16, ASTM G-1, ASTM G-33, ASTM G-92, ASTM G-31

  -ISO Series

  ISO-9223, ISSO-9224, ISO-9225, ISO-4628(1-10), ISO-17872, ISO8407, ISO 14993, ISO 16151

CHAPTER 2
REVIEW OF LITERATURE

2.1 Introduction

Review of literature chapter aims to present a thorough summary of all the theories, research findings, and scholarly works that have already been done related to the study topic. In addition to providing context for the study, this section highlights disagreements, gaps, and areas in which more research is required. The scope of this literature review includes the following: chemical reactions that cause steel to corrode in order to understand the factors that cause steel corrosion; atmospheric exposure tests that may demonstrate test procedures and thickness loss findings; corrosion equations that demonstrate the processes of creating a corrosion equation and the parameters in the equation; corrosion maps that demonstrate the methods of creating a corrosion map; and thickness loss projection of steel.

2.2 Corrosion of steel from chemical reaction

2.2.1 Bare steel

When steel without corrosion protection is exposed to the atmosphere, the surface will take on a reddish-brown color after a short time, and this reddish-brown color indicates the formation of corrosion. The electrolyte it is submerged in or the surface wetness on the exposed steel surfaces cause fluctuations in electrical potential. Anodes and cathodes are formed. Negatively charged electrons move from the anode to the cathode as a result of variations in electrical potential within the cell. Positively charged ions are created from iron atoms in the anode area. Iron oxide, sometimes known as rust, is created when positively charged iron ions from the anode interact with negatively charged hydroxyl ions in the electrolyte. Hydrogen gas is created when negatively charged electrons and positively charged hydrogen ions react at the cathode surface. On a piece of steel, the anode and cathode regions are essentially tiny. When viewed under a powerful microscope, the surface may resemble the mosaic of anodes and cathodes shown in Figure 2.1, which are all electrically connected via the underlying steel. There is corrosion in the anode sections.

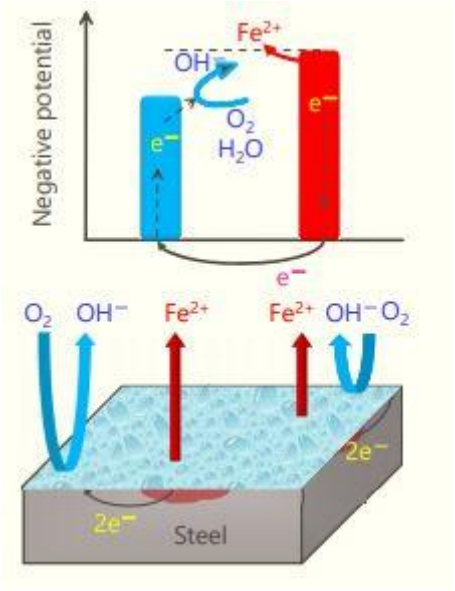

Figure 2.1 Anode and cathode reaction to forming corrosion on steel (Yokota, 2020)

Anode reaction:

$Fe \rightarrow Fe^{2+} + 2e^{-}$

Cathode reaction:

$O_2 + 2H_2O + 4e^{-} \rightarrow 4OH^{-}$

$2Fe + O_2 + 2H_2O \rightarrow 2Fe(OH)_2$

Anodic and cathodic reactions, in which one region of the steel serves as the anode (for oxidation) and another as the cathode (for reduction), can cause corrosion. By transferring electrons from the anode to the cathode, this establishes an electrochemical cell. While the cathodic process may involve the reduction of oxygen or hydrogen ions, the anodic reaction entails the oxidation of iron to iron ions.

Another chemical equation of the corrosion process of steel

$Fe + SO_2 + O_2 \rightarrow FeSO_4$ (Peibker, 2011)

Chloride-induced corrosion

The creation of passive layers in the presence of chlorides is due to localized concentrations of chloride ions. The chloride depassivates the steel surface, and then the steel easily reacts with the atmosphere.

Overall, environmental elements like moisture, oxygen levels, pH, temperature, and the presence of pollutants all play a role in the complex process of steel corrosion.

In order to create successful corrosion prevention measures, such as the application of protective coatings, cathodic protection, or the use of corrosion inhibitors, it is helpful to understand the chemical reactions involved in corrosion.

2.2.2 HDG steel

A form of steel known as hot-dipped galvanized (HDG) steel has undergone the hot-dip galvanization process, which coats the steel with a layer of zinc. The steel behind the zinc coating has high corrosion resistance. Galvanized steel, however, can nevertheless experience a type of corrosion known as white rust or zinc hydroxide corrosion under specific circumstances. The following chemical processes contribute to the corrosion of hot-dipped galvanized steel:

Dissolution of Zinc:

$$Zn + 2OH^- \rightarrow Zn(OH)_2 + 2e^-$$

Zinc hydroxide ($Zn(OH)_2$) is created when zinc (Zn) on the surface of galvanized steel combines with hydroxide ions (OH^-) in the presence of moisture and oxygen. Zinc dissolves as a result of this reaction, and electrons are released ($2e^-$).

Reduction Reaction:

$$O_2 + 2H_2O + 4e^- \rightarrow 4OH^-$$

At the same time, as zinc dissolves, oxygen (O_2) from the air combines with water (H2O) and takes the electrons that are released. Hydroxide ions (OH-) are produced during this reduction reaction.

Formation of Zinc Hydroxide:

$$Zn(OH)_2 + 2OH^- \rightarrow [Zn(OH)_4]^{2-}$$

The zinc hydroxide ($Zn(OH)_2$) reacts further with the hydroxide ions (OH^-) produced in the reduction reaction and zinc dissolution to form the complex ion $[Zn(OH)_4]^{2-}$. This complex ion is soluble in water and quickly removed, which causes the development of white rust, a powdery substance that appears on the surface of galvanized steel. Figure 2.2 shows the corrosion of hot-dip galvanized steel.

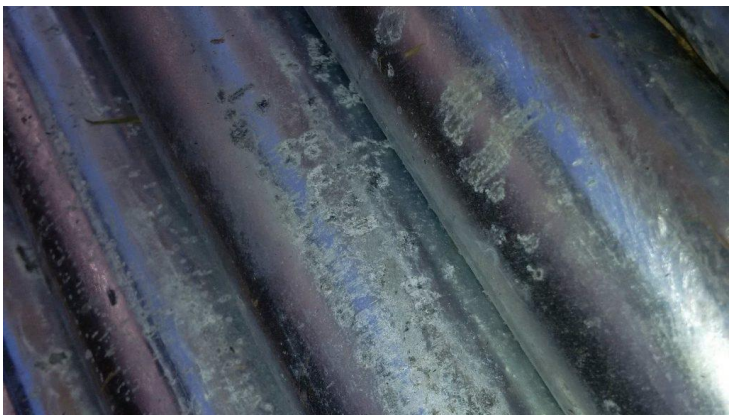

Figure 2.2 Corrosion of Hot-dipped galvanized steel

Overall, zinc dissolution, oxygen reduction, and zinc hydroxide production occur during the corrosion of hot-dipped galvanized steel. It is significant to remember that white rust, a kind of corrosion, predominantly damages the zinc coating rather than the steel substrate. White rust can damage the galvanized coating's integrity and protective qualities if it is not treated, rendering the steel more susceptible to other types of corrosion. Galvanized steel must be handled carefully and maintained regularly to avoid white rust and ensure the material's long-term durability.

2.3 Atmospheric exposure test

Steel samples or buildings are tested for their resistance to corrosion and deterioration by being exposed to outdoor ambient conditions for a predetermined amount of time. This kind of testing offers useful information on how steel performs and holds up under real-world conditions, assisting engineers and researchers in making knowledgeable choices about material selection, design enhancements, and corrosion prevention techniques.

The following steps are commonly included in the atmospheric exposure test:

- Test location Selection: An appropriate test location is selected to simulate the actual environment to which the steel will be exposed. When choosing the location, factors like humidity, temperature range, pollution levels, and closeness to industrial or coastal areas are taken into account (ASTMD1014, 2009; ASTMG50, 2015).
- Steel samples are prepared in accordance with ASTM G92 standards (ASTMG92, 2010) for the intended test goals. Depending on the individual

study or quality control requirements, the samples may be in the form of coupons, panels, or complicated shapes.

- Exposure Length: The test's length is decided by the desired research goals. For the purpose of simulating the real conditions the steel will face throughout the complete cycle of the season, at least one year of exposure testing has been conducted.
- Environmental Monitoring: Throughout the exposure time, a number of environmental parameters are regularly inspected. These include the following: air quality, rainfall, relative humidity, and temperature. The gathering of this information aids in the correlation of steel corrosion behavior with certain environmental elements.
- Measurement of the Corrosion Rate or thickness loss of the steel: Corrosion rate measurements give numerical information about how much corrosion is taking place on the steel surface. The corrosion rate is determined using methods like weight loss studies.
- Data Collection, Analysis, and Reporting: To assess the steel's performance in real-world scenarios, the data gathered from the air exposure test is examined. A thorough report is produced by compiling corrosion rates or thickness loss, and any other pertinent factors. The study might make suggestions for techniques to prevent corrosion, alterations to materials, or adjustments to design and maintenance procedures.

For sectors where steel is often utilized, including construction, infrastructure, automotive, and marine, atmospheric exposure testing offers useful information. It helps engineers and researchers in comprehending the long-term behavior of steel.

In order to know the thickness loss of each material, atmospheric exposure test is needed. Several atmospheric tests have been performed by several researchers. For example:

- Atmospheric corrosion in the Canary Islands has been studied by J. J. Santana et al. (Souto et al., 2014). Carbon steel plates with measurements of 100 x 40 x 20 mm were studied. The study followed ASTM G1-90 standards (ASTMG1, 2003) for the specimen cleaning processes before exposure. Seven study exposure periods were followed: 3, 6, 9, 12, 18, 24, and 36

months. The corrosion products of the study specimens were eliminated chemically according to ISO/DIS 8403.3. Weight loss measurements were used to calculate the rates of corrosion. The 74 test locations were studied over the Canary Islands. The test sites were categorized into various corrosive groups in order to take into account the variation in the aggressiveness of the surroundings present in the geographical area under consideration. The result showed that, even within a single island after just one year, the data variations range from 3.09 μm/year to 247.27 μm/year for Tenerife and from 10.47 μm/year to 299.98 μm/year for Gran Canaria. First year corrosion rates for bare steel ranged from 10.47 μm/year to 222.33 μm/year for Las Palmas and from 5.44 μm/year to 250.18 μm/year for Santa Cruz de Tenerife, respectively. Third year corrosion rates ranged from 6.40 μm/year to 145.78 μm/year for Las Palmas and from 2.34 μm/year 58.43 μm/year, respectively. It showed that the corrosion rate at the third year is lower than the first year. It proved that the rust on bare steel surfaces acted as the barriers to slow down the corrosion rate of the bare steel.

- Atmospheric corrosion of carbon steel in Colombia was studied by J. G. Castano et al. (Castaño et al., 2010). Castano et al. (2010) aim to study the influence of atmospheric parameters in Colombia on the corrosion of steel. For their atmospheric exposure test, commercial AISI-SAE 1016 carbon steel plates with dimensions of 100 mm x 150 mm x 2 mm were used. The study of 14-month period was conducted. Every two months, test specimens were recovered. Three samples were taken from each site for the weight loss test during each sampling period. The lead dioxide candle was used to determine the SO_2 deposition rate at each station. The results showed that all the test sites had high time of wetness (TOW) values. The three stations (Barranquilla, Cartagena, and Chinu) with greater temperatures also had the highest TOW. Throughout the test period, there were noticeable differences in the deposition of chlorides, particularly in Barranquilla and Cartagena. In semi-industrial stations (Bogota and Medellin), there were some variances in SO_2 levels. They found that the following are the cities with the largest mass

losses during the 14th month of exposure: Barranquilla, Bogota, Cartagena, Medellin, Chinu, and San Bernardino. Figure 2.3 displays the X-Ray diffraction analysis (XRD) spectra of the corrosion products in San Bernardino (rural), Barranquilla (marine), and Bogota (semi-industrial) after 14 months of exposure. Lepidocrocite (ɤ-FeOOH) and goethite (α-FeOOH), the most prevalent rust elements in natural environments, were discovered in the three stations. Akaneite (β-FeOOH) and the spinel-type oxides known as magnetite (Fe_3O_4), which are frequently found in marine environments, were also discovered at Barranquilla.

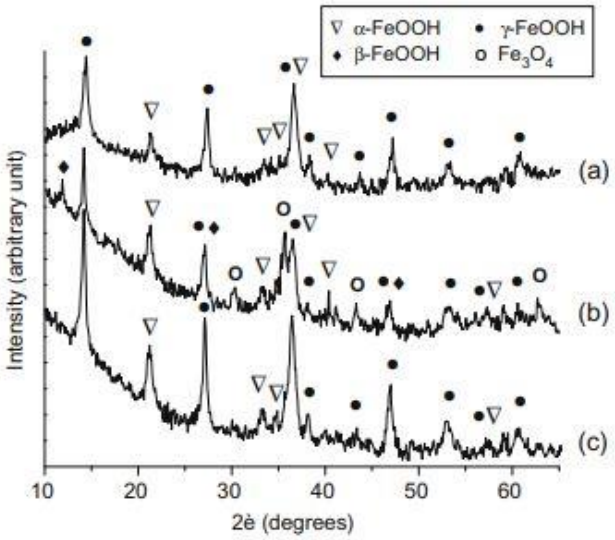

Figure 2.3 XRD spectra obtained after 14-month exposure. (a) San Bernardino, (b) Barranquilla and (c) Bogota (Castano et al., 2010)

- Annual atmospheric corrosion rate and dose-response function for carbon steel in Bogotá was studied by J. F. ROIS-ROJAS et al. (Rios-Rojas, Aperador Rodriguez, Hernandez, & Arroyave, 2017). In their study, corrosion rate were assessed using commercial AISI-SAE 1006 carbon steel plates (100 x 150 x 1.6 mm). After 3, 6, 9 and 12 months, specimens were withdrawn to evaluate. RH and temperature recording were continuously taken at each location. In their study, the deposition rates of SO_2 and particulate matter (PM) were determined every three months. The lead dioxide method was used to calculate the rate of SO_2 deposition at each location. The exposure was taken in eight different locations across Bogotá. The exposure sites were chosen based on the quantity of pollutants and

meteorological parameters reported by the city network of environmental assessment, and located in accordance with criteria for the siting of ambient air monitoring sites as well as standards for sampling total sulfation activity and chloride deposition from the atmosphere. The results showed that the corrosion rate and the behavior of the pollutants, especially the SO_2 level, were in good agreement; nevertheless, the magnitude of corrosion rate is not directly proportional to the SO_2 deposition. Low SO_2 and PM deposition test sites had nearly constant corrosion rates, indicating that carbon steel does not form a protective corrosion layer there. They concluded that, in Bogotá, the average atmospheric corrosivity value for ordinary carbon steel could be between 5 and 35 μm/year. The highest values are typically linked to higher SO_2 levels, which are linked to areas with greater anthropogenic activity.

- Atmospheric corrosion of weathering steels was studied by Morcillo et al. (Morcillo, Díaz, Cano, Chico, & de la Fuente, 2019). This paper offered engineers, designers, and steel producers a view into the current knowledge regarding this significant structural material and presents essential research findings in a way that encourages their practical implementation.

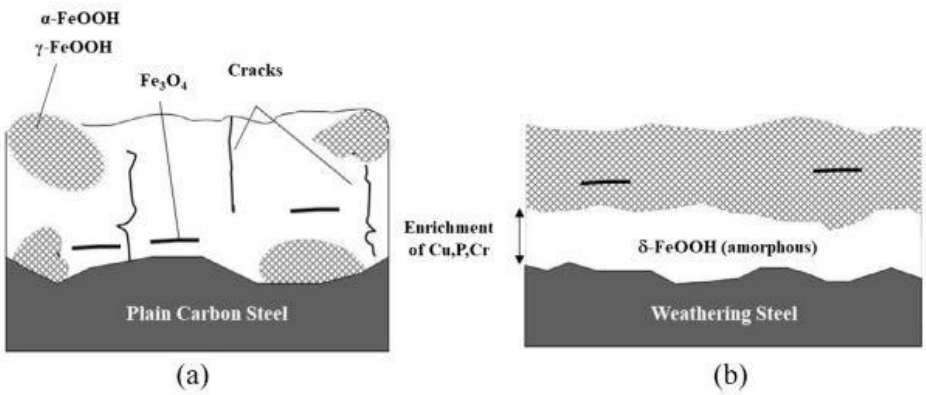

Figure 2.4 Schematic representation according to Misawa et al. of rust layers formed on plain carbon steel (a) and weathering steel (b) after exposure to the atmosphere for long periods of time.

Table 2.1 Corrosion products usually found in rust layers.

Name	Composition
Oxides	
Hematite	α-Fe_2O_3
Maghemite	γ-Fe_2O_3
Magnetite	Fe_3O_4
Ferrihydrite	Fe_3HO_8 $4H_2O$
Oxyhydroxides	
Goethite	α-FeOOH
Akaganeite	β-FeOOH
Lepidocrocite	γ-FeOOH
Feroxyhyte	δ-FeOOH

Table 2.1 lists the corrosion products that are most frequently discovered in the rust layers that form on carbon and weathering steel after being exposed to the atmosphere. Other noncrystalline (amorphous) and non-stoichiometric phases are frequently seen in atmospheric corrosion products on steel, including a group of Fe(II/III) hydroxyl salts known as green rusts due to their greenyblue/grey color. Iron can also combine with sulfur or chlorine to generate compounds like kornelite [$Fe(SO4)_3$] or $FeCl_3$, which have a substantial impact on corrosion in urban-industrial and marine environments, respectively.

- The prediction of atmospheric corrosion of metals and alloys in Chile using artificial neural networks was studied by Vera and Ossandon (Vera & Ossandón, 2014). Their study gives findings regarding the corrosion of metals exposed to the environment for 3 years at 9 distinct sites around Chile: carbon steel, galvanized steel, copper, and aluminum. They found that, over time, the weight loss increases and then stabilizes. The meteorological factors and the ambient pollutants at each station determine the gradient of the graph at earlier exposure times and the time at which stability is reached. After one year and three years of exposure, the carbon steel from the Coronel station's surface appearance and a cross-section are shown in Figure 2.5. They found that a substantial amount of corrosion product has fully covered the steel. However, the covering has cracks that let pollutants inside, confirming the increased rate of corrosion during specific times. In the cross-section, the attack morphology after a year is visible, along with corrosion products that range in thickness from 40 to 60 microns on the surface. Additionally, the

existence of cracks were found. After three years of, this behavior becomes even more obvious with more corrosion product and less adhesion to the base material. After a year of exposure, Figure 2.6 illustrates the morphology of the corrosion products on the galvanized steel at the stations in Quintero (A) and Easter Island (B). In contrast to Easter Island, where the corrosion product is significantly smaller in size and other sites where it is flat, the galvanized steel at Quintero generates a significant amount of granular corrosion product throughout the entire surface.

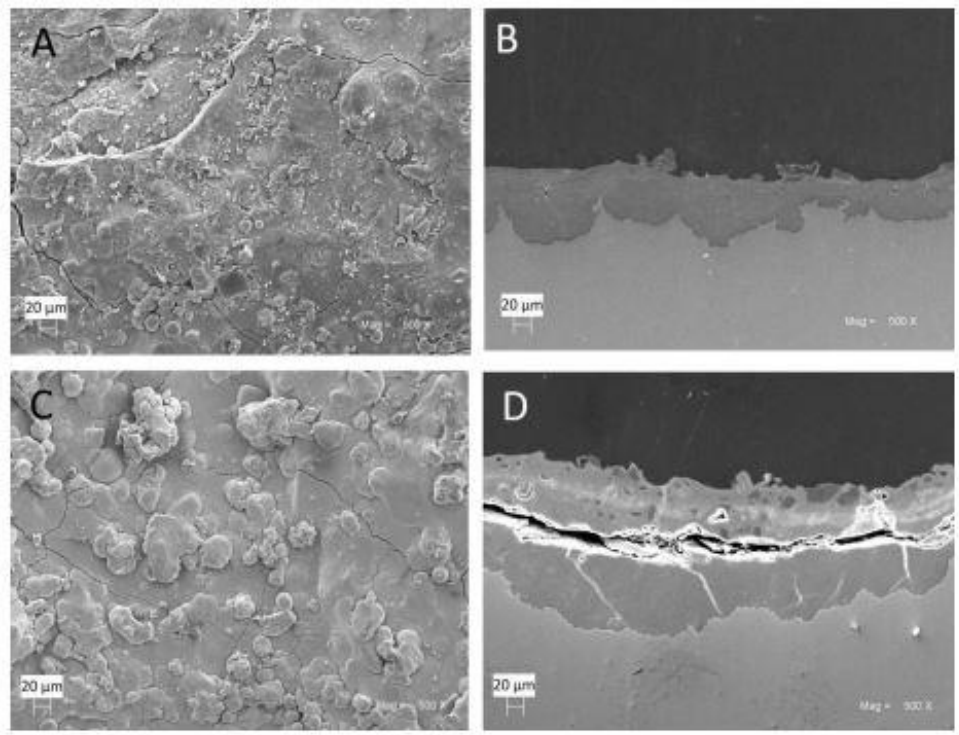

Figure 2.5 Surface and cross-section of the carbon steel from the Coronel station. A and B: 1 year, C and D: 3 years, 500x.

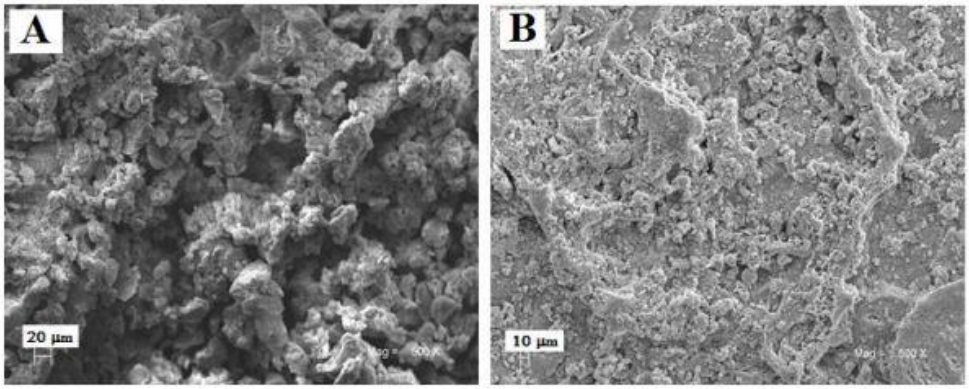

Figure 2.6 Surface of the galvanised steel after one year of exposure at the stations in Quintero(A) and Isla de Pascua (B), 500x.

- Characterization of corrosion products on carbon steel exposed to natural weathering and to accelerated corrosion tests was studied by R. A. Antunes et al. (Antunes, Ichikawa, Martinez, & Costa, 2014). The size of specimens for their study was 150 mm x 150 mm. The specimens were cleaned with a blast of organic solvent before exposure. Two different locations in Sao Paulo State, Brazil were chosen in their study. The corrosion products examined in their study were made with the exposure times of 1, 2, 3, 6, and 9 months. Figure 2.7 (a) and (b) show the XRD patterns of the specimens exposed at Cubatao and Paula Souza, respectively.

(a).

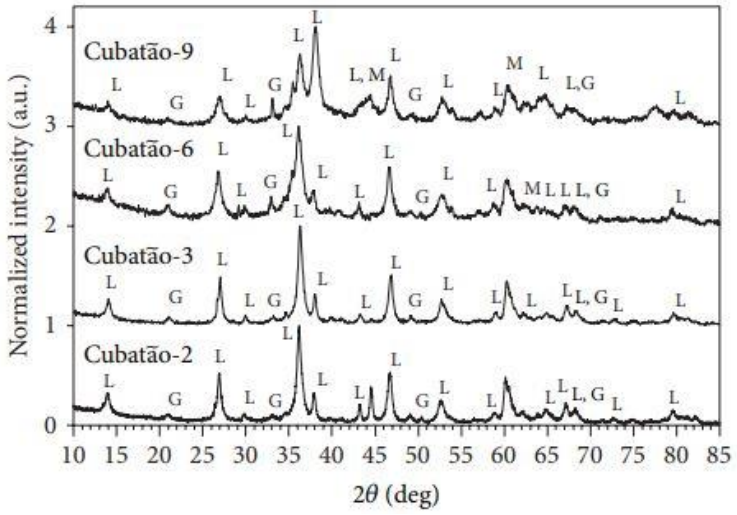

(b).

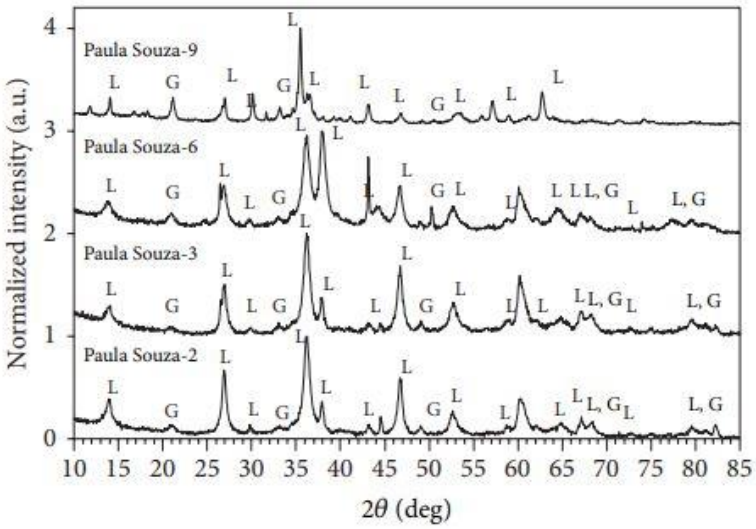

Figure 2.7 XRD patterns of specimens exposed in (a) Cubatao, and (b) Paula Souza station for different periods. G = goethite; L = lepidocrocite; M = magnetite

They fund that lepidocrocite and goethite were the primary corrosion products in Cubatao, according to quantitative X-ray analyses, after up to six months of exposure. On the specimen that had been exposed for 6 months, magnetite was found to be a small component. But after 9 months of exposure, it overtook the rust layer as the dominant phase. Paula Souza was found to have lepidocrocite and goethite as well. The primary phase was lepidocrocite, which was followed by goethite. The specimens exposed for six and nine months in Cubatao have this recognized magnetite, but not at Paula Souza.

- The effect of environmental variables on atmospheric corrosion of carbon steel in Shenyang, China was studied by C. Wang et al. (Wang, Wang, & Ke, 2009). In their study, carbon steel Q235 was used. The specimens with dimensions of 100 mm x 50 mm x 3 mm were used to measure corrosion losses, while the specimens with dimensions of 10 mm x 10 mm x 5 mm were utilized to evaluate the morphology and byproducts of the rust layer. Their exposure study period was up to 18 months at Shenyang test site. They found that, throughout time, the rate of corrosion varies. The corrosion rate is often high during the early stage. The mass loss increases rapidly from the start to about 120 days in the first process, and stays rather constant between 120 and around 360 days in the second step. The mass loss again accelerates quickly in the third phase, from 360 to around 510 days. The third segment's slope is less steep than the first segment's. For the appearance of the exposed specimens, they found that, after 10 days of exposure, the majority of the sample surfaces had yellow corrosion products partially covering them; after 30 days of exposure, the majority of the sample surfaces had all of them completely covered with corrosion products, and the color of the rust had changed to a light brown. In addition to the exposure time being increased, the hue of the rust turns dark brown. Figure 2.8 (a) – (e) show their results of XRD analysis for the periods of exposure with 10, 20, 30, 90, and 120 days, respectively. Lepidocrocite was the only corrosion product found in the Shenyang test station after 10 and 20 days, and its amount rose as the exposure period increased based on the XRD results. Maghemite Fe2O3 was

visible in the corrosion products after a 30-day exposure period. Magnetite Fe_3O_4 was found after 90 days of testing. At 120 days of exposure, goethite was found in the corrosion products.

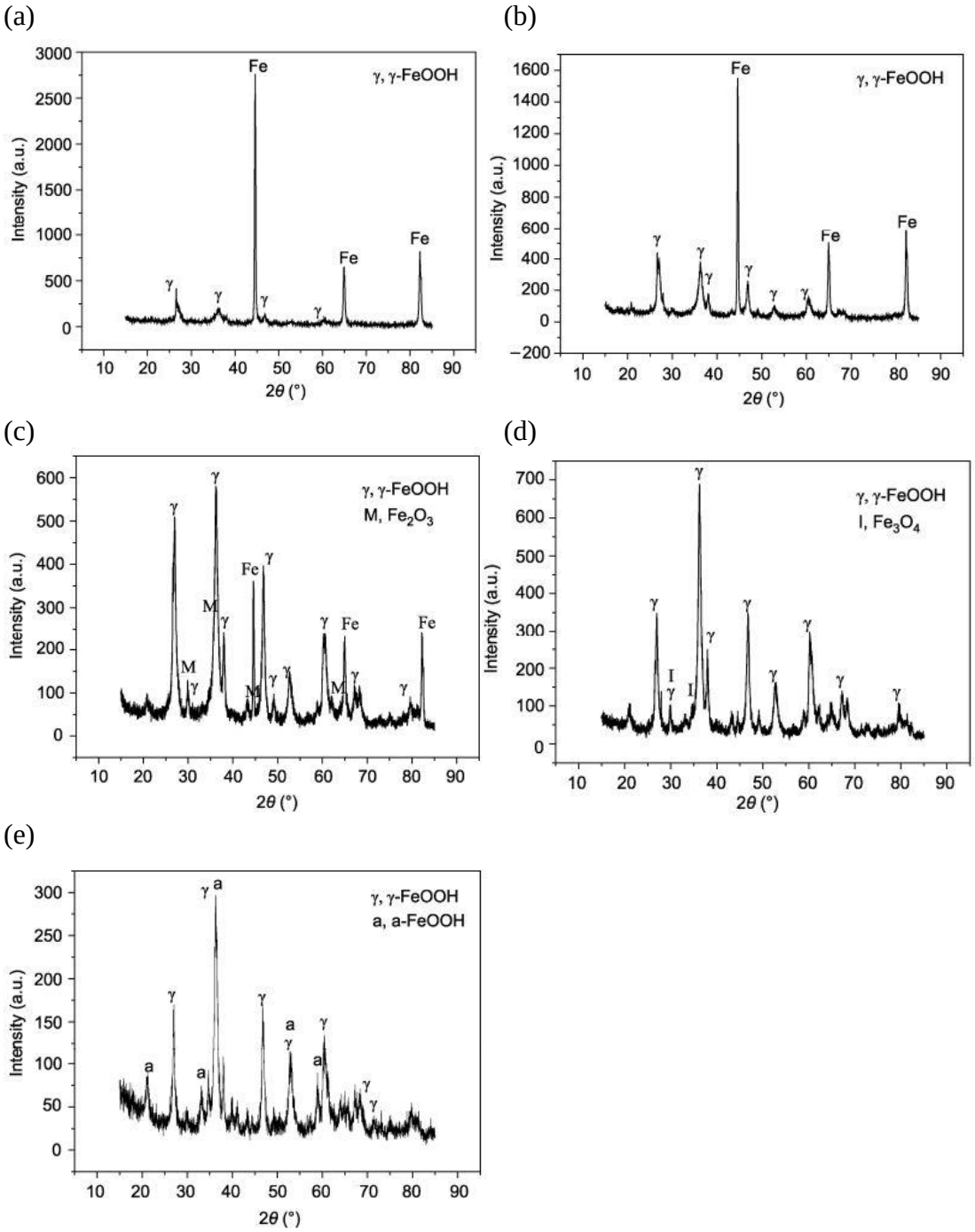

Figure 2.8 XRD of corrosion products of Q235 exposed: (a) 10 days, (b) 20 days, (c) 30 days, (d) 90 days, and (e) 120 days.

- Atmospheric corrosion of zinc and zinc alloyed coated steel was studied by D. Thierry et al. (Thierry, Persson, & Lebozec, 2017). Based on their study,

they reported that basic zinc salts containing anions, such as carbonate, chloride, and sulfate, are the predominant corrosion products observed in field exposures on zinc and zinc coated steel. Both zinc oxide and zinc hydroxide have been observed regularly. It has also been reported that zinc non-basic salts like $ZnCO_3$ and $ZnSO_4.nH_2O$ exist, as shown in Table 2.2.

Table 2.2 Zinc compounds reported in corrosion products on zinc and zinc coated steel after field exposure and laboratory investigations.

Compound	**Field exposures/atmosphere**
ZnO	Rural, urban, marine, industrial
$Zn(OH)_2$	Rural, urban, marine, industrial
$ZnCO_3$	Rural, urban, marine
$Zn_4(OH)_6CO_3 . H_2O$	Marine
$Zn_5(OH)_6(CO_3)_2$	Rural, urban, marine, industrial
$Zn_5(OH)_8Cl_2 . H_2O$	Marine, industrial
$ZnSO_4$	Industrial
$Zn_4(OH)_6SO_4 .nH_2O$	Rural, urban, marine, industrial
$NaZn_4Cl(OH)_6SO_4 . 6H_2O$	Urban, marine
$Zn_4Cl_2(OH)_6SO_4 . 5H_2O$	Rural, urban, marine, industrial

Adapted from References Zhang, X. G. (1996). Corrosion and Electrochemistry of Zinc. Plenum Press: New York; Graedel T. E. (1989). Corrosion mechanisms for Zinc Exposed in the Atmosphere. J. Electrochem. Soc. 136, 193C–203C.

- Studies of galvanized steel atmospheric corrosion in Saudi Arabia was studied by S. Syed (Syed, 2010). Four pure marine and five mixed marine (SO_2 polluted) sites in the Saudi Arabia region were chosen in his study. In his study, galvanized steel specimens were exposed for four years. The surface of the specimen is 100 x 150 x 2 mm in rectangular shape. Four samples of each metal were then subjected to the various atmospheres (marine and marine industrial) on open racks. Facing the south was his exposure angle. The loss of their shiny appearance and the development of a white patina were characteristics of exposed galvanized steel surfaces, especially on all the specimens exposed in marine and marine industrial stations. It is important to know whether the corrosion rate of the galvanized steel decreases with the exposure time or not. The decline in corrosion rates was reported for his studied stations: Khober, Jubail-1, Jubail-2, Farsan, Khafji, and Hakhal. He stated that the development of adhering corrosion products on the surface is most likely to make the slowing down of the corrosion rate with exposure time. Table 2.3 shows the corrosion compounds

of exposed galvanized steel specimens of his study. The analysis was made by the XRD method.

Table 2.3 Crystalline compounds of galvanized steel specimens identified by XRD

Stations / Corrosion Products	Khober	Jubail-2	Farsan	Jeddah	Yanbu	Wajah	Hakhal
ZnO	Yes	Yes	Yes	No	No	No	No
$Zn(OH)_2$	Yes	No	No	Yes	No	No	No
$Zn_5((OH)_8Cl_2).H_2O$	Yes	No	No	No	No	No	No
$ZnCl_2$	Yes	Yes	No	Yes	No	No	No
$NaZn(SO_4)(OH)_6Cl.6(H_2O)$	Yes	No	No	Yes	Yes	Yes	Yes
$Zn((OH)_2)_3(ZnSO_4)(H_2O)_3$	No	Yes	No	No	Yes	No	No
$Zn(SO_4)(OH)_2.4H_2O$	No	Yes	No	Yes	Yes	No	No
$Zn_4O_3(SO_4).7H_2O$	No	Yes	No	No	No	No	No
Zincite	No	No	Yes	No	No	No	No
SiO_2	No	No	Yes	No	No	Yes	Yes
Fe_2O_3	No	No	Yes	No	No	No	No
$Zn(HSO_4)_2$	No	No	No	Yes	No	No	No
$Zn(SO_3)_250(H_2O)$	No	No	No	No	Yes	No	No
$ZnSO_4$	No	No	No	No	Yes	No	No
$ZnCO_3$	No	No	No	No	No	Yes	Yes
Fe_3O_4	No	No	No	No	No	Yes	Yes
NaCl	No	No	No	No	No	No	Yes

- Corrosion resistance of painted zinc alloy coated steels was studied by Edavan et al. (Edavan & Kopinski, 2009). Five different kinds of hot-dip coated steel, zinc (type-A), Galvalume (type-B), Galfan (type-C), ZAM (type-D) and SuperDyma (type-E), were chosen in their study. The specimen sizes of their study were 120 x 300 mm, with a thickness of 0.45–0.6 mm. Only 14 months of exposure had been completed at the time this article was submitted for the atmospheric corrosion tests under sheltered of the painted panels at the Akzo Nobel exposure site in Muriwai, New Zealand. Their study results were obtained from the exposed specimen naturally exposed for 14 months under sheltered conditions at Muriwai, New Zealand (Table 2.4). Despite the short period of the exposure, the test still revealed significant corrosion creep at the cut edges due to the aggressive environmental conditions. In their test, Type-A panels with chromate-based paint systems displayed low to moderate facial blistering while others did not. All of the panels were practically blister-free because to the Cr-free paint technique. Panel D was good coating system under this exposure. The ability to resist blistering from natural exposure can be summarized as follows:

  Cr-system: B = D = E = C > A

  Cr-free system: B = D = E = C = A

They found that the adhesive properties of the substrates appear to have a substantial impact on the creep process. A model on a schematics of the corrosion creep mechanism is illustrated and described in Figure 2.9.

Table 2.4 Summary of the natural exposure test results of the painted coated steel panels at Muriwai, New Zealand, after 16 months of exposure in sheltered conditions.

Panel No.	Paint system	Blistering (density, D and size, S) Scale 0–5 (nil–max)			Corrosion product 3T	Cut edge corrosion creep, mm					
		Scribe	Face	Bend (3T)		Scribe	Left	Bottom	Top	Right	Average
A	Chrome system	D3S2	D2S2–3	D3S2	0	1	3	5	1.5	5	3.6
B		D0S0	D1S2	D0S0	0	0	0	1	0	2	0.8
C		D0S0	D1S2	D0S0	0	0	3	4	3	9	4.8
D		D0S0	D0S0	D0S0	0	0	0	0.5	0.5	0	0.3
E		D0S0	D0S0	D0S0	0	0	0	0	0	0	0.0
A	Chrome free system	D3S2	D1S2	D3S2	4	0.5	3	5	1.5	2	2.9
B		D0S0	D1S2	D0S0	0	0	1	2	2	6	2.8
C		D0S0	D1S2	D2S2	0	0	1	10	2	1	3.5
D		D2S1	D0S0	D3S2	2	0	1.5	2	1.5	1	1.5
E		D0S0	D1S2	D2S1	0	0	2	2	1.5	1.5	1.8

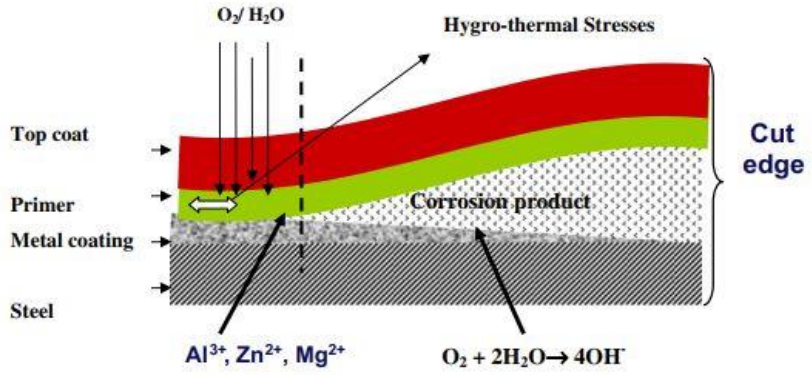

Figure 2.9 A schematics of the corrosion creep mechanism taking place on the painted and coated steel sheet.

After reviewing many studies related to atmospheric exposure tests, it can be concluded as follows: the dimensions of the specimens were mostly 100 mm × 150 mm. The most important pollutant factor is SO_2, which makes steel corrode. The weight loss method is used to find the thickness loss of the exposure specimen. Blistering and corrosion creep are the criteria for making an assessment of painted steel.

2.4 Corrosion equation

The relationship between a substance's corrosion level and the response or effect it generates is known as the dose-response function. The idea of a dose-response fucntion is typically correlated with atmospheric conditions when it comes to the corrosion of steel. The dose-response function of corrosion of steel and atmopheric paprameter is called corrosion equation.

Numerous factors, including those already mentioned such humidity, temperature, oxygen concentration, air pollution, salinity, and rainfall, have an impact on the rate of corrosion and the thickness loss of steel. However, there is not just a straightforward dose-response relationship between these variables and corrosion rate or thickness loss; rather, there is a complicated interplay between a number of variables.

Researchers utilize corrosion models that include these many characteristics and their interactions to analyze steel corrosion and forecast its behavior. To understand and forecast the corrosion behavior based on the many affecting elements, researchers employ corrosion equations.

Several corrosion equations based on their atmospheric tests have been developed by several researchers. For example:

- Annual atmospheric corrosion rate and dose-response function for carbon steel in Bogotá was studied by J. F. ROIS-ROJAS et al. (Rios-Rojas et al., 2017). In their study, initial analyses were performed by including data on PM deposition, which improved goodness of fit or R^2, but because PM was correlated with SO_2 concentration and included in the equations, it produced an underestimate of SO_2's actual effect, leading to its eventual exclusion from the statistical analysis. The latest equation, on the other hand, provided a superior estimate of the corrosion rates than before, taking into account both the best-fit and individual importance of the parameters. As a result, the equation below illustrates the annual dose-response function of carbon steel in the city of Bogotá in accordance with the experimental results:

$$r_{corr,it} = 0.071\left[{D_{SO2_{it}}}^{0.37}\right] exp^{(0.045\,RH + 0.14\,T)} \quad (2.1)$$

  A reliable approach to find the rate of corrosion of carbon steel during the first year of exposure to the Bogotá atmosphere was provided by the yearly dose-response function that was obtained.

- Prediction model of corrosion losses based on probabilistic approach was studied by Krivy et al. (Krivy, Kubzova, Kreislova, & Krejsa, 2018). Their study discusses the use of dose-response functions to predict corrosion losses of weathering steels. Utilizing statistical and probabilistic techniques, the following environmental characteristic entering the dose-response functions is examined: mean annual values of the temperature T, sulfur dioxide

concentration SO_2, relative air humidity RH, and chloride deposition Cl^-. Probabilistic analysis can be used to forecast the predicted range of corrosion rates and examine how certain environmental factors affect the corrosion process.

- Development of mathematical models to predict the atmospheric corrosion rate of carbon steel in fragmented subtropical environments was studied by Souto et al. (Souto et al., 2014). In order to accurately forecast corrosion rates from environmental elements including the pace at which chemical agents (namely chloride and Sulphur dioxide) deposit on metals, the duration of metal exposure, and the impacts of the climate (such as moisture and time of wetness), new modeling approaches are needed. Utilizing data collected over the course of three years of carbon steel exposure at 74 sites spread across the seven major islands of the Canary Islands (Spain) in their study, the validity of the method was examined. The impact of environmental conditions on the degree of corrosion was clearly assessed, and positive outcomes were determined in terms of the fitting quality. They believed that their model adequately captures the corrosion rates of carbon steel throughout the entire archipelago.

$$\begin{aligned}\mathrm{Ln}(CR) = {} & 2.9378+0.0738(SO2)+0.097(CL)+0.1987\ln(TOW)-0.0018(SO2)(CL) \\ & -0.5985\ln(TEXP)+0.0067(CL)\ln(TEXP)-0.0014(SO2)(CL)\ln(TEXP) \\ & +0.5544D2+1.1423D3+1.4916D4 \end{aligned} \quad (2.2)$$

where *CR*: corrosion rate (µm/year); *TEXP*, the exposure time (year); *TOW*, time of wetness (year); *CL*, concentration of chlorides (g/m^2 year); and *SO2*, concentration of SO2 (g/m^2 year). The qualitative variables (*D2*, *D3*, and *D4*)

- Optimization of the atmospheric corrosivity mapping of Guangdong Province, China was studied by Huang et al. (Huang, Meng, Zheng, & Gao, 2018). The on-site exposure test was conducted using Q235 steel as the material. Their specimen dimension is 100 x 50 x 3 mm. The specimens were exposed at a 30 degree angle, facing south. In their study, the specimens were retrieved a year later, and the rust layers were removed in accordance with

ISO 9226. The calculation of the corrosion rate was made with the weight loss method. Their atmospheric corrosion tests were conducted at 48 locations throughout Guangdong Province. During the test period, environmental data impacting corrosion, such as temperature, relative humidity, sulfur dioxide, nitrogen dioxide, ozone, and particle content, were collected from 102 environmental monitoring stations spread across 21 cities in Guangdong Province. The results were statistically averaged. Different factors, including temperature, relative humidity, sulfur dioxide, nitrogen dioxide, ozone, and particulate matter, influences in different impacts on the atmospheric corrosion of materials. Their method was based on data gathered from monitoring stations and on-site exposure experiments conducted in Guangdong Province about corrosion rates and environmental corrosion factors. The dose response function below was discovered to be appropriate for the corrosion rate calculation for the province of Guangdong:

$$\ln(r_{corr}) = -8.908+0.422\cdot\ln(SO_2)+1.126\cdot\ln(O_3)+1.902\cdot\ln(RH),\ \ R^2 = 0.87 \qquad (2.3)$$

where: r_{corr} (g/[m^2·a]); SO_2 (μg·m^{-3}); O_3 (μg·m^{-3}); RH (%).The function provides a mathematical relationship between atmospheric corrosion rate and environmental parameters so that corrosion rate can be calculated using environmental information from monitoring stations.

- The effect of environmental variables on atmospheric corrosion of carbon steel in Shenyang, China was studied by Wang et al. (Wang et al., 2009). As mentioned in the above section, carbon steel Q235 with specimen dimensions of 100 mm x 50 mm x 3 mm was chosen for the study over an 18 months of exposure in their scope. In their study, twelve significant meteorological characteristics with data matching to the test period were all examined in order to fully characterize industrial atmospheric corrosion. The suggested model takes into account how the most significant environmental factors affect the urban air corrosion of carbon steel. To find the most accurate regression model in their study, the data were subjected to a stepwise multiple regression analysis. SPSS statistical software program was used to conduct the statistical analysis in their study. To find the optimal regression

model, stepwise multiple regression analysis was used on the data from 12 meteorological indicators and 7 contaminants. A model describing the interaction between the total amount of time it rains, the total amount of time it is sunny, and the concentration of H_2S was created: $C = 1.185 \times \sum$rain time $+ 0.066 \times \sum$sunshine time $+ 377.847 \times [H_2S] + 2.325$. The model shows that carbon steel will increase in corrosion rate as the sum of rainfall time, the sum of sunshine time and the concentration of H_2S increase.

2.5 Corrosion map

A corrosion heat map is a visual description or tool used to evaluate and show the degree and severity of corrosion throughout the map. It helps in determining the locations most susceptible to corrosion and offers a visual assessment of the risks associated with corrosion. The corrosion heat map is often constructed by collecting data on corrosion rates or thickness loss at various points within the exposure test. This data can be gathered through weight loss measurement method. Factors such as ambient conditions, and exposure to corrosive agents are taken into account to determine the corrosion hazards.

Data is collected, examined, and given a color scheme based on the level of corrosion after analysis. The colors can range from green (which denotes little danger of corrosion) through yellow, orange, and red (which denotes rising risk or severity of corrosion). Darker colors denote higher degrees of risk, and color intensity can be used to signify the extent of corrosion.

Engineers, maintenance workers, and facility managers may quickly grasp the overall corrosion status of the steel with the help of the corrosion heat map. Based on the severity shown by the heat map, it enables them to prioritize areas for inspection, maintenance, or corrosion control methods. They can effectively allocate their efforts and resources to prevent the potential corrosion damage by concentrating attention on locations with the highest corrosion risk.

In environment including pollutants, marine, transportation, infrastructure, and manufacturing where corrosion can pose serious concerns, corrosion heat maps are very helpful. In order to limit the influence of corrosion on the integrity, safety, and dependability of the systems or structures, they provide a brief and unambiguous picture

of the corrosion status. This enables proactive maintenance planning and decision-making.

Overall, corrosion heat maps are effective tools for evaluating the extent and severity of corrosion, identifying vulnerable locations, and directing preventive actions to reduce hazards associated with corrosion.

Corrosion maps have been created successfully by several researchers:

- Steel corrosion map of Vietnam was studied by Ivan Cole et al. (Cole, Corrigan, & Nguyen, 2012). For their study, mild steel, zinc, and copper were tested on a variety of sites that represented various climatic situations, including harsh marine, marine, industrial, urban, and rural. Specimens of mild steel, zinc, and copper with dimensions of 10 x 16 x 1 mm were taken to perform the exposure for collecting data for corrosion mapping. The specimens were exposed at a 45-degree angle and faced the ocean. Their periods of exposure were 1, 3, 6, 9, 12, 24, and 36 months. Continuous records of the following variables were made: surface temperature, humidity, rainfall, solar radiation, and the duration of daylight. The Inverse Distance Weight (IDW) method was used in creating the corrosion map. They made a comparison between the data from the map and the real test and could conclude that the data obtained from the map and those chosen from field tests are quite close, with 2% to 3% differences. Their corrosion map of mild steel in Vietnam is shown in Figure 2.10.

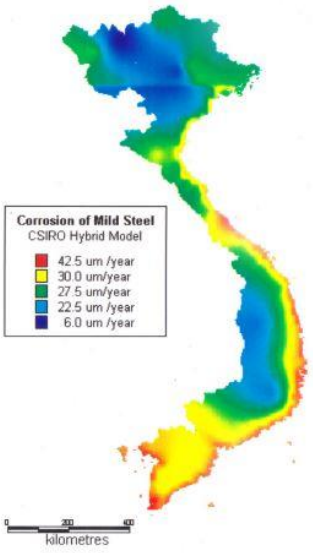

Figure 2.10 Corrosion map of Vietnam by IDW model

- Corrosion map of South Africa's macro atmosphere was studied by Rensburg et al. (Janse van Rensburg, Cornish, & van der Merwe, 2019). Based on 12-month mild steel corrosion rates at more than 100 sites throughout the country, their study's corrosion map of South Africa's macro atmosphere is presented. Their test sites cover all aspects of the South African atmosphere (marine, urban, industrial, rural, and desert environments). The process of their research comprised exposing mild steel (low carbon steel) coupons to various atmospheric conditions for a period of 12 months, after which metal specimens' weight loss was measured. Their test specimens had been chemically cleaned, dried out, and then reweighed according to ISO 9226. The 12-month corrosion rate of each mild steel coupon was then determined. Using the geographic information system (GIS) software package Esri ArcGIS 10.2, their corrosion data were then used to create an atmospheric corrosion map of South Africa. Their corrosion map results, as shown in Figure 2.11, showed that, at all corrosion monitoring locations more than 30 km from the ocean, the average first-year corrosion rate of mild steel was around 21 ± 12 µm/a [95% CI: 18-23 µm/a]. The Central Karoo, a hot, semi-arid region, was the site of the lowest inland measurement, which was roughly 1.3 µm/a. In South Africa's heavily industrialized Highveld and Vaal Triangle regions, where typical rainfall is about 550–600 mm/a, the highest, of about 51 µm/a and 50 µm/a, were reported at Germiston (Gauteng) and Sasolburg (Free State), respectively. The average first-year corrosion rate of mild steel exposed within the first 150 meters from the shoreline in South Africa's coastal districts was 319 ± 112 µm/a (95% Cl: 215–422 µm/a). Salisbury Island in Durban reported the lowest value, which was about 134 µm/a, while Melkbosstrand in the Western Cape recorded the highest value, which was about 460 µm/a. The average first-year mild steel corrosion rate for sites between 150 and 1000 m from the coast was 60 ± 22 µm/a [95% Cl: 45–75 µm/a]. The average first-year corrosion rate of mild steel drops much more at 1–3 km from the ocean, to around 43 ± 14 µm/a [95% Cl: 28–58 µm/a]. At all sites within 3 to 10 km of the coast, the average first-year

corrosion rate of mild steel was recorded at 37 ± 13 μm/a (95% Cl: 27–47 μm/a). The average first-year corrosion rate of mild steel for the 10–30 km region was 35 ± 14 μm/a (95% Cl: 22–48 μm/a), which indicates that the average corrosivity of the atmosphere has decreased by 1%.

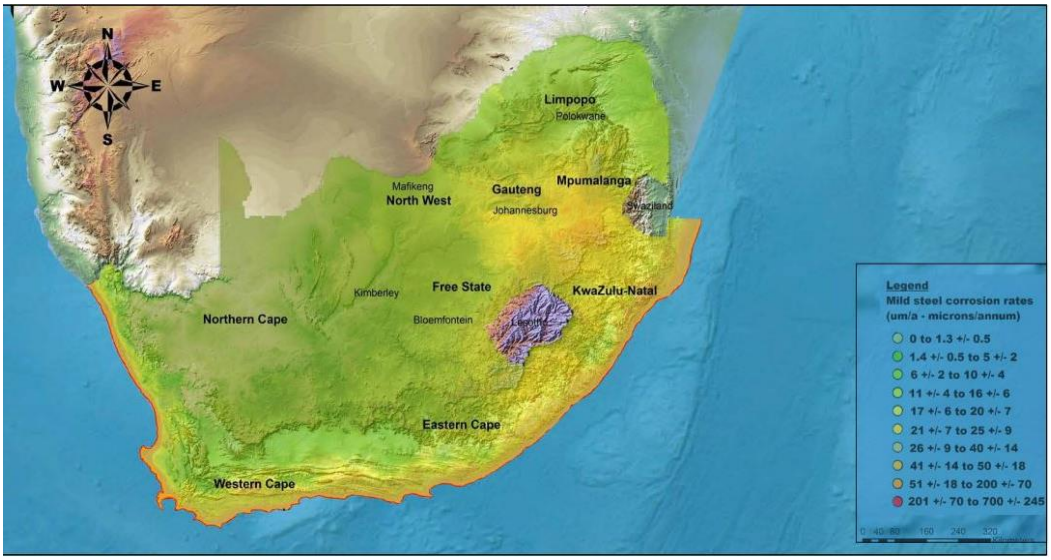

Figure 2.11 Atmospheric corrosion map of South Africa

- Optimization of the atmospheric corrosivity mapping of Guangdong Province, China was studied by Huang et al. (Huang et al., 2018). In their study, the dose response function was discovered to be appropriate for the corrosion rate calculation for the province of Guangdong. The spatial interpolation of the data was carried out using the kriging method in the ArcGIS 10.2 software. A geostatistical procedure called kriging creates an approximated surface from a dispersed collection of data points. The kriging method calculates the output value for each place by matching a mathematical function with a predetermined number of data points, or all points within a predetermined radius. The findings of the kriging method offer the most accurate and ideal estimates. By using the dose response function and the ArcGIS 10.2 software, they came up with the atmospheric corrosion map of Guangdong province, as shown in Figure 2.12. The corrosion rate of each range was shown in the different colors.

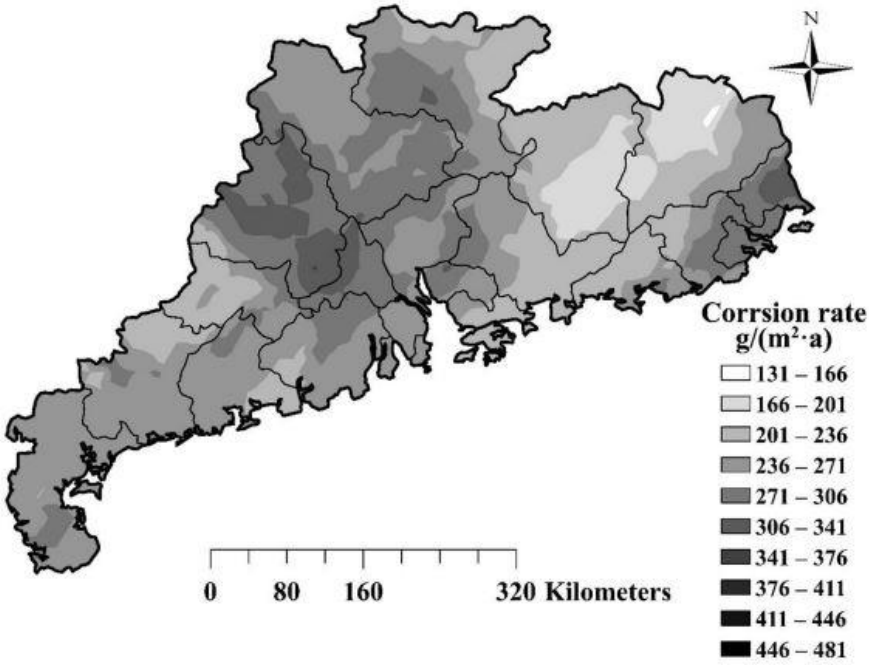

Figure 2.12 Atmospheric corrosion map of Guangdong Province (150 points including exposure test data and calculated data)

2.6 Thickness loss projection of steel

Loss of thickness Steel projection is the calculation or forecast of the thickness loss that occurs over time as a result of corrosion in steel structures. It is a crucial component of corrosion management and helps in establishing maintenance schedules, determining how long steel components will last, and guaranteeing structural integrity. The thickness loss projection method for steel has been shown and used successfully by several researchers, as presented below. Some of the standards, like ISO 9224 (ISO9224, 2012) or ASTM G16 (ASTMG16, 2013), showed the formula and method to calculate the thickness loss projection.

- "The prediction of atmospheric corrosion from meteorological and pollution parameters–I and II. Long-term forecast" was studied by Feliu et al. (Feliu, Morcillo, & Feliu, 1993). Forecasts for long-term atmospheric corrosion frequently depend on the satisfaction of equations of the type:

$$C = At^n \tag{2.4}$$

where C denotes corrosion after t years and A denotes corrosion after the first year of exposure. Constants A and n must be given appropriate values. The

feasibility of expressing *A* as a function of typically available environmental characteristics was examined in the first section of their work. In their following second section, it is determined whether the exponent *n* of the preceding equation can also be represented as a function of such environmental characteristics using data gathered after a thorough literature review. The exponent n can be found by plotting the corrosion data against the exposure duration (in years) in a log-log plot. After performing linear regression, they obtained the equations for *A* and *n* as shown in Table 2.5 and 2.6. As a result, the constant *A* and the exponent *n* in the atmospheric corrosion power law connected with pollution and meteorological conditions were successfully created in their study.

Table 2.5 Relationships between *A* in equation 2.4 and the environmental parameters: carbon steel for equations (5) & (6); zinc for equations (7) & (8). (Feliu, 1993)

Equations	Remarks
$A = 132.4\ Cl\ (1 + 0.038\ T - 1.96\ t_w - 0.53\ S + 74.6\ t_w(1+1.07\ S) - 6.3$ ($R = 0.79$) equation (5) $A = 33.0 + 57.4\ Cl + 26.6\ S$ ($R = 0.73$) equation (6)	A = annual corrosion (μm), t_w = wetness time (annual fraction), T = temperature annual average (°C), S = SO_2 pollution annual average ($mgSO_2dm^{-2}d^{-1}$), Cl = chloride pollution annual average ($mgCl^{-}dm^{-2}d^{-1}$), R = multiple correlation coefficient
$A = 0.703 + 4.40\ Cl(1 + 0.11\ T - 3.5\ t_w) + 5.23\ S(1 - 0.054\ T)$ ($R = 0.91$) equation (7) $A = 0.785 + 5.01\ Cl + 2.26\ S$ ($R = 0.73$) equation (8)	A = annual corrosion (μm), t_w = wetness time (annual fraction), T = temperature annual average (°C), S = SO_2 pollution annual average ($mgSO_2dm^{-2}d^{-1}$), Cl = chloride pollution annual average ($mgCl^{-}dm^{-2}d^{-1}$), R = multiple correlation coefficient

Note: equations (5) & (7) are the best least-squares fits with the interaction terms; equations (6) & (8) are without the interaction terms.

Table 2.6 Relationships between the values of exponent *n* in equation 2.4 and the environmental parameters. (Feliu, 1993)

Materials	Equations	Remarks
Carbon steel	$n = 0.570 + 0.0057\ \mathrm{Cl}\ T + 7.7 \times 10^{-4}\ D - 1.7 \times 10^{-3}\ A$ ($R = 0.40$) equation (2)	n = exponent in equation (1), A = first-year corrosion (μm), t_w = wetness time (annual fraction), T = temperature annual average (°C), D = number of rainy days per year, RH = relative humidity annual average (%), MAQ = marine atmosphere quality (variable coded as 1 or 0), S = SO_2 pollution annual average ($mgSO_2dm^{-2}d^{-1}$), Cl = chloride pollution annual average ($mgCl^-dm^{-2}d^{-1}$), R = multiple correlation coefficient
Carbon steel	$n = 0.531 + 0.115\ \mathrm{MAQ} + 0.00112\ D - 0.221\ t_w$ ($R = 0.44$) equation (3)	
Zinc	$n = 0.526 + 0.545\ S\ (1 - 0.068\ T) + 0.0246\ T$ ($R = 0.62$) equation (4)	
Copper	$n = 0.822 - 0.0684\ T\ (1 - 0.011\ \mathrm{RH})$ ($R = 0.47$) equation (5)	

- Practically, the prediction models can be separated into two categories: (a) models for predicting corrosion rate (or corrosion loss) following the first year of exposure; and (b) models for predicting corrosion loss following the structure's long-term exposure. Prediction model of corrosion losses based on probabilistic approach was studied by Vit Krivy et al. (Krivy et al., 2018). They studied about the prediction of weathering steel thickness losses. Their long-term corrosion loss is in the form of:

$$D = r_{corr} \cdot t^b \qquad \textbf{2.1}$$

where D is corossion loss (μm), r_{corr} is the corrosion rate during the first exposure year (μm/year), t is exposure time (years), b is the coefficient, which is often smaller than 1.

The first year corrosion loss rate (r_{corr}) is the primary input variable for the long-term prediction models of corrosion development on weathering steel. The atmospheric variable properties determine the r_{corr} value.

2.7 Summary

The literature review chapter can be summarized as below:

- Chemical component reactions to make steel corrosion are in the combination of H_2O, and oxygen. The main environmental pollutants that make steel corrode are SO_2 and chloride.
- Many researchers have carried out the atmospheric exposure tests. Therefore, we can learn about their testing method, the differences between each researcher, their weak points, and their limitations. Even though it has many studies, the atmospheric exposure tests for bare steel, HDG steel, and painted steel in Thailand have not yet been conducted.
- Corrosion equations with dose response functions for atmospheric corrosion with the complexity of atmospheric characteristics like Thailand have not yet been developed.
- The corrosion map was successfully developed by many researchers. Therefore, a corrosion map for Thailand should be developed.
- Thickness loss projection could be done by the first year thickness loss results.

CHAPTER 3
ATMOSPHERIC EXPOSURE TEST

3.1 Introduction

In order to understand the corrosive resistance performance of each type of steel, the atmospheric exposure test has to be conducted. In this chapter, all research methodologies are explained in detail. The atmospheric exposure test was conducted following the relevant standards, which are mentioned for each type of method and procedure.

3.2 Research framework

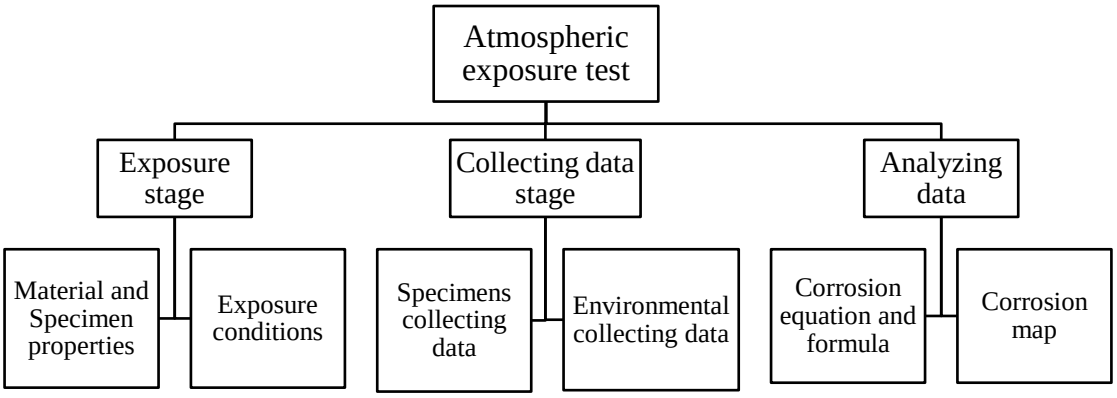

Figure 3.1 Atmospheric exposure test framework

As shown in Figure 3.1, the research framework was divided into three major stages:

Exposure stage: this phase is an essential step in determining the effectiveness of materials or coatings exposed to outside atmosphere. In order to mimic and evaluate test specimens' resistance to weathering, corrosion, deterioration, and other environmental effects, the test specimens and exposed to real-world air conditions for a prolonged length of time. For this exposure stage, material and specimen properties and exposure conditions are the points to consider. The materials or coatings being evaluated are prepared in accordance with the test's precise specifications. This could entail applying coatings or surface treatments, cutting or shaping specimens to

predetermined dimensions, and making sure fixation or mounting for exposure is done correctly. In exposure conditions, testing location is one of the considering case. A suitable outdoor testing location is chosen to ensure that it reflects the environmental conditions that the materials or coatings would experience throughout their intended use. To ensure that the test settings adequately reflect the desired exposure scenario, variables such as temperature, humidity, rainfall, air pollution, and proximity to coastal or industrial areas are taken into consideration. Another case of exposure conditions is the exposure setup. To expose the test specimens to the outdoor environment in a representative manner, they are erected or placed in strategic locations at the test site. The closest possible representation of the real-world conditions is achieved by taking into account variables like orientation, inclination, and separation from other objects. Depending on the test criteria and objectives, the exposure stage often involves at least one year exposure time in order to complete understand the full cycle of the season.

Monitoring and data collection stage: Various monitoring techniques are used to collect data on environmental factors like temperature, humidity, and rainfall throughout the exposure period. Additionally, the test specimens are subjected to routine inspections and measurements to evaluate any alterations in their appearance, corrosion, deterioration, adhesion, color fading, or other pertinent criteria. This stage of collecting data could be divided into two cases. The first one is specimen collection data, including rust removal, thickness loss, and assessment of exposed painted steel. Another is environmental data collection.

Evaluation and analysis stage: Following the exposure phase, the test specimens are closely examined, and the results are assessed using predetermined standards or criteria. After collecting data, those data will be analyzed using the corrosion equation and creating the corrosion heat map that could provide the thickness loss information throughout the map.

3.3 Exposure stage

3.3.1 Material and specimen properties

Two commercial types of steel were used to perform the atmospheric exposure test, SS400 and SM490A, with six different kinds of coating. The specimen types and name codes are provided in Table 3.1. The specimen was designed with the dimensions

100 x 150 x 4.5 mm, based on the ASTM G92 (ASTMG92, 2010) and ASTM D1014 (ASTMD1014, 2009) standards. The SS400 specimen has been conformed to JIS G3101 (JISG3101, 2015) and the SM490A has been conformed to JIS G3106 (JISG3106, 2004). The chemical composition of steel specimens was tested and as presented in Table 3.2. Each type of specimen had its own thickness of coating and painting. Table 3.3 shows the number of coating layers and the thickness of the specimen coating.

Table 3.1 Specimen types

Specimen Type	Specimen name code	
	SS400	SM490A
1. Bare Steel (Control Specimen)	V	W
2. Hot-Dip Galvanized	X	Y
3. Low grade paint with scribed mark	A	B
4. Medium grade paint with scribed mark	C	D
5. Premium grade Paint with scribed mark	E	F
6. Hot-Dip Galvanized + Paint with Scribed Mark (Duplex System)	G	H

Table 3.2 Chemical composition of base steel

Element composition (% by wt)	Steel types	
	SS400	SM490A
C	0.117	0.199
Mn	0.430	1.220
Si	0.014	0.010
P	0.012	0.014
S	0.009	0.010
Al	0.050	0.042
Ni	0.011	0.013
Cr	0.020	0.030
Mo	0.003	0.007
V	0.000	0.002
Cu	0.017	0.008
B	0.0000	0.0000
Cr+Mo	0.023	0.41
Cu+Ni+Cr+Mo	0.051	0.26

Table 3.3 Coating layer and thickness

Specimens	Coating layer 1 Binder	Thk.	Coating layer 2 Binder	Thk.	Coating layer 3 Binder	Thk.	Standards
Bare steel	-	-	-	-	-	-	
HDG steel	Zn	100 µm	-	-	-	-	(ASTMA123, 2008)
Low grade paint	EP	80 µm	PUR	40 µm	-	-	DPT 1333-61
Medium grade paint	EP	80 µm	PUR	80 µm	-	-	DPT 1333-61
Premium grade paint	EP	150 µm	PUR	150 µm	-	-	DPT 1333-61
Duplex system	Zn	100 µm	EP	80 µm	PUR	40 µm	ASTM A123

Note: Zn = Zinc, EP = Epoxy, PUR = Polyurethane

3.3.2 Specimen preparation

For bare steel and HDG steel, all specimen preparation procedures conformed to the ASTM G1 (ASTMG1, 2003) and ASTM G31 (ASTMG31, 2004) standards. Mill scale and steel rust were removed by the sandblasting method. After the sandblasting method, a rough surface was observed on the specimen's surfaces, which provided a bad condition for the atmospheric exposure test. Therefore, a sandpaper smoothing machine was used to smooth the specimen's surfaces. The grade of sandpaper is 600. Subsequently, all specimens were marked with the name code for identification. Thereafter, the dimensions of the specimens were measured three times for width, three times for height, and eight points for thickness. The average value of those three measurements for width and height was used. In addition, the average value of those eight measurements for the thickness was used. For all dimension measurements, a digital caliper with an accuracy ± 0.2 mm was used. After measuring the dimensions of the specimens, dust, oil, and chemical substances were removed with deionized (DI) water and acetone. Then, the drying process was carried out by using a hair dryer. The specimens were weighed on a digital balance with a 0.001 g sensitivity after they had completely dried. Finally, all specimens were stored in a dried and absorbent box, called a desiccator box, prior to exposure. For HDG steel, the specimen preparation processes are almost the same as with bare steel. It started from smoothing the specimen's surfaces with a sandpaper smoothing machine up to storing it in the desiccator boxes. The specimen preparation and procedure activities for bare steel and HDG steel are provided in Figure 3.2.

For the painted steel, the specimens were painted at the desired thickness. Each paint system has its own thickness that adheres to the DPT 1333–61 standards

(DPT1333–61, 2018). Subsequently, an artificially scribed mark with a single line shape was made following the ISO 17872 (ISO17872, 2019) standards. The scribed mark length is 70 mm, and the scribed width is 0.6 mm. In order to define the study area, UV-resistant tape was applied on the specimens. The specimen preparation and procedure activities for painted steel are provided in Figure 3.3. The position and dimension of scribed mark and taping is shown in Figure 3.4.

The specimens were organized and marked for identification in order to control all the data. The numbering identification should be in the simplest form since it has a lot of specimens. An example of specimen name identification is shown in Figure 3.5. The specimens were also properly organized on the rack.

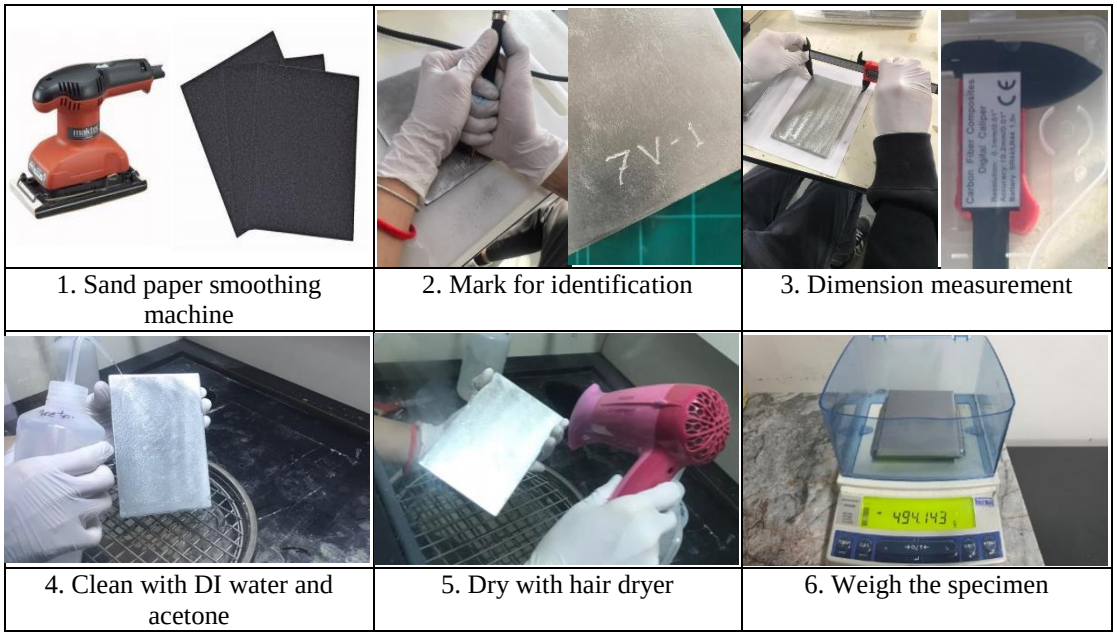

1. Sand paper smoothing machine	2. Mark for identification	3. Dimension measurement
4. Clean with DI water and acetone	5. Dry with hair dryer	6. Weigh the specimen

Figure 3.2 Specimen preparation procedures for bare steel and HDG

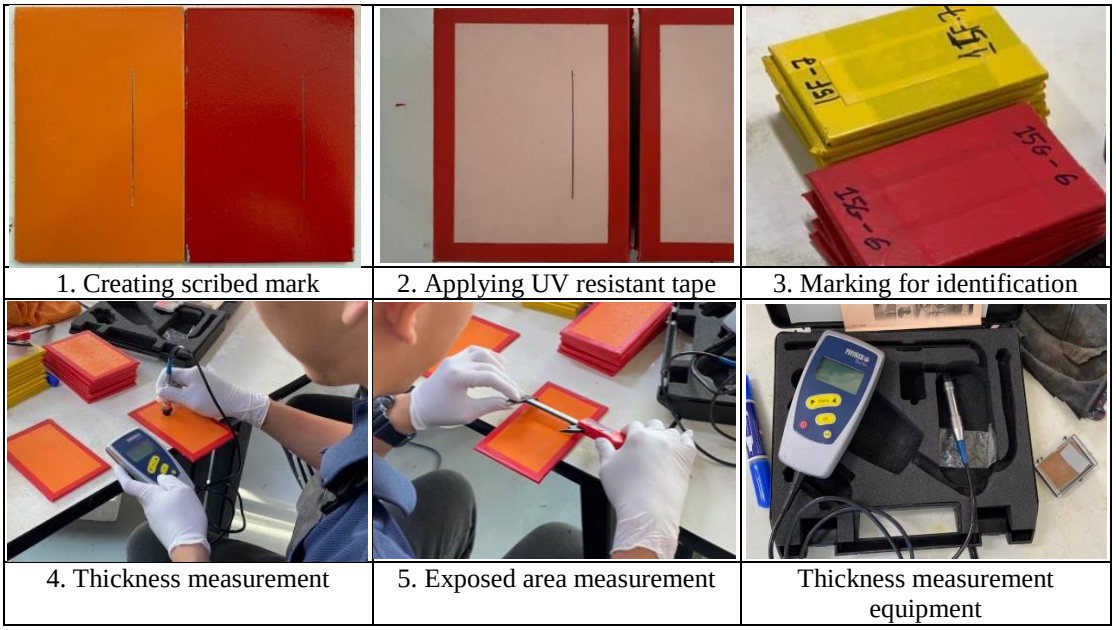

1. Creating scribed mark	2. Applying UV resistant tape	3. Marking for identification
4. Thickness measurement	5. Exposed area measurement	Thickness measurement equipment

Figure 3.3 Specimen preparation procedures for painted steel

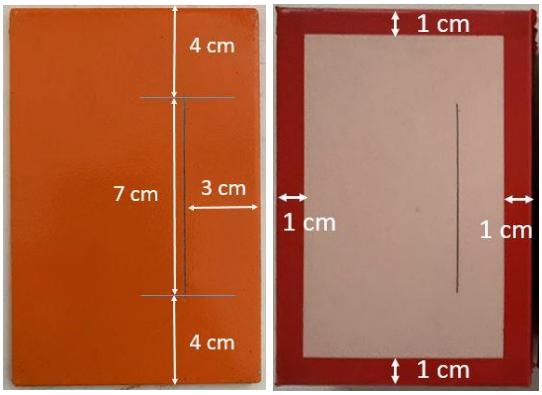

Figure 3.4 Position and dimension of scribed mark and taping

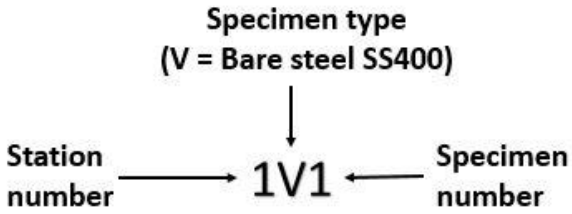

Figure 3.5 An example for a specimen identification name

3.3.3 Exposure condition

3.3.3.1 Atmospheric exposure test locations

19 locations were chosen to perform the atmospheric exposure test, as shown in Figure 3.6. Those locations were selected to have geographic and atmospheric characteristics that followed the ASTM G50 standards (ASTMG50, 2015). The names of the test locations are listed in Table 3.4. The criteria for choosing the test location are:

- Distance from shoreline.
- Natural atmospheric characteristics.
- Areas with a high corrosion tendency (industrial zone, construction growth area, pollution zone, etc).

3.3.3.2 Exposure rack and environmental station

The exposure rack was positioned at a 30° angle facing the sea, as shown in Figure 3.7. HDG steel was used for the structure of the rack and the environmental station. ASTM G50 was followed. The ISO 9225 standard (ISO9225, 2012) was followed for environmental and weather stations. Its height should be greater than one meter, as shown in Figure 3.8. Moreover, the environmental and weather station was placed not far from the specimen exposure rack.

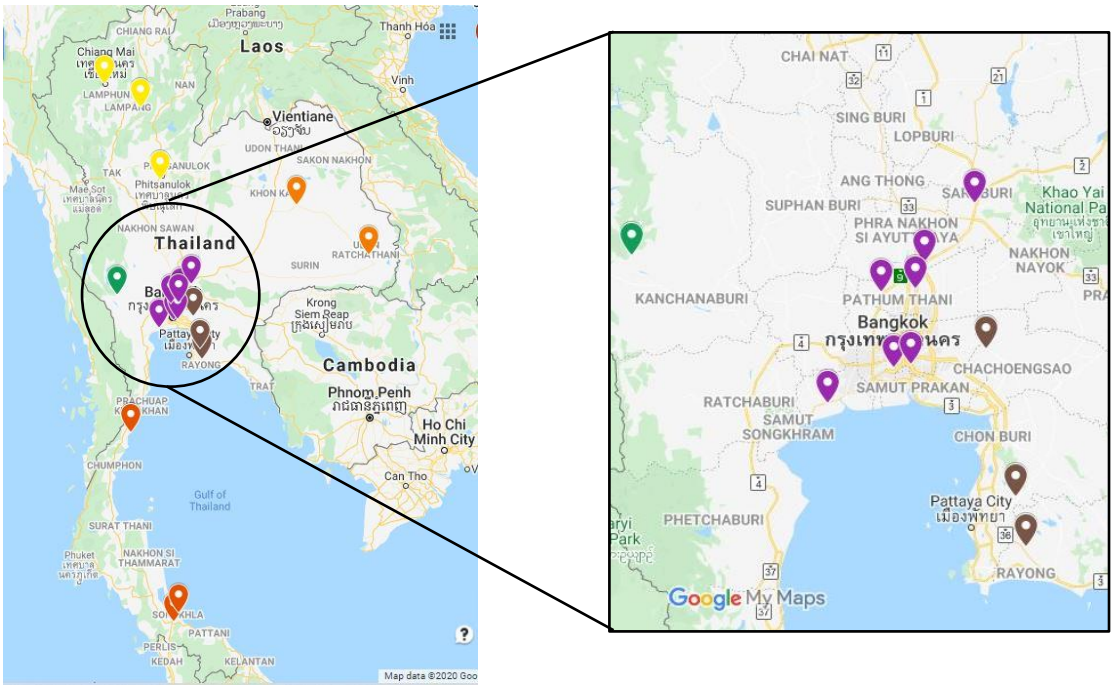

Figure 3.6 Exposure test locations

Table 3.4 Name list of test locations

N0.	Location	Category	Number of Rack	Environmental parameter station
1	Cotco-SV Eastern Steel Pipe LTD.	East	1	
2	Mae Moh power plant	North	2	
3	Faculty of Engineering Naresuan University	North	1	
4	Maha Sarakham University	North-East	2	
5	Ubon Ratchathani University Faculty of Engineering	North-East	1	
6	Private House (Saraburi province)	Center	2	Weather and pollution
7	Thai Metal Trade Company Limited (Wangnoi)	Center	1	
8	Sangcharoen Galvanizing Limited.	Center	1	
9	Sirindhorn International Institute of Technology (SIIT)	Center	2	
10	Thai Premium Pipe Company Limited	Center	2	Weather and pollution
11	Thai Metal Trade Company Limited (Bangkok)	Center	1	
12	Iron and Steel Institute of Thailand	Center	2	
13	Union Galvanizer	East	2	Weather and pollution
14	Sangchareon Eastern Galvanize Co., Ltd	East	2	Weather and pollution
15	Faculty of Engineering, Chiang Mai University	North	1	
16	Tha Thung Na Dam Power Plant	West	1	
17	Sahaviriya Steel Industries Public Company Limited	South	2	Weather and pollution
18	Sonkla nakarin University	South	2	Weather and pollution
19	Rajamangala University of Technology	South	2	Weather and pollution

Figure 3.7 Exposure rack (Saraburi province)

Figure 3.8 Environmental collector station

3.4 Collecting data

3.4.1 Specimen collecting data

For each period of exposure time (after exposure: 3 months, 6 months, and 12 months), three main category types of specimen have been divided. There are three types of steel: bare steel, HDG steel, and painted steel. All the data were recorded in accordance with ASTM G33 (ASTMG33, 2010). The specimen data collection frame work is shown in Figure 3.9.

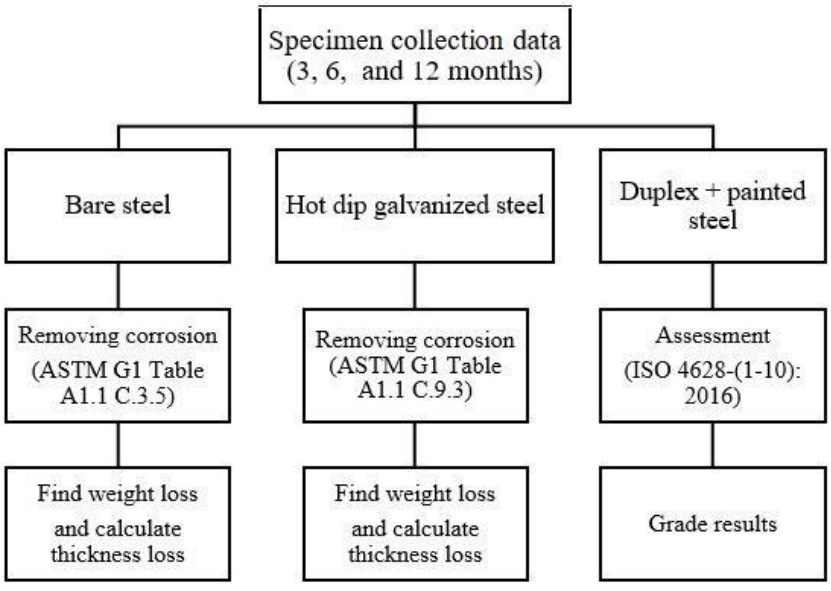

Figure 3.9 Framework of specimen collecting data

a) Method of removing rust and thickness loss calculation of bare steel

After reaching each exact period of time of atmospheric exposure (3, 6, and 12 months), two specimens of bare steel were retrieved from each site for analysis. The collected bare steel specimens were transported to the laboratory to undergo the corrosion-removing process. The corrosion-removing procedure was carried out in accordance with the ASTM G1 standard (ASTMG1, 2003), using the chemical materials listed in Table A1.1 C.3.5. The materials used for the bare steel rust removal are shown in Figure 3. 10. The rust removal procedure was carried out on two types of specimens (exposed specimen and control specimen, non-corroded specimen, for adjustment of the mass loss according to ASTM G1 standard).

The rust removal procedures for bare steel are as follows:

- Make an acid solution with 500 ml of hydrochloric acid and DI water to make 1000 ml of solution.
- Immerse the specimen in the acid solution (hydrochloric acid and DI water).
- Set the timer for 10 minutes and the temperature to 20-25°C (according to ASTM G1).
- Wait until it is complete, then use the steel pliers to catch the specimen.
- Clean with DI water and acetone.
- Dry the specimen with a hair dryer.
- Weigh the specimen and record the weight.
- Repeat several times with the same procedures until the rust is completely removed.

After completing the rust removal processes (Figure 3.11), the graph of mass loss versus the number of cleaning cycles was plotted. The mass loss due to corrosion will correspond approximately to point B (based on the ASTM G1 standard), as shown in Figure 3.12.

The control specimen (non-corroded specimen) was performed with the same procedure and the same number of cycles as the corroded specimen for adjustment of the mass loss according to the ASTM G1 standard. At last, the final mass loss of each specimen was calculated by subtracting the mass loss of the control specimen (a non-corroded specimen).

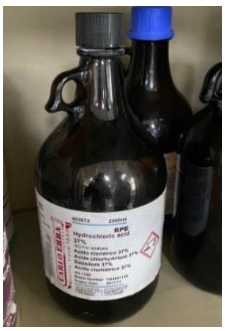
Hydrochloric acid


DI water

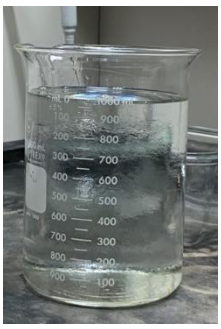
Beaker 1000 ml


Chemical protection masks

Figure 3. 10 Materials needed for removing rust of bare steel

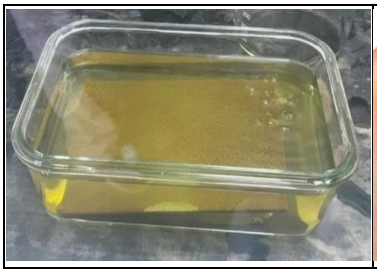		
1. Submerge the specimen into HCL acid solution	2. Set 10 mins for the submerging time	3. Clean with DI water and acetone
		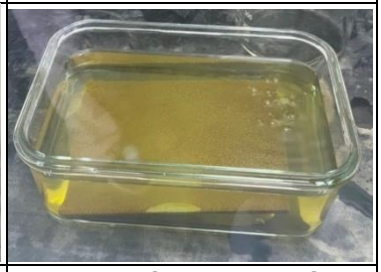
4. Dry with hair dyer	5. Weigh with digital balance	6. Repeat the same procedure until the rust is completely removed

Figure 3. 11 Rust removal procedures for bare steel

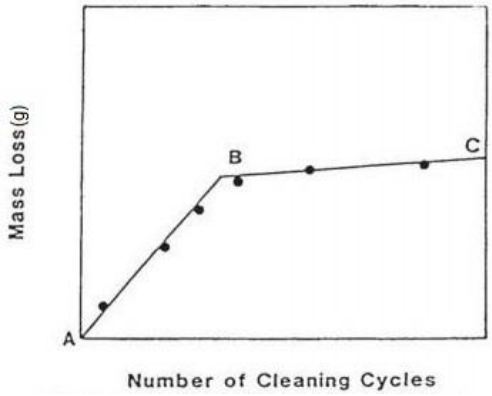

Figure 3.12 Mass loss of corroded specimen resulting from repetitive cleaning cycles (ASTMG1, 2003)

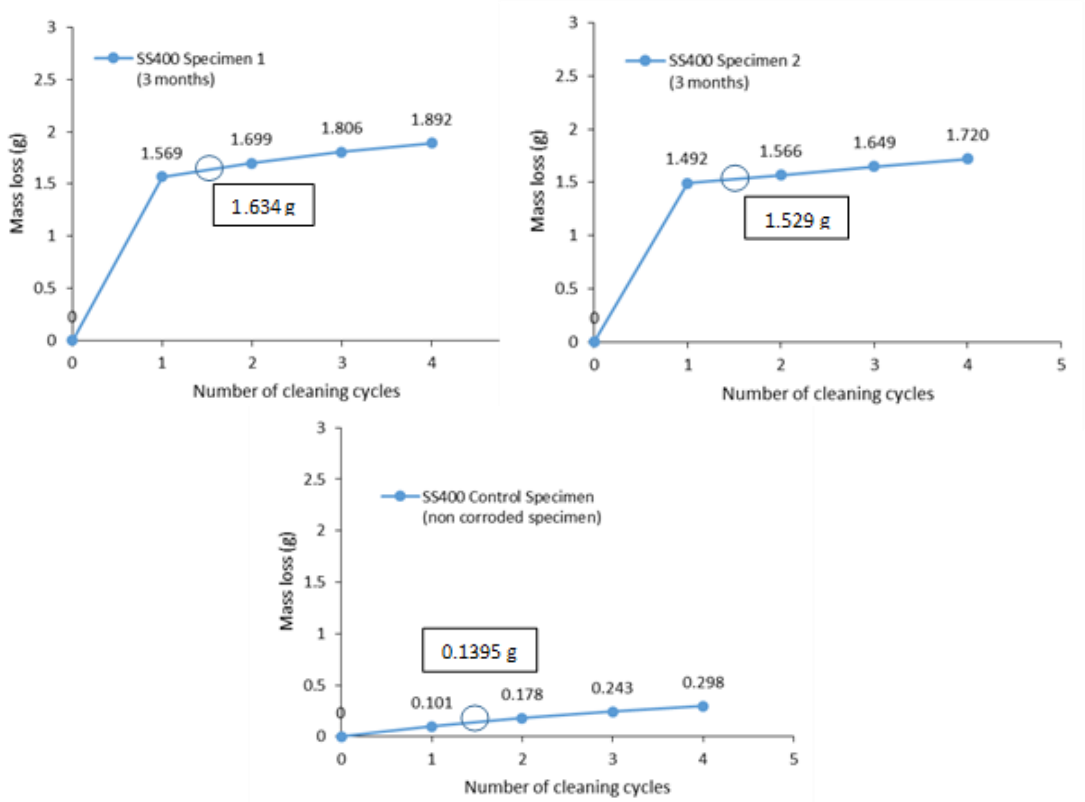

Figure 3.13 Mass loss graph of bare steel SS400 station 9 (3 months)

In Figure 3.13, the mass loss graph of bare steel SS400 station 9 (3 months) is shown as an example of the thickness loss calculation. Below is an example of the mass loss calculation procedure and the thickness loss calculation procedure:

Mass loss for a 3 month exposed specimen of bare steel at SIIT (station 9):

- Thus, the final mass loss for SS400 specimen 1 is: 1.634 – 0.1395 = 1.495 g
- Thus, the final mass loss for SS400 specimen 2 is: 1.529 – 0.1395 = 1.390 g

The area of POM plastic that is not exposed for specimen = 1275.56 mm^2

- Thus, the exposed area for SS400 specimen 1 is:

31904.7 –1275.56 = 30629.14 mm^2 = 306.291 cm^2

- Thus, the exposed area for SS400 specimen 2 is:

31359.9 –1275.56 = 30084.37 mm^2 = 300.844 cm^2

The thickness loss has been calculated by following formula below:

$$C = \frac{W}{D \times A} \times 10^4 \quad (3.1)$$

where C is thickness loss (µm), W is weight loss (g), A is the specimen exposed area (cm^2), and D is the density of steel (7.86 g/cm^3) or the density of zinc (7.13 g/cm^3) in the case of HDG specimens.

The specimen has been exposed for 91 days

- Therefore, the thickness loss for SS400 specimen 1 is:

$$\frac{1.495 \times 10^4}{306.391 \times 7.86} \times \frac{90}{91} = 6.14 \text{ micron}$$

- Therefore, the thickness loss for SS400 specimen 2 is:

$$\frac{1.390 \times 10^4}{300.844 \times 7.86} \times \frac{90}{91} = 5.81 \text{ micron}$$

Average thickness loss for both specimens:

$$\frac{(6.14+5.81)}{2} = 5.98 \text{ micron}$$

b) Method of removing rust and thickness loss calculation of HDG steel

After reaching each exact period of time (3, 6, and 12 months) of atmospheric exposure, 3 specimens of hot-dip galvanized steel were collected from each site for analysis. The collected hot dip galvanized specimens were transported to the laboratory to undergo the corrosion-removing process. The corrosion-removal processes were carried out in accordance with the ASTM G1 standard, and the chemical materials were chosen in accordance with Table A1.1 C.9.3. The materials using for the HDG steel rust removal are shown in Figure 3.14. Two types of specimens were also subjected to the rust removal procedure for HDG steel (exposed specimen and control specimen, non-corroded specimen, for adjustment of the mass loss according to ASTM G1 standard)

The rust removal procedures for HDG steel are as follows:

- Make a solution with 200 g of chromium trioxide and DI water to make a 1000 ml solution. Put the solution on the temperature plate and use a thermometer to check that the solution temperature has reached 80°C.
- Immerse the specimen into the Chromium Trioxide solution.

- Set the timer for one minute and the temperature to 80°C (as per ASTM G1).
- Wait until it is complete, then use the steel pliers to catch the specimen.
- Clean with DI water and acetone. Dry the specimen with a hair dryer.
- Weigh the specimen.
- Repeat several times with the same procedures until the rust is completely removed.

After completing the rust removal processes (Figure 3.15), the graph of mass loss versus the number of cleaning cycles was plotted. The mass loss due to corrosion will correspond approximately to point B (based on the ASTM G1 standard), as shown in Figure 3.12.

Chromium Trioxide | DI water | Beaker 1000 ml | Chemical protection mask

Figure 3.14 Materials needed for removing rust of HDG steel

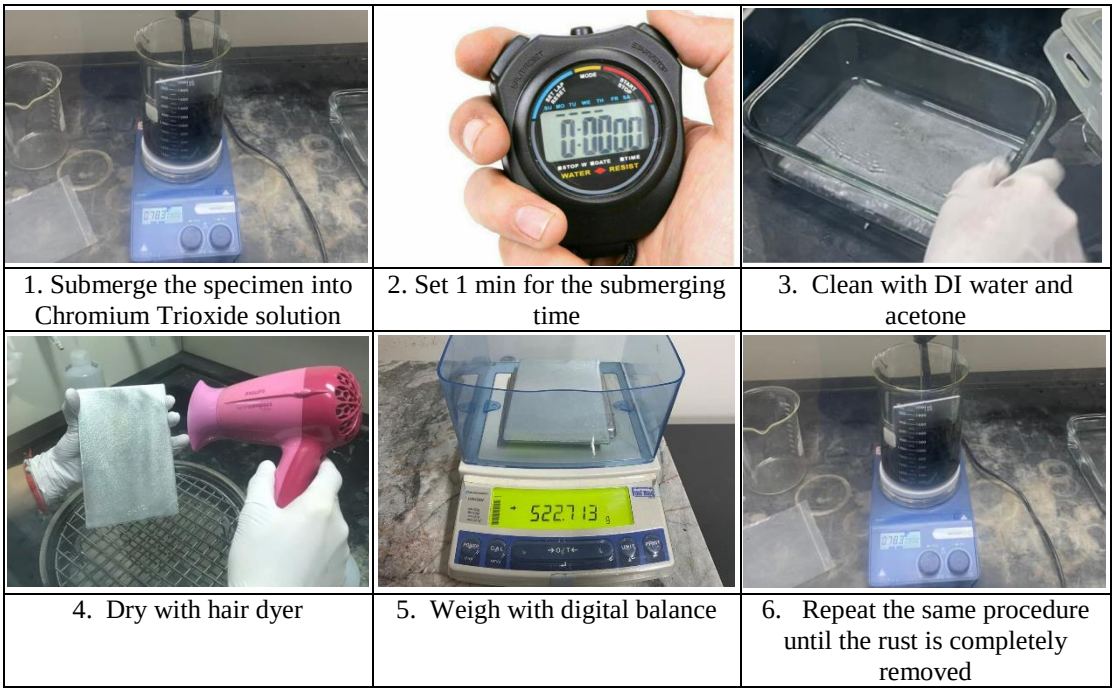

1. Submerge the specimen into Chromium Trioxide solution	2. Set 1 min for the submerging time	3. Clean with DI water and acetone
4. Dry with hair dyer	5. Weigh with digital balance	6. Repeat the same procedure until the rust is completely removed

Figure 3.15 Rust removal procedures for HDG steel

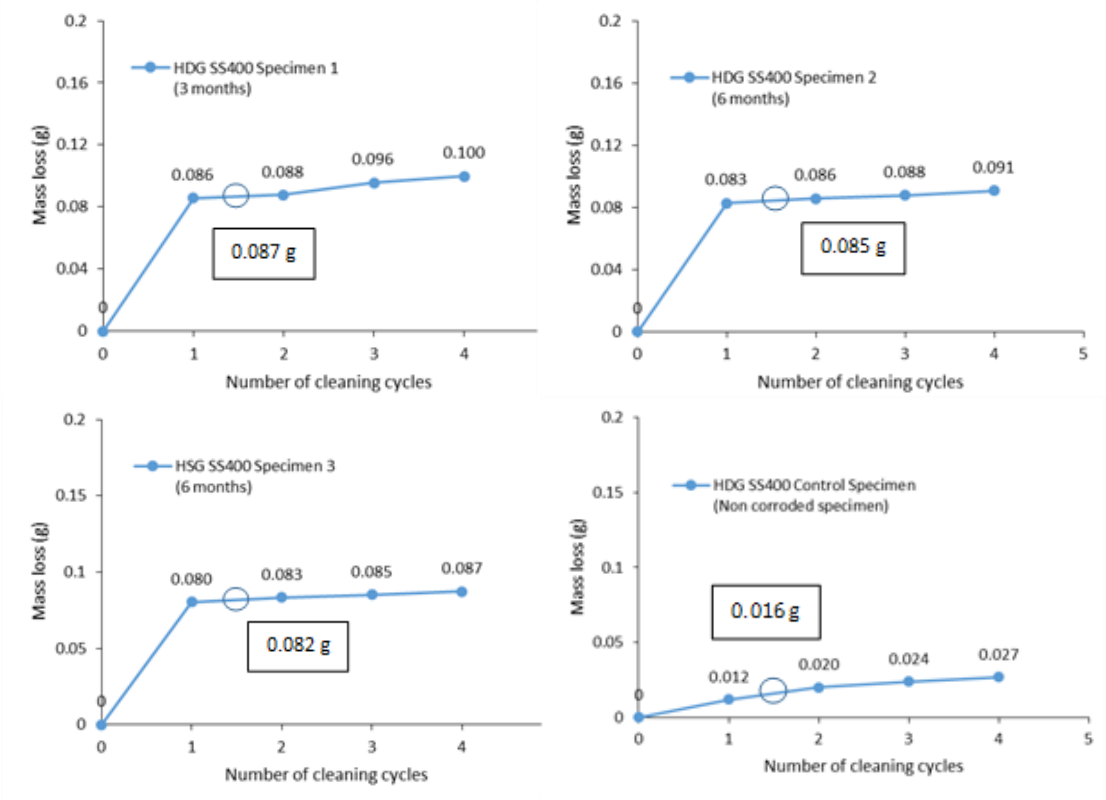

Figure 3.16 Example of mass loss graph of HDG steel SS400 station 9 (6 months)

In Figure 3.16, the mass loss graph of HDG steel SS400 station 9 (3 months) is shown as an example of the thickness loss calculation.

Mass loss for a 3-month exposed specimen of HDG steel at station 9:

- Thus, the final mass loss for SS400 specimen 1 is: 0.087 – 0.016 = 0.071 g
- Thus, the final mass loss for SS400 specimen 2 is: 0.085 – 0.016 = 0.068 g
- Thus, the final mass loss for SS400 specimen 2 is: 0.082 – 0.016 = 0.066 g

The area of POM plastic that is not exposed area for specimen = 1275.56 mm^2

- Thus, the exposed area for HDG SS400 specimen 1 is:
  32033.82 – 1275.56 = 30758.78 mm^2 = 307.5878 cm^2
- Thus, the exposed area for HDG SS400 specimen 2 is:
  32557.83 – 1275.56 = 31282.79 mm^2 = 312.8279 cm^2
- Thus, exposed area for HDG SS400 specimen 3 is:
  32277.31 – 1275.56 = 31002.27 mm^2 = 310.0227 cm^2

The specimen has been exposed for 181 days

- Therefore, the thickness loss for SS400 specimen 1 is:

$$\frac{0.071 \times 10^4}{307.5878 \times 7.13} \times \frac{180}{181} = 0.320 \text{ micron}$$

- Therefore, the thickness loss for SS400 specimen 2 is:

$$\frac{0.068 \times 10^4}{312.8279 \times 7.13} \times \frac{180}{181} = 0.304 \text{ micron}$$

- Therefore, the thickness loss for SS400 specimen 3 is:

$$\frac{0.066 \times 10^4}{310.0227 \times 7.13} \times \frac{180}{181} = 0.296 \text{ micron}$$

Average thickness loss for all three specimens =

$$\frac{0.320 + 0.304 + 0.296}{3} = 0.31 \text{ micron}$$

c) Method assessment on painted steel

The exposed painted steel specimens were retrieved at the determined period to be assessed in accordance with ISO 4628 (1–10) standards (ISO4628, 2016). In the ISO 4628 standard, it contains 9 parts, including:

- Part 1: General introduction and designation system

In part 1, there are three main categories of general guidelines. The categories are quantity of defect, size of defect, and intensity of changes. The general guideline and rating are illustrated in Table 3.5.

Table 3.5 General guideline and rating

Rating	Quantity of defect	Size of defect	Intensity of change
0	No	Not detectable	Unchanged
1	Very few	Only visible	Very slight
2	Few	Just visible	Slightly change
3	Moderate	Clearly visible	Moderate
4	Considerable	Bigger than 0.5 mm up to 5 mm	Considerable
5	Dense defects	Larger than 5 mm	Marked change

- Part 2: Assessment of degree of blistering

Blistering is one of the corrosion modes of painted steel that could cause the paint to fail. In Figure 3.17, scanning electron microscope (SEM) images of blisters with corrosion products from Saarimaa's study (2022) (Saarimaa, Virtanen, Laihinen, Laurila, & Väisänen, 2022) clearly show the failure of the painted steel due to blistering. The quantity and size of the blisters are used to determine the level of blistering. Q and S represent the quantity and size of blisters, respectively, for expressing results. The quantity and size were rated on a scale of 0 to 5, with "0" representing no blistering and "5" representing maximum blistering. The assessment was carried out by comparing it to a pictorial standard in accordance with ISO 4628 standards. Figure 3.18 shows an

example of a pictorial standard to use for the assessment. The results were given in short form, for example “Q2S2,” which represents quality 2 and size 2.

- Part 3: Assessment of degree of rusting

The degree of rusting is determined by referring to the percentage of the rusted area on the exposed surface of the specimens. The assessment results show in term of Ri 0 – 5. Figure 3.19 shows the pictorial standards for the assessment of rusting.

- Part 4: Assessment of degree of cracking

Paint will bubble when moisture, heat, or both are present. Bubbles are one of the causes of paint that is peeling or breaking. Paint has the ability to entirely fracture after it bubbles. The degree of cracking is rated based on the pictorial standards indicated in ISO 4628-4. Figure 3.20 shows the pictorial standards for the assessment of cracking.

- Part 5: Assessment of degree of flaking

  Paint that has been exposed to excessive humidity may peel easily. Humidity can weaken the adhesion of the paint and eventually cause it to start flaking off. Figure 3.21 shows the pictorial standards for the assessment of flaking.

- Part 6 & 7: Assessment of degree of chalking

Ultraviolet (UV) radiation from sunshine damages the paint coating and causes chalking. The exposed pigment particles will eventually become less tightly attached to the surface due to UV-induced breakdown of the resin or binder in the paint film. This leaves a surface that is powdery. The tape is used in part 6 to check the chalking. In contrast, the cloth is used for inspecting the chalking in part 7. Although the material is different, both use the same checking process. Figure 3.22 shows the pictorial standards for the assessment of chalking.

- Part 8: Assessment of degree of delamination and corrosion around a scribe or other artificial defect

Eight points along the scribed mark were measured to determine or calculate the mean overall width of delamination or corrosion. Thereafter, the effective width of delamination was calculated by taking the mean overall width of corrosion and subtracting it from the original scribed width. At last, the final delamination or corrosion is the equivalent of half the effective width of delamination. The delamination

at the scribed mark and pictorial standards for assessment of delamination (ISO 4628-8) is shown in Figure 3.23.

- Part 10: Assessment of degree of filiform corrosion

A type of corrosion known as "filiform corrosion" resembles tiny worms or filaments spreading beneath the coating. When moisture seeps through the coating of a painted surface, this form of corrosion occurs. The procedures for measuring the filiform and reporting the results are outlined below:

- When the filiform is in a regular form, as shown in Figure 3.24 (a)
    1. Measure the maximum distances L_l and L_r, in millimeters.
    2. Measure the distances M_l and M_r, in millimeters.
- When the filiform is in an irregular form, as shown in Figure 3.24 (b)
    1. Measure L
    2. Measure M_{l1}, M_{r1}, M_{l2}, M_{r2}, etc.,
    3. Calculate the overall values of M_l and M_r

$$M_{l=}\frac{x_1M_{l1}+x_2M_{l2}+\cdots+x_nM_{ln}}{z} \tag{3.2}$$

$$M_{r=}\frac{x_1M_{r1}+x_2M_{r2}+\cdots+x_nM_{rn}}{z} \tag{3.3}$$

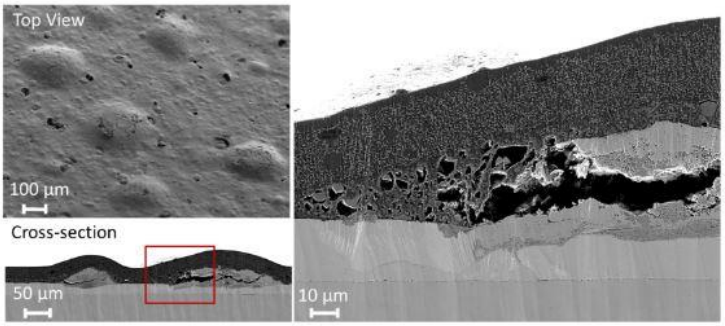

Figure 3.17 SEM images of blisters with corrosion product (Saarimaa et al., 2022)

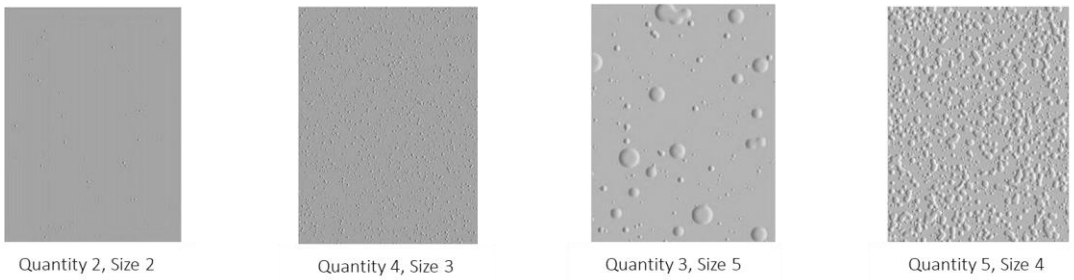

Figure 3.18 Example of pictorial standards of blistering assessment (ISO 4628-2)

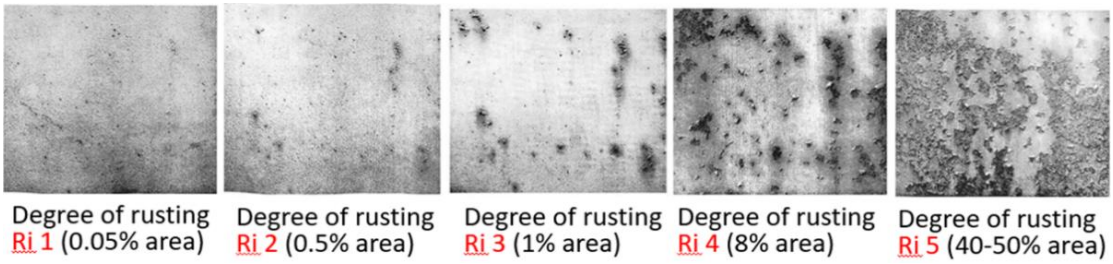

Figure 3.19 Pictorial standards of degree of rusting (ISO 4628-3)

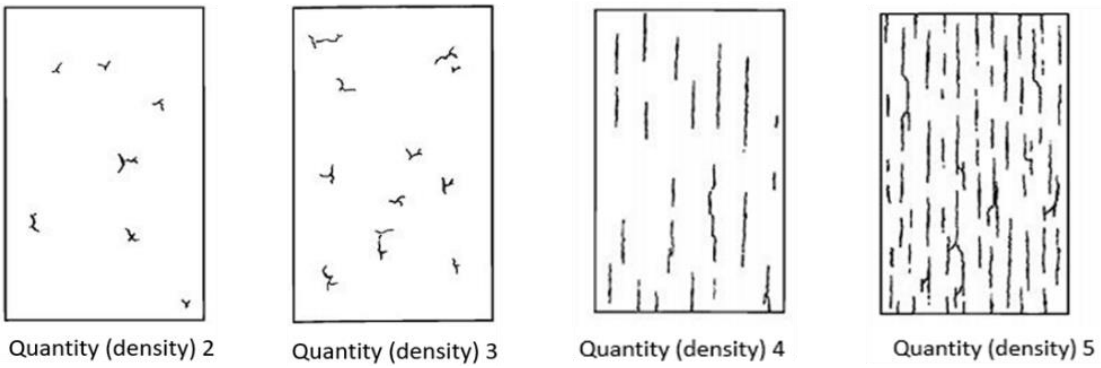

Figure 3.20 Pictorial standards of degree of cracking (ISO 4628-4)

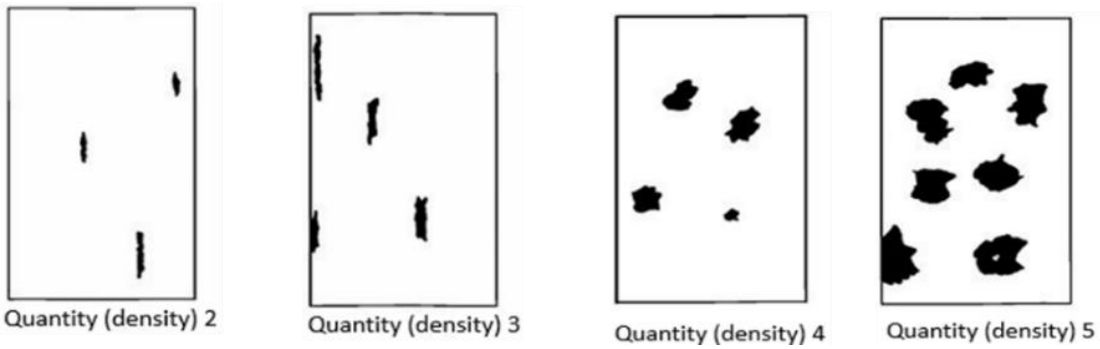

Figure 3.21 Pictorial standards of degree of flaking (ISO 4628-5)

Figure 3.22 Chalking pictorial standards (ISO 4628-6&7)

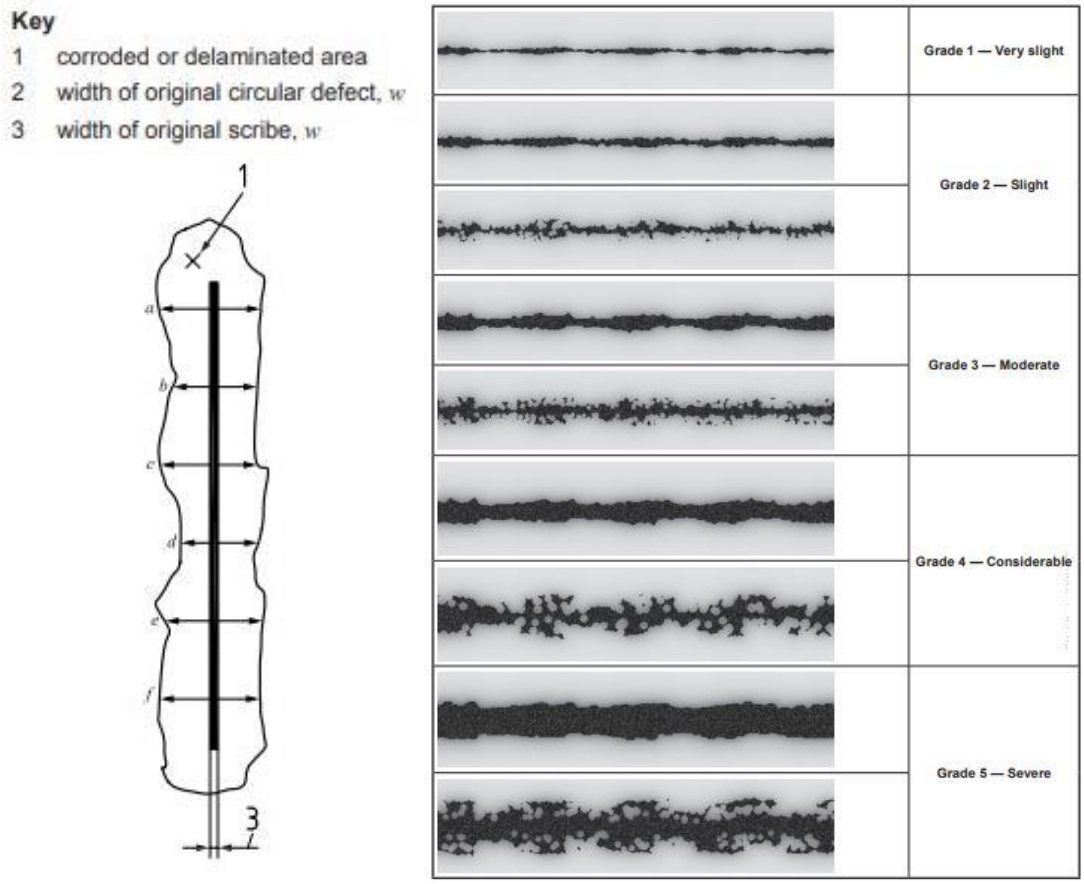

Figure 3.23 Delamination at the scribed mark and pictorial standards for assessment of delamination (ISO 4628-8)

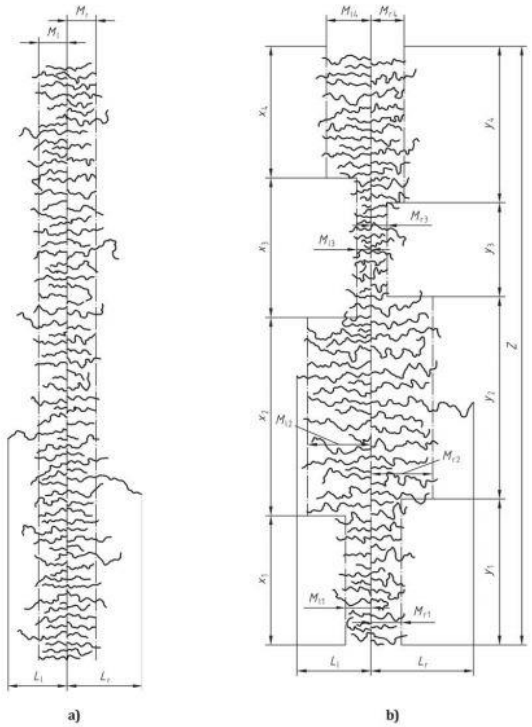

Figure 3.24 Filiform corrosion at scribed mark (ISO 4628-10)

3.4.2 Environmental parameters collecting data

The following atmospheric parameters were collected: temperature, relative humidity, and rainfall. Those parameters were collected by the atmospheric collecting equipment as shown in Figure 3.25. The duration of each capture was set to 5 minutes. However, the data must have a monthly average value. According to ISO 9225 (ISO9225, 2012), environmental pollutants, SO_2 and chloride, were collected.

- **SO_2**

The following are the conditions for placing a lead cylinder for collecting SO_2 at the exposure site:

- exposed vertically in a shelter
- place near the exposure test rack
- Keep it away from rain and sunshine, and keep it at a well-ventilated location

The data was collected on a monthly basis, and the methodology followed ISO 9225-2012. Preparing lead cylinder procedures:

- Measure 95 ml of DI water, 5 ml of ethanol, and 1 g of gum tragacanth by putting them in separate chemical containers.
- Mix 1 g of gum tragacanth and 5 ml of ethanol in the chemical mixing bottle.
- Put 95 ml of DI water and mix them together in the same chemical mixing bottle.
- Measure 5 ml out of the mixed gum tragacanth solution by putting it in a beaker
- Measure 5 g of lead (IV) oxide and put in the beaker which contained 5 ml of gum tragacanth solution
- Mix that solution with a painting brush
- Put the mixed lead dioxide solution on the gauze and paint it until it is empty on the desired exposure area
- Keep it dry for 24 hours, and finally, that lead cylinder (Figure 3.26) can be used to expose it to the atmosphere on the test site in order to collect SO_2. Figure 3.27 shows photos of the activities of lead cylinder preparation.

After exposure for a determined period, the lead cylinders were retrieved to do the analysis. Sulfate amount was analyzed by the sulfate reader machine with the model

HANNA-HI96751 Sulfate ISM, and then that data was able to be calculated to SO_2 deposition rate.

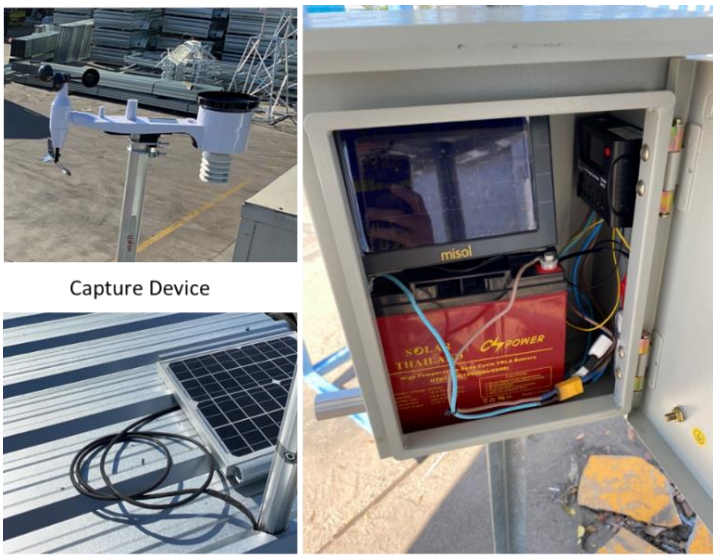

Figure 3.25 Atmospheric parameter collecting equipment

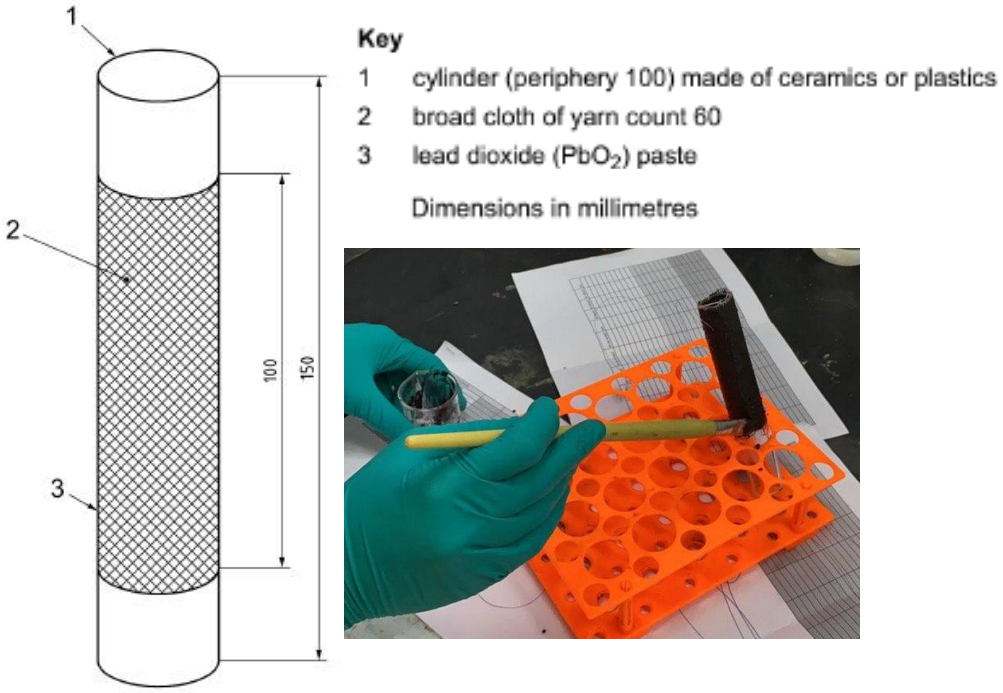

Figure 3.26 Lead dioxide cylinder (ISO 9225-2012)

		
1. Mix 1 g of Gum Tragacanth and 5 ml of ethanol	2. Then put 95 ml of DI water and mix together	3. Measure 5 g of lead (IV) oxide
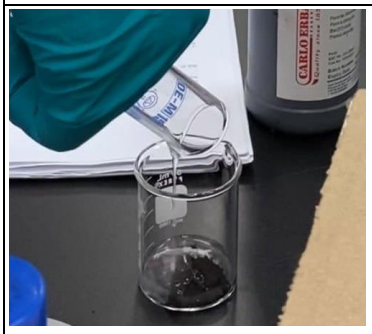	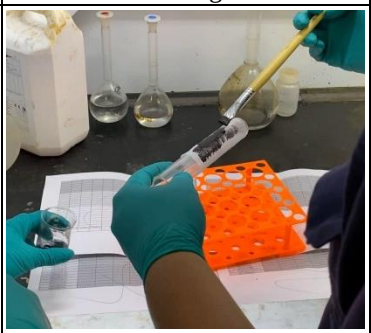	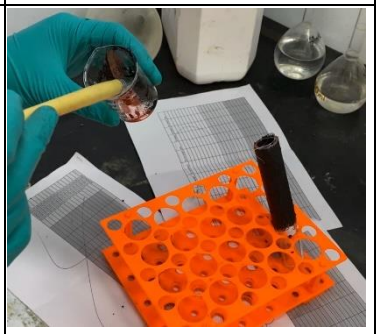
4. Mix 5 ml of Gum Tragacanth solution and 5 g of lead (IV) oxide	5. Put the mix lead dioxide solution on the gauze	6. Paint the solution until empty and keep it 24 hours prior exposure

Figure 3.27 Lead cylinder preparation procedures

- **Airborne chloride**

Airborne chloride has been collected by two methods, such as the wet candle method and the dry gauze method. The methodology for collecting airborne chloride was according to the ISO 9225-2012 standard, as shown in Figure 3.28.

The conditions for placing dry gauze at the exposure site are:

- exposed vertically in a shelter
- keep close to the exposure test rack
- keep it away from rain and direct sunlight, and keep it in a well-ventilated location
- the distance between the grounds to the bottle must be at least 1 m.
- fixed firmly so that is not swung by the wing.

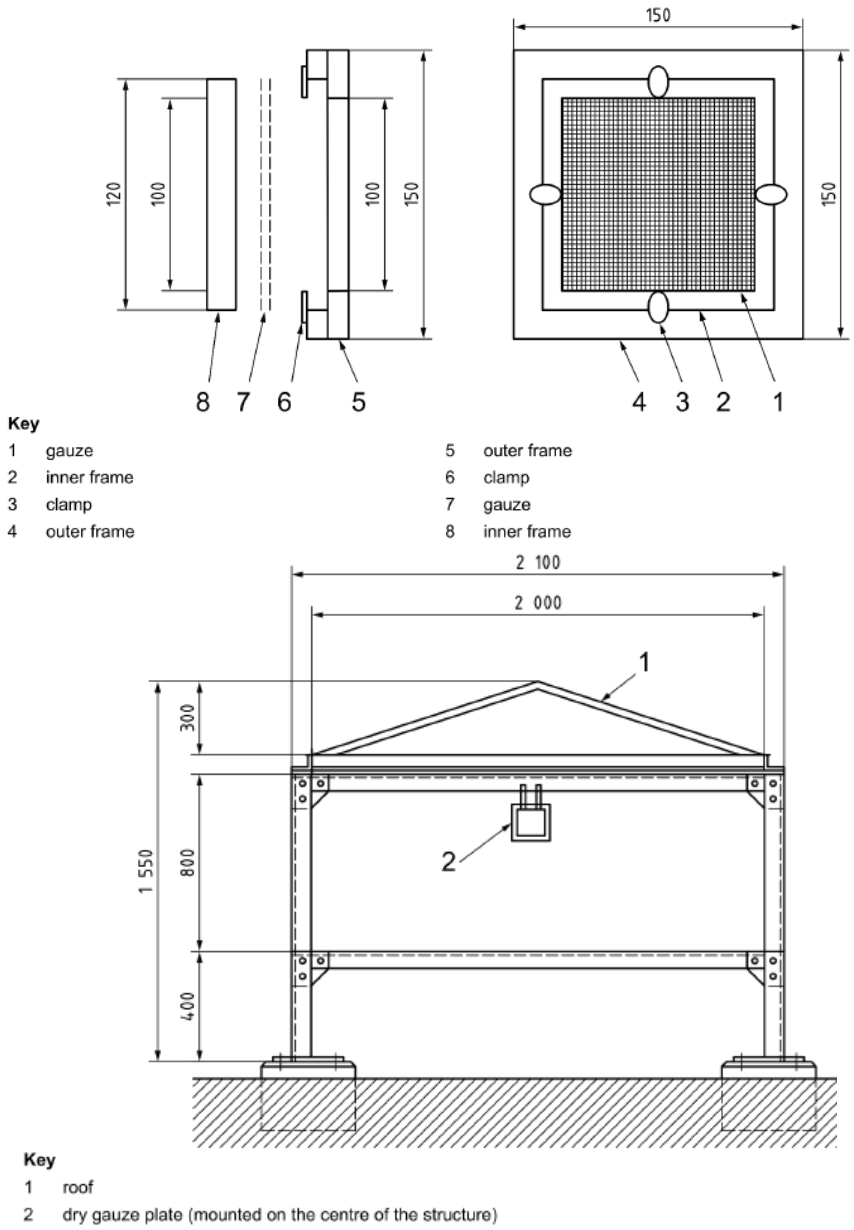

Figure 3.28 Collecting chloride by dry gauze method (ISO 9225-2012)

3.5 Analyzing data

3.5.1 Corrosion equation

Since the corrosion of steel is correlated with the condition of the surrounding atmosphere, the relationship between the atmospheric parameters and environmental pollutants should be studied. Multiple variable linear regression analysis was performed in order to find the value of the coefficient in front of the parameters. The central, north, northeastern, and west regions are represented by equation 3.4 since those regions are

far from the sea and the chloride can be neglected. For the central region, 6 test locations (station 6, 7, 8, 9, 11, and 12) were used to perform multilinear regression. Five test locations (station 3, 4, 5, 15, and 16) were used to perform multilinear regression for the north, northeastern, and west.

$$C = \alpha \times T\ (℃) + \beta \times RF\ (m) + \gamma \times RH\ (\%) + \delta \times SO_2(\mu g/m^3) + \varepsilon \times T_{exp}(month) \quad (3.4)$$

where T : average temperature during exposure ($^{\circ}$C)

RF: cumulative rainfall during exposure (m)

RH: average relative humidity during exposure (percentage)

SO_2: cumulative sulfur dioxide during exposure (μg/m^3)

T_{exp}: Time of exposure (month)

α, β, γ, δ, and ε are constants

The east and south regions are close to the shoreline and are affected by chloride, which is one of the main causes of steel corrosion. Therefore, those regions are represented by equation 3.5, which includes chloride and the distance of those locations to the sea.

$$C = \alpha \times T\ (℃) + \beta \times RF\ (m) + \gamma \times RH\ (\%) + \delta \times SO_2(\mu g/m^3) + \mu \times Cl^{-}(\mu g/m^2) + \theta \times T_{exp}(month) + \varepsilon \times \exp\big(\gamma D(km)\big) \quad (3.5)$$

where T : average temperature during exposure (^{0}C)

RF: cumulative rainfall during exposure (m)

RH: average relative humidity during exposure (percentage)

SO_2: cumulative sulfur dioxide concentration rate during exposure (μg/m^3)

Cl^{-}: cumulative chloride deposition rate during exposure (μg/m^2)

T_{exp}: Time of exposure (month)

D: Distance of the location to the sea (km)

α, β, γ, δ, μ, θ, ε, and γ are constants

In order to have chloride data at the meteorological department locations and the test locations that do not have chloride data, chloride equations have to be created.

Since the chloride deposition rate at one location depends on the distance to the sea, as was observed and also recommended by many researchers, the chloride equation as a function of the distance to the sea should be created as shown in equation 3.6. Six locations from CONTEC (Construction and Maintenance Technology Research Center) (CONTEC, 2023), twelve locations from MTEC (the National Metal & Materials Technology Center) (MTEC, 2023), and four locations from the test locations were chosen to create the chloride equation. Table 3.6 shows chloride test locations.

Table 3.6 Chloride test locations

Station	Station	Category	Province	Distance to the sea (km)	mg/(m2.d)
T1	Union Galvanizer Company	East	Chachoengsao	36	0.89
T2	Sangchareon Eastern Galvanized	East	Chon Buri	18.5	5.82
T3	Prince of Sonkla University	South	Songkla	22	3.55
T4	Rajamangala University of Technology	South	Songkla	0.3	6.40
CON1	Wat Komut Rattanaram	East	Chon Buri	0.008	30
CON2	Si Ratcha	East	Chon Buri	0.011	38
CON3	South Pattaya Beach	East	Pattaya	0.015	60
CON4	Map Ta Phut	East	Rayong	0.000	320
CON5	Khung Kraben Bay	East	Chanthaburi	0.037	192
CON6	Laem Sok	East	Trat	0.008	49
M1	P0	South	Phangnga	0.15	40
M2	P1	South	Phangnga	0.4	2.5
M3	P2	South	Phangnga	0.5	1
M4	P3	South	Phangnga	1	1.2
M5	P4	South	Phangnga	2	2.8
M6	P5	South	Phangnga	4	2
M7	S0	South	Songkla	0.02	200
M8	S1	South	Songkla	0.5	3.5
M9	S2	South	Songkla	0.9	2
M10	S3	South	Songkla	2.3	4
M11	S4	South	Songkla	3.5	2.8
M12	S5	South	Songkla	4.9	4

Note: T1, T2,..., T4: are test locations; CON1, CON2,..., CON6: are test locations from CONTEC, M1, M2,..., M12: are test locations from MTEC.

The chloride deposition rate equation:

$$y = me^{nx} \tag{3.6}$$

where y is chloride deposition rate ($\mu g/m^2$)

x is the distance to the sea (km)

m and n are constants.

For the east chlordie equation, 2 test locations and 6 locations from CONTEC were taken to find the representing curve equation. Two test locations and twelve MTEC locations were chosen for the south to determine the representing curve equation and the representing relationship of the chloride deposition rate. For the south, two conditions were established: locations that are less than 0.5 km from the sea and locations that are more than 0.5 km from the sea. For the location that is less than 0.5 km from the sea, the chloride equation was established. For the locations that are more than 0.5 km from the sea, the average deposition rate value was used.

3.5.2 Corrosion map

The corrosion map is useful because it shows the thickness loss value at each location. A map of steel's atmospheric corrosion was generated successfully by many researchers (Ivaskova, Kotes, & Brodnan, 2015; Santa et al., 2022; Sica, Kenny, Portella, & Filho, 2007). Nineteen test locations and 72 locations from TMD were taken to create the corrosion heat map for bare steel and HDG steel. Two main portions of the map were divided in order to create the whole country map as shown in Figure 3.29. The 44 locations belong to the TMD, and 11 locations from exposure tests were taken to create the central and northern portions of the map. The 28 locations belong to TMD, and 7 locations from exposure tests were taken to create the eastern and southern portions of the map. After obtaining the equations, atmospheric parameter data and environmental pollutant data were substituted back into the corrosion equations, which were provided by the TMD (TMD, 2022) and the Thailand Pollution Control Department (PCD, 2022), respectively. QGIS software (QGIS, 2022) were used in order to create the corrosion heat map. All locations were inserted on the map in QGIS

software. Thereafter, interpolation with the inverse distance weight method (IDW) was used to create the heat map.

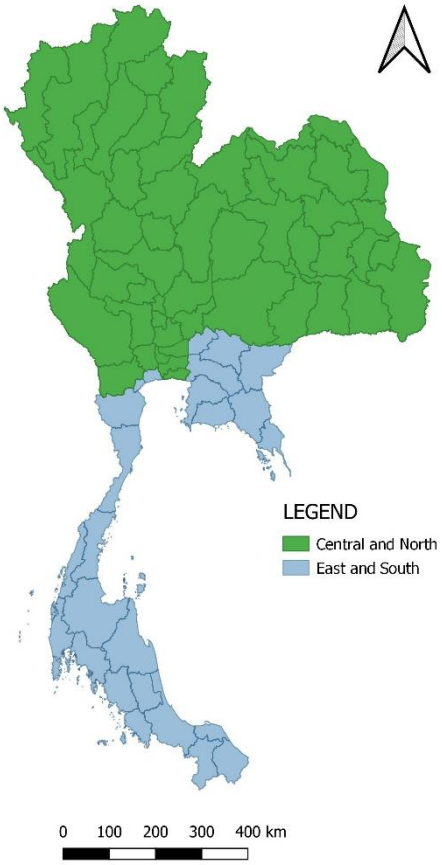

Figure 3.29 Portion map for creating a corrosion heat map

3.5.3 Thickness loss projection

3.5.3.1 Thickness loss projection for bare steel

Plotting thickness loss versus exposure time was done when the exposure test data were obtained. A power law function link between the findings at each exposure interval was seen in the case of bare steel. As a result, the atmospheric corrosion equation with the change in the bare steel's exposure duration can be written as follows:

$$D = At^n \tag{3.7}$$

where t is the exposure duration (year), D is the thickness loss (μm), and A and n are constants obtained from the fitting curve.

After applying a logarithmic function to both sides of equation (3.7), the equation became

$$\log D = n\log t + \log A \tag{3.8}$$

The log-log of thickness loss with time can be plotted to obtain the constants *A* and *n* in equation (3.7). The log-log plot's curve was fitted using the linear function fitting curve to obtain the line slope, which is equal to *n*. The fitting equation's intercept, log*A*, allows for the calculation of *A*. An example of how to find *A* and *n* is performed with Station 9 (SIIT). The log-log curve and its corresponding linear equation for SS400 and SM490A, respectively, are displayed in Figure 3.30.

(a) (b)

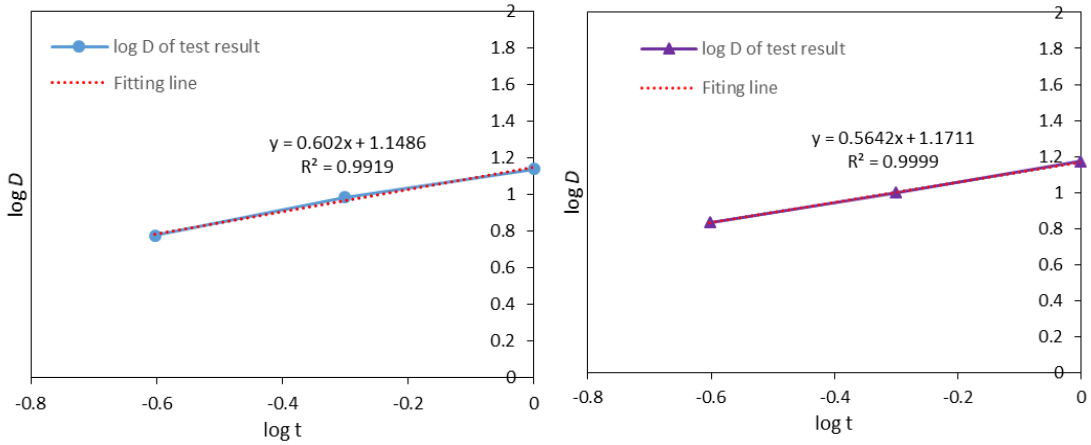

Figure 3.30 Log of thickness loss for bare steel versus log of exposure time for station 9 (SIIT): (a) SS400, (b) SM490A

Numerous data from field exposure corrosion test studies indicate that there are two distinct stages to the real atmospheric corrosion process. The corrosion reaction starts at the first stage, which is also known as the initial stage. The quantity of corrosion grows linearly with time. The coefficient *n* from a power function can be used to explain the relationship between corrosion loss and exposure duration in the second stage, which is known as the steady state. Consequently, the following bi-linear model form based on ISO 9224 (ISO9224, 2012) can be used to describe the corrosion process:

$$D = \begin{cases} D_1 t & , t \leq 10 \\ D_1 t + \alpha(t - 10) & , t > 10 \end{cases} \tag{3.9}$$

where *D* is the thickness loss (μm) at *t* years. *t* is exposure years. D_1 stands for the first year thickness loss getting from exposure test (μm/year). After ten years, at the steady stage, corrosion loss rises at the average rate α. The values of α for carbon steel can be calculated from expression below:

$$\alpha = A \cdot n \cdot t^{n-1} \tag{3.10}$$

where *A* and *n* are constants from equation (3.7) obtained from curve fitting.

3.5.3.2 Thickness loss projection for HDG steel

Numerous studies as well as the ASTM G16 standard (ASTMG16, 2013) suggest HDG steel corrosion behavior with a mathematical function. The relationship between the thickness loss magnitudes versus time was considered to be a linear function. The observation of partial white powder rust on the specimen's surfaces following the exposure test is another factor supporting the use of linear behavior. In contrast to bare steel that was completely covered in rust, HDG steel had some rust on it on some surfaces where it was unable to function as a barrier to slow down the rate of deterioration. It means HDG steel specimens could rust at the same rate during exposure time. When compared to bare steel, the thickness loss magnitude of HDG steel was found to be substantially less. It was probably going to corrode more as exposure time increased. Thus, a linear relationship was established as follows:

$$D = kt \tag{3.11}$$

where D is the thickness loss (μm) at t years. t is exposure years. k is a constant from the fitting curve.

An example of how to find k is performed with Station 9 (SIIT). The curve and its corresponding linear equation for SS400 and SM490A, respectively, are displayed in Figure 3.31.

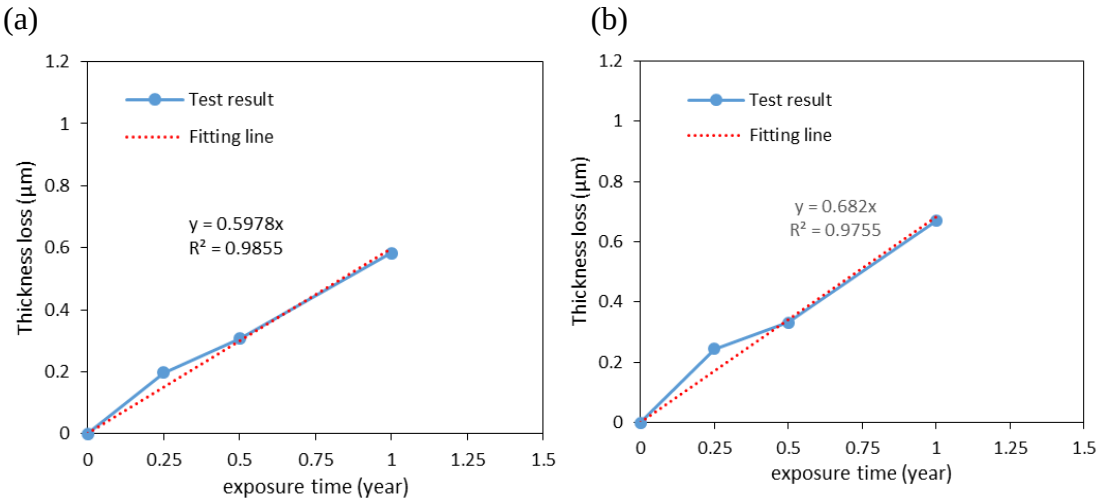

Figure 3.31 Thickness loss of HDG steel versus exposure time with a linear function fitting curve (Station 9: SIIT): (a) SS400, (b) SM490A.

3.6 Summary

Atmospheric exposure test chapter shows the systematic process of data collection, analysis, and interpretation. The methods guarantee the validity and reliability of the research findings and act as a guide for carrying out the study. The following is the summary of this chapter:

- Material characterization and atmospheric exposure test: Two grades of steel (SS400 and SM490A) with six different types of coating were selected to perform the test. The exposure periods are 3, 6, and 12 months. Specimens were prepared following ASTM G1 and ASTM G31 standards. Nineteen locations were chosen following ASTM G50 as the test location. The exposure test conformed to the ASTM G50 standard.
- Corrosion measurement techniques: Rust on exposed specimens was removed by a chemical method for bare and HDG steel. Thickness loss was calculated at the determined period for bare and HDG steel. Both methods (rust removal and thickness loss calculation) conformed to ASTM G1 standards. For exposed painted steel, the specimens were taken for assessment based on ISO 4628 (1–10) standards.
- Environmental factor: Temperature, Rainfall, Relative Humidity, SO_2, and Chloride were collected during the exposure period.
- Data analysis: Corrosion equation was created using multivariable linear regression. Corrosion map was created using IDW method and QGIS software. Bi-linear model form based on ISO 9224 was used to perform the thickness loss projection for bare steel. Linear relationship and linear fitting curve of thickness loss vs exposure time were used to perform the thickness loss projection for HDG steel.

CHAPTER 4
THICKNESS LOSS AND ASSESSMENT

4.1 Introduction

The results of the atmospheric test are shown in this chapter. The results include atmospheric parameters and environmental pollutants at test locations, thickness loss of bare steel, thickness loss of HDG steel, appearance of both types of steel (bare and HDG steel), assessment results of painted steel, and microscopic pictures of painted steel. The climate and geographic features of Thailand will also come up for discussion. The discussion of the thickness loss and assessment will be made in this chapter.

4.2 The geography and climate of Thailand

Thailand is located between latitudes of 5.4˚N and 20.3˚N and longitudes of 97.7˚E and 105.45˚E. The total area is 513,115 square kilometers or around 200,000 square miles. Thailand's borders with its neighboring countries are as follows: the north has borders with Myanmar and Laos; the east has borders with Laos, Cambodia, and the Gulf of Thailand; the south has border with Malaysia; and the west has borders with Myanmar and the Andaman Sea.

Thailand can be split into 6 regions, namely the Northern, Northeastern, Western, Central, Eastern, and Southern regions, in accordance with the climatic patterns and meteorological circumstances. Each region's topography differs greatly in the ways listed below.

- Northern region: The majority of the region is mountainous and hilly, and several significant rivers originate there. Doi Inthanon in Chiang Mai is the highest mountain, rising to a height of approximately 2,595 meters above mean sea level. Known as the central highlands, these mountains run along the northeastern portion's eastern border. A central valley can be found in the southern portion of the region.
- Northeastern region: The northeast plateau is a naturally high plain in this area. The northeastern portion is divided into two basins by the northwest-southeast oriented Phu Phan ridge. One is a significant high level plain in the west. Another one is smaller and slopes eastward.

- West region: The western region's geography is characterized by tall mountains and narrow river valleys. Most of Thailand's less-developed forest areas are found in the west of the country. Minerals and water are significant natural resources. Many of the country's largest dams are located in this area, and mining is a significant sector. The physical landscape of the area is prominently reflected in the names of many villages in western Thailand.
- Central region: This region is a sizable low-lying plain where the Chao Phraya River, which originates in the Northern region, joins the Ping, Wang, Yom, and Nan Rivers.
- Eastern region: The Gulf of Thailand touches directly the south and southwest of this region.
- Southern region: The topography of this region is surrounded by the Andaman Sea on the western side and the South China Sea on the eastern side.

Overall, Thailand has a wide variety of geography, including mountains, plains, islands, and coasts. It consists of inland and shorelines.

The Southeast Asia region is impacted by large-scale climate fluctuation due to the Asian monsoon, one of the most prominent elements of the global climate system. The term "monsoon" describes the seasonal winds and precipitation. Thailand is a tropical country that is influenced by monsoon winds and experiences hot and humid characteristics of the atmosphere. Hot and humid climates make steel corrode easily and quickly. The major factor sustaining the Asian summer monsoon cycle is the disparity in heat capacity between land and sea. The climate in Thailand differs geographically as well. Compared to the center and southern regions, the northern and northeastern regions often have cooler temperatures. Due to their orientation and proximity to the seas, the southern region, in particular the coasts of the Andaman Sea and the Gulf of Thailand, can see slightly varied rainfall pattern.

The climate of Thailand can be classified into two seasons, rainy and dry season, based on meteorological data. Rainy season starts from May to October and dry season starts from October to April. During March to May, it is the hottest period of the year, and the maximum temperatures are around 40°C except along coastal areas where the sea will help moderate the temperature. From mid of May, the rainy season also

drastically lowers temperatures, which are typically below 40°C. During December and January, cold air from China lower the temperature, especially in the Northern and Northeastern regions. Due to this region's marine characteristics, temperatures in the Southern region are typically mild throughout the year. Rarely do the high temperatures typical of upper Thailand occur. Temperature changes throughout the day and throughout the seasons are much fewer than they are in upper Thailand.

From mid of May through early October, the monsoon leads to have rainfall. When the rainfall peaks, usually in August or September, some places may flood. Unlike higher Thailand, the southern region of Thailand has a different rainy season. Both the northeast and southwest monsoons bring about a lot of rain. The Southern Thailand West Coast experiences heavy rainfall during the southwest monsoon, which peaks in September. On the other hand, the Southern Thailand East Coast has heavy rainfall from November through January of the following year, which marks the start of the northeast monsoon.

4.3 Atmospheric parameters and pollutants at test locations

At 19 test locations, atmospheric variables and pollutant data were gathered and measured. For stations without the capture equipment to collect atmospheric data, they were also gathered via the Thai Meteorological Department's website. The monthly averages for temperature, precipitation, and relative humidity are displayed in Figure 4.1 to 4.3, respectively.

Figure 4.1 (a) shows that the central region (Stations 6, 7, 8, 9, 11, and 12) had the country's highest temperatures. Thailand's central area, which is home to cities like Bangkok, Pathum Thani, and Ayutthaya, has a tropical climate with high temperatures. These cities are in urban and metropolitan areas. The central Thailand region's scorching heat is to blame for these conditions. The temperature graph reveals a tendency that starts to decline from November to December and then starts to rise in February. In the central region, the hot season normally starts in February and lasts until May. During this time, temperatures can rise above 35°C during the daytime. In the central region, the rainy season often begins in June and lasts until October. Rainfall is frequent throughout this time, frequently in the form of afternoon showers or thunderstorms. The range of temperatures during the rainy season is slightly lower than

the hot season. In the central region, the cool season starts in November and lasts until February. Even though it is considered chilly at this time of year, it is still quite warm compared to other regions of the country that are experiencing winter. Evenings and early mornings can see lows of about 20°C, while daytime temperatures typically range from about 25°C to 30°C. Figure 4.1 (a) also shows the eastern region (Stations 13, 14, and 1). Thailand's eastern section is a coastal region that runs the length of the Gulf of Thailand. Like other regions of the country, it has a tropical environment with high annual temperatures and humidity. Figure 4.1 (a) also shows the south region (Stations 10, 17, 18, and 19). Thailand's southern region is known for its stunning beaches, islands, and lush tropical scenery. Although there are little differences between different regions of the region, the area has a tropical climate with high temperatures and humidity all year long. With rain and sporadic storms, the rainy season begins around October or November and lasts until December or January. The average temperature during the rainy season is between 25°C and 32°C. Temperatures during the cool season, which lasts from January through February, range from 25°C to 30°C. Figure 4.1 (b) shows the nothern, northeastern, and west region. In contrast to the country's center and southern regions, Thailand's northern and northeastern regions, which include towns like Chiang Mai, Lampang, Maha Sarakhram, and Ubon Ratchathani, feature distinctive weather patterns. A subtropical climate prevails in these areas, with temperatures that are a little bit colder, especially in the cool season. The cool season normally begins in November and lasts until February in the northern region. The average daily temperature is between 25°C and 30°C, however early mornings and evenings can be chilly, with lows of 15°C or even lower in some mountainous regions. The mild season in the north offers a welcome respite from the oppressive heat and humidity found in other regions of the nation. In the northern region, the hot season starts in March and lasts through May. High amounts of humidity are frequently present during the summer season, making it feel even hotter. In the northern region, the rainy season often begins in June and lasts until October. Significant rainfall occurs throughout this time, frequently in the form of afternoon showers or thunderstorms. The humidity is still high. The weather in Thailand's northeast and western are comparable to that in the country's north. The temperature of these regions is the lowest, as shown in Figure 4.1 (b), during December and January compared to other regions.

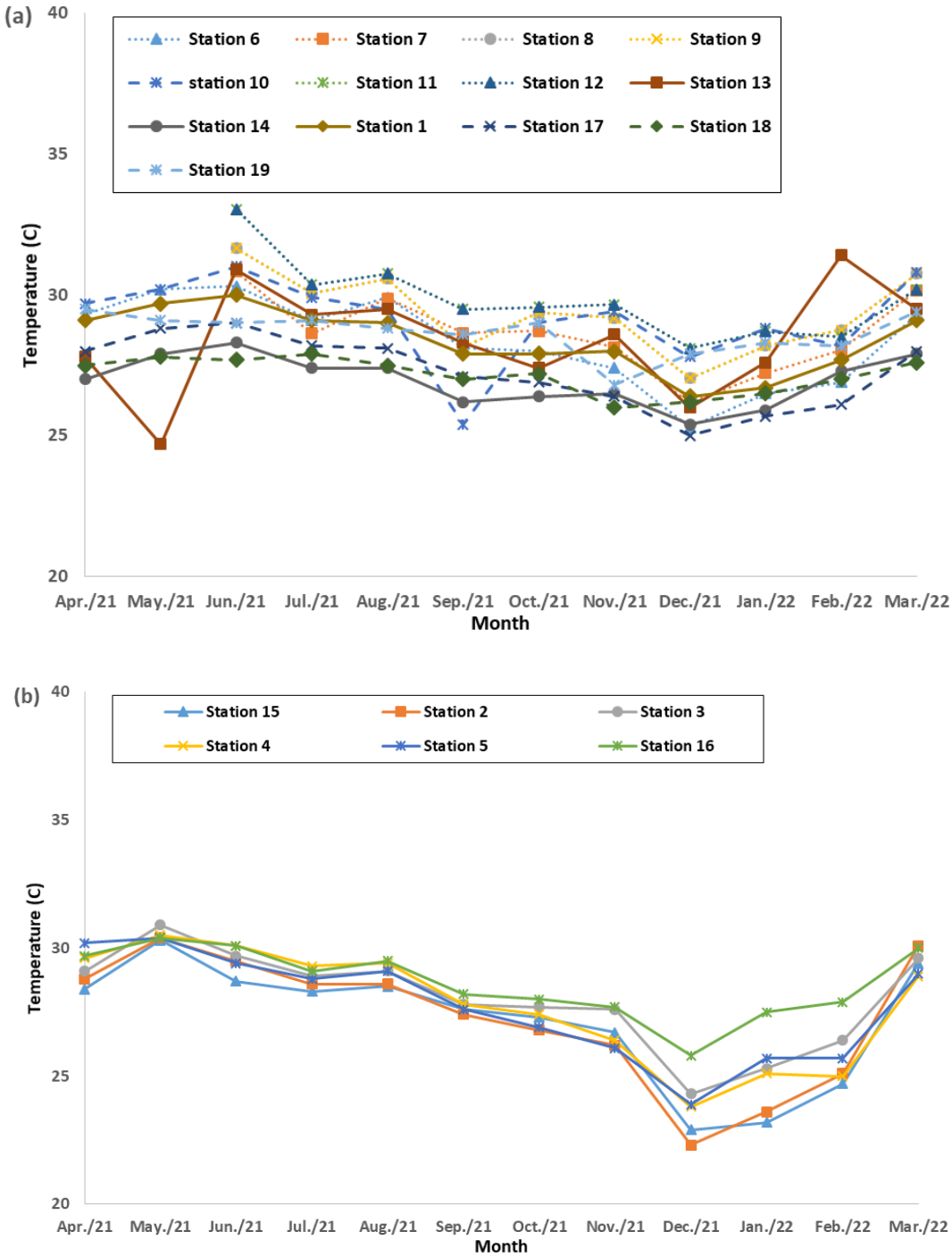

Figure 4.1 Monthly average temperature: (a) central and southern region; (b) northern, northeastern and west region

Figure 4.2 (a) represents the amount of rain that fell during the exposure of one year. The graph clearly demonstrates that due to its proximity to the sea, the station in Songkhla experiences the maximum quantity of rainfall, averaging about 1315 mm in November. Although not as much as in Songkhla, heavy precipitation was recorded at Hat Yai in November. The graph in Figure 4.2 (a) demonstrates that the highest precipitation was recorded in the central and eastern regions between August and October, whereas the peak was recorded in the southern region between October and November or early December. Overall, from March to June, all of the stations experienced little precipitation, which was consistent with the hot June temperatures. In Figure 4.2 (b), it shows that the northern, northeastern, and western region have the same behavior as the central and eastern region, which have high rainfall around September and very little rainfall in November and December.

(a)

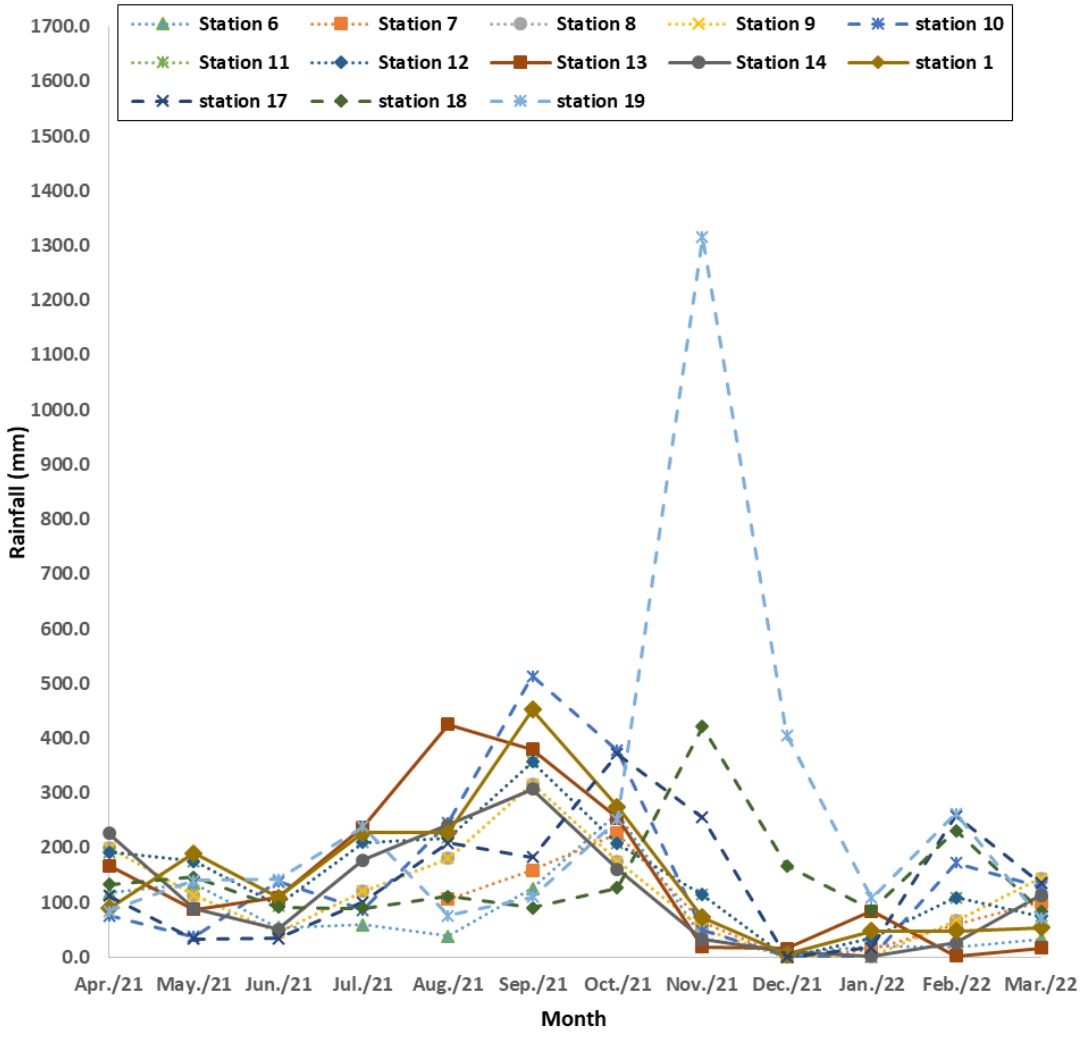

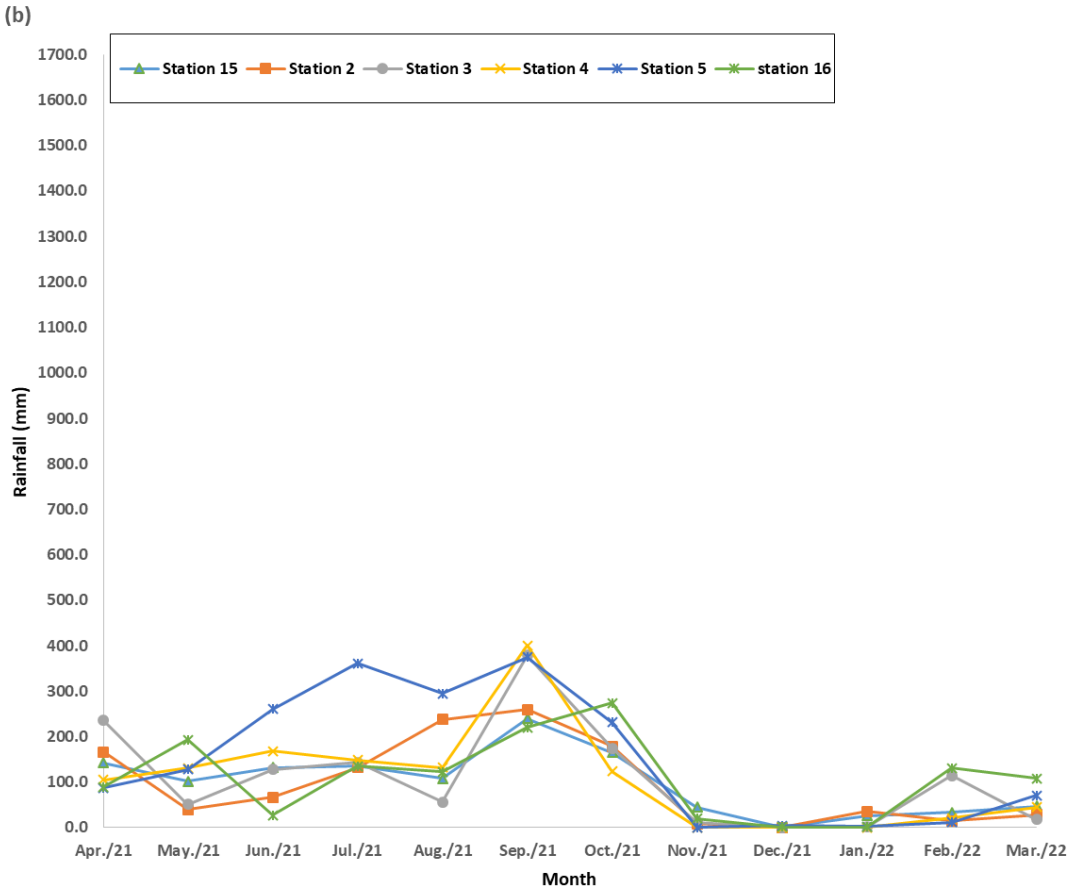

Figure 4.2 Monthly average temperature: (a) central and southern region; (b) northern, northeastern, and west region

During the exposure test, the monthly average relative humidity (RH) is depicted in Figure 4.3. Since there was a lot of precipitation during that time, the curves for the central and eastern regions grow from August to October and decline from November to December. From October through November, the Southern region saw high relative humidity, which is linked to heavy rainfall. Due to the month's minimal precipitation, the majority of the sites have low RH in December. The range of the monthly average RH was between 60% and 93%. Note that the RH data recording began in August 2021 for the stations in Pathum Thani, Ayutthaya, Hat Yai, and the northern regions due to the technical issue in collecting RH with those stations. However, the RH value at each station was calculated as an average value per year. It showed not much difference when compared with the data with TMD.

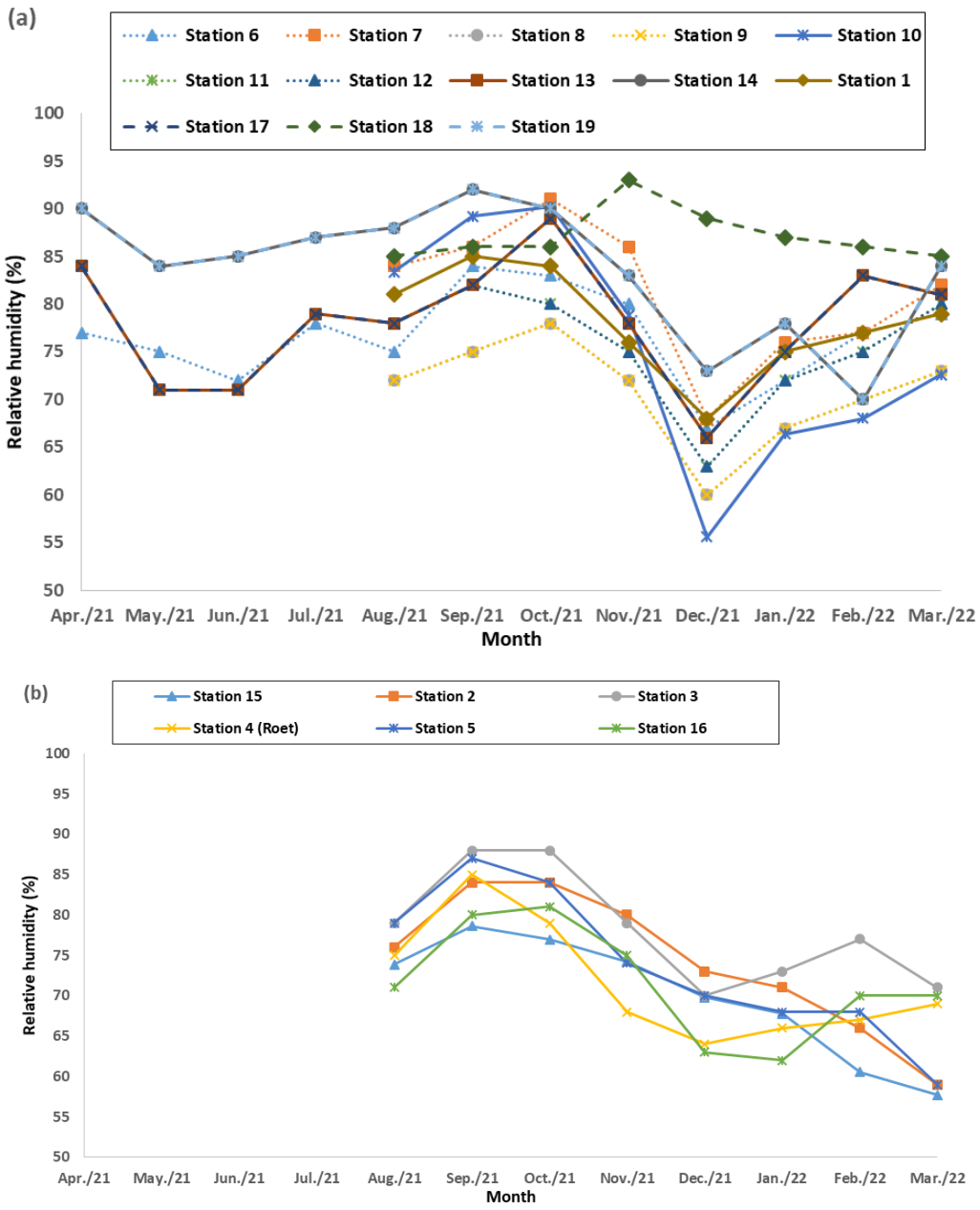

Figure 4.3 Monthly average relative humidity: (a) central and southern region; (b) northern, northeastern and west region

Table 4.1 displays the SO_2 content in the air as obtained from the website of the Thai Pollutant Department. According to the data in the table, major cities like Bangkok have higher SO_2 concentrations than other urban areas. Vehicles and factories both release SO_2 as a pollutant. The classification based on ISO 9223 (ISO9223, 2012) is used in Table 4.2 to display the SO_2 and chloride deposition rates at the test location. The categorization is shown as "P" and "S" for SO_2 and chloride, respectively, based on the aforementioned ISO standard. Class "P0" deposition rates for SO_2 range from 0 to

4 mg/m^2 per day, while class "P1" deposition rates range from 4 to 24 mg/m^2 per day. S0 and S1 are the chloride deposition rates for airborne chloride, with ranges of 0 to 3 and 3 to 60 mg/m^2 per day, respectively. Thailand's central area contains the province of Saraburi, which is far from the coast. With a value of 2.41 mg/m^2 per day, it is within the range of chloride class S0. Thailand's Southern area includes Songkla. PSU (Hat Yai) and RUT (Songkla) were designated as the two test sites in this province. RUT (Songkla) is around 300 meters from the water, while PSU (Hat Yai) is about 20 kilometers away. RUT (Songkla) displayed a greater rate of 15.36 mg/m^2 per day than PSU (Hat Yai), whose rate was 8.53 mg/m^2 per day. These places were classed as S1. Chon Buri, a seaside city in Thailand's East, was given the S1 classification and a daily presentation of 13.96 mg/m^2 per day. A lot of air pollution are present in the industrial area where Sangchareon Eastern Galvanize (Chon Buri) is located. According to the information in Table 4.2, a substantial SO_2 deposition rate was noted in this area. Due to the rise in SO_2 levels brought on by the usage of fossil fuels (Rios-Rojas et al., 2017), SO_2-induced air corrosion becomes a significant issue.

Table 4.1 Test locations and environmental pollutants at the test locations

No.	Location	Region	Province	Cumulative SO_2 (μg/m^3)
15	Chaing Mai U.	N	Chaing Mai	0
2	Mae Moh power plant	N	Lampang	75.98
3	Naresuan U.	N	Phitsanulok	18.34
4	Mahasarakham U.	NE	Mahasarakham	34.06
5	Ubon Ratchathani U.	NE	Ubon Ratchathani	34.06
6	Saraburi province	C	Saraburi	31.44
7	TMT Wangnoi	C	Ayutthaya	41.92
8	Sangcharoen	C	Pathum Thani	49.78
9	SIIT	C	Pathum Thani	49.78
10	Thai Premium Pipe	S	Samut Sakorn	89.08
11	TMT Bangkok	C	Bangkok	57.64
12	ISIT Bangkok	C	Bangkok	57.64
13	Union Galvanizer	E	Chachoengsao	49.78
14	Sangchareon Eastern Galvanize	E	Chon Buri	55.02
15	Cotco-SV Eastern Steel Pipe LTD	E	Rayong	57.64
16	Tha Thung Na Dam	W	Kanchanaburi	5.24
17	Sahaviriya Steel	S	Prachuap Khiri Khan	*
18	Prince of Sonkla U.	S	Songkhla	39.3
19	Rajamangala U.	S	Songkhla	39.3

Table 4.2 Average chloride deposition rate data

	Cl	
Site	mg/m^2 day	S
Saraburi	2.41	S_0
Sangchareon Eastern: Chon Buri	13.96	S_1
PSU: Hat Yai	8.53	S_1
RUT: Songkhla	15.36	S_1

Note: S categories obtained for chloride following ISO 9223 standard.

4.4 Thickness loss of bare steel

4.4.1 Graph

When exposed to corrosive environments, bare steel gradually loses thickness as a result of corrosion. The rate of thickness loss is influenced by a number of variables, such as the particular corrosive environment, time spent exposed, steel composition, and surface quality. For estimating corrosion rates, making predictions about the service life of structures, and putting the right maintenance and mitigation measures in place, it is crucial to comprehend the thickness loss of bare steel.

The corrosive environment can have a considerable impact on the rate of corrosion of exposed steel. The rate of thickness loss is significantly influenced by variables like temperature, humidity, the presence of corrosive chemicals (such as salts and acids), and air pollution levels. For instance, compared to inland or less corrosive locations, coastal sites with high air salinity or industrial settings with chemical emissions tend to speed up the corrosion process and cause faster thickness loss. Figure 4.4 shows the results of exposure test for all 19 stations.

All the test stations is classified into regions as follows: northern, northeastern, west, central, eastern, and southern region. The northern region consists of stations 15, 2, and 3. The northeastern region consists of stations 4 and 5. The west region consists of station 16. The central region consists of stations 6, 7, 8, 9, 11, and 12. The east region consists of station 13, 14, and 1. The southern region consists of stations 10, 17, 18, and 19.

Figure 4.4 show the progression of the thickness loss of bare steel for grades SS400 and SM490A over the course of a year at each of 19 test sites. The graph's steep

positive slope in the first three months indicates that the bare steel rusted quickly. For several sites, the slope of the graph remains high from three to six months. After six months, the graphs start to progressively flatten. By serving as a barrier layer against air chemicals, the corrosion layer lowers the rate of corrosion. The thickness loss of SM490A grade was found to be larger when compared to SS400 grade of bare steel. Since both forms of steel are carbon steel, there is not much of a difference in the thickness loss between the two. Table 3.2 revealed that SM490A contains a slightly lower percentage of copper (Cu) than SS400 and a slightly higher percentage of carbon than SS400. Copper (Cu) is one of the chemical elements that shields steel against corrosion.

For the northern, northeastern, and west (Stations 15, 3, 4, 5, and 16) region, it shows that one-year thickness loss of these station is not higher than 15 microns. Most of them is lower than 10 microns. As mentioned in the above section, this region consists of mountainous areas, and has low industrial activities. Thailand's northern area, which includes the provinces of Chiang Mai, Chiang Rai, and Lampang, consists the natural surroundings. The following are some sectors for business in northern Thailand: tourism, agriculture, handicrafts and textiles, and some industries.

For station 2, this station was placed at Mae Moh power plant, a sizable thermal power station known as the Mae Moh Power station. It is situated in northern Thailand's Lampang province's Mae Moh district. It is one of the biggest coal-fired power plants in Southeast Asia and the largest in Thailand. The Mae Moh Power Plant's development got under way in 1975, and it started running in 1978. The Electricity Generating Authority of Thailand (EGAT) is the company that owns and runs the facility. It is made up of many power plants with a total installed capacity of about 2,625 megawatts (MW). The plant's main fuel supply is lignite coal, which is plentiful at the neighboring Mae Moh mine. The Mae Moh Power Plant has raised questions about its environmental impact because it is a coal-fired power plant. When coal is burned to produce power, greenhouse gases like carbon dioxide are released, which accelerates global warming. Air pollutants such as sulfur dioxide (SO_2), nitrogen oxides (NOx), and particulate matter can also be produced by coal combustion. The power station has implemented pollution control technologies and other efforts over time to lessen its impact on the environment. It is based on official sources of the Electricity Generating

Authority of Thailand (EGAT). Station 2 is located in northern Thailand. However, this station is located at the power plant station. The environmental conditions at this station are dominated by the local environment. SO_2 concentration data from the Thai Pollution Control Department at the station near the Mae Moh Power Plant is shown with 75.98 $\mu g/m^3$ (Table 4.1) for the cumulative monthly average value during the exposure test at the Mae Moh power plant. The thickness loss for bare steel at this station is very severe. The one-year thickness losses for bare steel SS400 and SM490A are 41.82 and 42.31 microns, respectively. This station is a special case among the northern stations.

For central region (Stations 6, 7, 8, 9, 11, and 12), the thickness loss for both grades of steel (SS400 and SM490A) after one year of exposure was lower in Saraburi and Ayutthaya than in Pathum Thani and Bangkok, which were characterized by higher SO_2 concentrations (Table 4.1) and temperatures (Figure 4.1), respectively. Bangkok experiences issues with air pollution, and SO_2 is one of the pollutants of concern, like many other major urban centers (Pathum Thani). The main human activities that release SO_2 into the atmosphere include industrial processes, electricity generating, transportation, and home burning. The huge number of automobiles, and industrial activity all contribute to the discharge of SO_2 into the air in Bangkok. Additionally, the large number of automobiles on Bangkok's roads contributes to the SO_2 emissions. This pollutant is produced when gasoline and diesel fuels are used in engines, especially in older automobiles with less sophisticated emission control equipment. Traffic congestion makes the problem worse because emissions are increased by stop-and-go traffic and prolonged idle hours. These reasons may explain the high thickness loss of bare steel in this region.

In the eastern region (Stations 13, 14, and 1), greater thickness loss occurs in Chon Buri than in Chachoengsao at Union Galvanizer, followed by Cotco in Rayong. According to Table 4.2, Chon Buri had a higher daily SO_2 deposition rate of 8.27 mg/m^2 (ISO grade: P1). Thailand's eastern region, which includes provinces like Chonburi, Rayong, and Chachoengsao, is well-known for its economic growth and industrialization. As a result, this area struggles with air pollution, which includes sulfur dioxide (SO_2) as a pollutant. Industrial complexes, power stations, and refineries are present in Thailand's eastern region, which increases SO_2 emissions. Significant volumes of SO_2 are released into the atmosphere as a result of industrial activities,

especially those that involve the burning of fossil fuels. The region's industrial complexes, which include petrochemical plants and manufacturing facilities, frequently run on fossil fuels like coal and oil. So, when these fuels are burned, SO_2 is released into the environment. In addition, SO_2 emissions from marine boats may result from the heavy maritime activity and shipping in the eastern region's coastal areas.

According to Figure 4.4, Songkhla RUT in the southern region recorded the maximum thickness loss, which is associated with both the highest rainfall and the highest chloride deposition rate (15.36 mg/m^2 per day). The distance to the seashore from this point is about 300 meters. According to other research (Corvo et al., 1997; Mendoza & Corvo, 1999), high chloride deposition affects the atmospheric corrosion of steel at marine sites. Sea spray is a prominent component causing chloride deposition in Thailand's southern region, which includes islands and coastal areas. Sea moisture and marine aerosols can carry chloride ions inland. The atmospheric predominance of sea salt spray and its closeness to the ocean both contribute to the deposition of chloride on surfaces. Other variables, such as prevalent wind patterns and regional weather conditions, also affect the rate of chloride deposition. In general, it's expected that coastal areas and places closed to the sea will face higher chloride deposition rates than inland locations. The coastal environment has been found to be a major concern by multiple researchers (Feliu, Morcillo, & Chico, 1999; Jaén, Iglesias, & Hernández, 2012) for the steel degradation. This is concerning because steel constructions are weak to air corrosion. Station 18 at Prince Songkla University (PSU) had chloride deposition rate 8.53 mg/m^2 per day. This station is 22 kilometers from the seashore. The one-year thickness loss for this station is 19.75 and 23.29 microns for SS400 and SM490A, respectively. It is lower than Songkhla RUT (station 19), which has values of 23.76 and 28.79 microns for SS400 and SM490A, respectively. For station 17 at Sahaviriya steel in Prachuap Khiri Khan province, this station is 2.6 kilometers from the shoreline. The thickness loss value at this station is between stations 18 and 19. Station 10 at Thai Premium Pipe in Samut Sakhon province is 7.5 kilometers from the shoreline. However, this station is higher than station 17 since there is a lot of industrial activity in this province. The thickness reduction in the zones occurred in the following order after a 12-month exposure: South > East > Central.

(a)

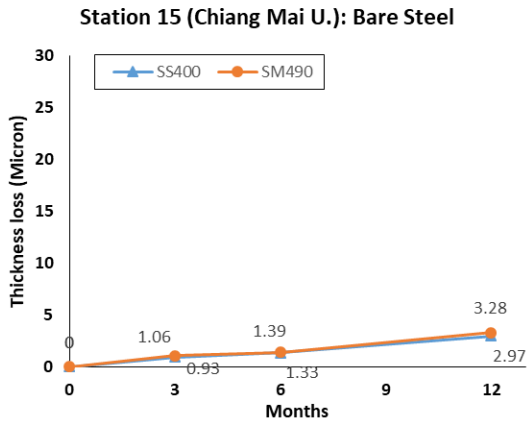
Station 15 (Chiang Mai U.): Bare Steel
SS400
SM490
Thickness loss (Micron)
Months
1.06
0.93
1.39
1.33
3.28
2.97

(b)

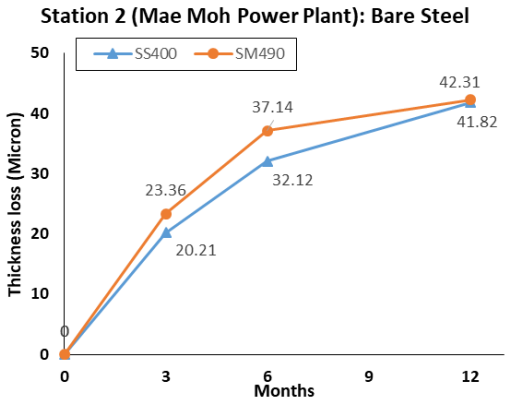
Station 2 (Mae Moh Power Plant): Bare Steel
SS400
SM490
Thickness loss (Micron)
Months
23.36
20.21
37.14
32.12
42.31
41.82

(c)

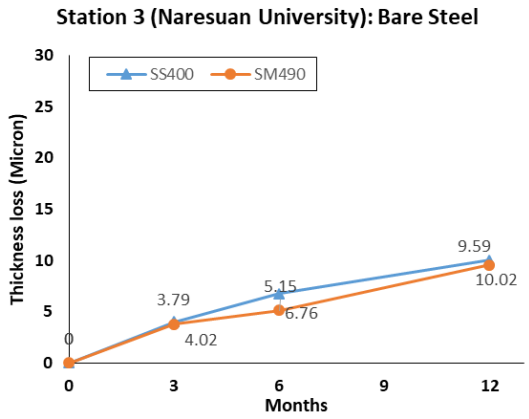
Station 3 (Naresuan University): Bare Steel
SS400
SM490
Thickness loss (Micron)
Months
3.79
4.02
5.15
6.76
9.59
10.02

(d)

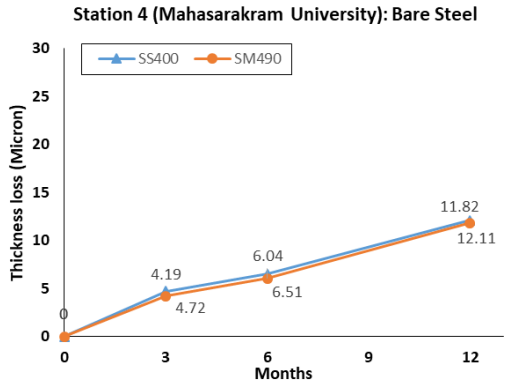
Station 4 (Mahasarakram University): Bare Steel
SS400
SM490
Thickness loss (Micron)
Months
4.19
4.72
6.04
6.51
11.82
12.11

(e)

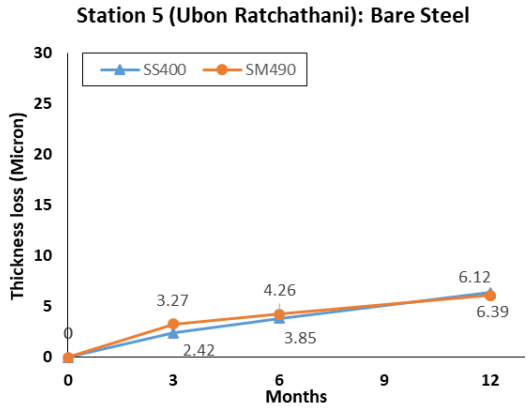
Station 5 (Ubon Ratchathani): Bare Steel
SS400
SM490
Thickness loss (Micron)
Months
3.27
2.42
4.26
3.85
6.12
6.39

(f)

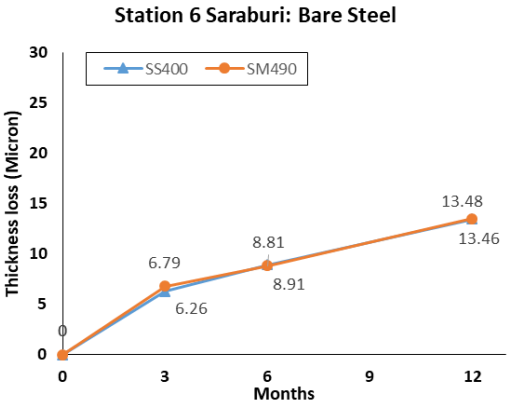
Station 6 Saraburi: Bare Steel
SS400
SM490
Thickness loss (Micron)
Months
6.79
6.26
8.81
8.91
13.48
13.46

(g)

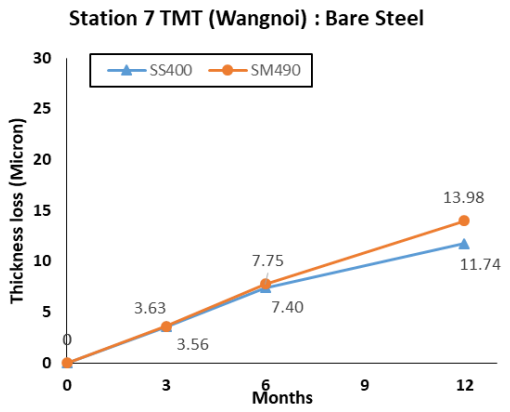
Station 7 TMT (Wangnoi) : Bare Steel
SS400
SM490
Thickness loss (Micron)
Months
3.63
3.56
7.75
7.40
13.98
11.74

(h)

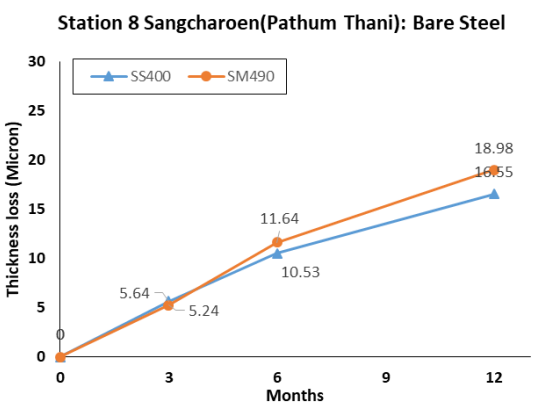
Station 8 Sangcharoen(Pathum Thani): Bare Steel
SS400
SM490
Thickness loss (Micron)
Months
5.64
5.24
11.64
10.53
18.98
16.55

(i)

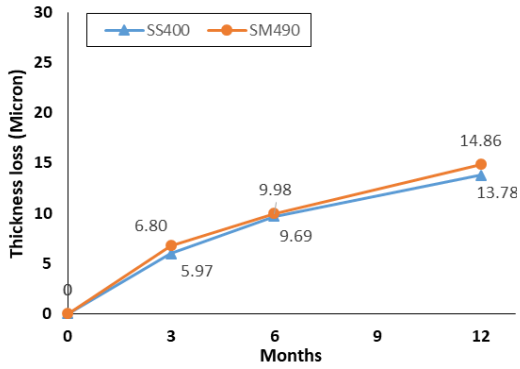
Station 9 SIIT: Bare Steel
SS400
SM490
Thickness loss (Micron)
Months
6.80
5.97
9.98
9.69
14.86
13.78

(j)

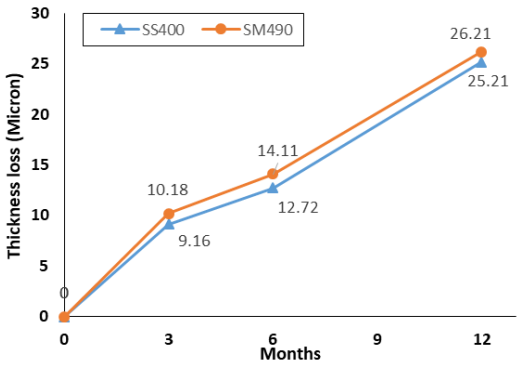
Station 10 (Thai Premium Pipe): Bare Steel
SS400
SM490
Thickness loss (Micron)
Months
10.18
9.16
14.11
12.72
26.21
25.21

(k)

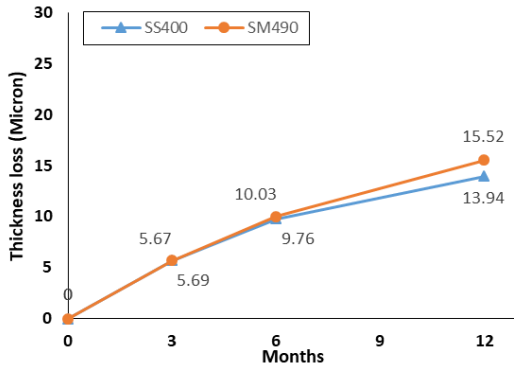
Station 11 TMT (Bangkok) : Bare Steel
SS400
SM490
Thickness loss (Micron)
Months
5.67
5.69
10.03
9.76
15.52
13.94

(l)

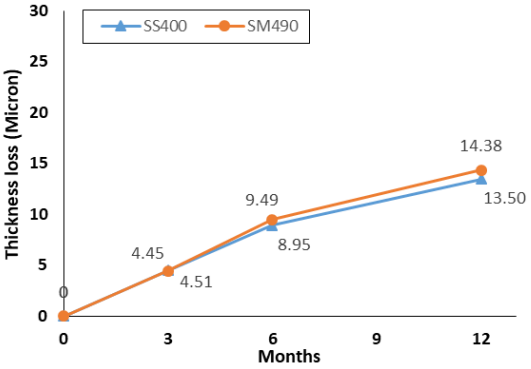
Station 12 ISIT (Bangkok) : Bare Steel
SS400
SM490
Thickness loss (Micron)
Months
4.45
4.51
9.49
8.95
14.38
13.50

(m)

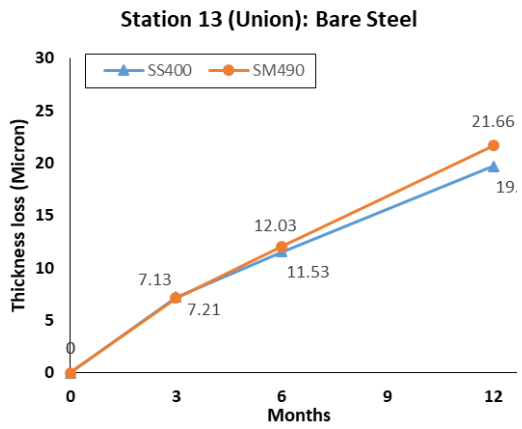
Station 13 (Union): Bare Steel
SS400
SM490
Thickness loss (Micron)
Months
0
7.13
7.21
12.03
11.53
21.66
19.

(n)

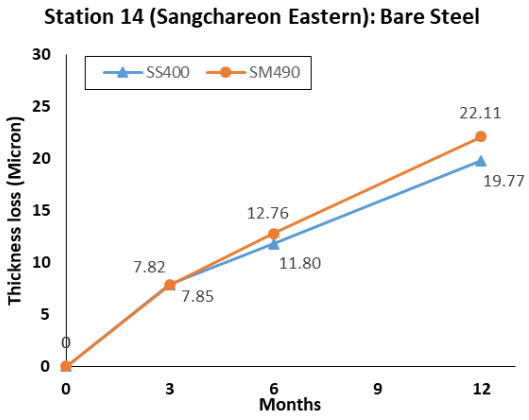
Station 14 (Sangchareon Eastern): Bare Steel
SS400
SM490
Thickness loss (Micron)
Months
0
7.82
7.85
12.76
11.80
22.11
19.77

(o)

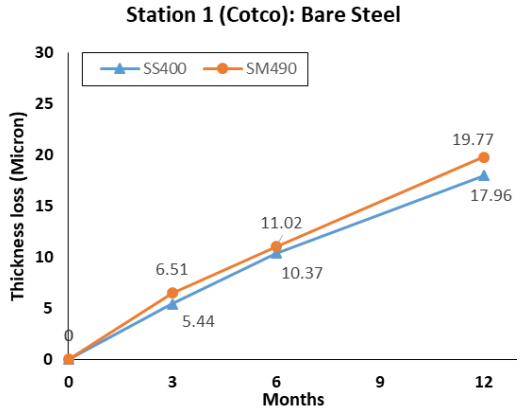
Station 1 (Cotco): Bare Steel
SS400
SM490
Thickness loss (Micron)
Months
0
6.51
5.44
11.02
10.37
19.77
17.96

(p)

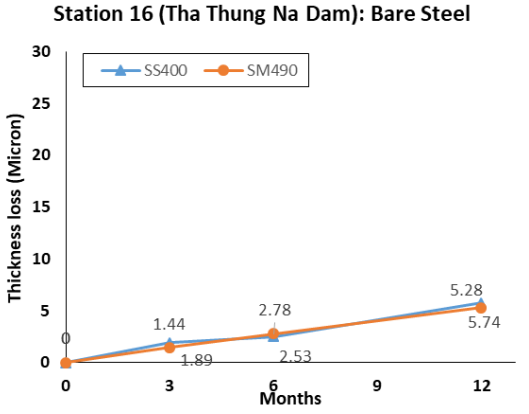
Station 16 (Tha Thung Na Dam): Bare Steel
SS400
SM490
Thickness loss (Micron)
Months
0
1.44
1.89
2.78
2.53
5.28
5.74

(q)

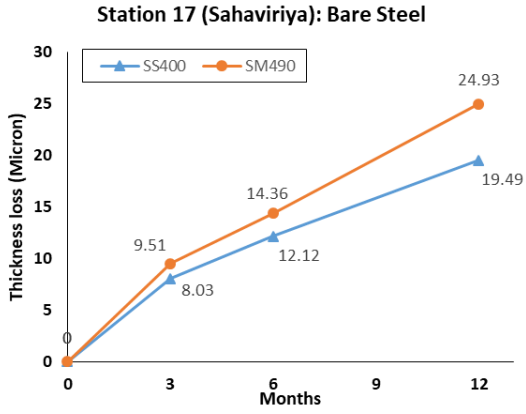
Station 17 (Sahaviriya): Bare Steel
SS400
SM490
Thickness loss (Micron)
Months
0
9.51
8.03
14.36
12.12
24.93
19.49

(r)

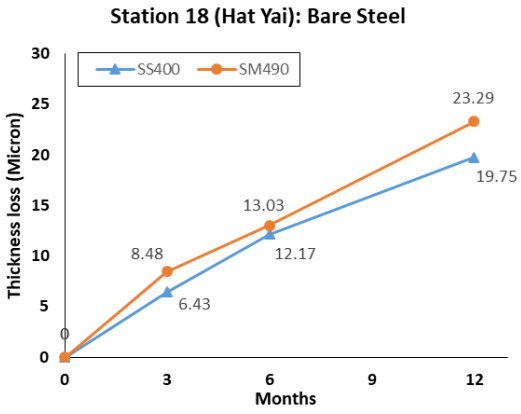
Station 18 (Hat Yai): Bare Steel
SS400
SM490
Thickness loss (Micron)
Months
0
8.48
6.43
13.03
12.17
23.29
19.75

(s)

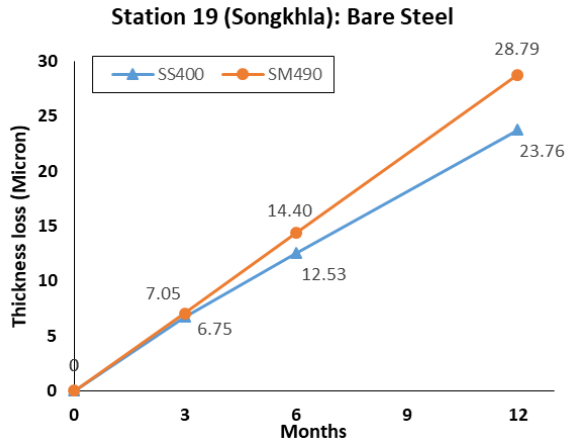

Figure 4.4 Thickness loss of bare steel versus exposure time at 19 test locations (a-s)

4.4.2 Appearance

Initially, bare steel has a clean and metallic appearance, with a surface that is bright and silver. But when it comes into touch with airborne moisture and oxygen, the oxidation process starts, which causes its look to gradually change. When steel first starts to corrode, the change in the surface's color starts to occur. Rust often manifests as a reddish or orange-brown color. Iron oxide, a byproduct of the corrosion process, is what is responsible for this coloring. After one-year exposure, all surface of the specimens are covered by the rust for all test locations. Without a covering or coating, the steel reacts with the atmosphere more sensitively. After one year of exposure, a darker orange-brown color was observed at stations near the coastline and the industrial stations than at stations far from the shoreline and industrial factory.

(a) Bare steel SS400 (b) Bare steel SM490A

Before exposure After one year Before exposure After one year

Figure 4.5 Bare steel after one year exposure at Songkla

4.5 Thickness loss of HDG steel

4.5.1 Graph

A popular corrosion protection technique for steel components and structures is hot-dip galvanizing. The procedure involves submerging the steel in molten zinc, which creates a protective zinc coating by forming a metallurgical link with the steel surface. Although hot-dip galvanized steel has good corrosion protection, atmospheric exposure over time may cause the zinc coating to gradually lose thickness. The following are some important points related to hot-dip galvanized steel's thickness loss:

- Corrosion Mechanisms: Sacrificial or galvanic corrosion, which gradually consumes the zinc coating, is the main cause of corrosion in hot-dip galvanized steel. Zinc corrodes in a sacrificial manner to protect the underlying steel substrate because it is more reactive than steel. Zinc consumption causes the coating's thickness to gradually decrease.
- Environmental Factors: The exposure conditions and the corrosive environment to which the structure is exposed determine the rate of thickness loss of hot-dip galvanized steel. Humidity, temperature, air pollution, airborne contaminants, and the presence of corrosive salts or chemicals can all affect how quickly the zinc coating corrodes and, as a result, how much of its thickness is lost.

Figure 4.6 shows the thickness loss of hot-dip galvanized steel for SS400 and SM490A over exposure time. For the majority of the stations, the graph shows a growth with time, suggesting that the basic zinc coating layers remain unprotected by the rust coatings after a year of exposure. Unlike bare steel, which developed a rust layer after a year of exposure, rust was seen on some of the exposed surface area. As a result, the rate at which HDG corrodes may remain constant or rise over time.

For the northern, northeastern, and west (Stations 15, 3, 4, 5, and 16) regions, it was discovered that two northeastern locations—Mahasarakham (station 4) and Ubon Ratchatani (station 5)—had greater values of thickness loss than the other test sites. It was determined that one-year thickness loss for both grades of HDG steel was approximately 0.7 microns. The two stations with higher thickness losses are Mahasarakham and Ubon Ratchatani, which have higher cumulative SO_2 levels among the northern region's tested stations (station No. 1–5), with a value of 34.06 $\mu g/m^3$, and

they also received higher cumulative rainfall, with values of 1.433 and 2.095 meters, as shown in Figure 4.2. For station 15 in Chiang Mai, one-year thickness loss for HDG is quite low compared to other stations (0.24 micron for the SS400 and 0.25 micron for the SM490A). For station 3 in Phitsanulok and station 16 in Kanchanaburi, one-year thickness loss is found with a value of around 0.3 microns for both grades. Station 2 in the Mae Moh power plant is a special station since this station is placed near the power plant, which receives a lot of pollutants, as mentioned in the above section 4.4, “Thickness loss of bare steel." The thickness loss of this station is found to be the highest. One-year thickness loss for this station are 1.82 and 2.12 microns for SS400 and SM490A, respectively.

For the stations located in the central regions (Stations 6, 7, 8, 9, 11, and 12) of Thailand, namely Saraburi, Ayuthaya, Pathum Thani, and Bangkok, the thickness loss in a year for SS400 ranges from 0.33 to 0.63 microns, while for SM490A, it varies from 0.38 to 0.69 microns.

Regarding the eastern regions (Stations 13, 14, and 1), the values of thickness loss for the eastern region vary from 0.60 to 0.68 microns and 0.58 to 0.79 microns for SS400 and SM490A, respectively.

Stations (Stations 10, 17, 18, and 19) in the southern region (Samut Sakorn, Prachuap Khiri Khan, Hat Yai, and Songkhla) had thickness losses ranging from 0.71 to 1.17 microns and 0.69 to 1.24 microns, respectively. High levels of chloride and prolonged moisture cause copper and zinc to corrode quickly in a variety of places (Santana Rodríguez et al., 2019). The corrosion process quickly when contaminants like SO_2 and chloride are present in the environment (Oesch, 1996).

(a)

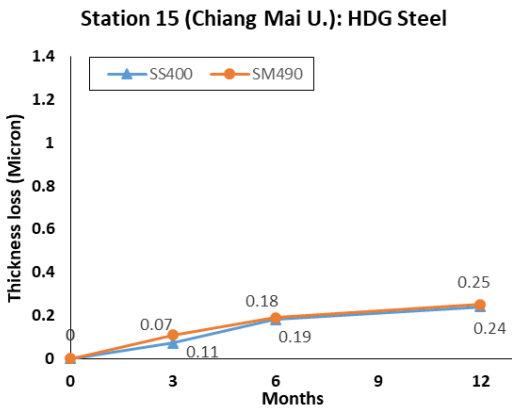
Station 15 (Chiang Mai U.): HDG Steel
SS400
SM490
Thickness loss (Micron)
Months
0.07
0.11
0.18
0.19
0.25
0.24

(b)

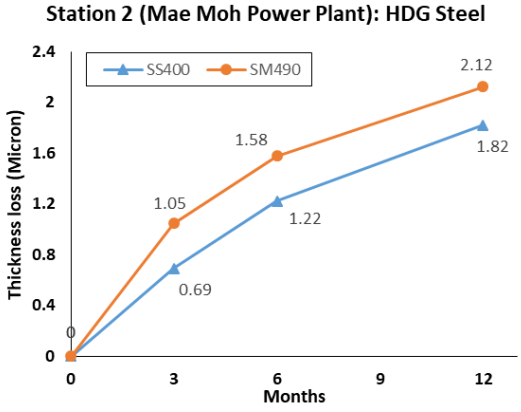
Station 2 (Mae Moh Power Plant): HDG Steel
SS400
SM490
Thickness loss (Micron)
Months
1.05
0.69
1.58
1.22
2.12
1.82

(c)

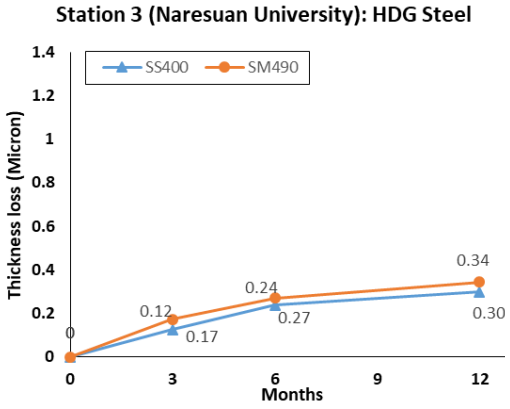
Station 3 (Naresuan University): HDG Steel
SS400
SM490
Thickness loss (Micron)
Months
0.12
0.17
0.24
0.27
0.34
0.30

(d)

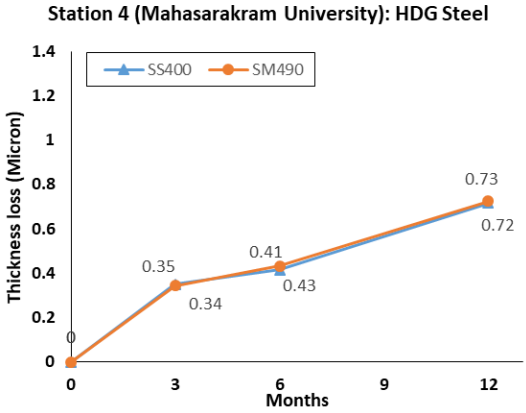
Station 4 (Mahasarakram University): HDG Steel
SS400
SM490
Thickness loss (Micron)
Months
0.35
0.34
0.41
0.43
0.73
0.72

(e)

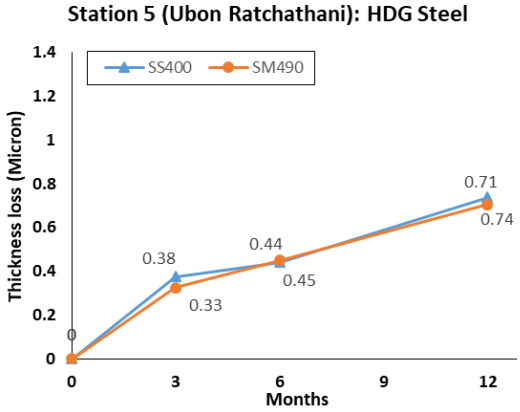
Station 5 (Ubon Ratchathani): HDG Steel
SS400
SM490
Thickness loss (Micron)
Months
0.38
0.33
0.44
0.45
0.71
0.74

(f)

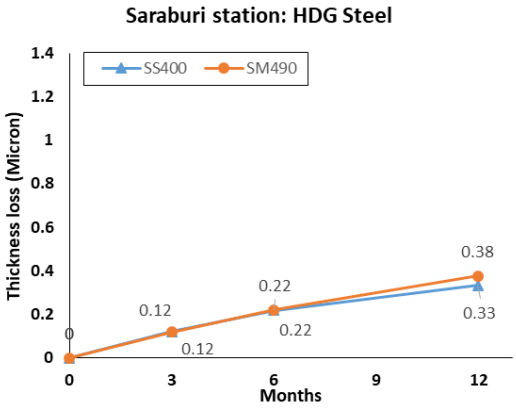
Saraburi station: HDG Steel
SS400
SM490
Thickness loss (Micron)
Months
0.12
0.12
0.22
0.22
0.38
0.33

(g)

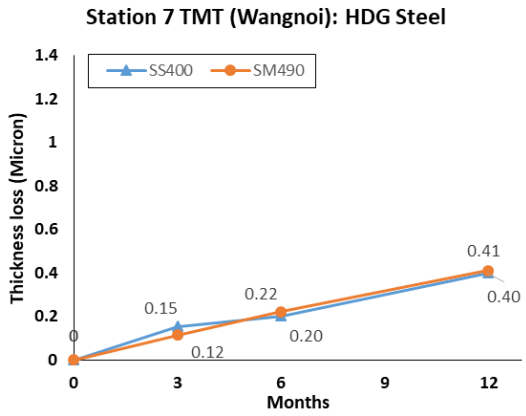
Station 7 TMT (Wangnoi): HDG Steel
SS400
SM490
Thickness loss (Micron)
Months
0.15
0.12
0.22
0.20
0.41
0.40

(h)

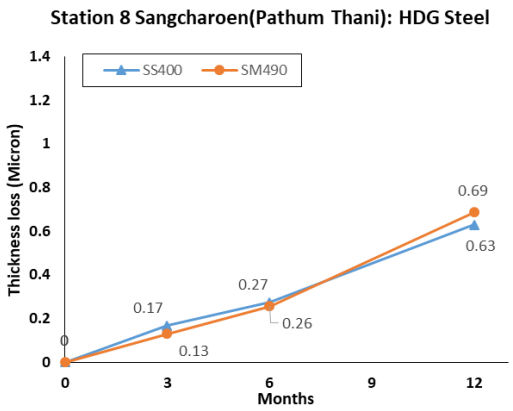
Station 8 Sangcharoen(Pathum Thani): HDG Steel
SS400
SM490
Thickness loss (Micron)
Months
0.17
0.13
0.27
0.26
0.69
0.63

(i)

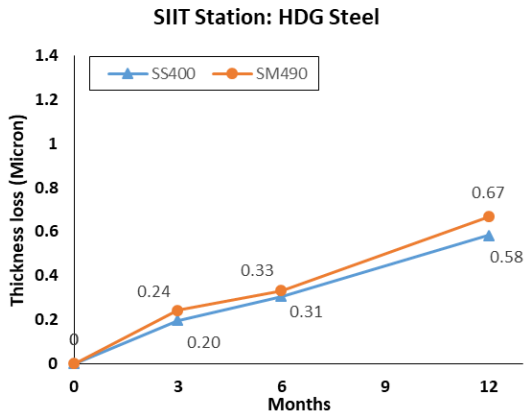
SIIT Station: HDG Steel
SS400
SM490
Thickness loss (Micron)
Months
0.24
0.20
0.33
0.31
0.67
0.58

(j)

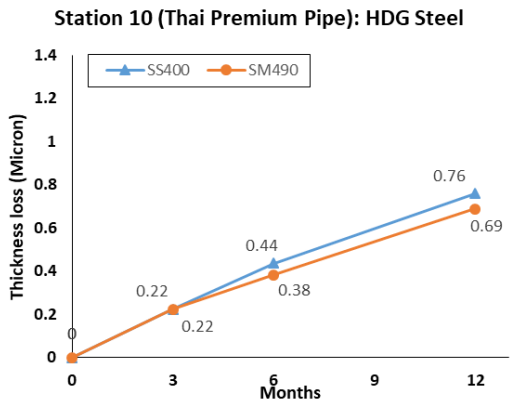
Station 10 (Thai Premium Pipe): HDG Steel
SS400
SM490
Thickness loss (Micron)
Months
0.22
0.22
0.44
0.38
0.76
0.69

(k)

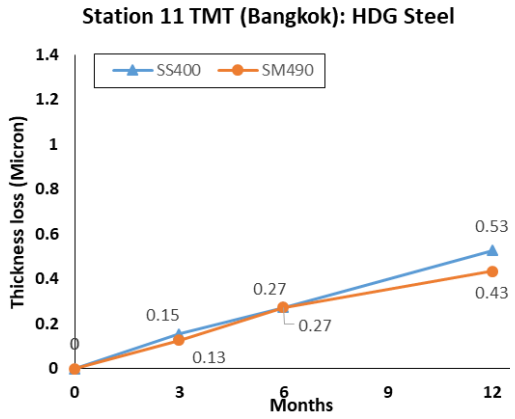
Station 11 TMT (Bangkok): HDG Steel
SS400
SM490
Thickness loss (Micron)
Months
0.15
0.13
0.27
0.27
0.53
0.43

(l)

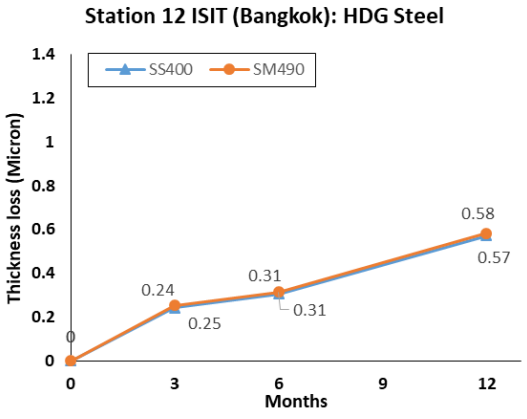
Station 12 ISIT (Bangkok): HDG Steel
SS400
SM490
Thickness loss (Micron)
Months
0.24
0.25
0.31
0.31
0.58
0.57

(m)

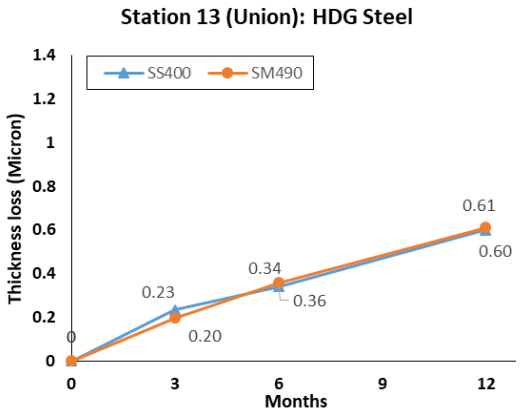
Station 13 (Union): HDG Steel
SS400
SM490
Thickness loss (Micron)
Months
0.23
0.20
0.34
0.36
0.61
0.60

(n)

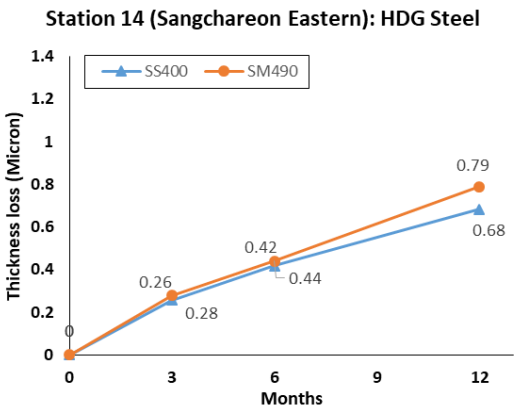
Station 14 (Sangchareon Eastern): HDG Steel
SS400
SM490
Thickness loss (Micron)
Months
0.26
0.28
0.42
0.44
0.79
0.68

(o)

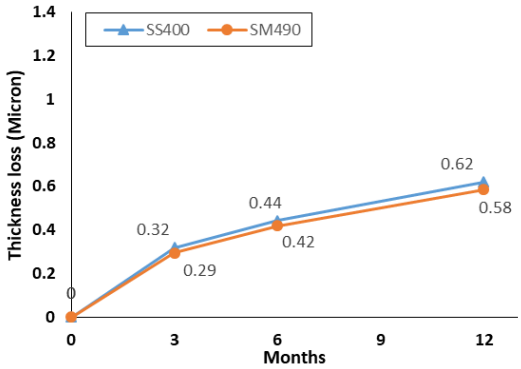
Station 1 (Cotco): HDG Steel
SS400
SM490
Thickness loss (Micron)
Months
0.32
0.29
0.44
0.42
0.62
0.58

(p)

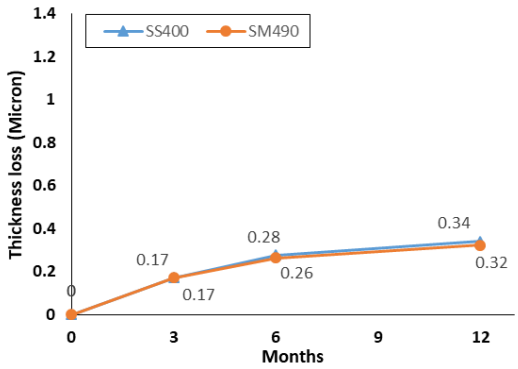
Station 16 (Tha Thung Na Dam): HDG Steel
SS400
SM490
Thickness loss (Micron)
Months
0.17
0.17
0.28
0.26
0.34
0.32

(q)

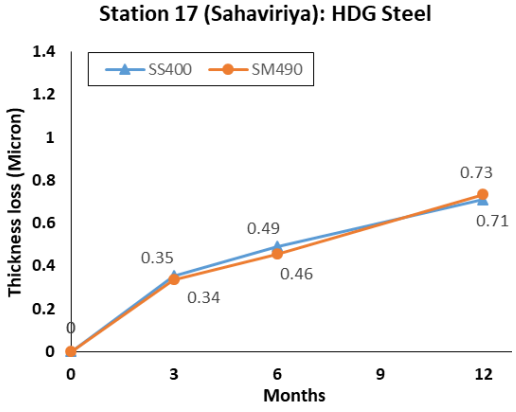
Station 17 (Sahaviriya): HDG Steel
SS400
SM490
Thickness loss (Micron)
Months
0.35
0.34
0.49
0.46
0.73
0.71

(r)

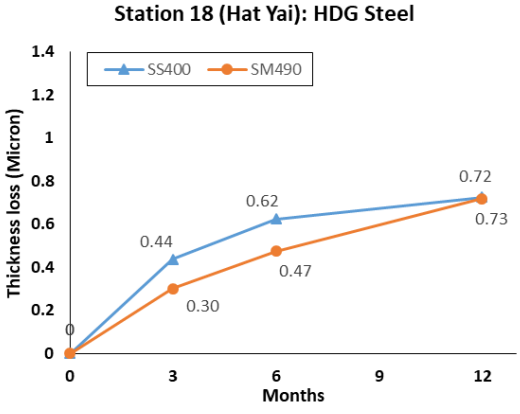
Station 18 (Hat Yai): HDG Steel
SS400
SM490
Thickness loss (Micron)
Months
0.44
0.30
0.62
0.47
0.72
0.73

(s)

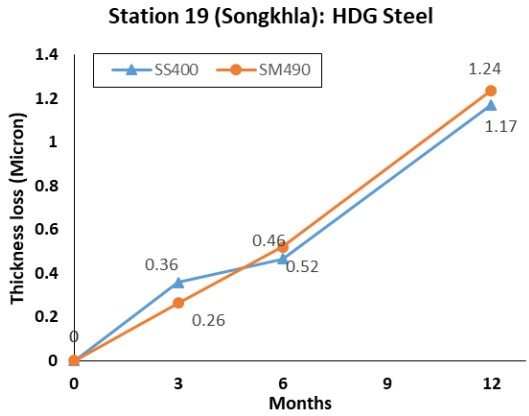

Figure 4.6 Thickness loss of HDG steel versus exposure time at 19 test locations(a-s)

4.5.2 Appearance

By submerging the steel in a bath of molten zinc, a protective coating is applied to the steel's surface during the hot-dip galvanizing process. In addition to offering superior corrosion protection, this coating gives the steel a unique visual appearance. After a year of exposure, white powder rust is seen on both steel grades of HDG steel at every station. Silver-gray color were discovered for HDG SS400, whereas silver-gray color and spangle shape were discovered for HDG SM490A as show in Figure 4.7. These tactile and visual characteristics add to HDG steel's functional durability and aesthetic appeal, making it a popular option for a variety of applications, including construction.

(a) HDG steel SS400 (b) HDG steel SM490A

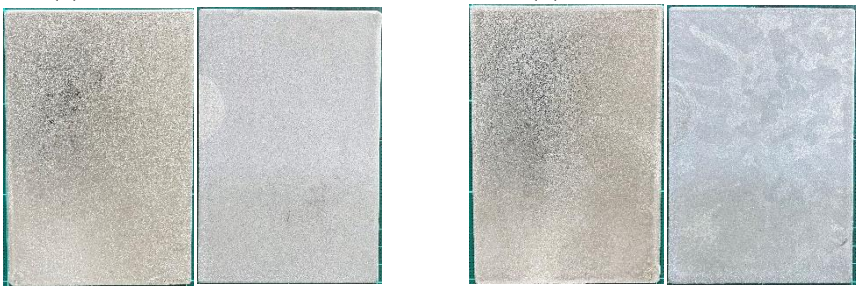

Before exposure After one year Before exposure After one year

Figure 4.7 HDG steel after one year exposure at Songkla

4.6 Assessment results of painted steel

To evaluate the effectiveness and longevity of protective coatings applied to steel surfaces, a painted steel exposure test, also known as a corrosion test, was carried out. In order to assess the coating's capacity to withstand corrosion, preserve its aesthetic quality, and offer long-term protection, painted steel panels are subjected to a variety of environmental conditions over a predetermined period of time. Here is a summary of the typical steps and goals of an exposure test for painted steel:

- Preparation of test panels: for the test, steel panels of a particular size (100 x 150 cm) and form are chosen. To get rid of any impurities, corrosion, or previous coatings, these panels were given a thorough cleaning. To obtain a consistent and clean substrate, the surface is prepared using chemical processes or abrasive blasting.
- Application of painting: the prepared steel panels are painted using the protective painted system that has been defined, which comprise primers, and topcoats. This is done in accordance with DPT 1333–61 standards. The method of painting application is spraying.
- Exposure conditions: to imitate real-world exposure, the painted steel panels are subjected to a variety of environmental conditions. These circumstances frequently include being exposed to the sun's ultraviolet (UV) rays, changing temperatures, humidity, rain, and atmospheric contaminants. Specific specifications for exposure angles, tilt, or height above the ground were set.
- Evaluation period: the tests last 3, 6, and 12 months.
- The assessment on the exposed painted steel followed ISO 4628 (1-10) standards.
- Test report and analysis: following the exposure test, a thorough report detailing the test asessment is generated. Photographs, ratings of coating performance, suggestions for enhancement, and comparisons to pertinent standards or specifications may all be included in the report.

The results of an atmospheric exposure test on painted steel with 19 exposure sites for SS400 and SM490A, respectively, are displayed in Table 4.3 and 4.4.

Table 4.3 Painted steel results for grade SS400

		3 months			6 months			12 months		
Sta.	Coated type	Blist.	Delam. (mm)	Others	Blist.	Delam. (mm)	Others	Blist.	Delam. (mm)	Others
15	A	Q1S1	0(0)	0	Q2S2	0(0)	0	Q2S2	0(0)	0
	C	Q1S1	0(0)	0	Q1S1	0(0)	0	Q2S2	0(0)	0
	E	Q0S0	1(0.06875)	0	Q0S0	1(0.091)	0	Q1S1	1(0.097)	0
	G	Q0S0	0(0)	0	Q0S0	0(0)	0	Q1S1	0(0)	0
3	A	Q1S1	0(0)	0	Q1S1	0(0)	0	Q2S1	0(0)	0
	C	Q1S1	0(0)	0	Q1S1	0(0)	0	Q2S2	0(0)	0
	E	Q0S0	1(0.031)	0	Q0S0	1(0.050)	0	Q0S0	1(0.131)	0
	G	Q0S0	0(0)	0	Q0S0	0(0)	0	Q1S2	0(0)	0
4	A	Q1S1	0(0)	0	Q1S1	0(0)	0	Q2S1	0(0)	0
	C	Q1S1	0(0)	0	Q2S1	0(0)	0	Q2S1	0(0)	0
	E	Q0S0	1(0.063)	0	Q1S1	1(0.166)	0	Q1S1	1(0.2125)	0
	G	Q0S0	0(0)	0	Q0S0	0(0)	0	Q1S1	0(0)	0
5	A	Q1S1	0(0)	0	Q2S2	0(0)	0	Q2S1	0(0)	Ri1
	C	Q1S1	0(0)	0	Q1S1	0(0)	0	Q2S2	0(0)	0
	E	Q0S0	1(0.038)	0	Q0S0	1(0.094)	0	Q1S1	1(0.109)	0
	G	Q0S0	0(0)	0	Q0S0	0(0)	0	Q0S0	0(0)	0
6	A	Q1S1	0	0	Q2S2	0	0	Q2S2	0	0
	C	Q1S1	0	0	Q2S2	0	0	Q2S2	0	0
	E	Q0S0	1(d=0.047)	0	Q0S0	1(d=0.066)	0	Q1S1	1(d=0.113)	0
	G	Q0S0	0	0	Q0S0	0	0	Q0S0	0	0
7	A	Q2S1	0	0	Q2S2	0	0	Q2S2	0	0
	C	Q2S1	0	0	Q2S2	0	0	Q2S2	0	0
	E	Q0S0	1(d=0.028)	0	Q0S0	1(d=0.066)	0	Q0S0	1(d=0.069)	0
	G	Q0S0	0	0	Q0S0	0	0	Q1S1	0	0
8	A	Q2S1	0	0	Q2S2	0	0	Q2S2	0	0
	C	Q1S1	0	0	Q2S2	0	0	Q2S2	0	0
	E	Q0S0	1(d=0.063)	0	Q0S0	1(d=0.081)	0	Q1S1	1(d=0.131)	0
	G	Q0S0	0	0	Q0S0	0	0	Q1S1	0	0
9	A	Q1S1	0	0	Q2S2	0	0	Q3S1	0	0
	C	Q1S1	0	0	Q2S2	0	0	Q3S1	0	0
	E	Q0S0	0	0	Q0S0	1(d=0.116)	0	Q1S1	1(d=0.125)	0
	G	Q0S0	0	0	Q0S0	0	0	Q1S1	0	0
10	A	Q1S1	0	0	Q2S2	0	0	Q1S2	0	0
	C	Q2S2	0	0	Q2S2	0	0	Q2S1	0	0
	E	Q0S0	1(d=0.047)	0	Q0S0	1(d=0.047)	0	Q2S1	1(d=0.081)	0
	G	Q0S0	0	0	Q0S0	0	0	Q0S0	0	0
11	A	Q2S1	0	0	Q2S2	0	0	Q2S2	0	0
	C	Q2S1	0	0	Q2S2	0	0	Q3S2	0	0

	E	Q1S1	1(d=0.05)	0	Q0S0	1(d=0.153)	0	Q1S1	1(d=0.153)	0
	G	Q0S0	0	0	Q0S0	0	0	Q1S1	0	0
12	A	Q1S1	0	0	Q1S1	0	0	Q2S2	0	0
	C	Q1S0	0	0	Q1S1	0	0	Q2S2	0	0
	E	Q0S0	1(d=0.066)	0	Q1S1	1(d=0.088)	0	Q1S1	1(d=0.109)	0
	G	Q0S0	0	0	Q1S1	0	0	Q1S1	0	0
13	A	Q1S1	0	0	Q2S2	0	0	Q2S2	0	0
	C	Q2S1	0	0	Q3S2	0	0	Q3S3	0	0
	E	Q1S1	1(d=0.025)	0	Q0S0	1(d=0.044)	0	Q1S1	1(d=0.106)	0
	G	Q0S0	0	0	Q0S0	0	0	Q1S1	0	0
14	A	Q2S1	0	0	Q2S2	0	0	Q3S2	0	0
	C	Q2S2	0	0	Q2S2	0	0	Q2S2	0	Ri1, Cr.(Q1 S1)
	E	Q1S1	1(d=0.075)	0	Q0S0	1(d=0.106)	0	Q1S1	1(d=0.166)	0
	G	Q0S0	0	0	Q0S0	0	0	Q1S1	0	0
1	A	Q1S1	0	0	Q1S1	0	0	Q1S1	0	0
	C	Q1S1	0	0	Q1S1	0	0	Q1S1	0	0
	E	Q0S0	1(d=0.044)	0	Q0S0	1(d=0.056)	0	Q0S0	1(d=0.066)	0
	G	Q0S0	0	0	Q0S0	0	0	Q1S1	0	0
16	A	Q1S1	0	0	Q1S1	0	0	Q1S1	0	0
	C	Q1S1	0	0	Q1S1	0	0	Q1S1	0	0
	E	Q0S0	1(d=0.022)	0	Q0S0	1(d=0.069)	0	Q0S0	1(d=0.081)	0
	G	Q0S0	0	0	Q0S0	0	0	Q1S1	0	0
17	A	Q1S1	0	0	Q2S2	0	0	Q2S2	0	0
	C	Q2S1	0	0	Q2S2	0	0	Q3S2	0	0
	E	Q0S0	1(d=0.078)	0	Q0S0	1(d=0.084)	0	Q1S1	1(d=0.109)	0
	G	Q0S0	0	0	Q0S0	0	0	Q1S1	0	0
18	A	Q1S1	0	0	Q2S2	0	0	Q3S2	0	0
	C	Q1S1	0	0	Q3S2	0	0	Q3S2	0	0
	E	Q0S0	1(d=0.059)	0	Q0S0	1(d=0.094)	0	Q1S1	1(d=0.106)	0
	G	Q0S0	0	0	Q0S0	0	0	Q1S1	0	0
19	A	Q1S1	0	0	Q3S2	0	0	Q3S2	0	0
	C	Q1S1	0	0	Q2S2	0	0	Q3S2	0	0
	E	Q0S0	1(d=0.056)	0	Q0S0	1(d=0.063)	0	Q1S1	1(d=0.109)	0
	G	Q0S0	0	0	Q0S0	0	0	Q1S1	0	0

Table 4.4 Painted steel results for grade SM490A

		3 months			6 months			12 months		
Sta.	Coated type	Blist.	Delam. (mm)	Others	Blist.	Delam. (mm)	Others	Blist.	Delam. (mm)	Others
15	B	Q1S1	0	0	Q2S2	0	0	Q2S2	0	0
	D	Q1S1	0	0	Q1S1	0	0	Q2S2	0	0
	F	Q0S0	1(d=0.0188)	0	Q0S0	1(d=0.028)	0	Q1S1	1(d=0.044)	0
	H	Q0S0	0	0	Q0S0	0	0	Q1S1	0	0
3	B	Q1S1	0	0	Q2S2	0	0	Q2S2	0	0
	D	Q1S1	0	0	Q2S2	0	0	Q2S2	0	0
	F	Q0S0	1(d=0.097)	0	Q0S0	1(d=0.169)	0	Q0S0	1(d=0.219)	0
	H	Q0S0	0	0	Q0S0	0	0	Q1S1	0	0
4	B	Q1S1	0	0	Q2S2	0	0	Q2S2	0	0
	D	Q1S1	0	0	Q2S1	0	0	Q2S3	0	0
	F	Q0S0	1(d=0.053)	0	Q0S0	1(d=0.066)	0	Q1S1	1(d=0.1625)	0
	H	Q0S0	0	0	Q0S0	0	0	Q1S1	0	0
5	B	Q1S1	0	0	Q2S2	0	0	Q2S2	0	0
	D	Q1S1	0	0	Q1S1	0	0	Q2S1	0	0
	F	Q0S0	1(d=0.144)	0	Q0S0	1(d=0.156)	0	Q1S1	1(d=0.122)	0
	H	Q0S0	0	0	Q0S0	0	0	Q1S1	0	0
6	B	Q1S1	0	0	Q1S1	0	0	Q2S2	0	0
	D	Q1S1	0	0	Q1S1	0	0	Q2S2	0	0
	F	Q0S0	1(d=0.100)	0	Q0S0	1(d=0.147)	0	Q1S1	1(d=0.166)	0
	H	Q0S0	0	0	Q0S0	0	0	Q0S0	0	0
7	B	Q2S1	0	0	Q2S2	0	0	Q2S2	0	0
	D	Q1S1	0	0	Q2S2	0	0	Q2S2	0	0
	F	Q0S0	1(d=0.078)	0	Q0S0	1(d=106)	0	Q1S1	1(d=103)	0
	H	Q0S0	0	0	Q0S0	0	0	Q1S1	0	0
8	B	Q2S1	0	0	Q2S2	0	0	Q2S2	0	0
	D	Q2S1	0	0	Q1S1	0	0	Q2S1	0	0
	F	Q0S0	1(d=0.116)	0	Q0S0	1(d=0.150)	0	Q1S1	1(d=0.206)	0
	H	Q0S0	0	0	Q0S0	0	0	Q0S0	0	0
9	B	Q1S1	0	0	Q2S2	0	0	Q3S2	0	0
	D	Q1S1	0	0	Q2S2	0	0	Q3S2	0	0
	F	Q0S0	1(d=0.094)	0	Q0S0	1(d=0.141)	0	Q1S1	1(d=0.144)	0
	H	Q0S0	0	0	Q0S0	0	0	Q1S1	0	0
10	B	Q2S2	0	0	Q2S2	0	0	Q2S2	0	0
	D	Q2S2	0	0	Q2S2	0	0	Q3S1	0	0
	F	Q0S0	1(d=0.041)	0	Q0S0	1(d=0.041)	0	Q1S1	1(d=0.059)	0
	H	Q0S0	0	0	Q0S0	0	0	Q0S0	0	0
11	B	Q2S1	0	0	Q2S2	0	0	Q3S2	0	0
	D	Q2S1	0	0	Q2S2	0	0	Q3S3	0	0

	F	Q1S1	1(d=0.100)	0	Q0S0	1(d=0.169)	0	Q1S1	1(d=0.194)	0
	H	Q0S0	0	0	Q0S0	0	0	Q1S1	0	0
12	B	Q1S1	0	0	Q1S1	0	0	Q2S2	0	0
	D	Q1S1	0	0	Q1S1	0	0	Q2S2	0	0
	F	Q0S0	1(d=0.038)	0	Q1S1	1(d=0.038)	0	Q1S1	1(d=0.044)	0
	H	Q0S0	0	0	Q1S1	0	0	Q1S1	0	0
13	B	Q1S1	0	0	Q2S2	0	0	Q2S2	0	0
	D	Q2S1	0	0	Q2S2	0	0	Q2S2	0	0
	F	Q0S0	1(d=0.075)	0	Q0S0	1(d=0.081)	0	Q1S1	1(d=0.175)	0
	H	Q0S0	0	0	Q0S0	0	0	Q1S1	0	0
14	B	Q2S1	0	0	Q3S2	0	0	Q3S2	0	0
	D	Q2S1	0	0	Q2S2	0	0	Q3S2	0	0
	F	Q0S0	1(d=0.050)	0	Q0S0	1(d=0.084)	0	Q1S1	1(d=0.116)	0
	H	Q0S0	0	0	Q0S0	0	0	Q1S1	0	0
1	B	Q1S1	0	0	Q1S1	0	0	Q1S1	0	0
	D	Q1S1	0	0	Q1S1	0	0	Q1S1	0	0
	F	Q0S0	1(d=0.041)	0	Q0S0	1(d=0.128)	0	Q0S0	1(d=0.178)	0
	H	Q0S0	0	0	Q0S0	0	0	Q0S0	0	0
16	B	Q1S1	0	0	Q1S1	0	0	Q1S2	0	0
	D	Q1S1	0	0	Q1S1	0	0	Q1S1	0	0
	F	Q0S0	1(d=0.056)	0	Q0S0	1(d=0.063)	0	Q0S0	1(d=0.063)	0
	H	Q0S0	0	0	Q0S0	0	0	Q0S0	0	0
17	B	Q2S1	0	0	Q2S2	0	0	Q3S2	0	0
	D	Q3S2	0	0	Q2S2	0	0	Q3S2	0	0
	F	Q0S0	1(d=0.091)	0	Q0S0	1(d=0.109)	0	Q1S1	1(d=0.169)	0
	H	Q0S0	0	0	Q0S0	0	0	Q1S1	0	0
18	B	Q2S2	0	0	Q2S3	0	0	Q2S3	0	0
	D	Q1S1	0	0	Q2S2	0	0	Q3S1	0	0
	F	Q0S0	1(d=0.047)	0	Q0S0	1(d=0.091)	0	Q1S1	1(d=0.175)	0
	H	Q0S0	0	0	Q0S0	0	0	Q1S2	0	0
19	B	Q2S2	0	0	Q2S2	0	0	Q3S2	0	0
	D	Q2S2	0	0	Q1S1	0	0	Q3S1	0	0
	F	Q0S0	1(d=0.031)	0	Q0S0	1(d=0.047)	0	Q1S1	1(d=0.059)	0
	H	Q0S0	0	0	Q0S0	0	0	Q1S1	0	0

Table 4.3 and 4.4 illustrate the assessment results of exposed painted steel with 19 test locations. It has four different types of paint systems, each with a different paint thickness. While other defects (such as rusting, cracking, flaking, chalking, and filiform corrosion) are displayed in the "Others" column, blistering and delamination assessment are shown in the result table. Below is a summary of the findings for comparing each exposed paint system at each station:

Resistance to blistering under atmospheric exposure:

For SS400: A ≈ C < E < G

For SM490A: B ≈ D < F < H

Resistance to delamination and corrosion at the scribed marks under atmospheric exposure:

For SS400: E < A ≈ C < G

For SM490A: F < B ≈ D < H

With the station 14 at Sangcharoen Eastern Galvanize Co., Ltd in Chon Buri, in the eastern region of Thailand, where there are many industrial sites, other defects were discovered. Paint system C (Medium Grade Paint) for the SS400 steel grade was discovered to have rusting with grade "Ri1" and cracking with grade "Q1S1". Pollutants in the air may have had an impact on the specimen. However, according to the ISO 4628 standard, the defects were minor and low grade. Station 5 in Ubon Ratchathani was found also the other defect of rusting with grade "Ri1" for paint system A (Low Grade Paint). It is unexpected defect that was found during the test at this location.

Below is a summary of the findings for comparing the level of corrosion of painted steel at each station:

SS400: Central: 1 ≈ 2 ≈ 3 ≈ 6 < 4 < 5, East: 7 ≈ 8, South: 9 < 10 ≈ 11

SM490A: Central: 1 ≈ 2 ≈ 3 ≈ 6 < 4 < 5, East: 7 < 8, South: 9 ≈ 10 ≈ 11

The comparison of the severity of painted steel corrosion for each zone's findings is as follows:

SS400: Central < Eastern < Southern

SM490A: Central < Eastern < Southern

According to the findings of the exposure test, the premium grade painting (E and F system painting) had more delamination and corrosion at the scribed marks than the other three coatings. A premium grade paint has a thickness of 300 microns, with 150 microns for the epoxy primer and 150 microns for the polyurethane top coat. The depth of the scribed mark for each of the paint systems is shown in Figure 4.8. The thicker premium quality paint intensifies the scribed mark, as shown in Figure 4.8 (d). Low grade painting, medium grade painting, and duplex systems all have shallow scribed lines, which make the rainwater along their edges quickly evaporate in the sun or under UV light when it rains. The premium grade painting had less moisture evaporation in the meanwhile. Since the mark was scribed, the loose epoxy paint layer beneath the top coat has been visible surrounding the scribed area. The thickness of the epoxy coating (150 microns), as observed during the scribing process, is excessively thick. The epoxy layer readily turns into white powder and gets looser around faults or damage, such as scribed marks. As demonstrated in Figure 4.8 (d), moisture from the

rain and moisture in the air may be present for longer and become difficult to drain when the loose component leaves beneath the top coat. As a result, the underlying steel rust at the scribed line can progress more quickly beneath the top coat or the paint layer. The compaction between the base steel with the primer and primer with the top coat work well for low grade painting (80 microns of epoxy and 40 microns of polyurethane) and medium grade painting (80 microns of epoxy and 80 microns of polyurethane). The epoxy layer beneath the top coat was solid with an 80 micron thickness. After the exposure testing, the adhesion for low grade, medium, and duplex systems is better than that of the premium grade painting system because, as previously mentioned, premium grade painting is worse when it has initial defects. However, as evidenced by the findings in Table 4.3 and 4.4, the premium grade painting system was discovered to have greater resistance to blistering, rusting, cracking, and flaking than the low and medium grade painting system. The premium grade painting system has the advantages of making the painting structure's surface appear smooth and durable in the face of the aforementioned corrosion failure of the paint, unless a severe initial defect has already reached the foundation steel.

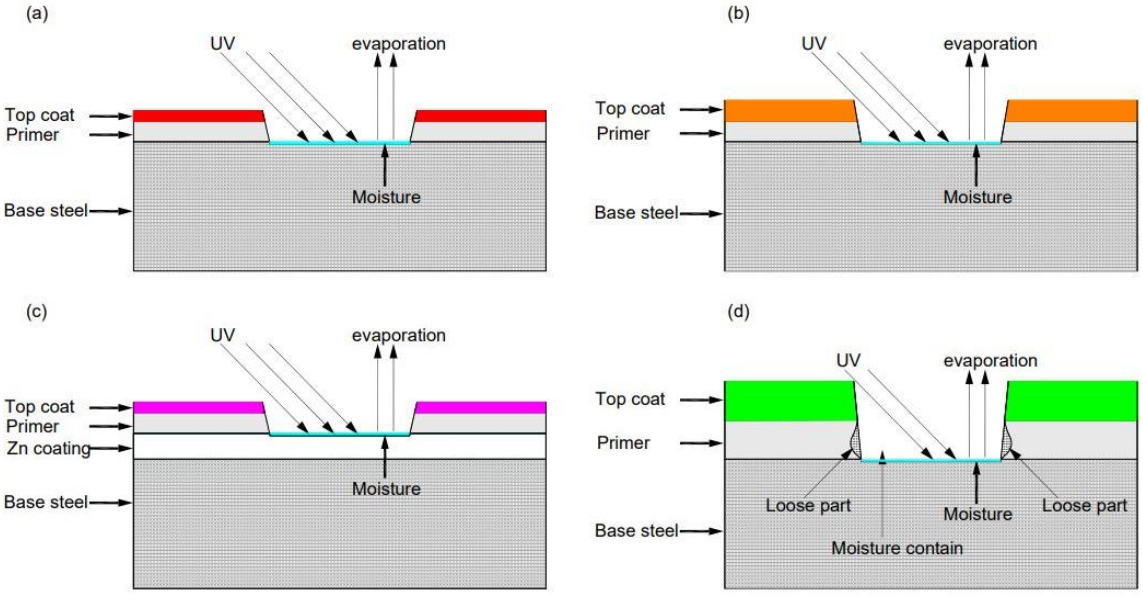

Figure 4.8 Cross section of painted steel at scribed mark (a): low grade painting, (b): medium grade painting, (c) duplex system, and (d): premium grade painting

4.7 Summary

Thickness loss and assessment chapter provides a summary of findings from the atmospheric exposure test. The summary of the main findings and highlights of significant trends in this chapter are as follows:

- The temperature is high in the central region. Rainfall is noticeably high in the southern region. SO_2 is low in the northern and northeastern regions, except station 2 at the Mae Moh power plant, since this station is placed close to the power plant.
- For bare steel, thickness loss of SM490A is slightly higher than SS400. SM490A contains a slightly lower percentage of copper (Cu) than SS400 and a slightly higher percentage of carbon than SS400.
- Thickness loss of HDG steel is noticeably low compared to bare steel.
- After a year of exposure, bare steel was completely covered in a layer of rust, while HDG had some white powder rust on it.
- Light dark color was found for HDG SS400, while light dark color and spangle shape were found for HDG SM490A.
- Based on the assessment results, the duplex system (G and H) for painted steel was determined to be the best coating system for withstanding corrosion even with paint defects or damages.
- The severity of the regions: South > East > Central > North, North-east

CHAPTER 5
CORROSIVITY CLASSIFICATION, EQUATIONS, AND MAP

5.1 Introduction

Corrosivity classification, equation and map are the essential part of this research study. The outcomes of the data analysis are presented in this chapter, along with an interpretation of the results and a discussion of the implications in relation to the research's aims. This chapter will show the corrosivity classification by ISO 9223 and the comparison of the corrosivity classification by DPT 1333-61. The corrosion equations with the dose response function that were created will be illustrated. The corrosion map is a graphical map that shows how corrosion is distributed and how severe it is on a certain structure or in a given location. The finding of corrosion maps for both steels (bare and HDG steel) with both grades (SS400 and SM490A) is presented in this chapter. When conducting corrosion studies, the correlation between thickness loss and sea distance is frequently taken into account, especially for structures exposed to marine environments. The topic of thickness loss versus the distance to the sea will be discussed.

5.2 Corrosivity classification

5.2.1 Corroivity classification by ISO 9223

Either the corrosion rate of exposed metals or the rating of climatic and pollutant elements can be used to determine how aggressive the atmosphere is (Natesan, Venkatachari, & Palaniswamy, 2006). According to the requirements of the application of building, particularly in terms of service life, the corrosivity category is a technical characteristic that serves as a basis for the selection of materials and protective measures in atmospheric conditions. Corrosivity classification by ISO9223 is based on the first year thickness loss.

The standard ISO 9223 offers a system of grading the corrosivity of atmospheres. It classifies various settings according to how corrosive they are, assisting in determining how these situations might affect metallic products. Understanding the different levels of corrosivity and choosing the right materials or safety precautions can be facilitated by using the classification system established in ISO 9223.

The corrosivity classification is divided into six categories by the ISO 9223 standard, ranging from C1 being the least corrosive to C5 being very high corrosivity, with CX being the most corrosive. Each group represents particular climatic factors and pollution concentrations that can cause corrosion. An overview of the corrosivity categories is provided below:

- C1 - Very low corrosivity: refers to situations with less pollution and corrosive material. C1 habitats often consist of indoor settings with controlled atmospheres or rural locations with little industrial activity. A few examples are heated structures, workplaces, or agricultural areas.
- C2 - Low corrosivity: C2 environments are a little bit more corrosive than C1 classification and may have a little bit more contaminants present. These settings are often found in low-pollution rural or metropolitan locations. Residential areas, tiny towns, or regions far from important industrial sources are a few examples.
- C3 - Medium corrosivity: C3 environments include moderate degrees of corrosivity and include places where there is more pollution and moisture exposure. This category includes urban and industrial settings where there is a moderate amount of pollution from industry, traffic, and other anthropogenic sources. Cities, suburbs, and seaside regions are among examples.
- C4 - High corrosivity: significant amounts of contaminants and corrosive chemicals in the atmosphere describe C4 classification, which are characterized by significant corrosivity. Typically, these settings can be found in chemical factories, industrial locations with a lot of industrial activity, or coastal regions with salty air. Ports, industrial complexes, and busy locations are a few examples.
- C5 – Very high corrosivity: the most hostile and corrosive environments are classified as C5 classification. They include places with exceptionally high pollution levels, dampness, and caustic substances. Heavy industrial zones, chemical factories, or salty coastal environments are the usual locations for

C5 environments. Examples include areas near significant industrial emissions, chemical plants, and coastal regions with marine splashing.

- CX – Extreme corrosivity: the CX classification was added by ISO 9223 to address extremely corrosive conditions that are more severe than those seen in C5 classification. Extreme and highly specialized settings, such as those found in particular industrial processes, chemical reactors, or heavily contaminated locations, fall under this category.

Understanding the anticipated corrosive conditions in various places is made easier with the help of the corrosivity categorization according to ISO 9223. The corrosivity classifications by ISO 9223 for bare and HDG steel are shown in Table 5.1 and 5.2.

Table 5.1 Corrosivity classification for bare steel by ISO9223

No.	Station name	Bare steel (SS400)		Bare steel (SM490A)	
		1 year (micron)	Category by ISO 9223	1 year (micron)	Category by ISO 9223
15	Faculty of Engineering, Chiang Mai University	2.97	C2	3.28	C2
2	Mae Moh power plant	41.82	C3	42.31	C3
3	Faculty of Engineering Naresuan University	10.02	C2	9.59	C2
4	Maha Sarakham University	12.11	C2	11.82	C2
5	Ubon Ratchathani University Faculty of Engineering	6.39	C2	6.12	C2
6	Private House (Saraburi province)	13.46	C2	13.48	C2
7	Thai Metal Trade Company Limited (Wangnoi)	11.74	C2	13.98	C2
8	Sangcharoen Galvanizing Limited.	16.55	C2	18.98	C2
9	Sirindhorn International Institute of Technology (SIIT)	13.78	C2	14.86	C2
10	Thai Premium Pipe Company Limited	25.21	C3	26.21	C3
11	Thai Metal Trade Company Limited (Bangkok)	13.94	C2	15.52	C2
12	Iron and Steel Institute of Thailand	13.50	C2	14.38	C2
13	Union Galvanizer	19.68	C2	21.66	C2
14	Sangchareon Eastern Galvanize	19.77	C2	22.11	C2
1	Cotco-SV Eastern Steel Pipe LTD.	17.96	C2	19.77	C2
16	Tha Thung Na Dam Power Plant	5.74	C2	5.28	C2
17	Sahaviriya Steel Industries Public Company Limited	19.49	C2	24.93	C2
18	Prince of Sonkla University	19.75	C2	23.29	C2
19	Rajamangala University of Technology	23.76	C2	28.79	C3

Table 5.2 Corrosivity classification for HDG steel by ISO9223

No.	Station name	HDG steel (SS400)		HDG steel (SM490A)	
		1 year (micron)	Category by ISO 9223	1 year (micron)	Category by ISO 9223
15	Faculty of Engineering, Chiang Mai University	0.24	C2	0.25	C2
2	Mae Moh power plant	1.82	C3	2.12	C4
3	Faculty of Engineering Naresuan University	0.30	C2	0.34	C2
4	Maha Sarakham University	0.72	C3	0.73	C3
5	Ubon Ratchathani University Faculty of Engineering	0.74	C3	0.71	C3
6	Private House (Saraburi province)	0.33	C2	0.38	C2
7	Thai Metal Trade Company Limited (Wangnoi)	0.40	C2	0.41	C2
8	Sangcharoen Galvanizing Limited.	0.63	C2	0.69	C2
9	Sirindhorn International Institute of Technology (SIIT)	0.58	C2	0.67	C2
10	Thai Premium Pipe Company Limited	0.76	C3	0.69	C2
11	Thai Metal Trade Company Limited (Bangkok)	0.53	C2	0.43	C2
12	Iron and Steel Institute of Thailand	0.57	C2	0.58	C2
13	Union Galvanizer	0.60	C2	0.61	C2
14	Sangchareon Eastern Galvanize	0.68	C2	0.79	C3
1	Cotco-SV Eastern Steel Pipe LTD.	0.62	C2	0.58	C2
16	Tha Thung Na Dam Power Plant	0.34	C2	0.32	C2
17	Sahaviriya Steel Industries Public Company Limited	0.71	C3	0.73	C3
18	Prince of Sonkla University	0.73	C3	0.72	C3
19	Rajamangala University of Technology	1.17	C3	1.24	C3

5.2.2 Corroivity classification by DPT 1333-61

There are two types of corrosion categories: those based on the environmental description in DPT 1333-61 and those based on the degree of the corrosion attack as determined by an experimental test conducted over the period of a year at various types of exposure sites. The corrosion categories serve as a rough estimate of the material's corrosion attack magnitude in micron per year. The DPT 1333-61 standard for corrosion and corrosion prevention systems for structural steel is used in Thailand. The foundation of the standard is found in ISO 9226 (1992), which was later translated and

changed to fit the Thai context. Corrosion categories based on environmental descriptions from DPT 1333-61 section 4.2 are shown in Table 5.3.

Table 5.3 Corrosion categories based on environmental descriptions from DPT 1333-61 section 4.2

Corrosion category	Low Carbon Steel µm/year	Zinc µm/year	Environmental description
C1	≤ 1.3	≤ 0.1	Area with extremely low corrosive environment.
C2	> 1.3 to 25	> 0.1 to 0.7	Area with low corrosive environment such as suburban area.
C3	> 25 to 50	> 0.7 to 2.1	Area with moderate corrosive environment such as suburban area, area with 500 m. or farther from industrial factory, and area with 1000 m. or farther from seacoast line.
C4	> 50 to 80	> 2.1 to 4.2	Area with high corrosive environment such as city area, area with 100-500 m. from industrial factory or area with 100-1000 m. from seacoast line.
C5-I	> 80 to 200	> 4.2 to 8.4	Area with extreme corrosive environment (industrial area) such as area with lesser than 100 m. far from industrial factory
C5-M	> 80 to 200	> 4.2 to 8.4	Area with extreme corrosive environment (seacoast line) such as area with lesser than 100 m. far from seacoast line.

Table 5.4 Corrosion categories of exposures test site in industrial areas

Station No.	Description of the station	Conditions match with environmental description	Corrosion categories based on environmental description
Station 2	The station was placed in the Mae Moh Power Plant	Area with less than 100 m far from industrial factory	C5-I
Station 7	The station was placed in the Thai Metal Trade Company Limited's factory in Wangnoi		C5-I
Station 8	The station was placed in Sangcharoen Galvanizing Limited's factory		C5-I
Station 10	The station was placed in Thai Premium Pipe Company Limited's factory		C5-I
Station 13	The station was placed in Union Galvanizer's factory		C5-I
Station 14	The station was placed Sangchareon Eastern Galvanize's factory		C5-I
Station 1	The station was placed Cotco-SV Eastern Steel Pipe LTD's factory		C5-I
Station 17	The station was placed in Sahaviriya Steel Industries Public Company Limited's factory		C5-I

In Table 5.4, eight separate industrial factories are the place for the eight exposure stations. A location that is less than 100 meters from an industrial factory is classified as C5-I based on the corrosion categories that are presented in DPT 1333-61 standard. In this category, zinc's corrosion attack magnitude is estimated to be between 4.2 and 8.4 microns. For bare steel, the range is thought to be between 80 and 200 microns. The corrosion categories acquired from the experimental exposure test for the above 8 stations are shown in Table 5.1 and 5.2 to be incredibly low in comparison to the category environmental description. The majority of locations only produce C2 and C3, where the thickness losses for zinc vary from 0.1 to 0.7 microns and 0.7 to 2.1 microns, respectively. For the C2 and C3 classifications of bare steel, thickness loss varies from 1.3 to 25 microns and 25 to 50 microns, respectively.

Table 5.5 Corrosion categories of exposures test site in urban area

Station No.	Description of the station	Conditions match with environmental description	Corrosion categories based on environmental description
Station 9	The station was placed at SIIT in Pathum Thani province	Area with high corrosive environment such as city area or urban area	C4
Station 11	The station was placed in the Thai Metal Trade Company Limited in Bangkok		C4
Station 12	The station was placed in Iron and Steel Institute of Thailand in Bangkok		C4

In Table 5.5, there were three exposure sites operated in densely populated urban areas. The corrosion category classification is designated as C4, and the corrosion attack magnitude for zinc ranges from 2.1 to 4.2 microns and for low carbon steel from 50 to 80 microns. From Table 5.1 and 5.2, it is obvious that the corrosion categories derived from experimental exposure tests are in C2 and that the thickness loss occurs in the following ranges for zinc and low carbon steel: 0.1–0.7 microns and 1.3–25 microns, respectively. This shows that most urban areas are not as corrosive as may be predicted. Stations 11 and 12 in the capital city, which has heavy traffic pollution, only delivered C2 rather than C4.

Table 5.6 Corrosion categories of exposures test site in suburban area

Station No.	Description of the station	Conditions match with environmental description	Corrosion categories based on environmental description
Station 15	The station was placed in Chiang Mai University in Chiang Mai Province.	Area with moderate corrosive environment such as suburban area, area with 500 m or farther from industrial factory	C3
Station 3	The station was placed in Naresuan University in Phitsanulok Province.		C3
Station 4	The station was placed in Maha Sarakham University in Maha Sarakham Province.		C3
Station 5	The station was placed in Ubon Ratchathani University in Ubon Ratchthani Province		C3
Station 18	The station was placed in Prince of Sonkla University in Hat Yai city, Songkla Province	Area with 1000 m. or farther from seacoast line.	C3

There are five exposure sites in four cities in the northern and northeastern regions and one city in the southern region, as shown in Table 5.6. The corrosion category classification based on environmental description is designated as C3, and the corrosion attack magnitude for low carbon steel is 25–50 microns and zinc is 0.7–2.1 microns. Through experimental exposure tests, the corrosion categories for these four stations were identified as C2 and C3. The corrosion attacks on low carbon steel and zinc, respectively, range from 1.3–25 microns and 25–50 microns, and on zinc, from 0.1–0.7 microns and 0.7–2.1 microns. The corrosivity classifications revealed that the classifications are close to each other based on the environmental description and the thickness loss obtained from the actual test.

Table 5.7 Corrosion categories of exposures test site in rural area

Station No.	Description of the station	Conditions match with environmental description	Corrosion categories based on environmental description
Station 6	The station was placed in rural area in Saraburi Province	Area with low corrosive environment	C2
Station 16	The station was placed in Tha Thung Na Dam Power Plant in Kanchanaburi		C2

In Table 5.7, there were two exposure sites in rural areas. The corrosion category standard is designated as C2, and the corrosion attack magnitude for zinc is 0.1-0.7 microns and for low carbon steel is 1.3-25 microns. The experimental exposure test's corrosion categories provided the same categories as the norm.

Table 5.8 Corrosion categories of exposures test site in shoreline area

Station No.	Description of the station	Conditions match with environmental description	Corrosion categories based on environmental description
Station 19	The station was placed in Rajamangala University of Technology in Songkla Province	Area with 100-1000 m. from seacoast line.	C4

In the southern region of Thailand, one exposure test site, shown in Table 5.8, was performed with 0.3 km from the seacoast line. It is classified as C4 based on environmental characteristics, with a corrosion attack magnitude of 50–80 microns for low carbon steel and 2.1–4.2 microns for zinc. According to Table 5.1 and 5.2, the results of the experimental exposure test fall into the C2 and C3 categories. In this test site, only bare steel with SS400 was in C2, but bare steel SM490A and HDG steel with both grades are in C3. The corrosivity classification based on the environmental description is higher than the actual test.

5.3 Corrosivity equation

5.3.1 Corrosivity equation term

Temperature, humidity, and the presence of pollutants are the atmospheric factors that have an impact on the corrosion process. The rate and severity of corrosion on various materials can be influenced by these factors. The relationship between environment factors and corrosion was drawn based on the specific material and environmental factors. Below are the form and conditions of the corrosion equation.

$$C = \alpha \times T\ (℃) + \beta \times RF\ (m) + \gamma \times RH\ (\%) + \delta \times SO_2(\mu g/m^3) + \varepsilon \times T_{exp}(month) \quad (3.4)$$

where T : average temperature during exposure (^{0}C)

RF: cumulative rainfall during exposure (m)

RH: average relative humidity during exposure (percentage)

SO_2: cumulative sulfur dioxide during exposure ($\mu g/m^3$)

T_{exp}: Time of exposure (month)

α, β, γ, δ, and ε are constants

Multiple variable linear regression analysis was performed in order to find the value of the coefficient in front of the parameters. For the central region, six test locations (station 6, 7, 8, 9, 11, and 12) were used to perform multilinear regression. Five test locations (station 3, 4, 5, 15, and 16) were used to perform multilinear regression for the north, northeastern, and west. Table 5.9 shows the results of creating corrosion equations for the central and northern regions.

Table 5.9 Dose response function results for central and northern regions

Type of steel	Regions	Dose response functions	R^2	Eq. No.
Bare steel	Central region	C (SS400) = 0.061 T + 1.779 RF + 1.00 RH + 0.012 SO_2 + 0.71 T_{exp}	0.91	(5.1)
		C (SM490A) = 0.050 T + 1.64 RF + 1.030 RH + 0.020 SO_2 + 0.825 T_{exp}	0.89	(5.2)
	Northern region	C (SS400) = 0.011 T + 0.15 RF + 3.460 RH + 0.271 SO_2 + 0.067 T_{exp}	0.80	(5.3)
		C (SM490A) = 0.028 T + 0.996 RF + 2.124 RH + 0.253 SO_2 + 0.018 T_{exp}	0.86	(5.4)
HDG steel	Central region	C (SS400) = 1.01×10^{-3} T + 0.181 RF + 0.011 RH + 0.406×10^{-3} SO_2 + 0.023 T_{exp}	0.88	(5.5)
		C (SM490A) = 0.247×10^{-3} T + 0.107 RF +0.027 RH + 0.069×10^{-3} SO_2 + 0.029 T_{exp}	0.81	(5.6)
	Northern region	C (SS400) = 1.08×10^{-3} T + 0.142 RF + 0.136 RH + 8.282×10^{-3} SO_2 + 0.0013 T_{exp}	0.76	(5.7)
		C (SM490A) = 1.73×10^{-3} T + 0.119 RF + 0.141 RH + 8.645×10^{-3} SO_2 + 0.0019 T_{exp}	0.80	(5.8)

The chloride, one of the main causes of steel corrosion, affects the east and south regions because they are close to the shoreline. Equation 3.5, which takes chloride into account as well as the sites' distances from the sea, is used to represent those regions.

$$C = \alpha \times T\ (℃) + \beta \times RF\ (m) + \gamma \times RH\ (\%) + \delta \times SO_2(\mu g/m^3) + \mu \times Cl^-(\mu g/m^2) + \theta \times T_{exp}(month) + \varepsilon \times \exp\left(\gamma D(km)\right) \quad (3.5)$$

where T : average temperature during exposure (^{0}C)

RF: cumulative rainfall during exposure (m)

RH: average relative humidity during exposure (percentage)

SO_2: cumulative sulfur dioxide concentration rate during exposure (μg/m^3)

Cl^-: cumulative chloride deposition rate during exposure (μg/m^2)

T_{exp}: Time of exposure (month)

D: Distance of the location to the sea (km)

α, β, γ, δ, μ, θ, and ε are constants

Multiple variable linear regression analysis was performed in order to find the value of the coefficient in front of the parameters. Table 5.10 shows the results of creating corrosion equations for the eastern and southern regions.

Table 5.10 Dose response function results for eastern and southern regions

Type of steel	Regions	Dose response functions	R^2	Eq. No.
Bare steel	Eastern and Southern region	C (SS400) = 0.059 T + 1.042 RF + 0.423 RH + 0.065 SO_2 +1.054 T_{exp} +0.018 CL +2.205 exp(-0.101 D_{sea})	0.96	(5.9)
		C (SM490A) = 0.021 T + 1.56 RF + 0.023 RH + 0.014 SO_2 +1.439 T_{exp} +0.013 CL +4.053 exp(-0.055 D_{sea})	0.96	(5.10)
HDG steel	Eastern and Southern region	C(SS400) = 0.001 T + 0.127 RF + 0.141 RH + 0.001 SO_2 +0.026 T_{exp} +0.002 CL +0.160 exp(-0.314 D_{sea})	0.83	(5.11)
		C (SM490A) = 0.001 T + 0.145 RF + 0.054 RH + 0.002 SO_2 +0.024 T_{exp} +0.004 CL +0.204 exp(-0.340 D_{sea})	0.87	(5.12)

5.3.2 Thickness loss from corrosion equation

Along with the corrosivity classification by ISO 9223 for bare steel and HDG steel, Table 5.11 shows the findings of first-year thickness loss at 44 locations from the Thai Meteorological Department (TMD). By replacing the atmospheric parameters and SO_2 concentration data in the dose response function, these first-year thickness loss values are achieved. All 44 locations for bare steel SS400 and SM490A were classified as C2. Even though SS400 and SM490A were under the C2 classification, their proportions of thickness loss values differed. Table 5.12 displays the percentage of thickness loss values for each interval for 44 locations from the Thai Meteorological Department. The thickness loss for SS400 was found to be 40.9% for the thickness loss range of 10 to 15 microns and 2.3% for the thickness loss range of 15 to 20 microns, while the thickness loss for SM490A was found to be 29.6% for the thickness loss range of 10 to 15 microns and 13.6% for the thickness loss range of 15 to 20 microns. This indicates that SM490A has more places than SS400 in the higher thickness loss range. The test findings proved that SM490A bare steel rusted more quickly than SS400 grade. The majority of the stations have SM490A thickness losses that are greater than SS400. The composition of the steel itself is another factor. Table 3.2 demonstrates that SM490A has a higher percentage of carbon (C) in its chemical composition than SS400. Since copper (Cu) is one of the chemical elements used to stop steel from corroding, SS400 contains a larger amount of Cu than SM490A.

87.7% of the 44 locations from the Thai Meteorological Department (TMD) for HDG steel SS400 and SM490A were categorized as C2, and 2.3% as C3. Since the zinc coating on HDG sacrifices itself to shield naked steel from corrosion, the proportion of each thickness loss interval is the same for both grades. Table 5.12 shows that the interval between 0.4 and 0.7 microns has greater percentages (81.8%) for both grades than other intervals. In the northern and central parts of Thailand, the thickness loss of HDG steel is thought to be between 0.4 and 0.7 microns.

Table 5.11 First-year thickness loss and corrosivity category by ISO 9223 of bare and HDG steel at 44 sites from TMD in Central, Northern, Northeastern, and Western Thailand.

No.	Location	Bare steel				HDG Steel			
		SS 400	Categ.	SM 490A	Categ.	SS 400	Categ.	SM 490A	Categ.
1	Chiang Rai	4.11	C2	4.54	C2	0.43	C2	0.41	C2
2	Mae Hong Son	3.84	C2	3.62	C2	0.30	C2	0.30	C2
3	Phayao	4.02	C2	4.15	C2	0.37	C2	0.36	C2
4	Chiang Mai	5.19	C2	5.31	C2	0.40	C2	0.40	C2
5	Tha wang pha	11.63	C2	11.33	C2	0.60	C2	0.61	C2
6	Nan	11.49	C2	10.99	C2	0.56	C2	0.57	C2
7	Lamphun	13.83	C2	15.06	C2	0.58	C2	0.52	C2
8	Lampang	14.01	C2	15.55	C2	0.56	C2	0.51	C2
9	Mae Sariang	4.16	C2	4.14	C2	0.36	C2	0.36	C2
10	Phrae	3.84	C2	3.85	C2	0.33	C2	0.33	C2
11	Uttaradit	9.54	C2	9.28	C2	0.52	C2	0.53	C2
12	Bhumibol Dam	4.27	C2	4.88	C2	0.46	C2	0.44	C2
13	Tak	4.22	C2	4.78	C2	0.45	C2	0.43	C2
14	Mae Sot	4.06	C2	4.80	C2	0.46	C2	0.44	C2
15	Umphang	4.12	C2	4.56	C2	0.43	C2	0.41	C2
16	Phitsanulok	8.97	C2	8.64	C2	0.50	C2	0.50	C2
17	Lom sak	6.30	C2	5.99	C2	0.36	C2	0.37	C2
18	Phetchabun	8.43	C2	8.00	C2	0.43	C2	0.44	C2
19	Wichian Buri	11.53	C2	11.43	C2	0.62	C2	0.62	C2
20	Kamphaeng Phet	9.05	C2	8.93	C2	0.54	C2	0.53	C2
21	Nong Khai	12.33	C2	12.50	C2	0.70	C3	0.69	C2
22	Loei	6.87	C2	6.76	C2	0.45	C2	0.45	C2
23	Udon Thani	7.16	C2	6.90	C2	0.41	C2	0.42	C2
24	Nakhon Phanom	11.76	C2	11.97	C2	0.69	C2	0.68	C2
25	Sakon Nakhon	12.49	C2	11.99	C2	0.62	C2	0.62	C2
26	Mukdahan	12.50	C2	12.06	C2	0.62	C2	0.63	C2
27	Khon Kaen	13.52	C2	14.80	C2	0.54	C2	0.50	C2
28	Kosum Phisai	14.02	C2	15.26	C2	0.59	C2	0.53	C2
29	Roi Et	14.08	C2	15.30	C2	0.60	C2	0.54	C2
30	Chaiyaphum	9.38	C2	9.13	C2	0.51	C2	0.51	C2
31	Ubon Ratchathani	13.20	C2	13.25	C2	0.73	C3	0.72	C3
32	Tha Tum	9.59	C2	9.02	C2	0.48	C2	0.49	C2
33	Surin	9.69	C2	9.66	C2	0.57	C2	0.57	C2
34	Nakhon Ratchasima	9.38	C2	9.05	C2	0.50	C2	0.50	C2
35	Chok Chai	9.45	C2	9.25	C2	0.52	C2	0.53	C2
36	Nang Rong	9.74	C2	9.63	C2	0.57	C2	0.56	C2
37	Nakhon Sawan	11.77	C2	11.36	C2	0.59	C2	0.60	C2
38	Bua Chum	11.49	C2	11.20	C2	0.59	C2	0.59	C2
39	Lop Buri	11.69	C2	11.21	C2	0.58	C2	0.58	C2
40	Suphan Buri	13.32	C2	12.53	C2	0.61	C2	0.62	C2
41	Thong Pha Phum	4.94	C2	5.74	C2	0.52	C2	0.49	C2
42	Kanchanaburi	4.61	C2	4.48	C2	0.34	C2	0.34	C2
43	Bangkok Airport	14.06	C2	15.48	C2	0.57	C2	0.52	C2
44	Bangkok Metropolis	15.13	C2	16.45	C2	0.68	C2	0.58	C2

Note: All locations are from Thailand Meteorological Department

Table 5.12 The proportion percentages of the thickness loss values in each interval of 44 meteorological stations: (a) Bare steel, (b) HDG steel.

(a).

Thickness loss range (µm)	Bare steel	
	SS400	SM490A
≤ 1.3	0%	0%
$1.3 < r_{corr} \leq 5$	25%	22.7%
$5 < r_{corr} \leq 10$	31.8%	34.1%
$10 < r_{corr} \leq 15$	40.9%	29.6%
$15 < r_{corr} \leq 20$	2.3%	13.6%
$20 < r_{corr} \leq 25$	0%	0%

(b).

Thickness loss range (µm)	HDG steel	
	SS400	SM490A
≤ 0.1	0%	0%
$0.1 < r_{corr} \leq 0.4$	15.9%	15.9%
$0.4 < r_{corr} \leq 0.7$	81.8%	81.8%
$0.7 < r_{corr} \leq 1$	2.3%	2.3%
> 1	0%	0%

Table 5.13 First-year thickness loss and corrosivity category by ISO 9223 of bare and HDG steel at 28 sites from TMD in Eastern and Southern Thailand.

No.	Location	Bare steel				HDG Steel			
		SS 400	Categ.	SM 490A	Categ.	SS 400	Categ.	SM 490A	Categ.
1	Prachin Buri	18.90	C2	21.13	C2	0.68	C2	0.66	C2
2	Kabin Buri	18.92	C2	21.26	C2	0.69	C2	0.67	C2
3	Aranyaprathet	18.27	C2	20.97	C2	0.65	C2	0.63	C2
4	Chon Buri	22.90	C2	25.54	C3	0.89	C3	1.04	C3
5	Ko Sichang	22.45	C2	25.67	C3	0.93	C3	1.08	C3
6	Pattaya	22.59	C2	26.00	C3	0.94	C3	1.09	C3
7	Sattahip	23.74	C2	27.63	C3	1.08	C3	1.26	C3
8	Rayong	22.61	C2	25.38	C3	0.83	C3	0.93	C3
9	Chanthaburi	21.61	C2	26.58	C3	0.99	C3	1.02	C3
10	Khlong Yai	23.55	C2	31.09	C3	1.40	C3	1.57	C3
11	Phetchaburi	17.36	C2	20.57	C2	0.60	C2	0.56	C2
12	Hua Hin	19.39	C2	24.06	C2	0.73	C3	0.73	C3
13	Prachuap Khiri Khan	19.96	C2	24.53	C2	0.81	C3	0.86	C3
14	Chumphon	21.31	C2	25.43	C3	0.82	C3	0.82	C3
15	Surat Thani	20.11	C2	23.73	C2	0.69	C2	0.68	C2
16	Ko Samui	21.44	C2	25.54	C3	0.82	C3	0.82	C3
17	Nakhon Si Thammarat	18.75	C2	25.09	C3	0.87	C3	0.84	C3
18	Songkhla	22.04	C2	26.45	C3	0.93	C3	0.95	C3
19	Hat Yai Airport	19.14	C2	21.78	C2	0.70	C2	0.68	C2
20	Pattani Airport	17.61	C2	23.40	C2	0.70	C2	0.64	C2
21	Narathiwat	19.35	C2	25.84	C3	0.88	C3	0.86	C3
22	Ranong	25.18	C3	31.29	C3	1.31	C3	1.38	C3
23	Takua Pa	22.89	C2	28.10	C3	1.06	C3	1.09	C3
24	Phuket	20.62	C2	24.61	C2	0.75	C3	0.74	C3
25	Phuket airport	22.50	C2	27.16	C3	0.98	C3	1.03	C3
26	Ko lanta	19.03	C2	25.40	C3	0.84	C3	0.81	C3
27	Trang Airport	17.53	C2	22.99	C2	0.77	C3	0.73	C3
28	Satun	21.24	C2	26.21	C3	0.89	C3	0.89	C3

Note: All locations are from Thailand Meteorological Department

Table 5.14 The proportion percentages of the thickness loss values in each interval of 28 meteorological stations: (a) Bare steel, (b) HDG steel.

(a).

Thickness loss range (µm)	Bare steel	
	SS400	SM490A
≤ 1.3	0%	0%
$1.3 < r_{corr} \leq 5$	0%	0%
$5 < r_{corr} \leq 10$	0%	0%
$10 < r_{corr} \leq 15$	0%	0%
$15 < r_{corr} \leq 20$	40%	0%
$20 < r_{corr} \leq 25$	56%	39%
$25 < r_{corr} \leq 35$	4%	61%

(b).

Thickness loss range (µm)	HDG steel	
	SS400	SM490A
≤ 0.1	0%	0%
$0.1 < r_{corr} \leq 0.4$	0%	0%
$0.4 < r_{corr} \leq 0.7$	25%	25%
$0.7 < r_{corr} \leq 1$	61%	43%
> 1	14%	32%

Along with the corrosivity classification by ISO 9223 for bare steel and HDG steel, Table 5.13 shows the findings of first-year thickness loss at 28 locations from the TMD. By replacing the atmospheric parameters, SO_2, and chloride data in the dose response function, these first-year thickness loss values are achieved. All 28 locations for bare steel SS400 were classified as C2, except only one station was in C3. For bare steel SM490A, 39% of the 28 stations were in C2, and 61% were in C3. It means that the bare steel SM490A has a more severe condition than the SS400. 75% of the 28 locations from TMD for HDG steel SS400 and SM490A were categorized as C3, and 25% as C2. HDG steel has the same percentage of stations in the same corrosivity classification for both grades. The proportions of thickness loss range values were shown in Table 5.14. For bare steel SM490A, 61% of TMD stations reached a thickness loss in the highest range of 25 to 35 microns, which was higher than SS400, only 4%. It is confirmed that bare steel SM490A has higher thickness loss than SS400. For HDG steel, 32% of TMD stations reached a thickness loss in the highest range of 1 to 2 microns, which was higher than SS400, only 14%.

5.4 Corrosion map

5.4.1 Corrosion map for central and northern region

The corrosivity map of the central, northern, northeastern, and western regions of Thailand for bare steel is displayed in Figure 5.1 using the generation of the map using the inverse distance weight method (IDW) in QGIS software. The bare steel

SS400 corrosivity map (Figure 5.1 (a)) illustrates the aggressiveness of bare steel corrosion as seen by some of the map's areas that range in color from orange to red. In comparison to other areas in the central region, Bangkok, Pathum Thani, Samut Prakan, and the neighboring areas were noted to be more severe. Since those cities are made up of urban areas and commercially active locations where airborne environmental pollutants like SO_2 are released into the atmosphere, high amounts of SO_2 were discovered there (data presented in section 4.3). The areas of Khon Kaen, Maha Sarakham, Roi Et, and other cities in the northeast were also noted to be aggressive. In those areas, one-year cumulative monthly average values of SO_2 were discovered to be higher than 35 µg/m^3 (Table 4.1). There was a significant thickness loss in the province of Lampang's northern regions. Lampang had a significant one-year cumulative monthly average value of SO_2 with 75.98 µg/m^3 (Table 4.1).

The degree of corrosion revealed a tendency to be slightly similar to that of the bare steel SS400 corrosivity map for the bare steel SM490A (Figure 5.1 (b)). However, compared to SS400, the value and pattern were different all over the map. For instance, the SS400 map displays the center region (Bangkok, Pathum Thani, and Samut Prakan) in a light orange color, indicating that the thickness loss value there ranges from 12.01 to 15 µm/year. However, the same sites in Bangkok, Pathum Thani, and Samut Prakan are demonstrated in orange on the SM490A map, suggesting that the thickness loss value ranges from 15.01 to 18 µm/year. It demonstrated that the thickness loss of SM490A is marginally greater than that of SS400.

The corrosivity map for HDG steel in the central, northern, northeastern, and western regions of Thailand is shown in Figure 5.1 (c) and (d). The map demonstrates that for both grades of HDG steel, the thickness loss value was not greater than 1 µm/year. The most aggressive regions of Thailand can be found in the northeastern provinces of Lampang, Maha Sarakham, and Ubon Ratchathani. The degree of the corrosion severity in the HDG steel SM490A corrosivity map (Figure 5.1 (d)) is not far different to that in the bare steel SS400 corrosivity map. However, compared to SS400, the value and pattern were different all over the map.

(a)

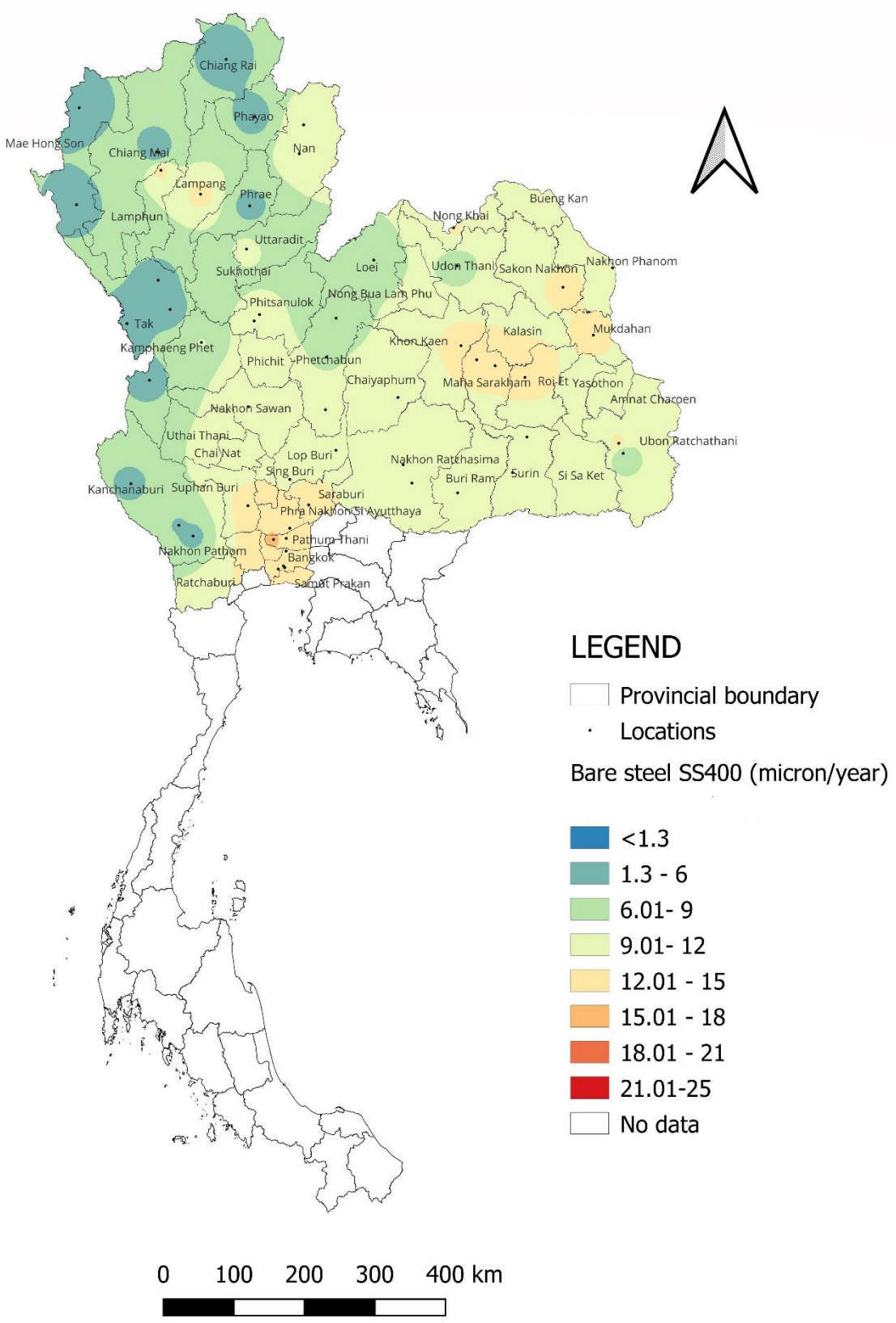
Chiang Rai
Phayao
Mae Hong Son
Chiang Mai
Nan
Lampang
Phrae
Bueng Kan
Nong Khai
Lamphun
Uttaradit
Loei
Udon Thani
Sakon Nakhon
Nakhon Phanom
Sukhothai
Nong Bua Lam Phu
Phitsanulok
Tak
Kalasin
Mukdahan
Khon Kaen
Kamphaeng Phet
Phichit
Phetchabun
Chaiyaphum
Maha Sarakham
Roi-Et
Yasothon
Amnat Charoen
Nakhon Sawan
Uthai Thani
Ubon Ratchathani
Chai Nat
Lop Buri
Nakhon Ratchasima
Sing Buri
Buri Ram
Surin
Si Sa Ket
Kanchanaburi
Suphan Buri
Saraburi
Phra Nakhon Si Ayutthaya
Pathum Thani
Nakhon Pathom
Bangkok
Ratchaburi
Samut Prakan
LEGEND
Provincial boundary
Locations
Bare steel SS400 (micron/year)
<1.3
1.3 - 6
6.01- 9
9.01- 12
12.01 - 15
15.01 - 18
18.01 - 21
21.01-25
No data
0
100
200
300
400 km

(b)

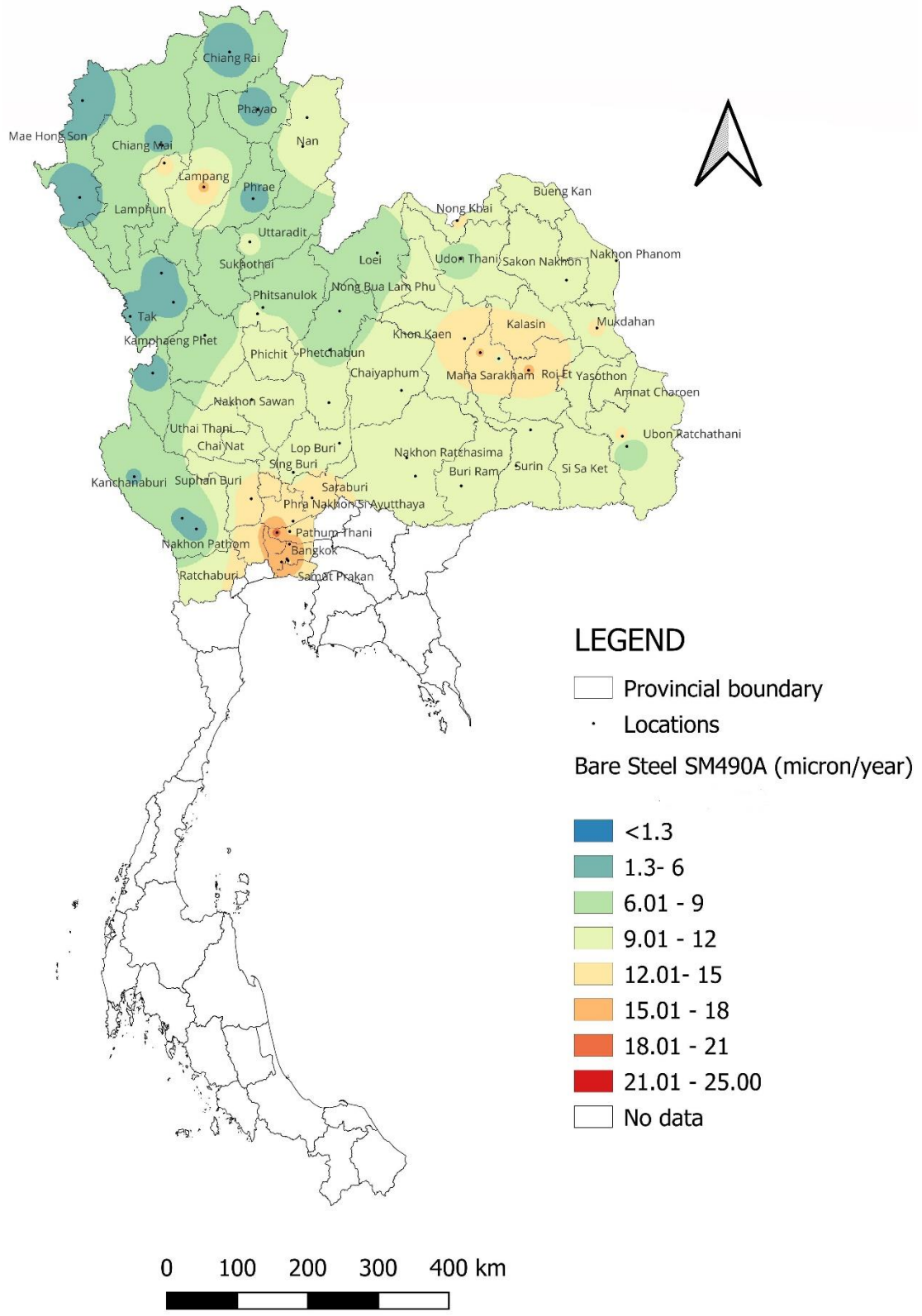
Chiang Rai
Phayao
Mae Hong Son
Chiang Mai
Nan
Lampang
Phrae
Lamphun
Uttaradit
Sukhothai
Loei
Phitsanulok
Nong Bua Lam Phu
Tak
Kamphaeng Phet
Phichit
Phetchabun
Khon Kaen
Chaiyaphum
Nakhon Sawan
Uthai Thani
Chai Nat
Lop Buri
Sing Buri
Kanchanaburi
Suphan Buri
Saraburi
Phra Nakhon Si Ayutthaya
Pathum Thani
Nakhon Pathom
Bangkok
Ratchaburi
Samut Prakan
Bueng Kan
Nong Khai
Udon Thani
Sakon Nakhon
Nakhon Phanom
Kalasin
Mukdahan
Maha Sarakham
Roi Et
Yasothon
Amnat Charoen
Ubon Ratchathani
Nakhon Ratchasima
Buri Ram
Surin
Si Sa Ket
LEGEND
Provincial boundary
Locations
Bare Steel SM490A (micron/year)
<1.3
1.3- 6
6.01 - 9
9.01 - 12
12.01- 15
15.01 - 18
18.01 - 21
21.01 - 25.00
No data
0
100
200
300
400 km

(c)

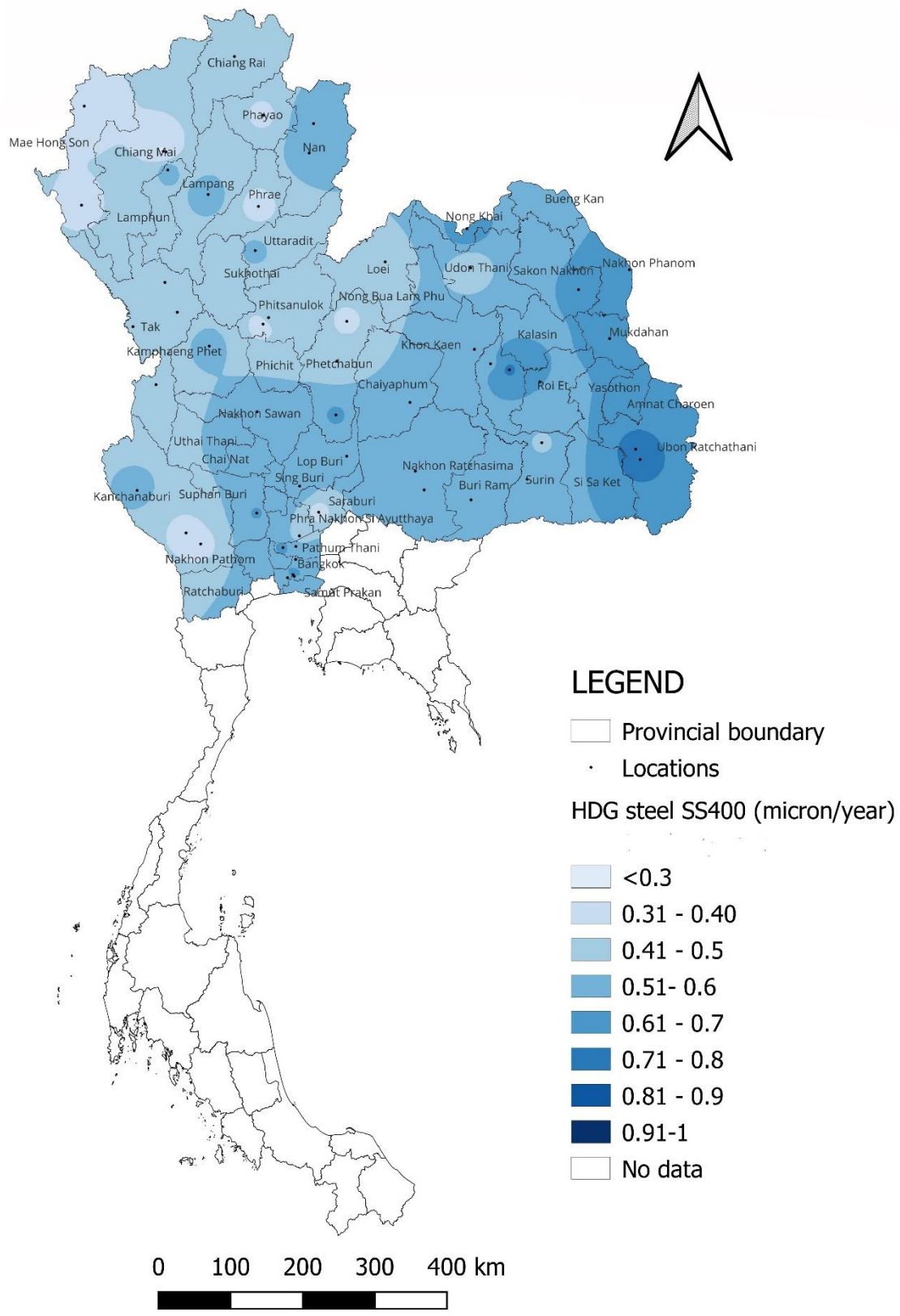
Chiang Rai
Phayao
Mae Hong Son
Chiang Mai
Nan
Lampang
Phrae
Lamphun
Uttaradit
Sukhothai
Loei
Nong Khai
Bueng Kan
Udon Thani
Sakon Nakhon
Nakhon Phanom
Phitsanulok
Nong Bua Lam Phu
Tak
Kamphaeng Phet
Phichit
Phetchabun
Khon Kaen
Kalasin
Mukdahan
Chaiyaphum
Roi Et
Yasothon
Amnat Charoen
Nakhon Sawan
Uthai Thani
Chai Nat
Lop Buri
Sing Buri
Nakhon Ratchasima
Buri Ram
Surin
Si Sa Ket
Ubon Ratchathani
Kanchanaburi
Suphan Buri
Saraburi
Phra Nakhon Si Ayutthaya
Nakhon Pathom
Pathum Thani
Bangkok
Samut Prakan
Ratchaburi
LEGEND
Provincial boundary
Locations
HDG steel SS400 (micron/year)
<0.3
0.31 - 0.40
0.41 - 0.5
0.51- 0.6
0.61 - 0.7
0.71 - 0.8
0.81 - 0.9
0.91-1
No data
0
100
200
300
400 km

(d)

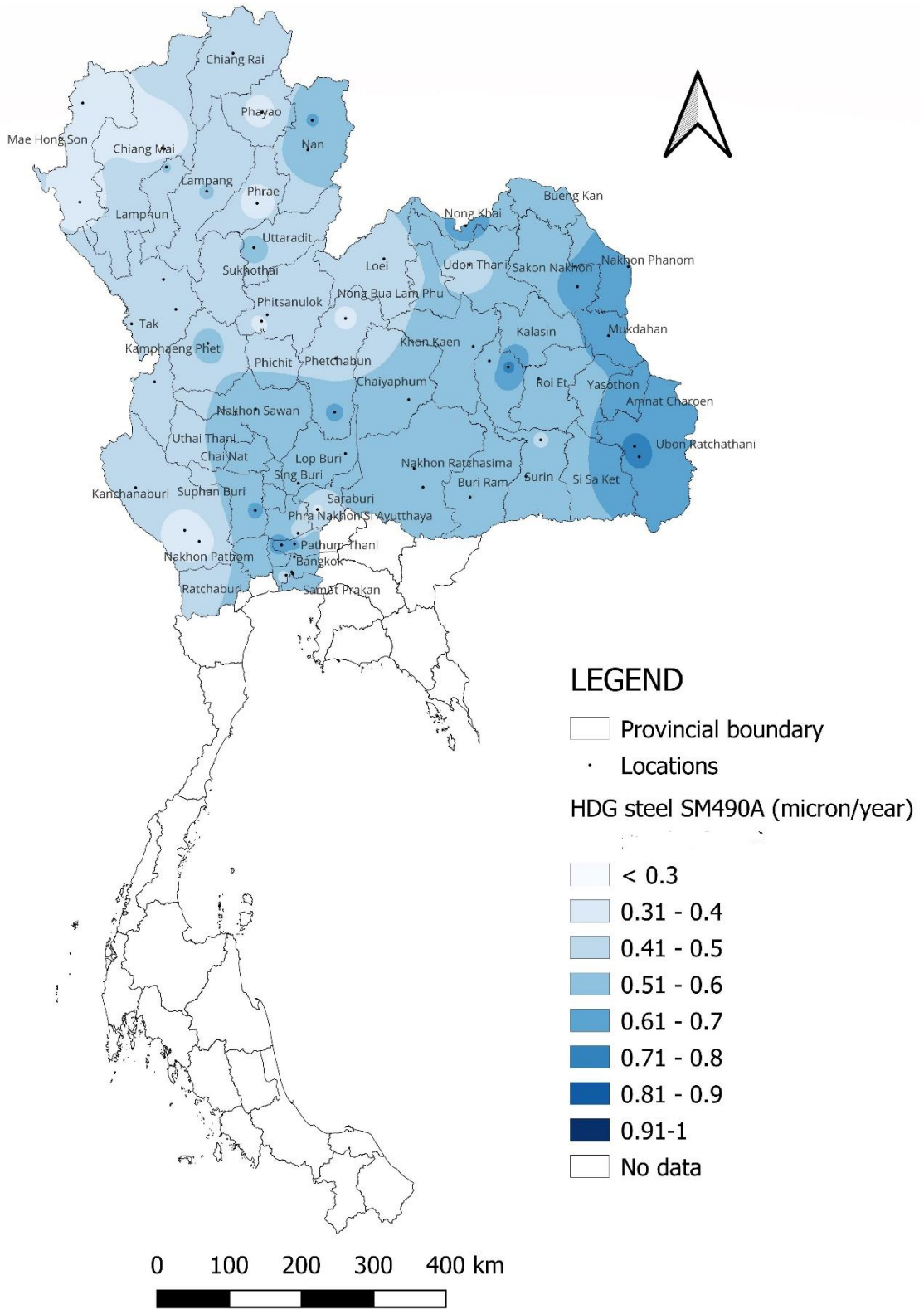

Figure 5.1 Corrosivity map for the northern and the central Thailand of bare steel: (a) SS400, (b) SM490A; HDG steel: (c) SS400, (d) SM490A

5.4.2 Corrosion map for eastern and southern region

Figure 5.2 shows the corrosivity map of the eastern and southern regions of Thailand for bare and HDG steel with both steel grades. Based on the map, it showed that along the shoreline, there is the most aggressive area or location. Steel corrosion along the shoreline is a common and significant issue due to the severe environmental conditions present in coastal areas. Chloride particles transported by sea breezes frequently pollute the air in coastal places. Airborne corrosion may result from these particles settling on steel surfaces. Steel deterioration is accelerated by the mixture of moisture and chloride. Chloride is a significant factor to corrosion due to its corrosive nature. Chloride ions can depassivate the steel, initiating the corrosion process. The corrosion map for bare steel SS400 (Figure 5.2 (a)) shows it is less aggressive than SM490A (Figure 5.2 (a)), as color observation shows a more severe color. This behavior was also found in the real exposure test. The thickness loss of SM490A was found to be slightly higher than SS400. For bare steel maps, it can be observed that at Ranong province (middle of the southern region), the corrosion severity covered the whole region since the shape of the country at this location is small. The west is the Andaman Sea, and the east is the Gulf of Thailand Sea. Both sides of this location are covered by the sea. The geographical characteristics of this location are special because of the shape of the country. For the HDG steel map, the severity of the map is not far different between SS400 and SM490A. However, the pattern of each map for each type of steel is different. All the maps in Figure 5.2 show that when the distance goes far from the shoreline, the severity of the map gets lighter and lighter. The influence of the distance to the sea on the thickness loss of steel will be discussed in Section 5.5.

(a)

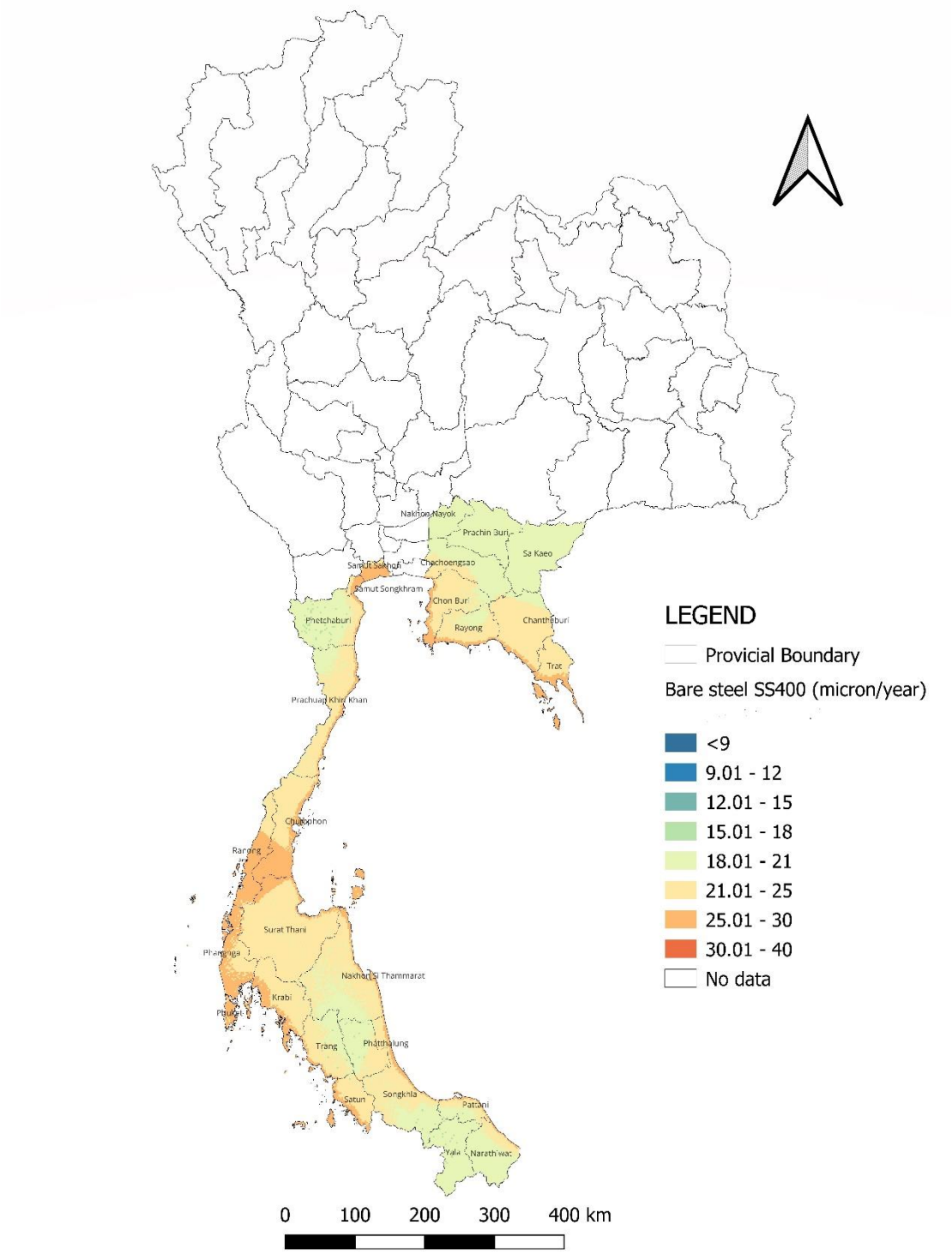
Nakhon Nayok
Prachin Buri
Sa Kaeo
Samut Sakhon
Chachoengsao
Samut Songkhram
Chon Buri
Phetchaburi
Rayong
Chanthaburi
Trat
Prachuap Khiri Khan
Chumphon
Ranong
Surat Thani
Phang Nga
Nakhon Si Thammarat
Krabi
Phuket
Trang
Phatthalung
Songkhla
Satun
Pattani
Yala
Narathiwat
LEGEND
Provicial Boundary
Bare steel SS400 (micron/year)
<9
9.01 - 12
12.01 - 15
15.01 - 18
18.01 - 21
21.01 - 25
25.01 - 30
30.01 - 40
No data
0
100
200
300
400 km

(b)

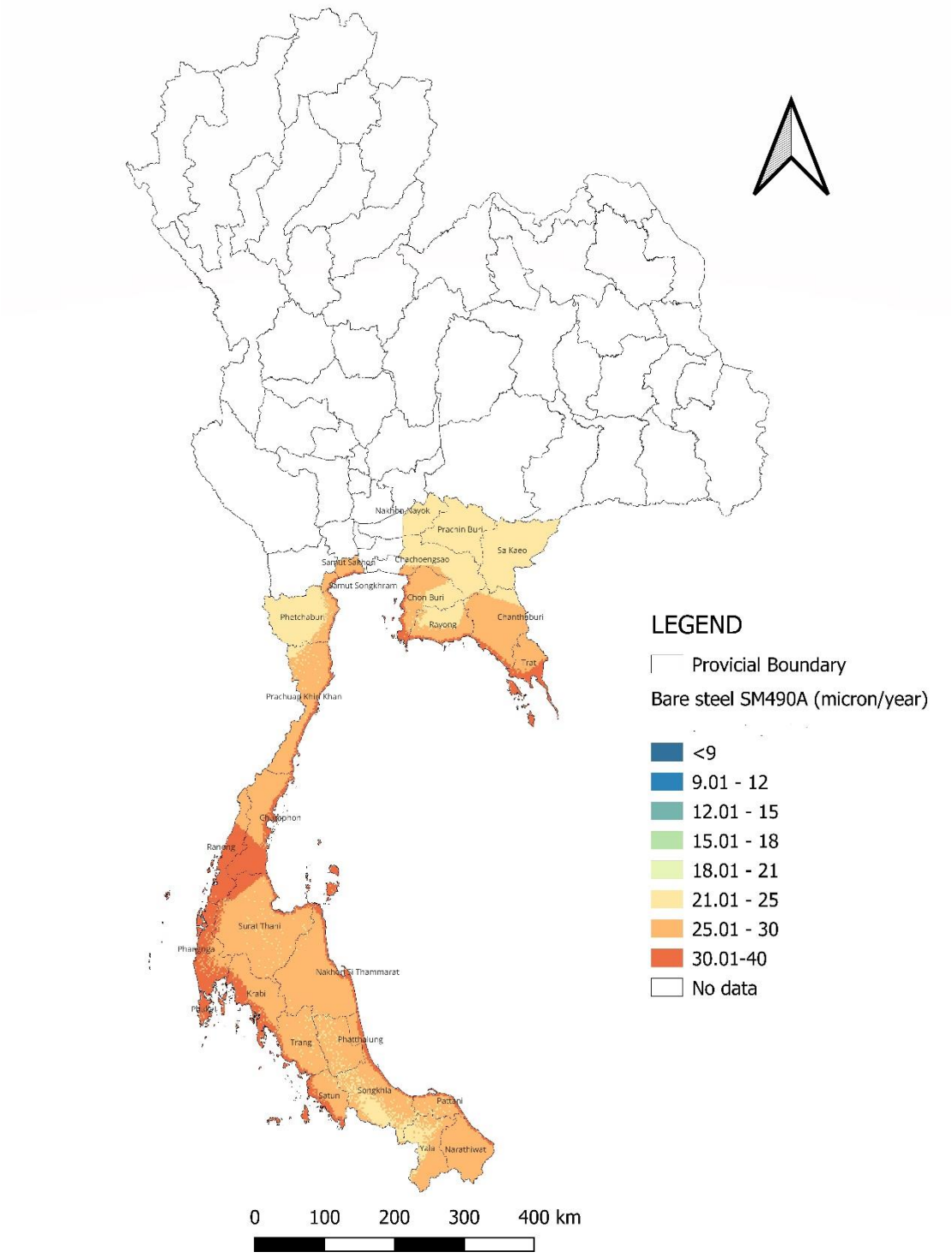
Nakhon Nayok
Prachin Buri
Sa Kaeo
Chachoengsao
Samut Sakhon
Samut Songkhram
Chon Buri
Phetchaburi
Rayong
Chanthaburi
Trat
Prachuap Khiri Khan
Chumphon
Ranong
Surat Thani
Phangnga
Nakhon Si Thammarat
Krabi
Phuket
Trang
Phatthalung
Satun
Songkhla
Pattani
Yala
Narathiwat
LEGEND
Provicial Boundary
Bare steel SM490A (micron/year)
<9
9.01 - 12
12.01 - 15
15.01 - 18
18.01 - 21
21.01 - 25
25.01 - 30
30.01-40
No data
0
100
200
300
400 km

(c)

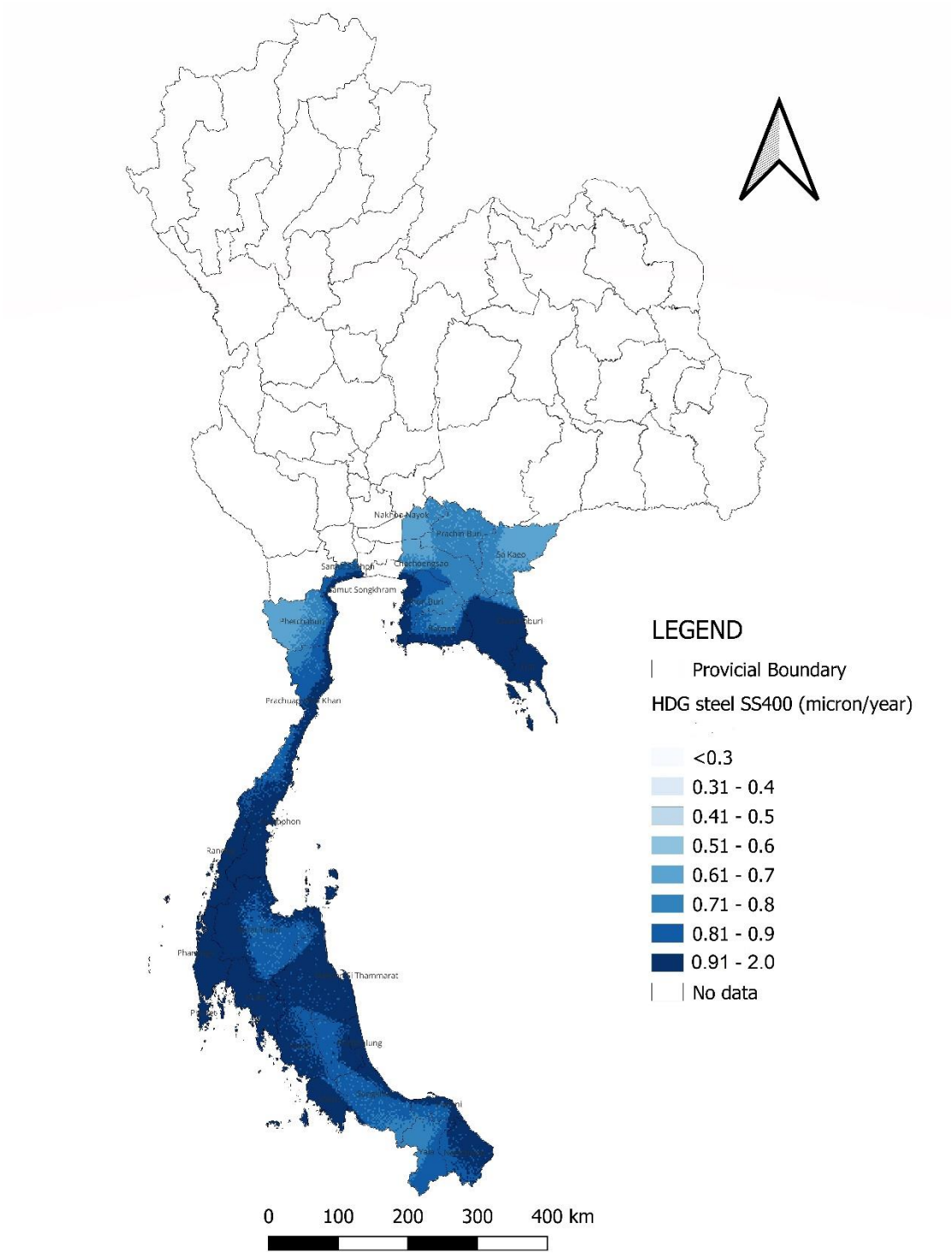
LEGEND
Provicial Boundary
HDG steel SS400 (micron/year)
<0.3
0.31 - 0.4
0.41 - 0.5
0.51 - 0.6
0.61 - 0.7
0.71 - 0.8
0.81 - 0.9
0.91 - 2.0
No data
0
100
200
300
400 km

(d)

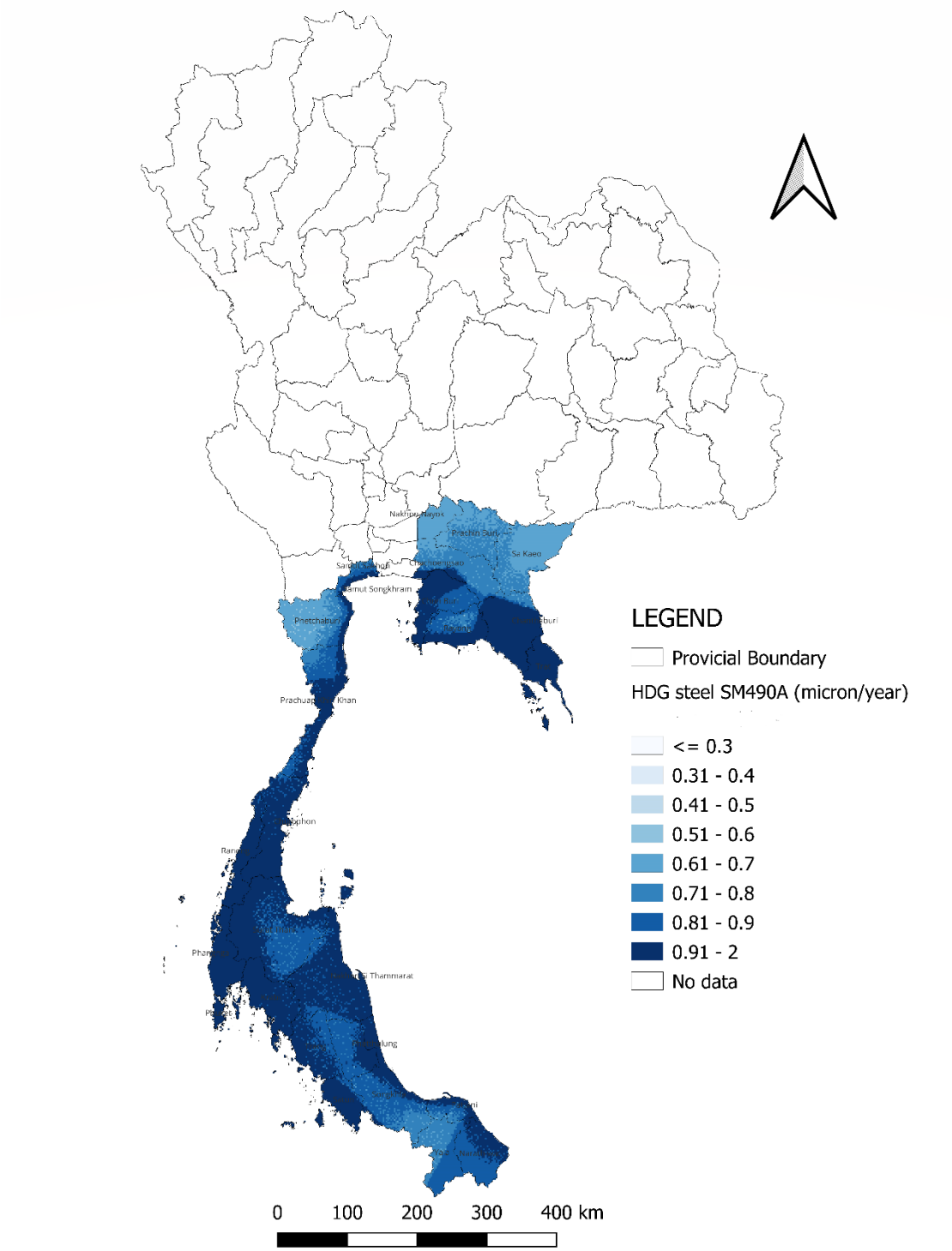

Figure 5.2 Corrosivity map for the eastern and southern Thailand of bare steel: (a) SS400, (b) SM490A; HDG steel: (c) SS400, (d) SM490A

5.5 Thickness loss vs distance to the sea

When conducting corrosion investigations, the correlation between thickness loss and sea distance is frequently taken into account, especially for structures exposed to marine environments. The corrosive processes that materials go through could be influenced by their closeness to the sea. Figure 5.3 shows the plot of the one-year thickness loss of bare steel versus the distance from the sea to the test stations. For bare steel, the graphs of both grades in Figure 5.3 were made with all test stations except station 2 (Mae Moh power plant), since this station is a special location. It is located in the northern region, and the distance to the sea is approximately 540 km. This station is very far from the sea, but the thickness loss obtained from the exposure test is very high since it is influent from the power plant.

Table 5.15 One-year thickness loss at test locations and the distance to the sea

No.	Station name	Bare steel (1 year)		HDG steel (1 year)		Distance to the sea (km)
		SS400 (micron)	SM490A (micron)	SS400 (micron)	SM490A (micron)	
15	Faculty of Engineering, Chiang Mai University	2.97	3.28	0.24	0.25	610.00
2	Mae Moh power plant	41.82	42.31	1.82	2.12	540.00
3	Faculty of Engineering Naresuan University	10.02	9.59	0.30	0.34	360.00
4	Maha Sarakham University	12.11	11.82	0.72	0.73	395.00
5	Ubon Ratchathani University Faculty of Engineering	6.39	6.12	0.74	0.71	425.00
6	Private House (Saraburi province)	13.46	13.48	0.33	0.38	111.00
7	Thai Metal Trade Company Limited (Wangnoi)	11.74	13.98	0.40	0.41	76.00
8	Sangcharoen Galvanizing Limited.	16.55	18.98	0.63	0.69	61.50
9	Sirindhorn International Institute of Technology (SIIT)	13.78	14.86	0.58	0.67	61.50
10	Thai Premium Pipe Company Limited	25.21	26.21	0.76	0.69	7.50
11	Thai Metal Trade Company Limited (Bangkok)	13.94	15.52	0.53	0.43	20.50
12	Iron and Steel Institute of Thailand	13.50	14.38	0.57	0.58	21.00
13	Union Galvanizer	19.68	21.66	0.60	0.61	36.00
14	Sangchareon Eastern Galvanized	19.77	22.11	0.68	0.79	18.50
1	Cotco-SV Eastern Steel Pipe LTD.	17.96	19.77	0.62	0.58	17.10
16	Tha Thung Na Dam Power Plant	5.74	5.28	0.34	0.32	127.00
17	Sahaviriya Steel Industries Public Company Limited	19.49	24.93	0.34	0.32	2.60
18	Prince of Sonkla University	19.75	23.29	0.71	0.73	22.00
19	Rajamangala University of Technology	23.76	28.79	0.73	0.72	0.30

Table 5.15 shows one-year thickness loss at each test location for bare and HDG steel with both grades and the distance to the sea of each lest location.

The estimate of thickness loss can be done by projecting the distance from the sea on the x axis to the trendline curve and then to the y axis in order to get the thickness loss of the steel. The drop trend of thickness loss in bare and HDG steel was observed in both grades while the distance went far from the sea.

(a)

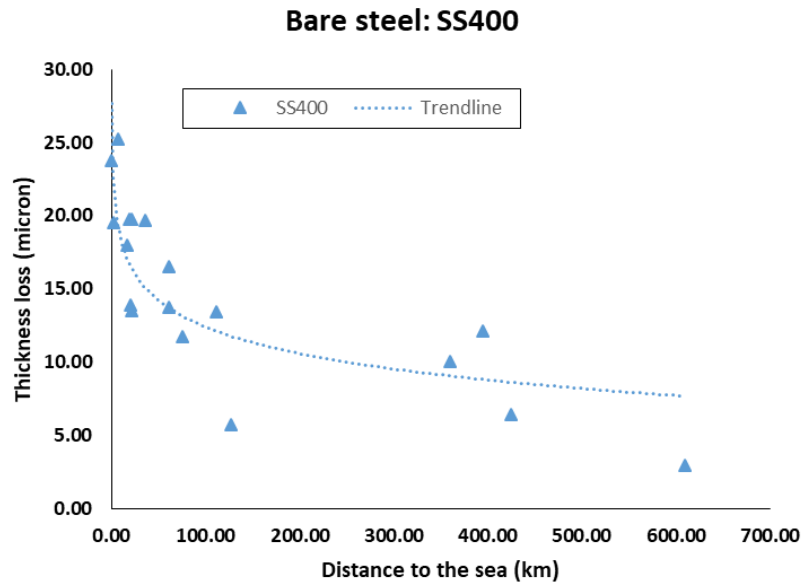

(b)

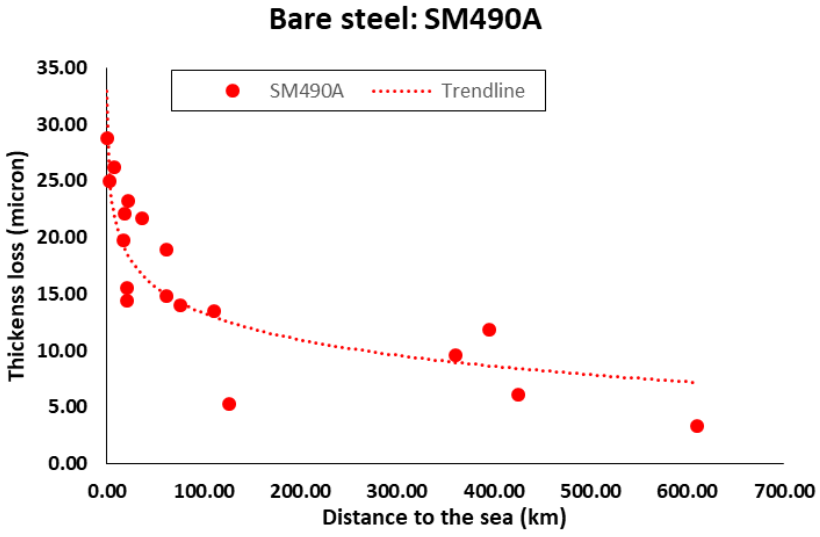

Figure 5.3 Thickness loss versus distance to the sea for bare steel: (a) SS400, (b) SM490A

Figure 5.4 shows the plot of the one-year thickness loss of HDG steel versus the distance from the sea to the test stations. For HDG steel, the graphs of both grades in Figure 5.4 were made with all test stations except stations 2 (Mae Moh power plant), 4, and 5, since these stations are the special locations. Those stations are located in the northern region, and those stations are very far from the sea, but the thickness loss obtained from the exposure test is very high since it is influenced by the power plant and the special conditions like high rainfall in stations 4 and 5. The drop trend of thickness loss in HDG steel was also observed in both grades while the distance went far from the sea.

(a)

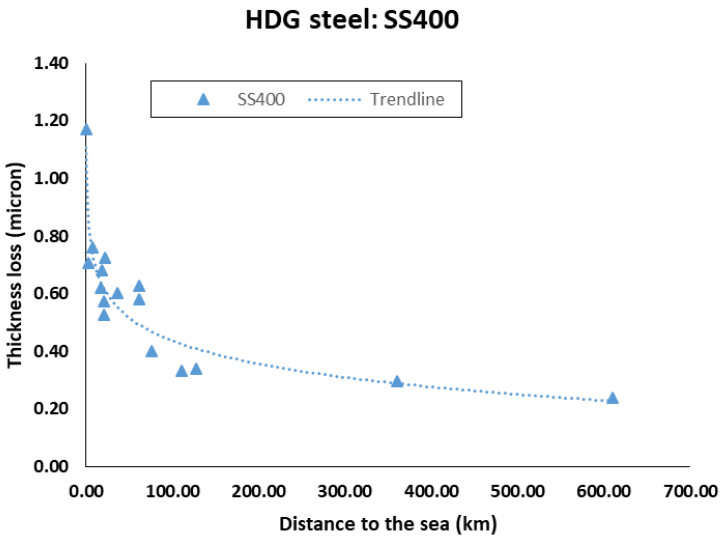

(b)

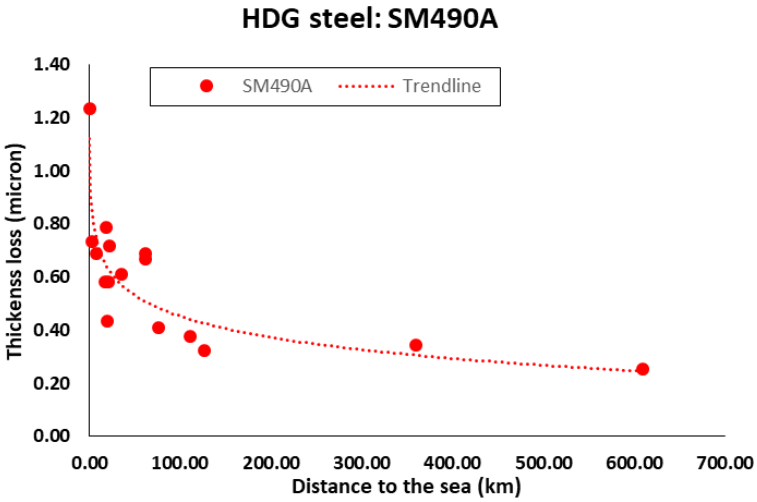

Figure 5.4 Thickness loss versus distance to the sea for HDG steel: (a) SS400, (b) SM490A

5.6 Summary

This chapter provides results of data analysis and findings for corrosivity classification, equations, and map. Presenting the finding results, interpreting them, and discussing their consequences in relation to the research objectives are all done in this chapter. This chapter can be summarized below:

- Corrosivity classification based on the environmental description in DPT 1333-61 was different from the actual exposure test. Corrosivity classification based on the environmental description in DPT 1333-61 should be modified or added more descriptions.
- Corrosion equations with the dose response function of each type of steel for each region were successfully developed.
- A corrosion map of each type of steel for both grades was successfully created. The maps give essential information on the thickness loss throughout the country.
- Thickness loss vs. the distance to the sea is one of the main factors to be studied. Thickness loss value dropped quickly while the distance was far away from the sea.

CHAPTER 6
LONG-TERM THICKNESS LOSS PROJECTION

6.1 Introduction

Projecting the future state of a material or structure, which is necessary to predict thickness loss over time as a result of corrosion, will be illustrated in this chapter. Thickness loss projection could be done by the first year thickness loss results that already made by many researchers, such as the studies of Feliu (Feliu et al., 1993), and Vit Krivy (Krivy et al., 2018). Thickness loss projection offers several advantages in various industries where corrosion is a significant concern. Projecting thickness loss enables the prediction of potential corrosion-related problems in the future. As a result, engineers can plan and schedule maintenance tasks in advance rather than having to respond to unexpected failures. Organizations may optimize resource allocation and save overall maintenance costs by using the thickness loss projection results and scheduling repair tasks in advance. Oftentimes, preventative efforts are more economical than corrective ones. The projection of thickness loss offers valuable information about the anticipated life of materials and structures, which is useful for efficient asset management. This helps organizations in making well-informed choices regarding the replacement or renovation of assets. In this chapter, the results and discussion of the projection thickness loss of bare and HDG steel are presented.

6.2 Thickness loss projection

6.2.1 Thickness loss projection for bare steel

The process of projecting thickness loss from corrosion entails calculating or forecasting the future thickness loss of a material. This estimate is useful for risk assessment, maintenance scheduling, and guaranteeing the long-term structural integrity of assets. Figure 6.1 shows the results of the thickness loss projection as a guide that will help engineers approach the thickness loss projection at each location for bare steel with both grades. The projection was done for a long-term period of up to 25 years. If the projection is made for a longer-term period, a long exposure period for a real exposure test should be conducted to confirm the predicted results. Based on the curve, it shows that the thickness loss increases linearly with time until 10 years. After

10 years, the slope decreases since the rust layer acted as a barrier to slow down the corrosion rate. According to ISO 9224 (ISO9224, 2012), 10 years is the year of corrosion rate of bare steel getting slow and stable.

(a)

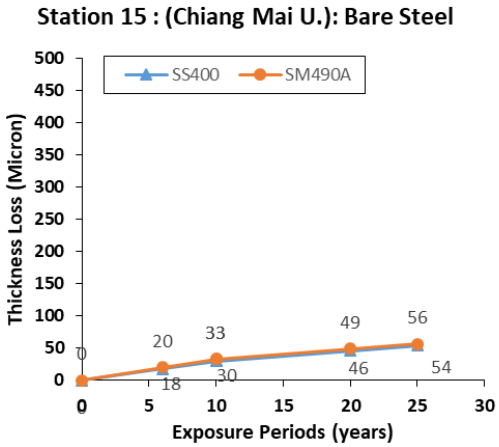

(b)

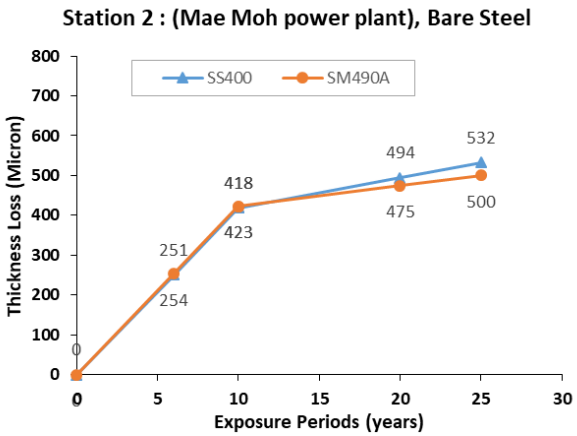

(c)

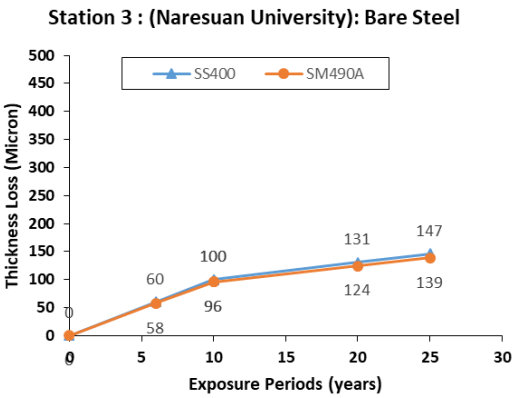

(d)

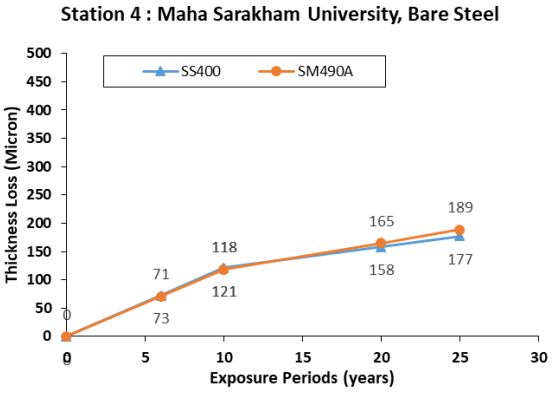

(e)

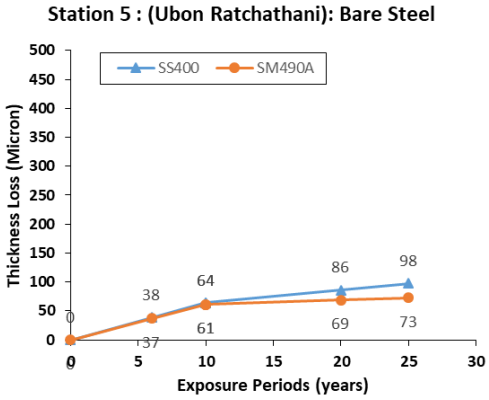

(f)

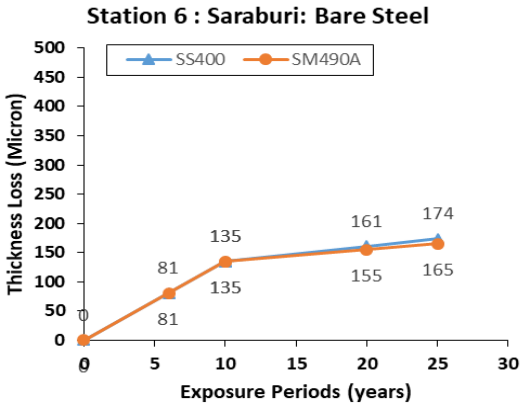

(g)

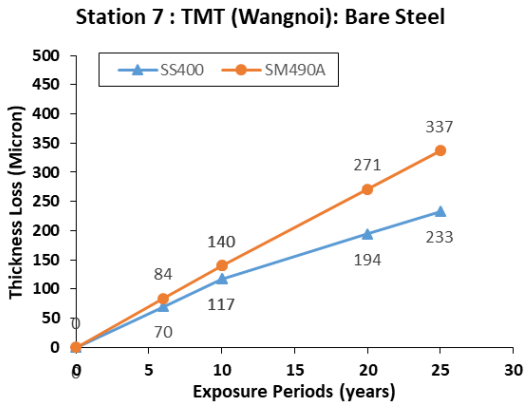
Station 7 : TMT (Wangnoi): Bare Steel
SS400
SM490A
Thickness Loss (Micron)
Exposure Periods (years)
0
84
140
271
337
0
70
117
194
233

(h)

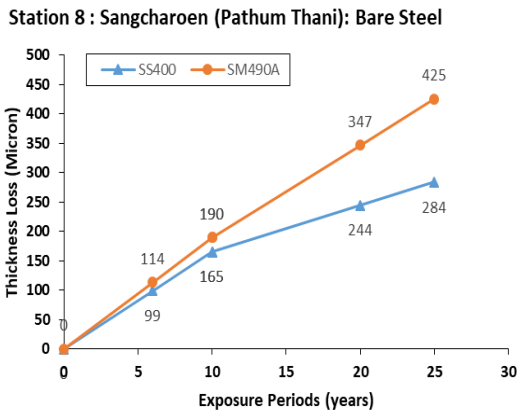
Station 8 : Sangcharoen (Pathum Thani): Bare Steel
SS400
SM490A
Thickness Loss (Micron)
Exposure Periods (years)
0
114
190
347
425
0
99
165
244
284

(i)

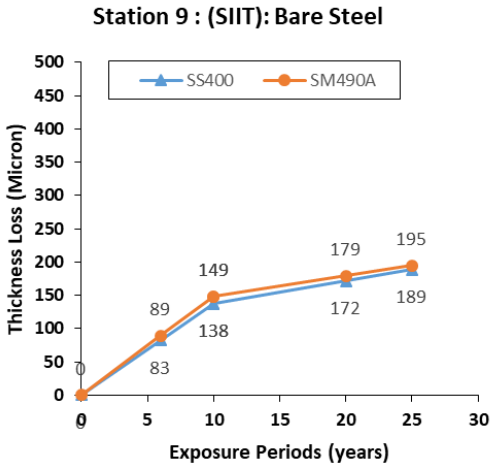
Station 9 : (SIIT): Bare Steel
SS400
SM490A
Thickness Loss (Micron)
Exposure Periods (years)
0
89
149
179
195
0
83
138
172
189

(j)

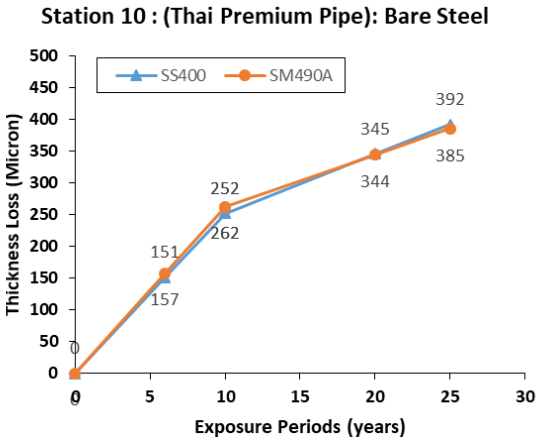
Station 10 : (Thai Premium Pipe): Bare Steel
SS400
SM490A
Thickness Loss (Micron)
Exposure Periods (years)
0
151
252
345
392
0
157
262
344
385

(k)

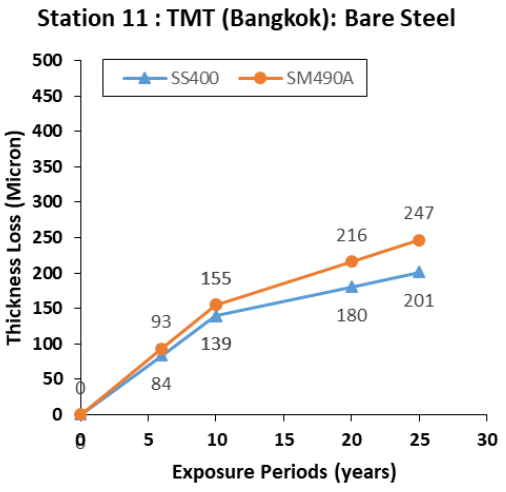
Station 11 : TMT (Bangkok): Bare Steel
SS400
SM490A
Thickness Loss (Micron)
Exposure Periods (years)
0
93
155
216
247
0
84
139
180
201

(l)

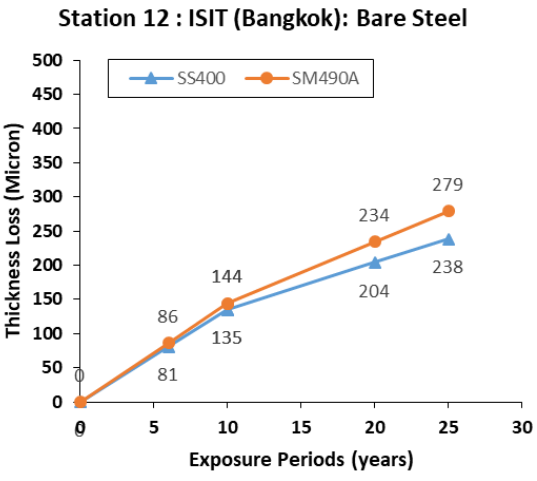
Station 12 : ISIT (Bangkok): Bare Steel
SS400
SM490A
Thickness Loss (Micron)
Exposure Periods (years)
0
86
144
234
279
0
81
135
204
238

(m)

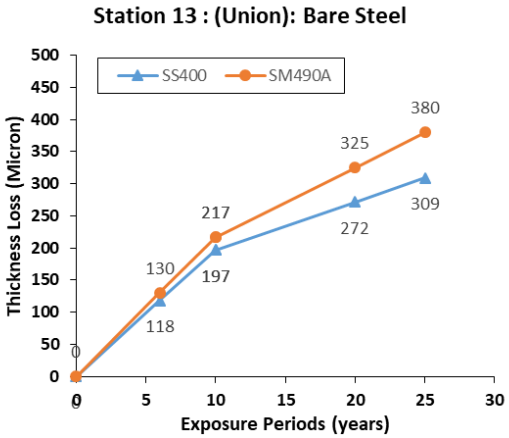
Station 13 : (Union): Bare Steel
SS400
SM490A
Thickness Loss (Micron)
Exposure Periods (years)
380
325
309
272
217
197
130
118

(n)

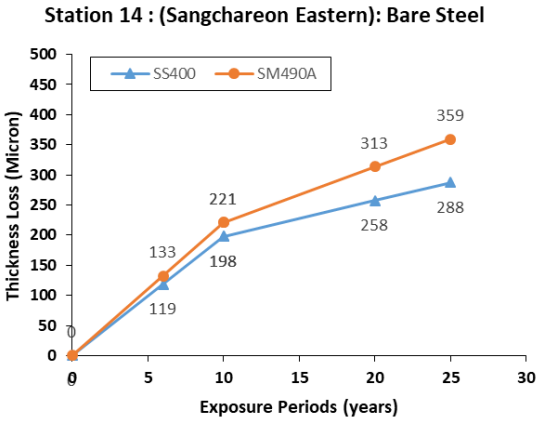
Station 14 : (Sangchareon Eastern): Bare Steel
SS400
SM490A
Thickness Loss (Micron)
Exposure Periods (years)
359
313
288
258
221
198
133
119

(o)

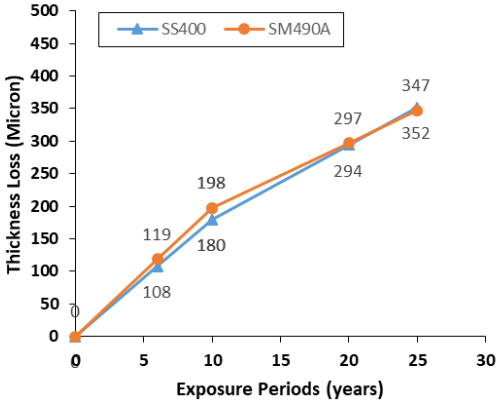
Station 1 : (Cotco-SV): Bare Steel
SS400
SM490A
Thickness Loss (Micron)
Exposure Periods (years)
347
297
352
294
198
180
119
108

(p)

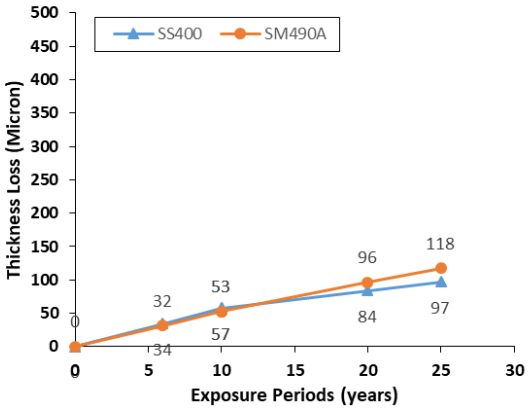
Station 16 : (Tha Thung Na Dam): Bare Steel
SS400
SM490A
Thickness Loss (Micron)
Exposure Periods (years)
118
96
97
84
53
57
32
34

(q)

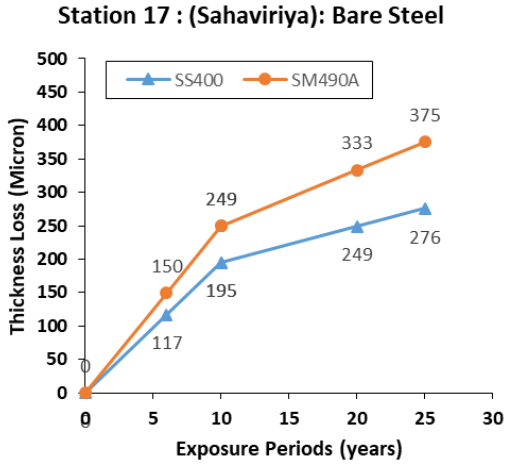
Station 17 : (Sahaviriya): Bare Steel
SS400
SM490A
Thickness Loss (Micron)
Exposure Periods (years)
375
333
276
249
249
195
150
117

(r)

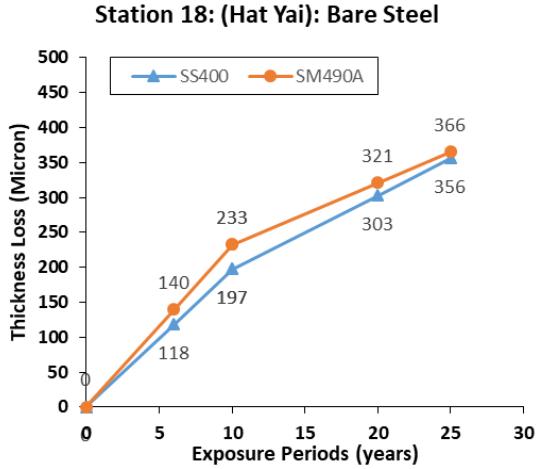
Station 18: (Hat Yai): Bare Steel
SS400
SM490A
Thickness Loss (Micron)
Exposure Periods (years)
366
321
356
303
233
197
140
118

(s)

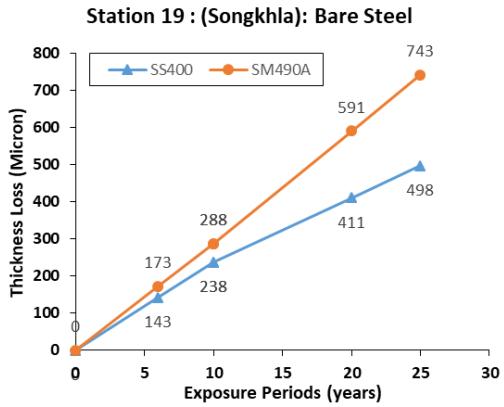

Figure 6.1 Thickness loss projection of bare steel versus exposure time at 19 test locations (a-s)

6.2.2 Thickness loss projection for HDG steel

Figure 6.2 shows the results of the thickness loss projection as a guide that will help engineers approach the thickness loss projection at each location for HDG steel with both grades. Thickness loss projection gives a thorough assessment of the expected long-term corrosion protection effectiveness of HDG steel. This helps in determining how effective the galvanized coating will be in the long run. Organizations are able to forecast when galvanized coating maintenance or refurbishment may be necessary by forecasting thickness loss. This could lower the possibility of unanticipated failures and downtime by enabling proactive planning of maintenance tasks. Cost savings can be achieved by proactively managing the hot-dip galvanized steel maintenance program based on thickness loss forecasts. Thickness loss projection helps in demonstrating and ensuring the continued protective capabilities of the galvanized coating. The projection was done for a long-term period of up to 25 years. If the projection is made for a longer-term period, a long exposure period for a real exposure test should be conducted to confirm the predicted results. Based on the graph, it can be observed that the thickness loss is linear with time, unlike bare steel, where the corrosion rust layer acts as a barrier to slow down the rate of corrosion some years later. Even for that reason (slowing down the rate from bare steel), it also illustrated that the thickness loss of HDG steel is markedly low compared to bare steel.

(a)

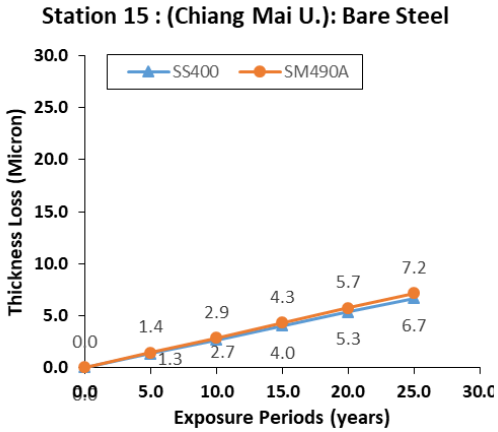
Station 15 : (Chiang Mai U.): Bare Steel
SS400
SM490A
Thickness Loss (Micron)
Exposure Periods (years)
0.0
1.4
2.9
4.3
5.7
7.2
0.0
1.3
2.7
4.0
5.3
6.7

(b)

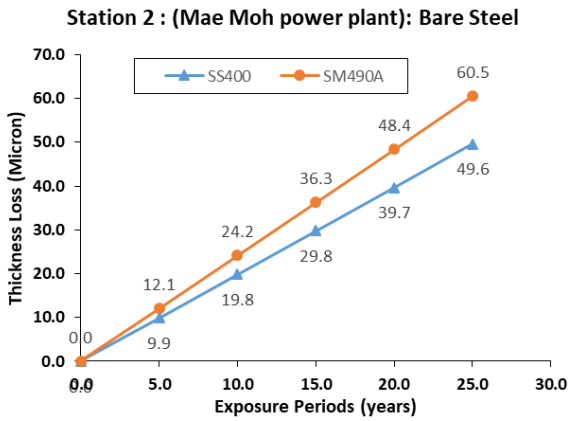
Station 2 : (Mae Moh power plant): Bare Steel
SS400
SM490A
Thickness Loss (Micron)
Exposure Periods (years)
0.0
12.1
24.2
36.3
48.4
60.5
0.0
9.9
19.8
29.8
39.7
49.6

(c)

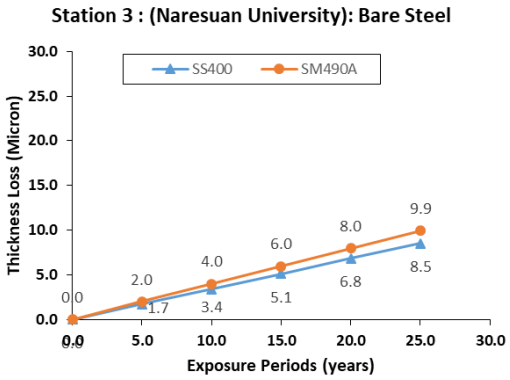
Station 3 : (Naresuan University): Bare Steel
SS400
SM490A
Thickness Loss (Micron)
Exposure Periods (years)
0.0
2.0
4.0
6.0
8.0
9.9
0.0
1.7
3.4
5.1
6.8
8.5

(d)

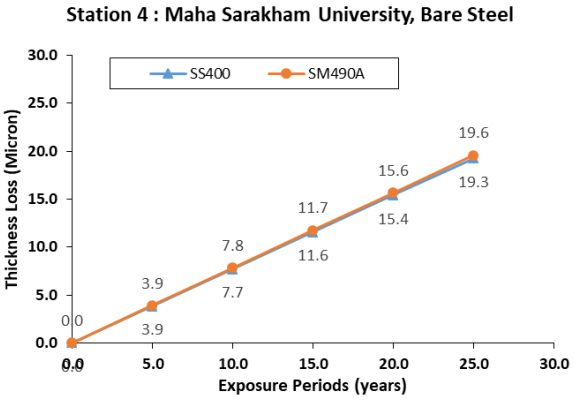
Station 4 : Maha Sarakham University, Bare Steel
SS400
SM490A
Thickness Loss (Micron)
Exposure Periods (years)
0.0
3.9
7.8
11.7
15.6
19.6
0.0
3.9
7.7
11.6
15.4
19.3

(e)

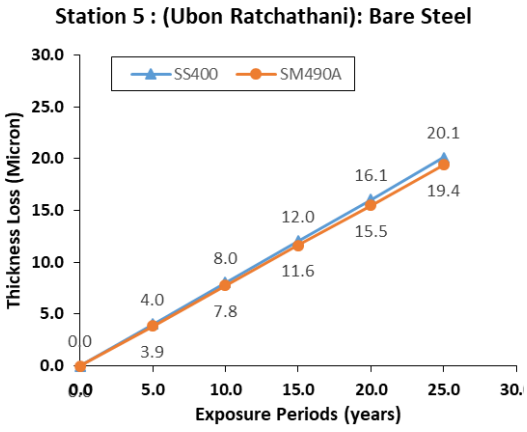
Station 5 : (Ubon Ratchathani): Bare Steel
SS400
SM490A
Thickness Loss (Micron)
Exposure Periods (years)
0.0
4.0
8.0
12.0
16.1
20.1
0.0
3.9
7.8
11.6
15.5
19.4

(f)

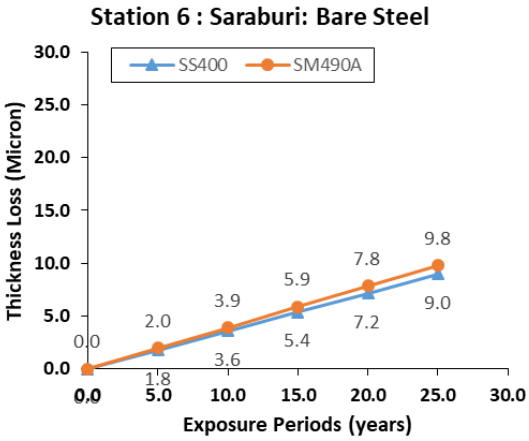
Station 6 : Saraburi: Bare Steel
SS400
SM490A
Thickness Loss (Micron)
Exposure Periods (years)
0.0
2.0
3.9
5.9
7.8
9.8
0.0
1.8
3.6
5.4
7.2
9.0

(g)

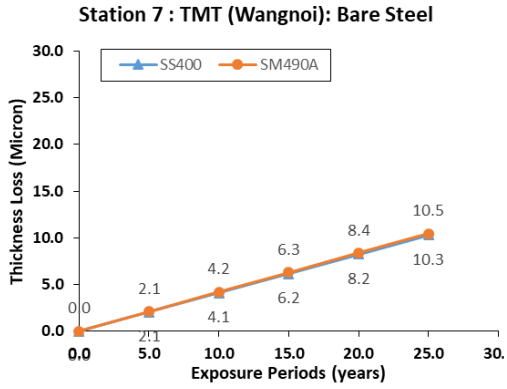
Station 7 : TMT (Wangnoi): Bare Steel
SS400
SM490A
Thickness Loss (Micron)
Exposure Periods (years)
0.0
2.1
4.2
6.3
8.4
10.5
0.0
2.1
4.1
6.2
8.2
10.3

(h)

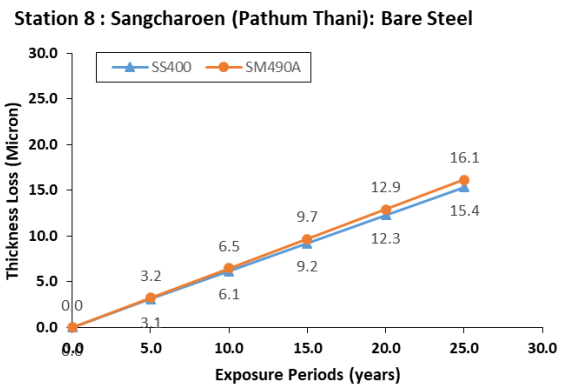
Station 8 : Sangcharoen (Pathum Thani): Bare Steel
SS400
SM490A
Thickness Loss (Micron)
Exposure Periods (years)
0.0
3.2
6.5
9.7
12.9
16.1
0.0
3.1
6.1
9.2
12.3
15.4

(i)

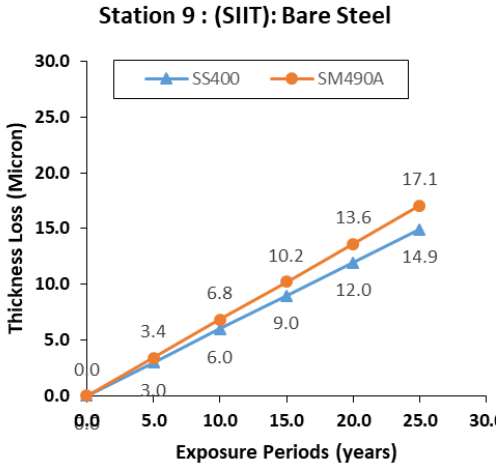
Station 9 : (SIIT): Bare Steel
SS400
SM490A
Thickness Loss (Micron)
Exposure Periods (years)
0.0
3.4
6.8
10.2
13.6
17.1
0.0
3.0
6.0
9.0
12.0
14.9

(j)

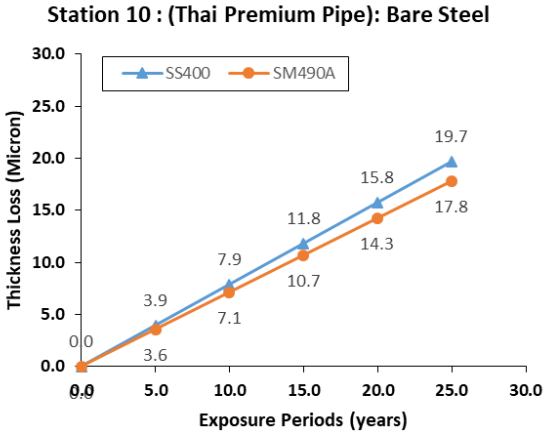
Station 10 : (Thai Premium Pipe): Bare Steel
SS400
SM490A
Thickness Loss (Micron)
Exposure Periods (years)
0.0
3.9
7.9
11.8
15.8
19.7
0.0
3.6
7.1
10.7
14.3
17.8

(k)

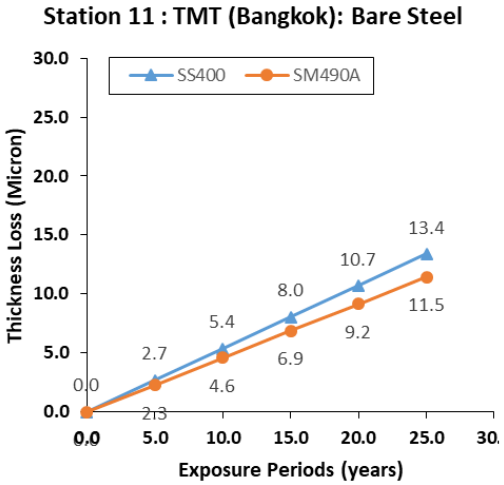
Station 11 : TMT (Bangkok): Bare Steel
SS400
SM490A
Thickness Loss (Micron)
Exposure Periods (years)
0.0
2.7
5.4
8.0
10.7
13.4
0.0
2.3
4.6
6.9
9.2
11.5

(l)

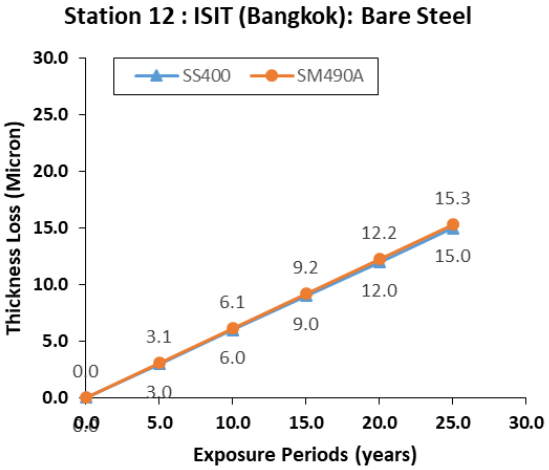
Station 12 : ISIT (Bangkok): Bare Steel
SS400
SM490A
Thickness Loss (Micron)
Exposure Periods (years)
0.0
3.1
6.1
9.2
12.2
15.3
0.0
3.0
6.0
9.0
12.0
15.0

(m)

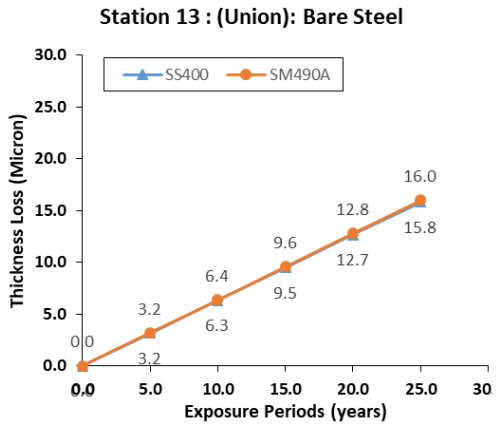
Station 13 : (Union): Bare Steel
SS400
SM490A
Thickness Loss (Micron)
Exposure Periods (years)
0.0
5.0
10.0
15.0
20.0
25.0
30
0.0
3.2
6.4
9.6
12.8
16.0
0.0
3.2
6.3
9.5
12.7
15.8

(n)

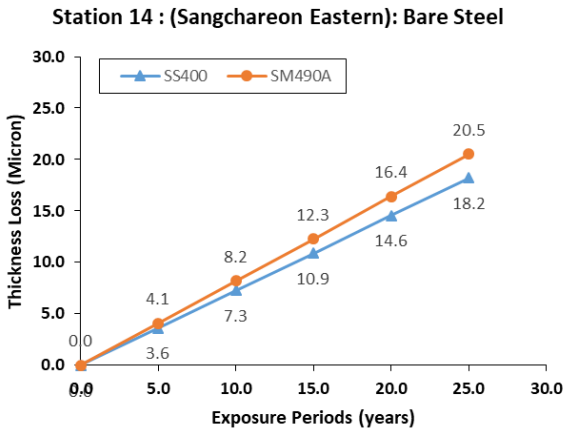
Station 14 : (Sangchareon Eastern): Bare Steel
SS400
SM490A
Thickness Loss (Micron)
Exposure Periods (years)
0.0
5.0
10.0
15.0
20.0
25.0
30.0
0.0
4.1
8.2
12.3
16.4
20.5
0.0
3.6
7.3
10.9
14.6
18.2

(o)

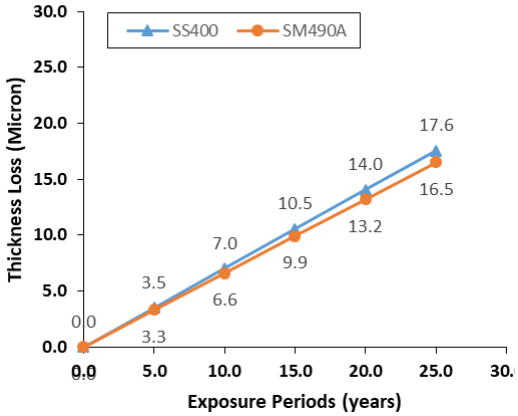
Station 1 : (Cotco-SV): Bare Steel
SS400
SM490A
Thickness Loss (Micron)
Exposure Periods (years)
0.0
5.0
10.0
15.0
20.0
25.0
30.
0.0
3.5
7.0
10.5
14.0
17.6
0.0
3.3
6.6
9.9
13.2
16.5

(p)

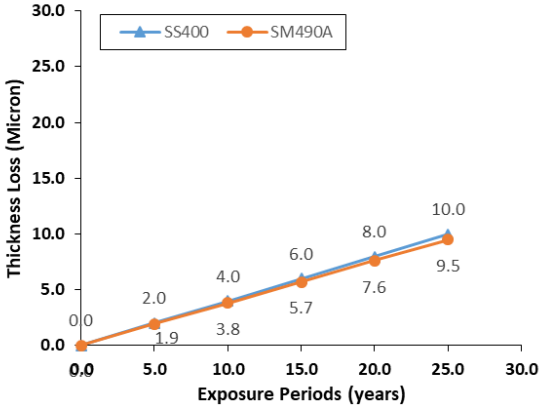
Station 16 : (Tha Thung Na Dam): Bare Steel
SS400
SM490A
Thickness Loss (Micron)
Exposure Periods (years)
0.0
5.0
10.0
15.0
20.0
25.0
30.0
0.0
2.0
4.0
6.0
8.0
10.0
0.0
1.9
3.8
5.7
7.6
9.5

(q)

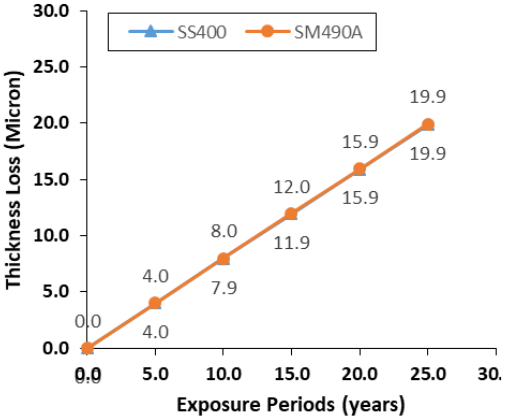
Station 17 : (Sahaviriya): Bare Steel
SS400
SM490A
Thickness Loss (Micron)
Exposure Periods (years)
0.0
5.0
10.0
15.0
20.0
25.0
30.
0.0
4.0
8.0
12.0
15.9
19.9
0.0
4.0
7.9
11.9
15.9
19.9

(r)

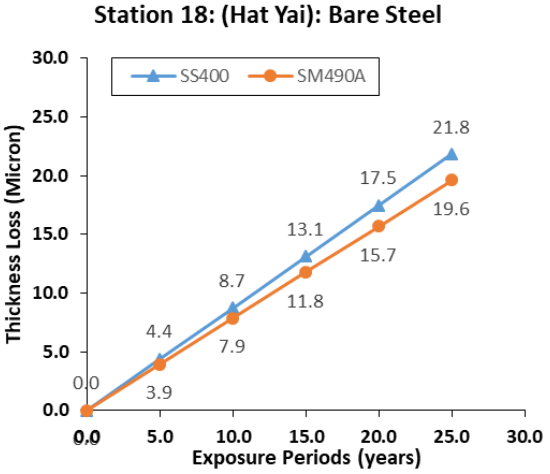
Station 18: (Hat Yai): Bare Steel
SS400
SM490A
Thickness Loss (Micron)
Exposure Periods (years)
0.0
5.0
10.0
15.0
20.0
25.0
30.0
0.0
4.4
8.7
13.1
17.5
21.8
0.0
3.9
7.9
11.8
15.7
19.6

(s)

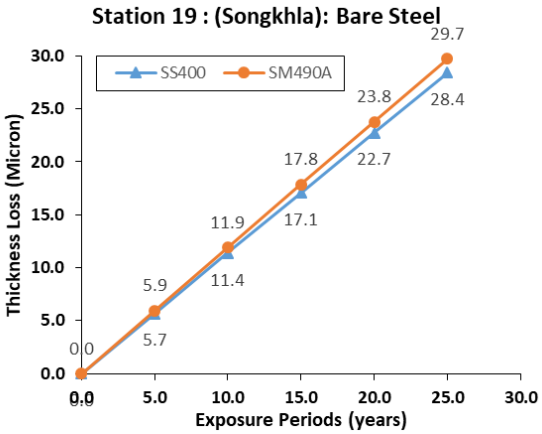

Figure 6.2 Thickness loss projection of HDG steel versus exposure time at 19 test locations (a-s)

Based on a one-year exposure test, the long-term thickness loss projection for both bare steel and HDG steel was examined and displayed. The thickness loss of bare steel was projected using a linear approach for the beginning stage and a power law function fitting curve approach thereafter. On the other hand, the thickness loss prediction for HDG steel was made using the linear fitting curve approach using a plot of thickness loss and exposure duration. Even though HDG steel has a linear development pattern over time, the thickness loss prediction findings at each station were found to be much smaller than bare steel. Without conducting a very long exposure, those results provide important data or valuable information for designers.

For HDG steel, even though the exposure test was conducted over a longer period, the results are not much different since the thickness loss projection of HDG steel was made by multiplying directly with the exposure time. After one year of exposure, the white powder rust was found partly on the HDG specimen, as shown in Figure 4.7 (which does not fully cover all surfaces of the specimen). The rust of HDG steel in the form of powder was easily rinsed away by the rain. It was not strong and packed like bare steel. Most of the researchers recommended that it multiply directly with time since its behavior is linear with time. For bare steel, if the exposure test was conducted over a longer period of time, the result of the thickness loss projection in the first 10 years would be much different since the first part of the thickness loss projection was made by multiplying directly with time. According to ISO 9224, the rust layer of the bare steel would not reduce the corrosion rate after some years of exposure. They

recommended that, after 10 years, the corrosion layer will act as a barrier to slow down the corrosion rate. If the exposure test was conducted over a longer period of time for bare steel, the thickness loss projection value would be lower than the current results at the last part of the projection after 10 years. However, in terms of safety margin, higher results in thickness loss are better. These thickness loss projections will help users and engineers ensure the long-term structural integrity of assets and plan ahead for maintaining strategy. However, the precautions for safety measurement are recommended below.

The following safety measures should be taken into account while working with steel thickness loss projection:

- Make sure the initial thickness measurements are precise and thorough.
- Establish a regular inspection program to monitor the steel structure's condition over time.
- Make sure the corrosion rate variability (chemical reaction or natural disaster influence corrosion rate) will not dramatically change.
- Conduction more longer exposure test to project more long period like 50-100 years.

6.3 Initial and life cycle cost comparison

The aim of the life cycle cost analysis was to compare the costs of different corrosion protection strategies for a structure. The outcomes will be established and can be utilized to identify the corrosion prevention coating that makes the most economical protection method. Figure 6.3 shows the results of the life cycle cost of the structure for public toilet studied by Cocks (Cocks, 2009) for HDG, stainless, painted, and duplex system (HDG + paint) steel. The study structure is located in Roughton Park, Coolangatta, Australia. LLC study of Cocks was followed AS/NZS 4536:1999 standard. The criteria of the life cycle cost are as follows:

- Initial construction: supply materials, fabrication, and application of coating.
- Service life and maintenance: cleaning, and maintenance of coatings
- Decommissioning and demolition: salvage value

The graph in Figure 6.3 shows that at the initial stage, the painted coating cost a bit less than HDG steel, but after using it for a longer period, it cost more than HDG since painted steel costs more for maintenance and decommissioning. The gap between the cost of paint and HDG gets larger and larger while the life of the structure gets longer and longer. For the duplex system, the initial stage costs more than HDG coating and continues to cost even longer for the structure since this coating needs to maintain and decompose the paint, sometimes also maintaining HDG.

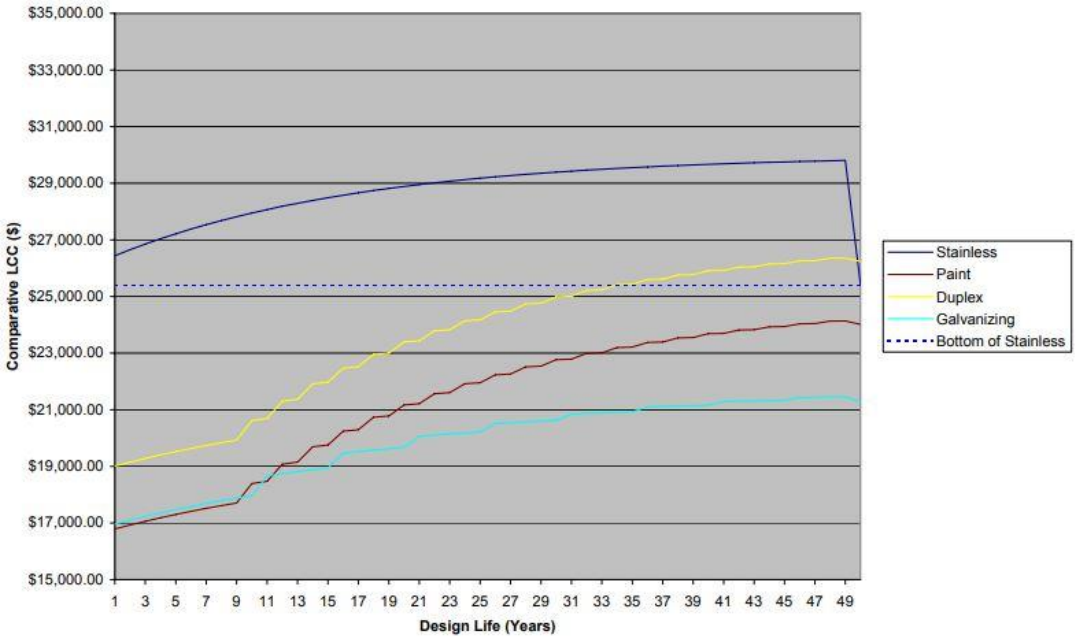

Figure 6.3 LCC of structure (Cocks, 2009)

Table 6.1 Initial and LCC cost ratios of each coating system compared to HDG steel based on Cocks' studies.

Type of steel	Thickness of coating (micron)	Service life		
		Initial	25 years	50 years
HDG	85	1	1	1
Paint	350	0.97	1.09	1.15
Duplex system (HDG+paint)	400 (85+325)	1.12	1.19	1.23

For painted steel in the Cocks study, there are two layers (epoxy and polyurethane). It is the same case with this study. Table 6.1 shows the cost ratios of each coating system compared to HDG steel. The value "1" in the row of HDG steel means that the whole cost is referenced to HDG steel. At 25 or 50 years for HDG steel, the

whole cost includes maintaining and decommissioning the structure for its entire life. For other coatings, the ratio below 1 means that the cost is lower than HDG. The ratio higher than 1 means that the cost is higher than HDG.

Table 6.2 Initial and LCC cost ratios of each coating system compared to HDG steel.

Type of steel	Thickness of coating (micron)	Service life		
		Initial	25 years	50 years
HDG	100	1	1	1
Low grade paint	120	0.39	0.51	0.57
Medium grade paint	160	0.52	0.64	0.70
Premium grade paint	300	0.98	1.07	1.10
Duplex system (HDG+paint)	220 (100+120)	1.05	1.12	1.16

Based on Cocks' studies, linear interpolation was conducted to determine the initial price of HDG since the thickness of the HDG coating in this study is 100 microns. For other coatings, the coefficient was calculated based on the coefficient reference in Table 6.1. The results of the comparison of the initial and LCC cost ratios of each coating system compared to HDG steel in this study are shown in Table 6.2. Below is an example of the calculation ratio.

- Cocks' studies:

HDG: 85 microns, Paint: 350 microns

Thickness ratio (Paint/HDG) = 350/85 = 4.12

With the thickness ratio 4.12, the initial cost is different 3% (HDG=1, paint=0.97)

- This studies:

HDG: 100 microns, Premium grade paint: 300 microns

Thickness ratio (Paint/HDG) = 300/100 = 3

Therefore with the thickness ratio 3, the linear interpolation could be made:

The different initial cost = (3×3%)/4.12 = 2.18 % (HDG =1, paint = 0.98)

For medium grade paint = (160/300)×0.98 = 0.52

For low grade paint = (120/300)×0.98 = 0.39

Based on the coefficients in the table, the low and medium grades of the paint are much lower than HDG steel for the initial cost. However, after the longer life of the

structure, the whole cost of the project is closer and closer to HDG since the paint spends more on maintaining and decommissioning. For the maintenance of the paint, surface preparation, repaint, and paint removal & repaint are considered for the cost of the maintenance. At the end of the service life of a structure, it is the decommissioning stage. At this stage, paint costs more than HDG since paint is a non-recyclable material, whereas HDG (coating with zinc) is 100% recyclable.

For the premium grade paint, the initial cost is nearly equal to HDG steel but after the longer life of the structure, the whole cost of the project is higher than HDG. For the duplex system, the initial cost is a bit higher than HDG since the cost of structure component preparation before coating is the same with HDG and needs little cost for the preparation stage again for painting compared to painting directly with base steel. It costs more on preparation for painting directly with base steel. After the longer life of the structure like 50 years, the cost of duplex system is not much higher than HDG. However, based on the atmospheric test results of this study, duplex system was found to be the best coating system in term of withstanding corrosion and esthetic of the structure.

6.4 Summary

In summary, thickness loss projection is a useful method that adheres to the values of safety, cost-effectiveness, and proactive asset management. It enhances the general sustainability and dependability of materials and structures subjected to corrosion in a variety of environments. Knowing the projected thickness loss helps organizations or engineer ensure the long-term structural integrity of assets. The thickness loss projection of bare and HDG steel could be made up to 25 years. Thickness loss projection gives the prediction of thickness loss over a long-term period. Thickness loss projection are useful to the manufacturing and material development industries because they may be used to improve the corrosion resistance of coatings and materials through this research findings.

CHAPTER 7
CONCLUSION AND RECOMMENDATIONS

Thailand is a tropical country which has a variety of atmospheric characteristics that need be researched in order to comprehend the corrosion behavior throughout the country. After a year of exposure, each coating system has its own corrosion resistance behavior, which can be summed up as follows:

When compared to bare steel, HDG steel's thickness loss was remarkably low. There was no significant difference in the thickness loss for bare steel and HDG steel between the two steel grades (SS400 and SM490A). After a year of exposure, bare steel was completely covered in a layer of rust, while HDG had some white powder rust on it. HDG steel should be used more and more since it is a durable material that can withstand corrosion.

The southern region, where the stations are along the shoreline, had the most aggressive behavior, followed by the eastern and central regions. The less aggressive regions were in the northern, northeastern, and west. According to ISO 9223, all of the stations in the central region were classified as C2. The C2 corrosivity classification for bare steel and C2 & C3 for HDG steel was discovered for the eastern region. Consequently, it could be concluded that this region's corrosivity classification was between C2 and C3. Designers or engineers need to be mindful of its corrosivity. C2 and C3 were discovered for bare steel and C3 for HDG steel in the southern region. In this area, corrosivity was typically classified as C3. For the northern, northeastern, and west regions, the corrosivity was classified as C2, even though the results of some stations were not expected to be that severe and were a special case of station 2 (Mae Moh Power Plant). The assumption was made based on the majority of the test results, geographical characteristics (mountain and forest), atmospheric behavior, and human activities such as business activities, industries, and transportation.

7.1 Contributions

7.1.1 Guidance for choosing coating system

According to the ISO 4628 assessment, the duplex system (G and H) for painted steel was determined to be the best coating system for withstanding corrosion even with paint defects or damages. The most severely corroded areas or areas with a high

concentration of industrial activities are advised to use this coating method. In comparison to premium grade painting (E and F) and the duplex system (G and H), low and medium grade paints (A, B, C, and D) performed the lowest in preventing blistering corrosion or other types of corrosion. The low and medium grade painting systems can be used in C1 corrosive zones. They are not advised for use in extremely corrosive environments. The results of premium grade paint (E and F) showed that they are the best for preventing corrosion types such as blistering, flacking, or rusting. Because of the thickness of the epoxy layer and the moisture maintained at the scribed mark, premium grade paint (E and F) was shown to function poorly at scribed marks. This paint system's epoxy layer should have less thickness. If the paint cannot be shielded from serious early defects that could expose the base steel, this kind of paint system is advised for low to medium corrosivity areas.

7.1.2 Practical contribution

Dose response functions, or relation functions, between the steel's thickness loss and environmental parameters were created by performing multivariable linear regression. The dose response function can be used to forecast thickness loss at specific sites by getting the data from the meteorological department. The dose response function results indicated that they did not deviate significantly from the test results or fall outside of expectations. According to ISO 9223, the results fell into the same corrosivity classification as the outcomes of the exposure test. With the data on environmental parameters, the calculation of the thickness loss of each type of steel can be made by substituting it into the equation.

QGIS software successfully produced an atmospheric corrosivity map using the inverse distance weight method (IDW). Users can obtain the relevant information regarding the thickness loss of HDG and bare steel throughout the corrosivity map. Users and designers can utilize the corrosivity maps to determine the thickness loss value at the site of their intended building. They have two options: either they can reserve thickness loss for the structure's intended year life, or they can estimate the structure's year life using the permitted thickness loss. The severity of the location is also depicted on such maps.

7.2 Limitations

There are certain limitations to this study that should be taken into account. First, the significant factors in this study are based on the current situation of the atmospheric and environmental conditions. As a result, it might not account for the future changes brought on by unexpected events like natural disasters or chemical explosion. Second, long-term thickness loss projections were made based on the first-year results since it had the limitation of study time and budget. It is recommended to conduct a longer exposure period to project a longer period. Last is the quotation price of HDG coating, which depends on each type of steel component of the structure and each company. It also varies depending on each project size. In addition, the quotation price for paint coating and maintenance depends on each construction company. In this study, the cost comparison ratio is based on Cocks' study. It is recommended to make more survey on the cost of HDG coating and painting. Despite these limitations, this study contributes to guidance to choose coating system and offers practical implications for thickness loss information throughout the map.

7.3 Recommendations for future studies

It is advised that more research should be done, particularly with regard to implementing the research's findings—such as the corrosion map—into a website or mobile application. It facilitates the user's control, access and data acquisition. Since, in this research, the thickness projection could be made in 25 years, it is recommended to conduct a longer period of exposure testing in order to predict it for up to 100 years. Other coating materials like zinc-aluminum, zinc-Fe, or zinc-aluminum-magnesium coating are recommended for future study in order to reduce the price of coating and optimize performance in the particular location.

7.4 Closure

This study was conducted to address the need for atmospheric exposure test to assess the durability and performance of bare, painted, and HDG steel under atmospheric exposure conditions. This findings facilitates the field of atmospheric corrosion of steel by providing empirical evidence of thickness loss value, their corrosion equation relationships among environmental factors, and their performance withstand corrosion.

REFERENCES

Antunes, R. A., Ichikawa, R. U., Martinez, L. G., & Costa, I. (2014). Characterization of Corrosion Products on Carbon Steel Exposed to Natural Weathering and to Accelerated Corrosion Tests. *International Journal of Corrosion, 2014*, 419570. doi:10.1155/2014/419570

AGA (2023). Process of hot-dip galvanizing Retrieved from https://galvanizeit.org/

ASTMA123. (2008). Standard Specification for Zinc (HDG) Coatings on Iron and Steel Products. In: ASTM.

ASTMD1014. (2009). Standard Practice for conducting exterior tests of paints and coatings on metal substrates. In. Pennsylvania: ASTM.

ASTMG1. (2003). Standard Practice for Preparing, Cleaning, and Evaluating Corrosion Test Specimens. In. Pennsylvania: ASTM.

ASTMG16. (2013). Standard Guide for Applying Statistics to Analysis of Corrosion Data. In. United States: ASTM.

ASTMG31. (2004). Standard Practice for Laboratory Immersion Corrosion Testing of Metals. In: ASTM.

ASTMG33. (2010). Standard Practice for Recording Data from Atmospheric Corrosion Tests of Metallic-Coated Steel Specimens. In. United States: ASTM.

ASTMG50. (2015). Standard Practice for Conducting Atmospheric Corrosion Tests on Metals. In. Pennsylvania: ASTM.

ASTMG92. (2010). Standard Practice for characterization of atmospheric test sites. In. Pennsylvania: ASTM.

Castaño, J. G., Botero, C. A., Restrepo, A. H., Agudelo, E. A., Correa, E., & Echeverría, F. (2010). Atmospheric corrosion of carbon steel in Colombia. *Corrosion Science, 52*(1), 216-223. doi:https://doi.org/10.1016/j.corsci.2009.09.006

Cocks, J. (2009). *Whole of Life Cost Comparison and Cost Benefit Analysis for Steel Structures Constructed in the Foreshore Zone* (thesis). Griffith University, Australia.

Cole, I., Corrigan, P., & Nguyen, V. (2012). Steel Corrosion Map of Vietnam. *Corrosion Science and Technology, 11*, 103-107. doi:10.14773/cst.2012.11.4.103

CONTEC. (2023). *Construction and Maintenance Technology Research Center*.

Corvo, F., Haces, C., Betancourt, N., Maldonado, L., Véleva, L., Echeverria, M., . . . Rincon, A. (1997). Atmospheric corrosivity in the Caribbean area. *Corrosion Science, 39*(5), 823-833. doi:https://doi.org/10.1016/S0010-938X(96)00138-2

DPT1333–61. (2018). Standard for Durability of Structural Steel Buildings. In. Bangkok: Department of Public Works and Town Planning.

Edavan, R., & Kopinski, R. (2009). Corrosion resistance of painted zinc alloy coated steels. *Corrosion Science - CORROS SCI, 51*, 2429-2442. doi:10.1016/j.corsci.2009.06.028

Feliu, S., Morcillo, M., & Chico, B. (1999). Effect of Distance from Sea on Atmospheric Corrosion Rate. *Corrosion, 55*(9), 883-891. doi:10.5006/1.3284045

Feliu, S., Morcillo, M., & Feliu, S. (1993). The prediction of atmospheric corrosion from meteorological and pollution parameters—II. Long-term forecasts. *Corrosion Science, 34*(3), 415-422. doi:https://doi.org/10.1016/0010-938X(93)90113-U

GAA (2023). Galvanizers Association of Australia. Retrieved from https://designmanual.gaa.com.au

Huang, J., Meng, X., Zheng, Z., & Gao, Y. (2018). Optimization of the atmospheric corrosivity mapping of Guangdong Province. *Materials and Corrosion, 70*. doi:10.1002/maco.201810306

ISIT (2018). Iron and Steel Institute of Thailand. Retrieved from https://www.isit.or.th

ISO4628. (2016). Paints and Varnishes- Evaluation of Degradation of Coatings - Designation of Quantity and Size of Defects, and of Intensity of Uniform. In. Switzerland: ISO.

ISO9223. (2012). Corrosion of metals and alloys — Corrosivity of atmospheres — Classification, determination and estimation. In: International Organization for Standardization.

ISO9224. (2012). Corrosion of metals and alloys — Corrosivity of atmospheres — Guiding values for the corrosivity categories In. Switzerland: ISO.

ISO9225. (2012). Corrosion of metals and alloys — Corrosivity of atmospheres — Measurement of environmental parameters affecting corrosivity of atmospheres. In. Switzerland: ISO.

ISO17872. (2019). Paints and Varnishes- Guidelines for the Introduction of Scribe Marks through Coatings on Metallic Panels for Corrosion Testing. In: ISO.

Ivaskova, M., Kotes, P., & Brodnan, M. (2015). Air Pollution as an Important Factor in Construction Materials Deterioration in Slovak Republic. *Procedia Engineering, 108*, 131-138. doi:https://doi.org/10.1016/j.proeng.2015.06.128

Jaén, J., Iglesias, J., & Hernández, C. (2012). Analysis of Short-Term Steel Corrosion Products Formed in Tropical Marine Environments of Panama. *International Journal of Corrosion, 2012*. doi:10.1155/2012/162729

Janse van Rensburg, D., Cornish, L., & van der Merwe, J. (2019). Corrosion map of South Africa's macro atmosphere. *South African Journal of Science, 115*. doi:10.17159/sajs.2019/4901

JISG3101. (2015). Rolled Steels for General Structure. In. Tokyo: JIS.

JISG3106. (2004). Rolled Steels for Welded Structure. In. Tokyo: JIS.

Krivy, V., Kubzova, M., Kreislova, K., & Krejsa, M. (2018). Prediction model of corrosion losses based on probabilistic approach. *Procedia Structural Integrity, 13*, 825-830. doi:https://doi.org/10.1016/j.prostr.2018.12.158

Mendoza, A. R., & Corvo, F. (1999). Outdoor and indoor atmospheric corrosion of carbon steel. *Corrosion Science, 41*(1), 75-86. doi:https://doi.org/10.1016/S0010-938X(98)00081-X

Morcillo, M., Díaz, I., Cano, H., Chico, B., & de la Fuente, D. (2019). Atmospheric corrosion of weathering steels. Overview for engineers. Part I: Basic concepts. *Construction and Building Materials, 213*, 723-737. doi:https://doi.org/10.1016/j.conbuildmat.2019.03.334

MTEC. (2023). *National Metal & Materials Technology Center*.

Natesan, M., Venkatachari, G., & Palaniswamy, N. (2006). Kinetics of atmospheric corrosion of mild steel, zinc, galvanized iron and aluminium at 10 exposure

stations in India. *Corrosion Science, 48*(11), 3584-3608. doi:https://doi.org/10.1016/j.corsci.2006.02.006

Oesch, S. (1996). The effect of SO2, NO2, NO and O3 on the corrosion of unalloyed carbon steel and weathering steel—The results of laboratory exposures. *Corrosion Science, 38*(8), 1357-1368. doi:https://doi.org/10.1016/0010-938X(96)00025-X

PCD. (2022). Thailand Pollution Control Department. Retrieved from http://air4thai.pcd.go.th/webV3/#/Home

Peibker, P. M. P. (2011). *Handbook of Hot-Dip Galvanization* (P. M. a. P. Peibker Ed.). Weinheim: Wiley-VCH.

QGIS. (2022). QGIS Association. Retrieved from https://www.qgis.org.

Rios-Rojas, J., Aperador Rodriguez, D., Hernandez, E., & Arroyave, C. (2017). Annual atmospheric corrosion rate and dose-response function for carbon steel in Bogotá. *Atmósfera, 30*, 53-61. doi:10.20937/ATM.2017.30.01.05

Saarimaa, V., Virtanen, M., Laihinen, T., Laurila, K., & Väisänen, P. (2022). Blistering of color coated steel: Use of broad ion beam milling to examine degradation phenomena and coating defects. *Surface and Coatings Technology*, *448*, 128913. doi:https://doi.org/10.1016/j.surfcoat.2022.128913

Santa, A. C., Tamayo, J. A., Correa, C. D., Gómez, M. A., Castaño, J. G., & Baena, L. M. (2022). Atmospheric corrosion maps as a tool for designing and maintaining building materials: A review. *Heliyon, 8*(9), e10438. doi:https://doi.org/10.1016/j.heliyon.2022.e10438

Santana Rodríguez, J., Ramos, A., Rodriguez-Gonzalez, A., Vasconcelos, H., Mena González, V. F., Fernández, B., & Souto, R. (2019). Shortcomings of International Standard ISO 9223 for the Classification, Determination, and Estimation of Atmosphere Corrosivities in Subtropical Archipelagic Conditions—The Case of the Canary Islands (Spain). *Metals, 9*, 1105. doi:10.3390/met9101105

Sica, Y., Kenny, E., Portella, K., & Filho, D. (2007). Atmospheric corrosion performance of carbon steel, galvanized steel, aluminum and copper in the North Brazilian coast. *J. Braz. Chem. Soc, 18*, 153-166. doi:10.1590/S0103-50532007000100017

Souto, R., Vasconcelos, H., Fernández, B., Morales, J., Gonzalez, S., Cano, V., & Santana Rodríguez, J. (2014). Development of Mathematical Models to predict the Atmospheric Corrosion Rate of Carbon Steel in Fragmented Subtropical Environments. *International journal of electrochemical science, 9*, 6514-6528. doi:10.1016/S1452-3981(23)10907-2

Syed, S. (2010). Studies of galvanised steel atmospheric corrosion in Saudi Arabia. *Corrosion Engineering Science and Technology - CORROS ENG SCI TECHNOL, 45*. doi:10.1179/147842209X12476568584250

Thierry, D., Persson, D., & Lebozec, N. (2017). Atmospheric Corrosion of Zinc and Zinc Alloyed Coated Steel. In.

TMD. (2022). Thai Meteorological Department. Retrieved from https://www.tmd.go.th/en/.

Vera, R., & Ossandón, S. (2014). On the Prediction of Atmospheric Corrosion of Metals and Alloys in Chile Using Artificial Neural Networks. *International journal of electrochemical science, 9*(12), 7131-7151. doi:https://doi.org/10.1016/S1452-3981(23)10956-4

Wang, C., Wang, Z., & Ke, W. (2009). The effect of environmental variables on atmospheric corrosion of carbon steel in Shenyang. *Chinese Science Bulletin, 54*(19), 3438-3445. doi:10.1007/s11434-008-0510-3

WSA (2021). World Steel Association. Retrieved from https://www.worldsteel.org

Yokota, H. (2020). Lecture of "Lifetime Engineering for Civil Infrastructure". In. Hokkaido, Japan: Hokkaido University.

APPENDIX

SPECIMEN PHOTOS

1. Station 15: (Faculty of Engineering, Chiang Mai University)

Bare steel

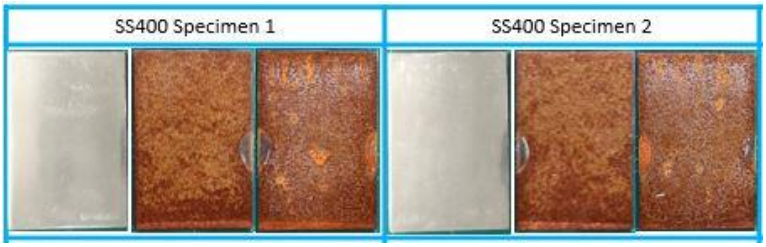

Front Back Front Back

Before after 1 year Before after 1 year

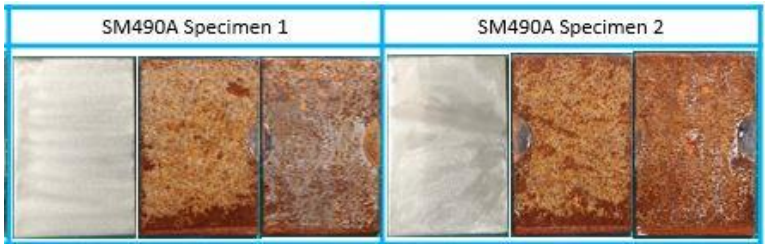

Front Back Front Back

Before after 1 year Before after 1 year

Hot dip galvanized

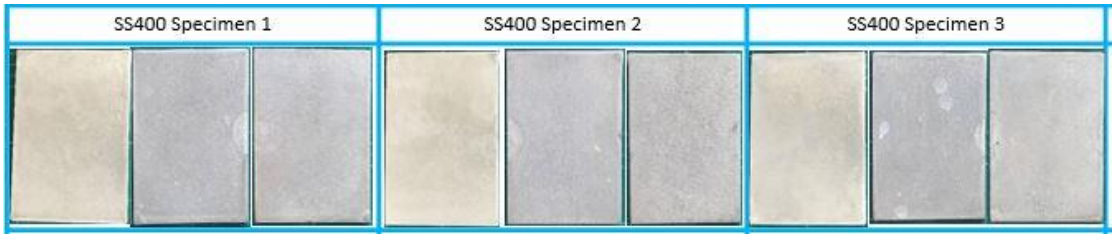

Front Back Front Back Front Back

Before after 1 year Before after 1 year Before after 1 year

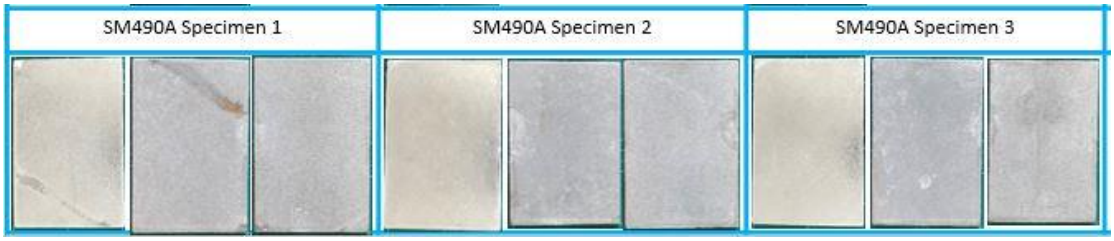

Front Back Front Back Front Back

Before after 1 year Before after 1 year Before after 1 year

2. Station 2: (Mae Moh Power Plant)

Bare steel

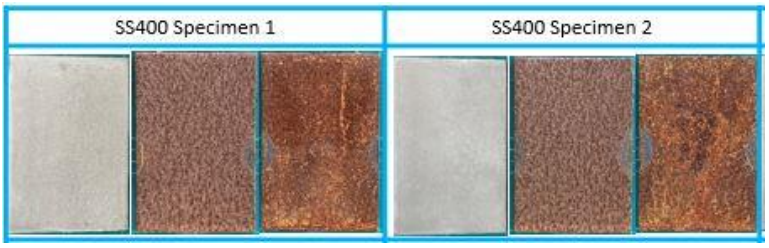

Front Back Front Back

Before after 1 year Before after 1 year

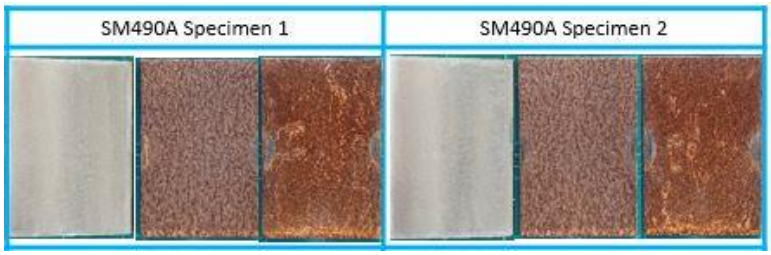

Front Back Front Back

Before after 1 year Before after 1 year

Hot dip galvanized

Front Back Front Back Front Back

Before after 1 year Before after 1 year Before after 1 year

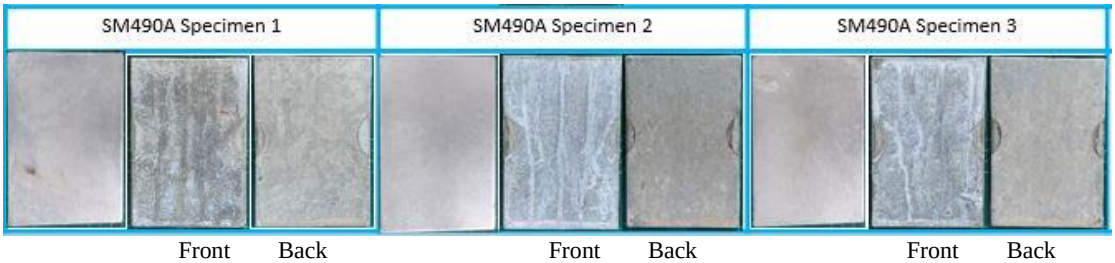

Front Back Front Back Front Back

Before after 1 year Before after 1 year Before after 1 year

3. Station 3: (Faculty of Engineering Naresuan University)

Bare steel

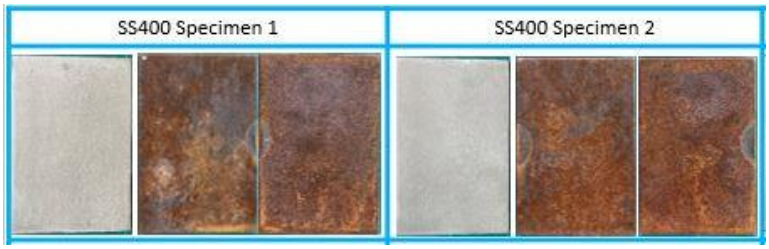

Front Back Front Back

Before after 1 year Before after 1 year

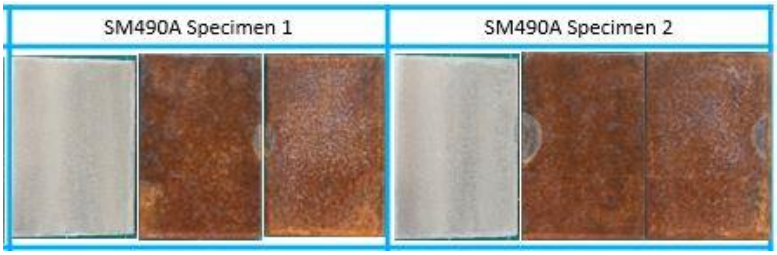

Front Back Front Back

Before after 1 year Before after 1 year

Hot dip galvanized

Front Back Front Back Front Back

Before after 1 year Before after 1 year Before after 1 year

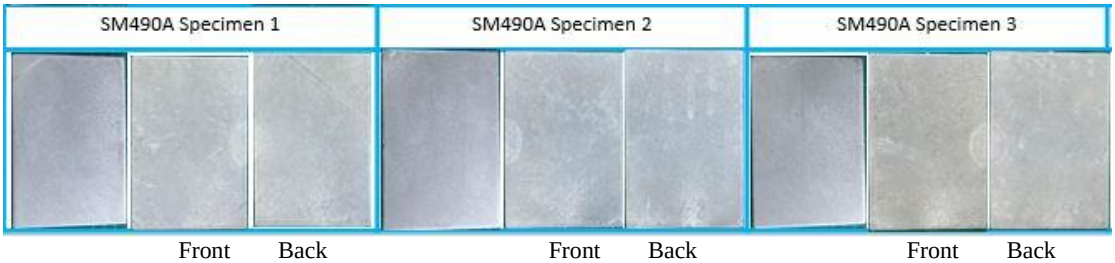

Front Back Front Back Front Back

Before after 1 year Before after 1 year Before after 1 year

4. Station 4: (Maha Sarakham University)

Bare steel

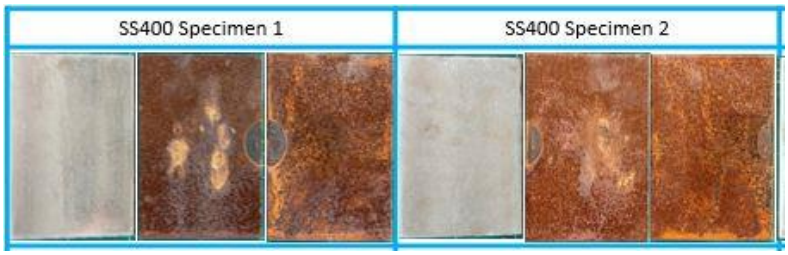

Front Back Front Back

Before after 1 year Before after 1 year

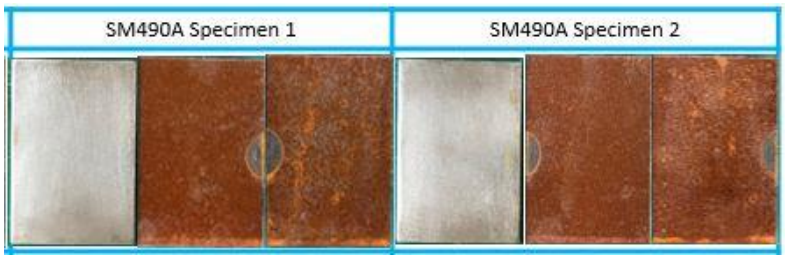

Front Back Front Back

Before after 1 year Before after 1 year

Hot dip galvanized

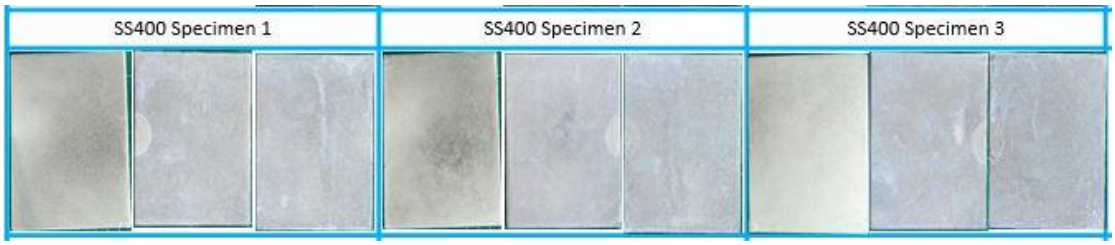

Front Back Front Back Front Back

Before after 1 year Before after 1 year Before after 1 year

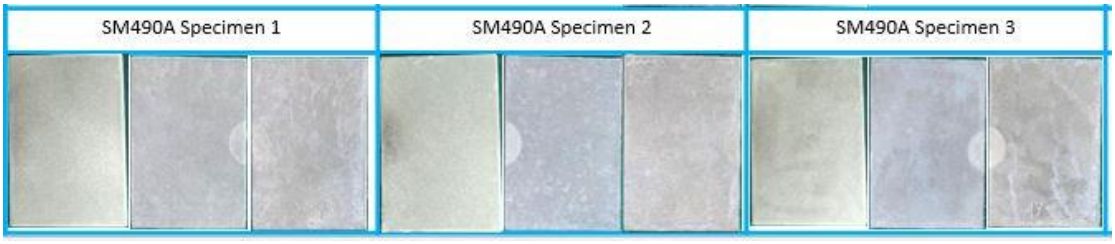

Front Back Front Back Front Back

Before after 1 year Before after 1 year Before after 1 year

5. Station 5: (Ubon Ratchathani University Faculty of Engineering)

Bare steel

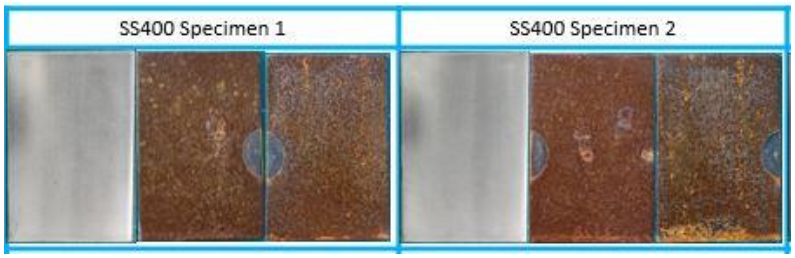

Front Back Front Back

Before after 1 year Before after 1 year

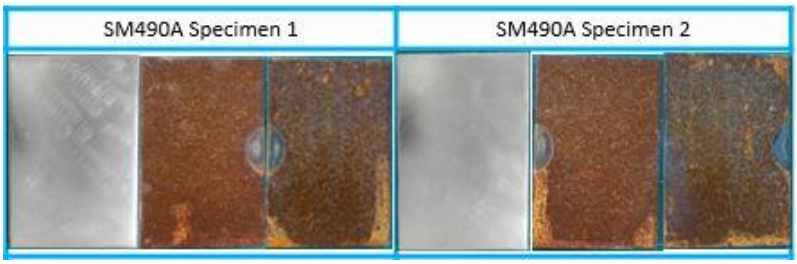

Front Back Front Back

Before after 1 year Before after 1 year

Hot dip galvanized

Front Back Front Back Front Back

Before after 1 year Before after 1 year Before after 1 year

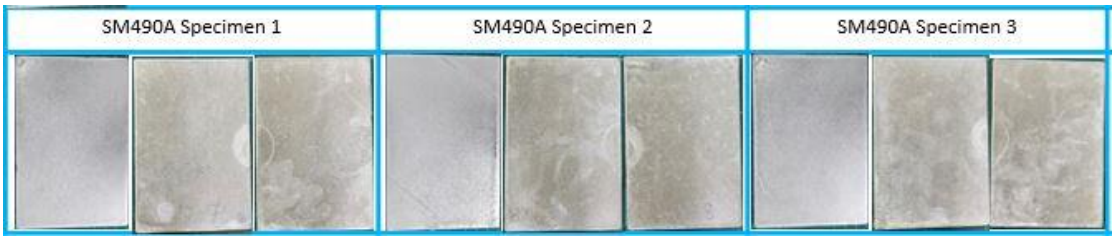

Front Back Front Back Front Back

Before after 1 year Before after 1 year Before after 1 year

6. Station 6: (Saraburi Province)

Bare steel

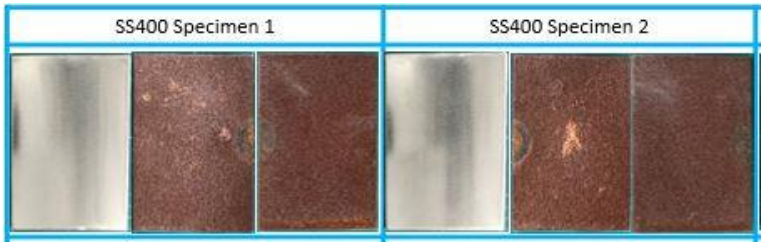

Front Back Front Back

Before after 1 year Before after 1 year

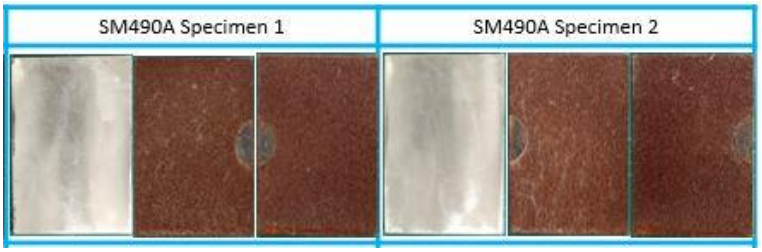

Front Back Front Back

Before after 1 year Before after 1 year

Hot dip galvanized

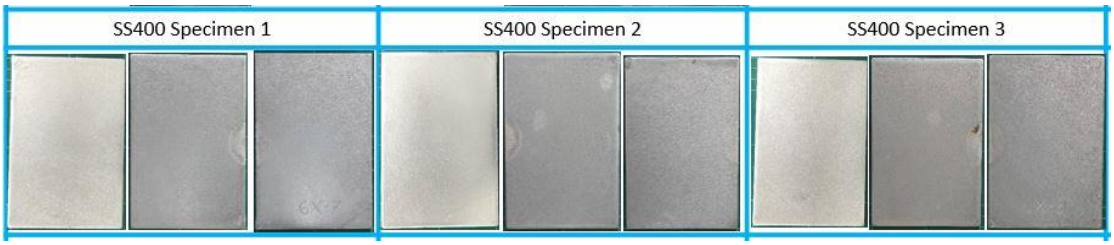

Front Back Front Back Front Back

Before after 1 year Before after 1 year Before after 1 year

Front Back Front Back Front Back

Before after 1 year Before after 1 year Before after 1 year

7. Station 7: (Thai Metal Trade Company Limited (Wangnoi))

Bare steel

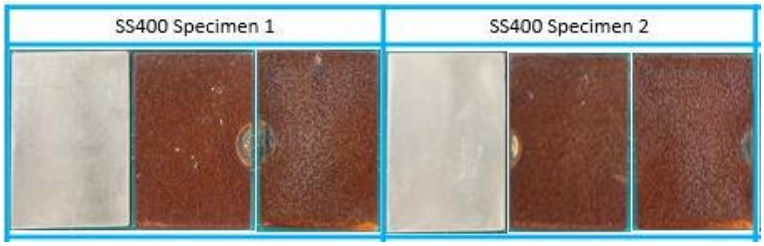

Front Back Front Back

Before after 1 year Before after 1 year

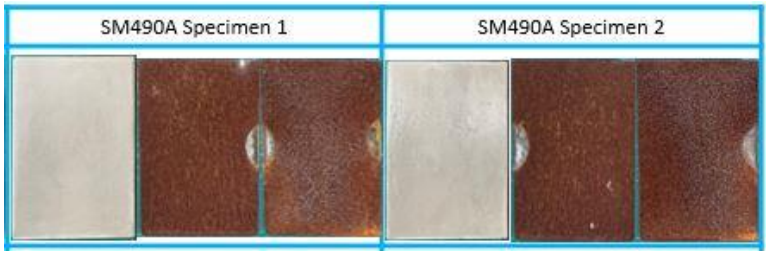

Front Back Front Back

Before after 1 year Before after 1 year

Hot dip galvanized

Front Back Front Back Front Back

Before after 1 year Before after 1 year Before after 1 year

Front Back Front Back Front Back

Before after 1 year Before after 1 year Before after 1 year

8. Station 8: (Sangcharoen Galvanizing Limited)

Bare steel

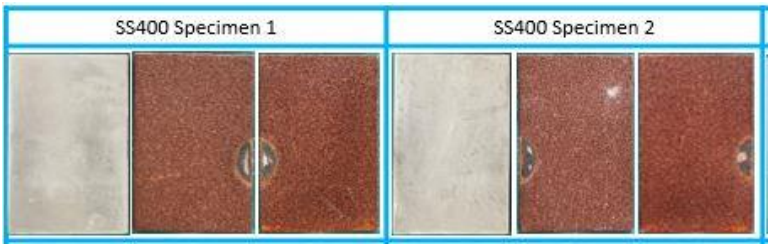

Front Back Front Back

Before after 1 year Before after 1 year

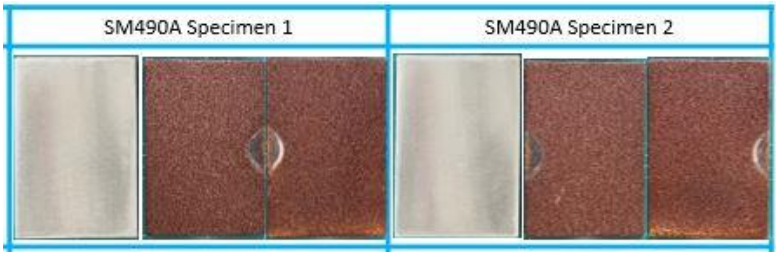

Front Back Front Back

Before after 1 year Before after 1 year

Hot dip galvanized

Front Back Front Back Front Back

Before after 1 year Before after 1 year Before after 1 year

Front Back Front Back Front Back

Before after 1 year Before after 1 year Before after 1 year

9. Station 9: (Sirindhorn International Institute of Technology (SIIT))

Bare steel

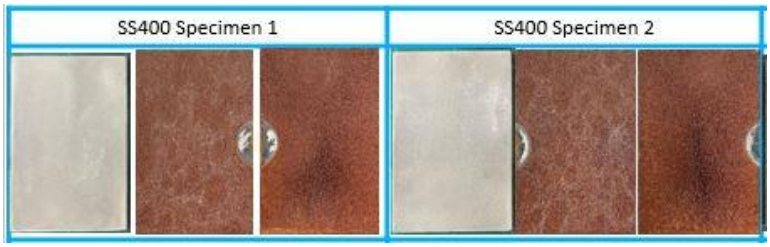

Front Back Front Back

Before after 1 year Before after 1 year

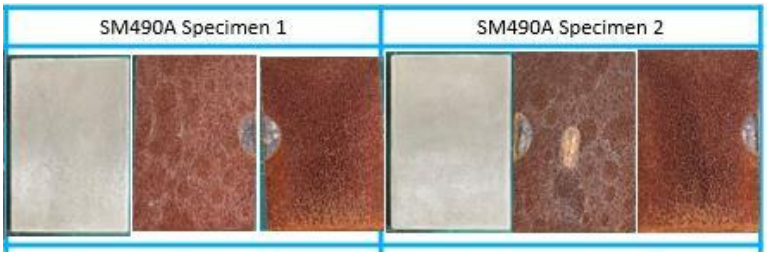

Front Back Front Back

Before after 1 year Before after 1 year

Hot dip galvanized

Front Back Front Back Front Back

Before after 1 year Before after 1 year Before after 1 year

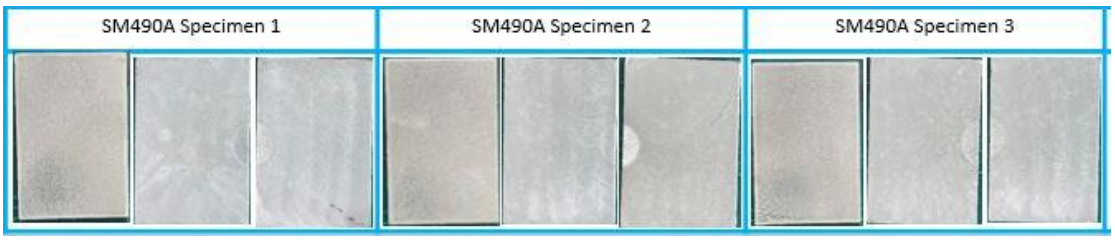

Front Back Front Back Front Back

Before after 1 year Before after 1 year Before after 1 year

10. Station 10: (Thai Premium Pipe Company Limited)

Bare steel

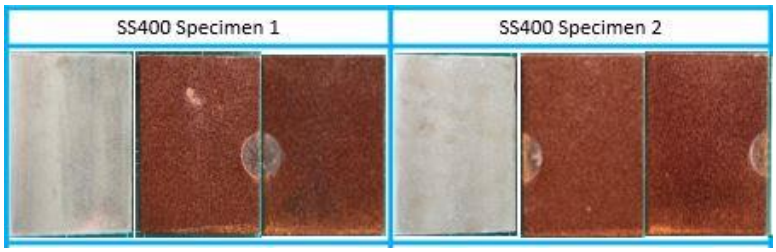

Front Back Front Back

Before after 1 year Before after 1 year

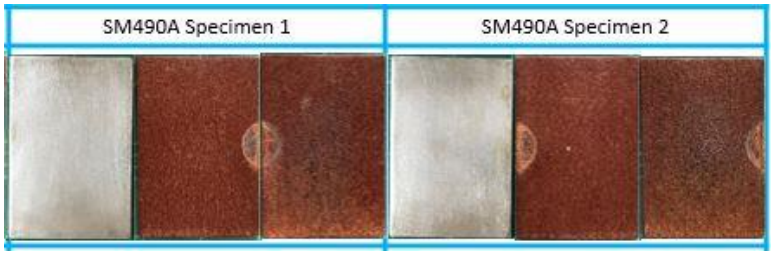

Front Back Front Back

Before after 1 year Before after 1 year

Hot dip galvanized

Front Back Front Back Front Back

Before after 1 year Before after 1 year Before after 1 year

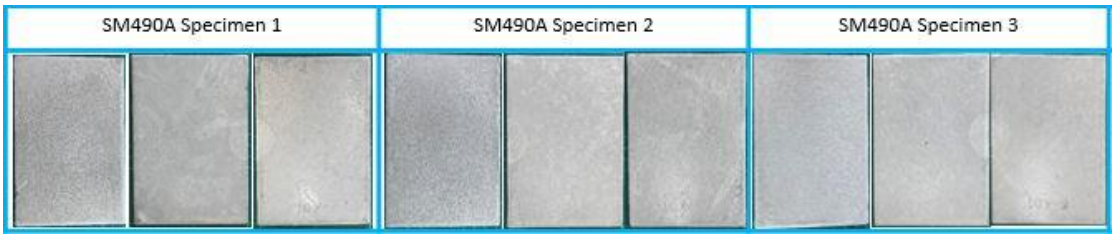

Front Back Front Back Front Back

Before after 1 year Before after 1 year Before after 1 year

11. Station 11: (Thai Metal Trade Company Limited (Bangkok))

Bare steel

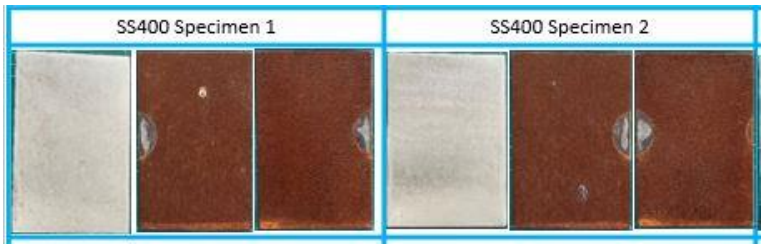

Front Back Front Back

Before after 1 year Before after 1 year

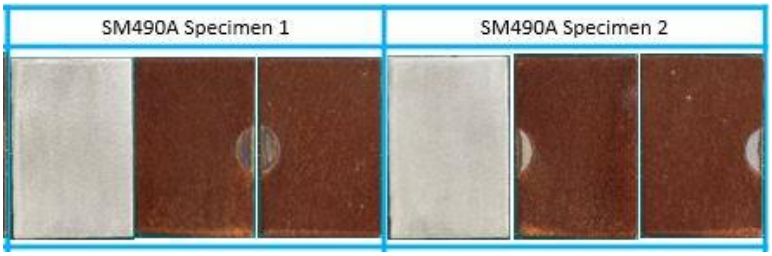

Front Back Front Back

Before after 1 year Before after 1 year

Hot dip galvanized

Front Back Front Back Front Back

Before after 1 year Before after 1 year Before after 1 year

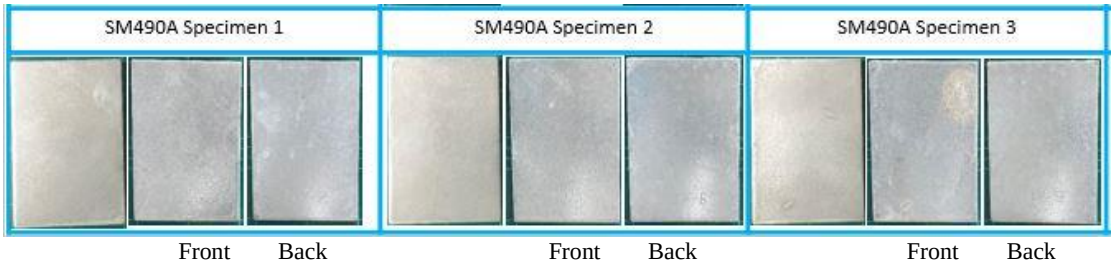

Front Back Front Back Front Back

Before after 1 year Before after 1 year Before after 1 year

12. Station 12: (Iron and Steel Institute of Thailand)

Bare steel

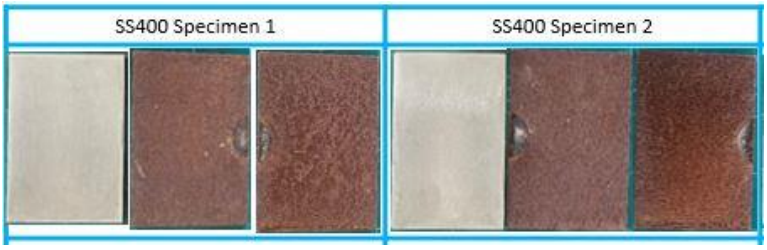

Front Back Front Back

Before after 1 year Before after 1 year

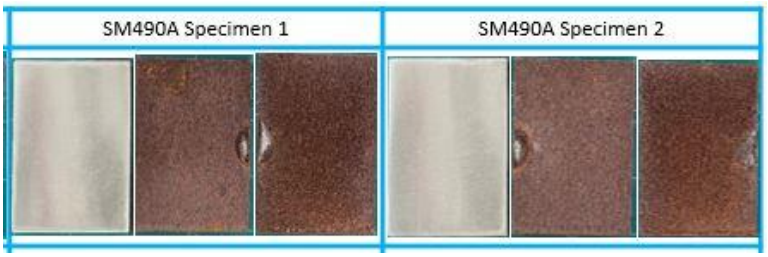

Front Back Front Back

Before after 1 year Before after 1 year

Hot dip galvanized

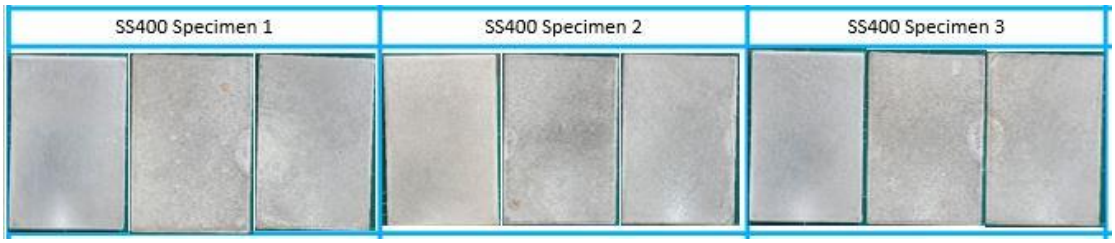

Front Back Front Back Front Back

Before after 1 year Before after 1 year Before after 1 year

Front Back Front Back Front Back

Before after 1 year Before after 1 year Before after 1 year

13. Station 13: (Union Galvanizer)

Bare steel

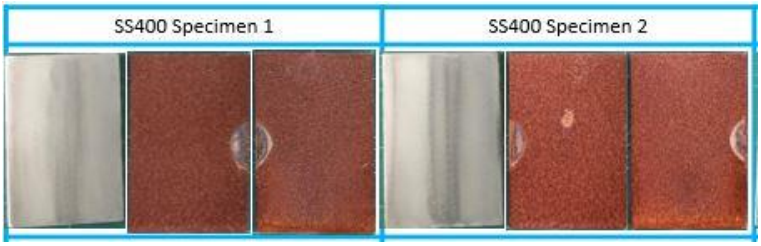

Front Back Front Back

Before after 1 year Before after 1 year

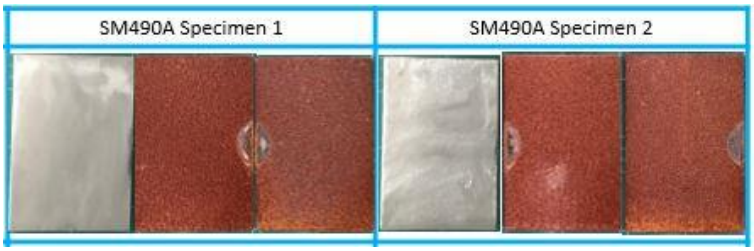

Front Back Front Back

Before after 1 year Before after 1 year

Hot dip galvanized

Front Back Front Back Front Back

Before after 1 year Before after 1 year Before after 1 year

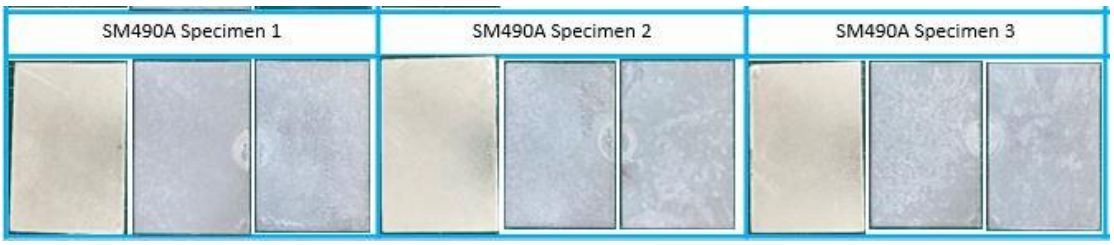

Front Back Front Back Front Back

Before after 1 year Before after 1 year Before after 1 year

14. Station 14: (Sangchareon Eastern Galvanized)

Bare steel

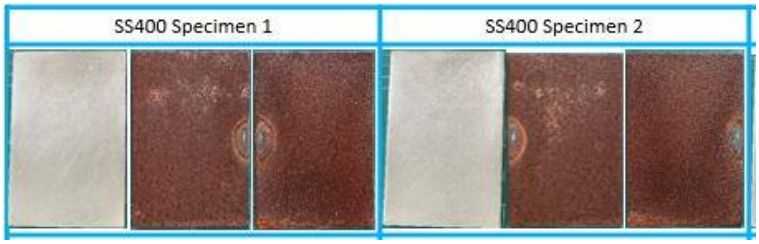

Front Back Front Back

Before after 1 year Before after 1 year

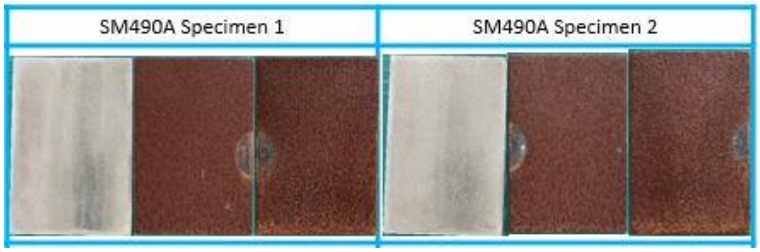

Front Back Front Back

Before after 1 year Before after 1 year

Hot dip galvanized

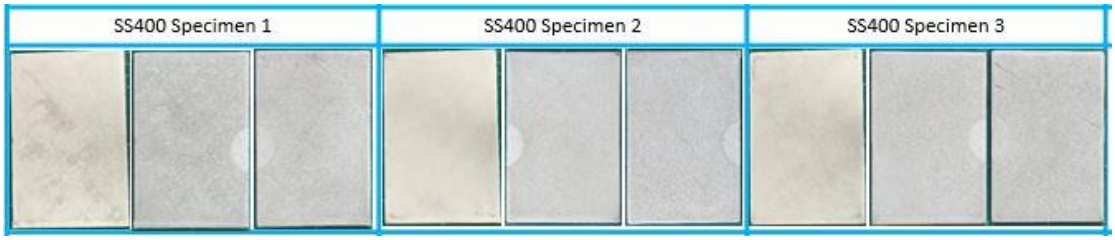

Front Back Front Back Front Back

Before after 1 year Before after 1 year Before after 1 year

Front Back Front Back Front Back

Before after 1 year Before after 1 year Before after 1 year

15. Station 1: (Cotco-SV Eastern Steel Pipe LTD)

Bare steel

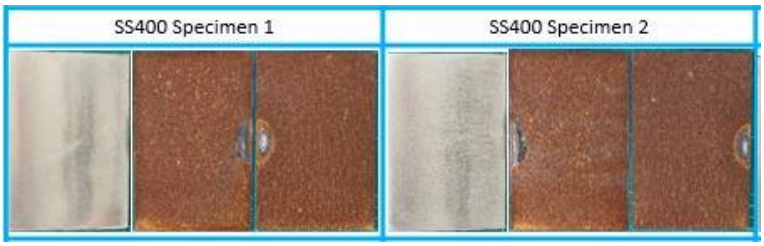

Front Back Front Back

Before after 1 year Before after 1 year

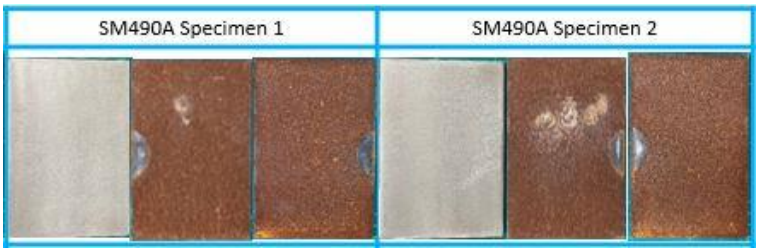

Front Back Front Back

Before after 1 year Before after 1 year

Hot dip galvanized

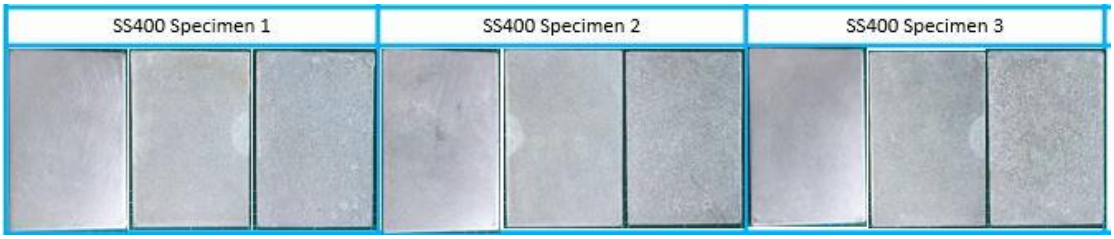

Front Back Front Back Front Back

Before after 1 year Before after 1 year Before after 1 year

Front Back Front Back Front Back

Before after 1 year Before after 1 year Before after 1 year

16. Station 16: (Tha Thung Na Dam Power Plant)

Bare steel

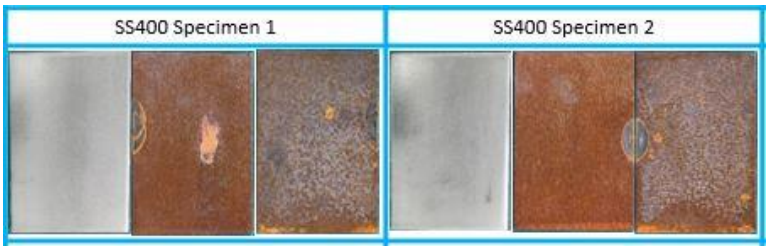

Front Back Front Back

Before after 1 year Before after 1 year

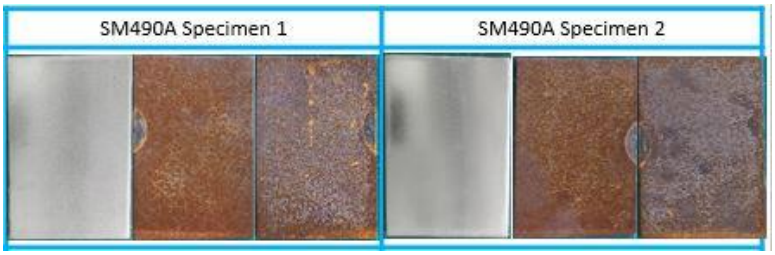

Front Back Front Back

Before after 1 year Before after 1 year

Hot dip galvanized

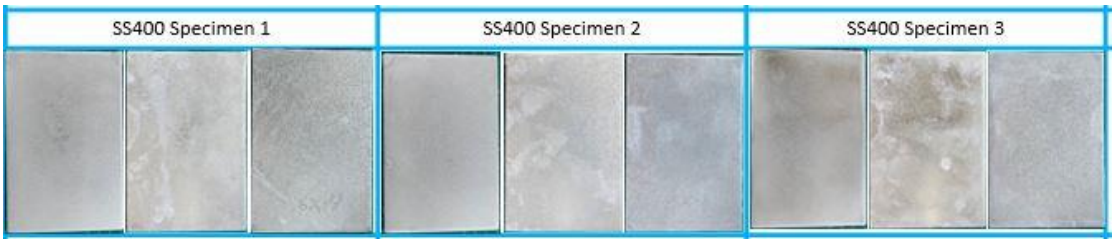

Front Back Front Back Front Back

Before after 1 year Before after 1 year Before after 1 year

Front Back Front Back Front Back

Before after 1 year Before after 1 year Before after 1 year

17. Station 17: (Sahaviriya Steel Industries Public Company Limited)

Bare steel

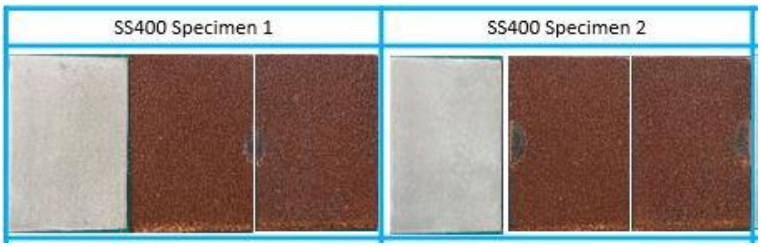

Front Back Front Back

Before after 1 year Before after 1 year

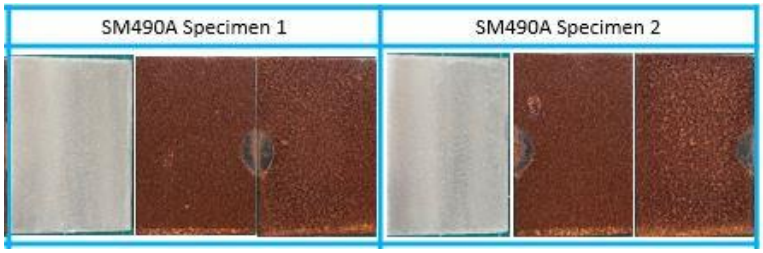

Front Back Front Back

Before after 1 year Before after 1 year

Hot dip galvanized

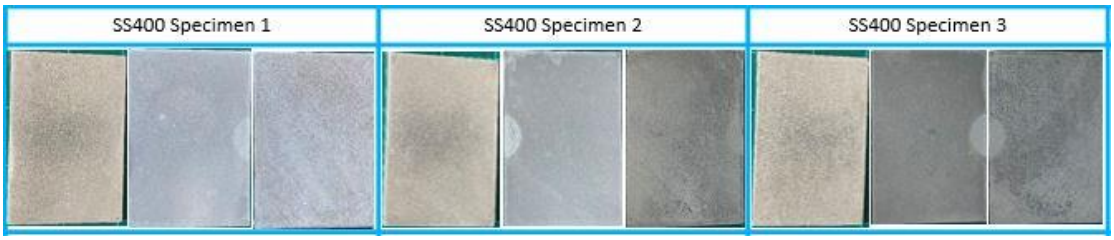

Front Back Front Back Front Back

Before after 1 year Before after 1 year Before after 1 year

Front Back Front Back Front Back

Before after 1 year Before after 1 year Before after 1 year

18. Station 18: (Prince of Sonkla University)

Bare steel

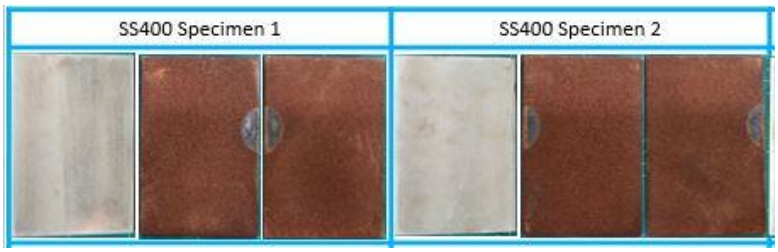

Front Back Front Back

Before after 1 year Before after 1 year

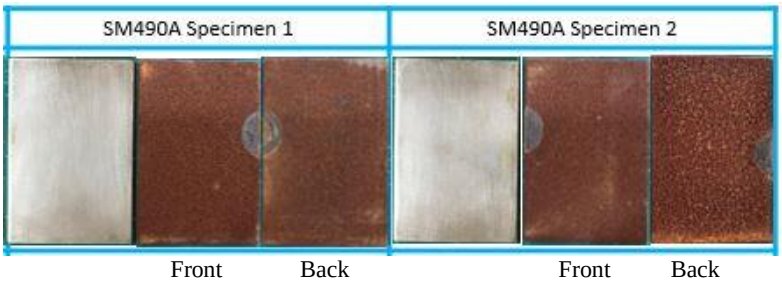

Front Back Front Back

Before after 1 year Before after 1 year

Hot dip galvanized

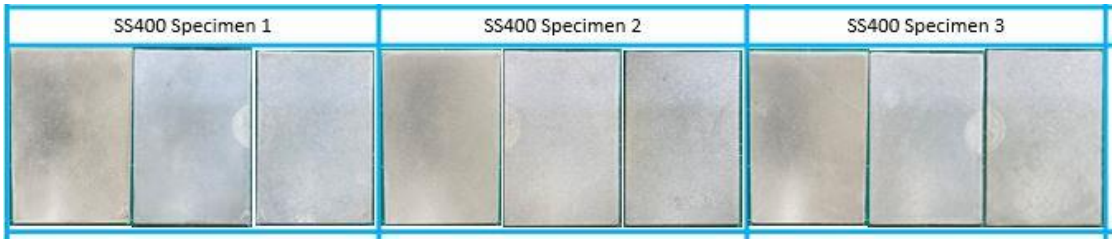

Front Back Front Back Front Back

Before after 1 year Before after 1 year Before after 1 year

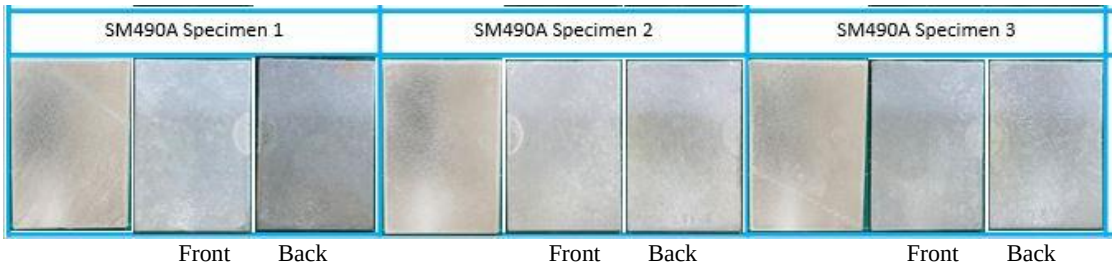

Front Back Front Back Front Back

Before after 1 year Before after 1 year Before after 1 year

19. Station 19: (Rajamangala University of Technology)

Bare steel

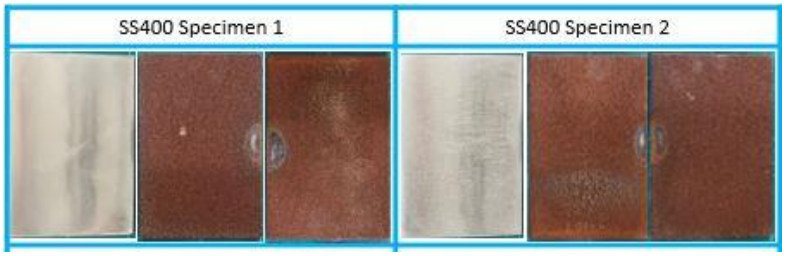

Front Back Front Back

Before after 1 year Before after 1 year

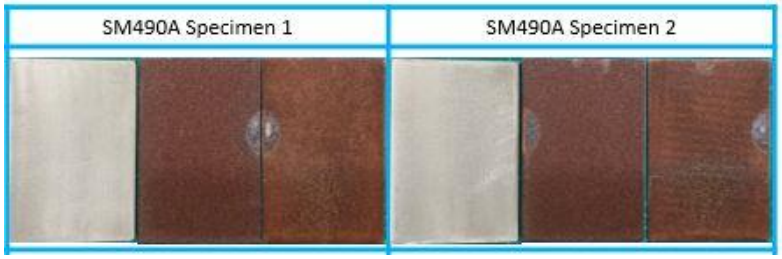

Front Back Front Back

Before after 1 year Before after 1 year

Hot dip galvanized

Front Back Front Back Front Back

Before after 1 year Before after 1 year Before after 1 year

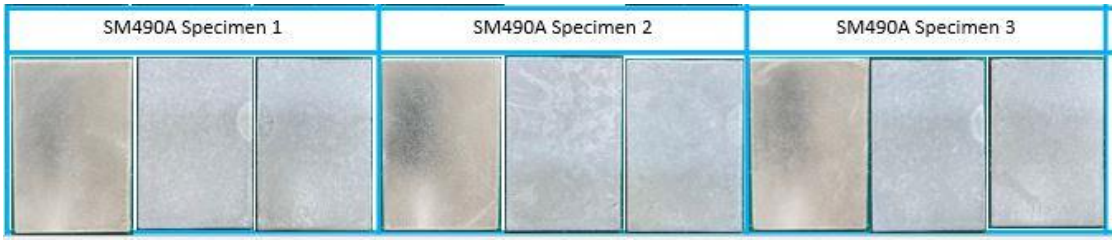

Front Back Front Back Front Back

Before after 1 year Before after 1 year Before after 1 year

Painted Steel

Specimens	Types			
	SS400		SM490A	
Low grade painting	A	Red	B	Red
Medium grade painting	C	Orange	D	Orange
Premium grade painting	E	Green	F	Green
Duplex system	G	Pink	H	Pink

1 Station 15: (Faculty of Engineering, Chiang Mai University)

A C E G

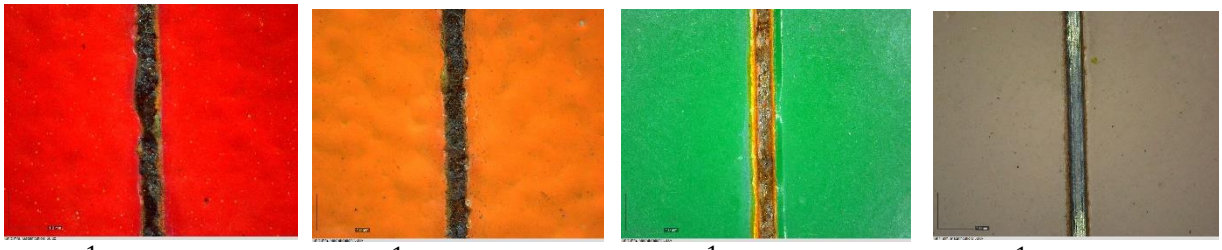

B D F H

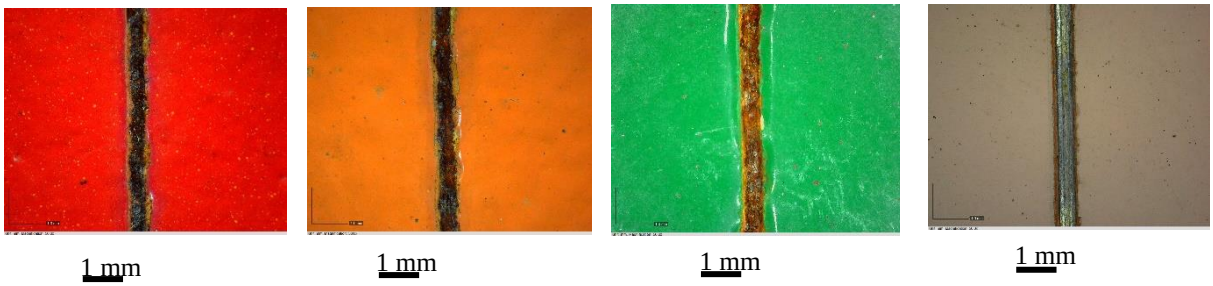

2 Station 2: (Mae Moh power plant)

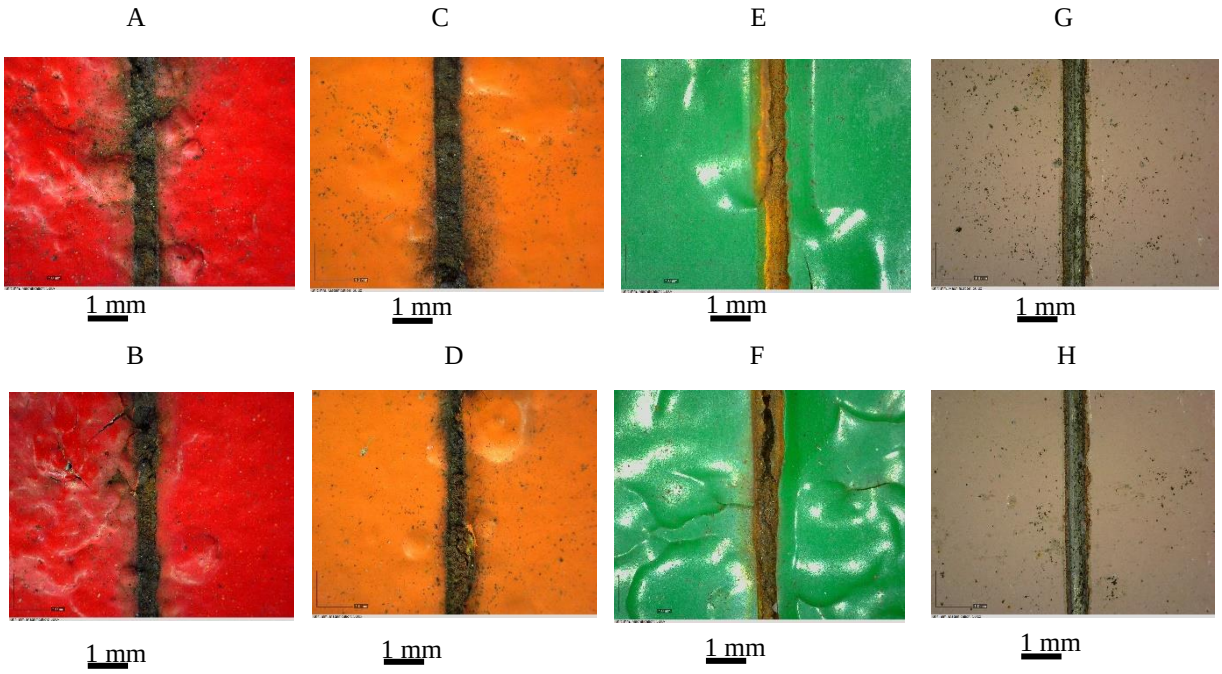

3 Station 3: (Faculty of Engineering Naresuan University)

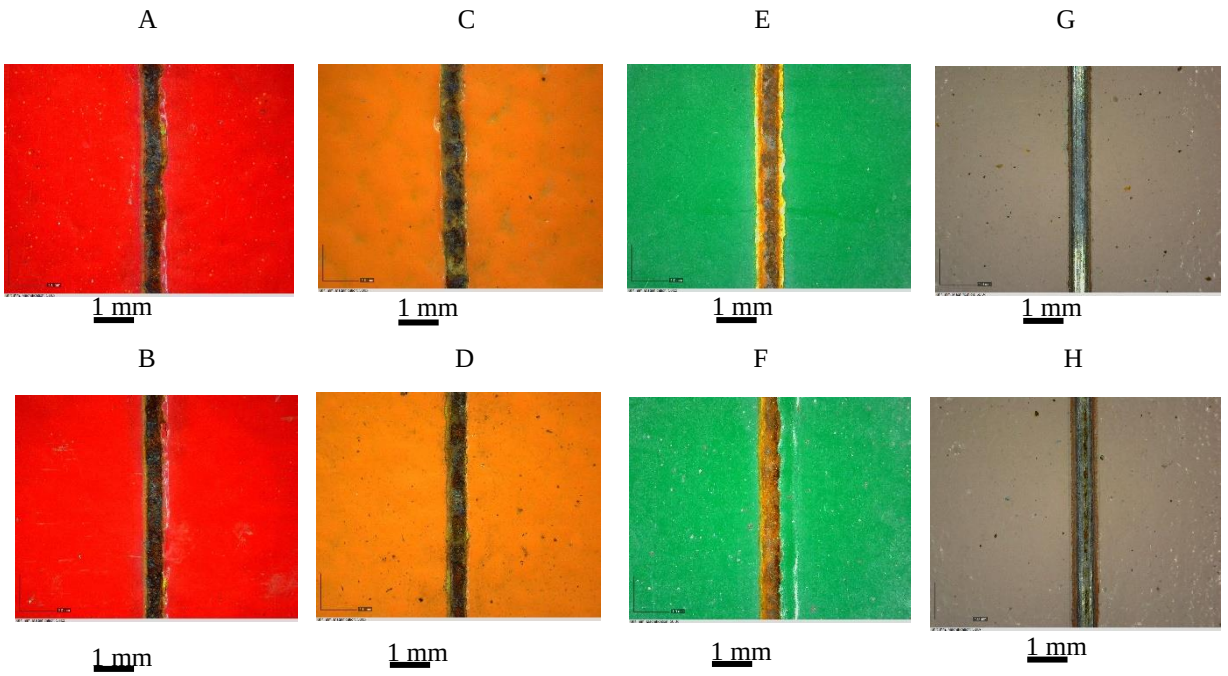

4 Station 4: (Maha Sarakham University)

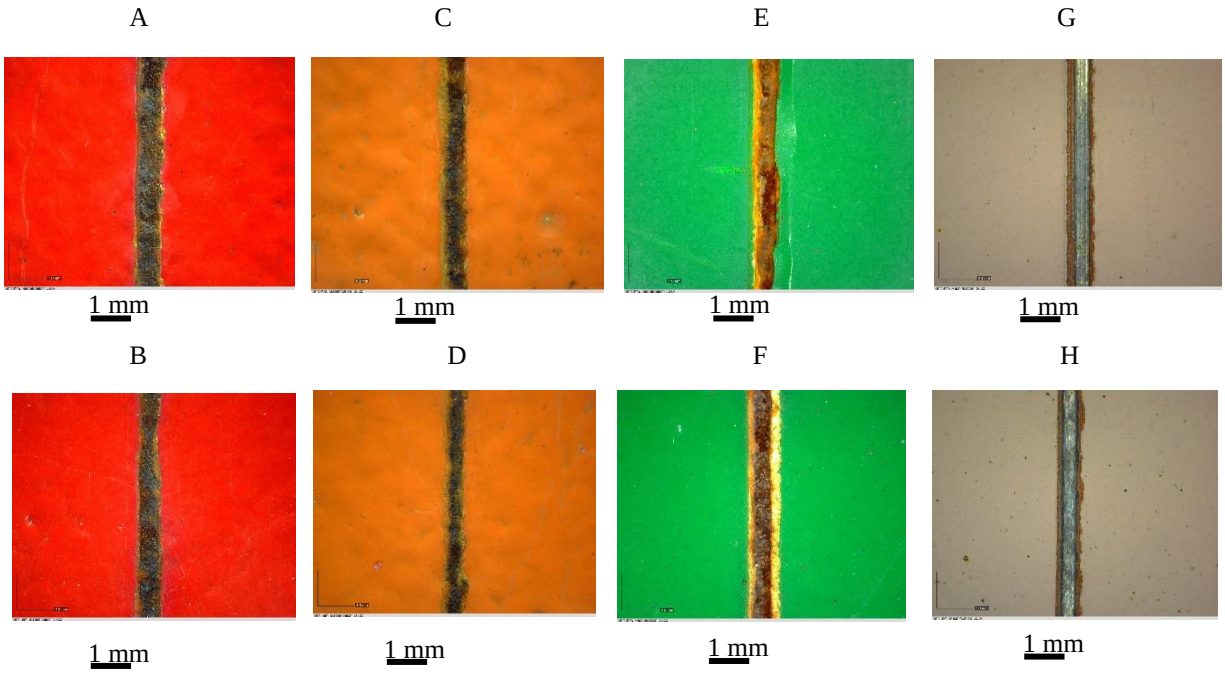

5 Station 5: (Ubon Ratchathani University Faculty of Engineering)

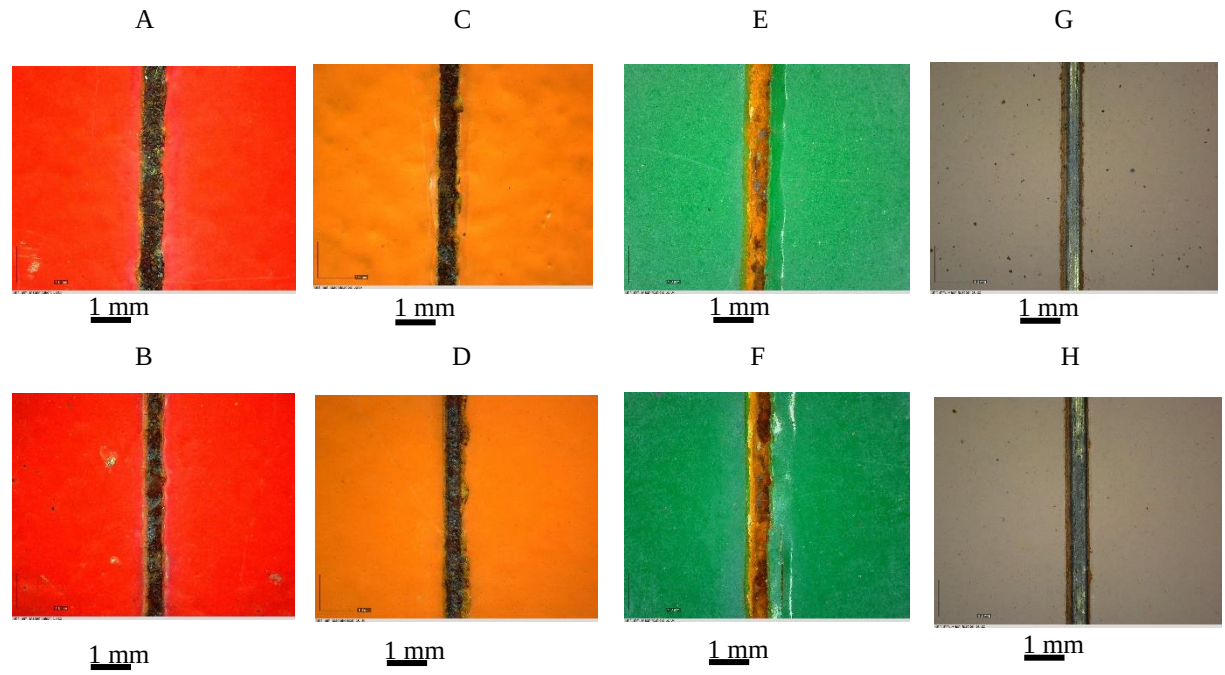

6 Station 6: (Saraburi province)

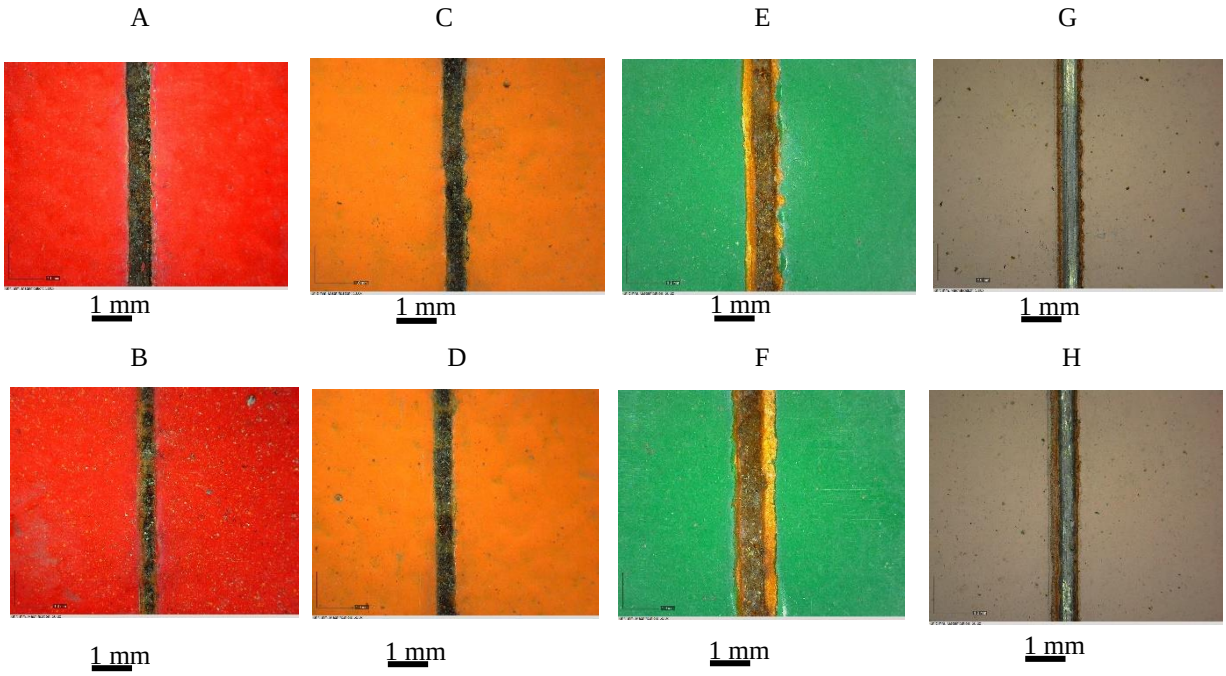

7 Station 7: Thai Metal Trade Company Limited (Wangnoi)

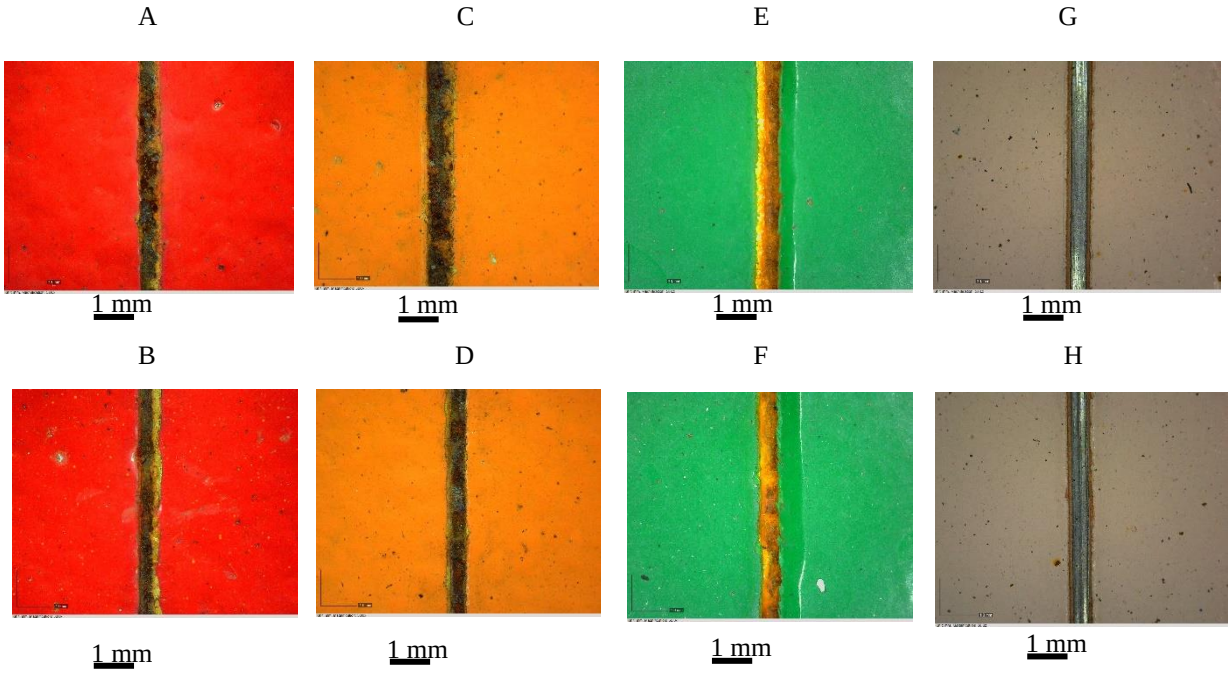

8 Station 8: (Sangcharoen Galvanizing Limited)

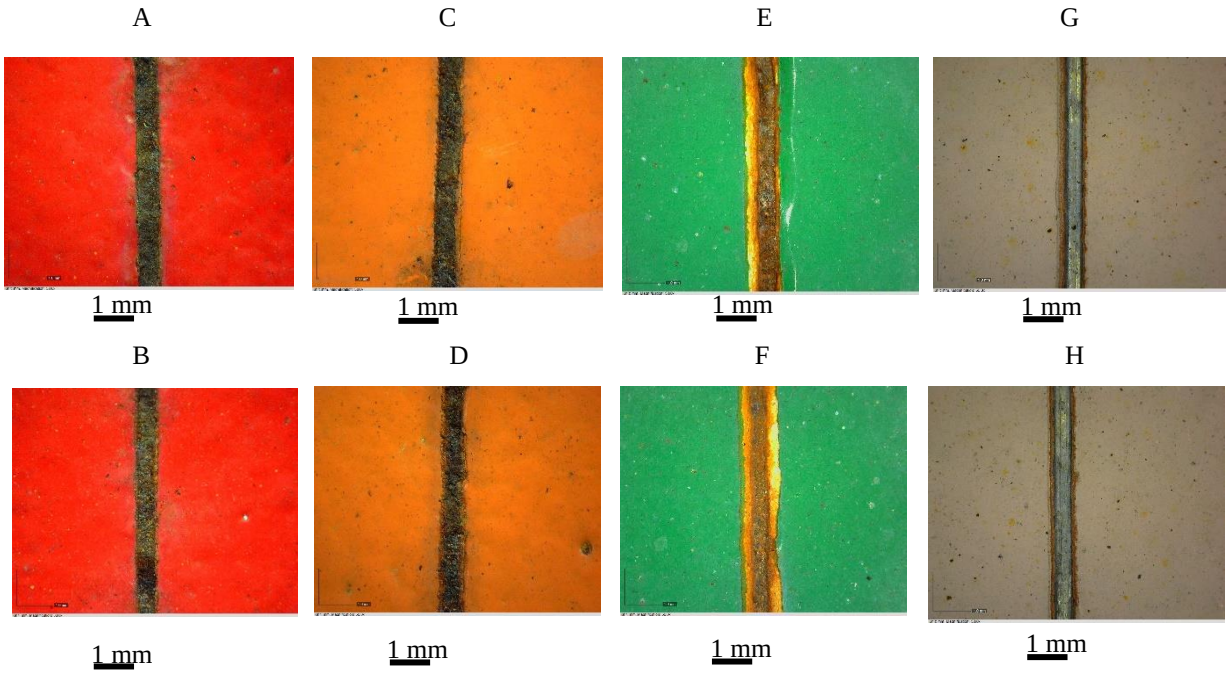

9 Station 9: Sirindhorn International Institute of Technology (SIIT)

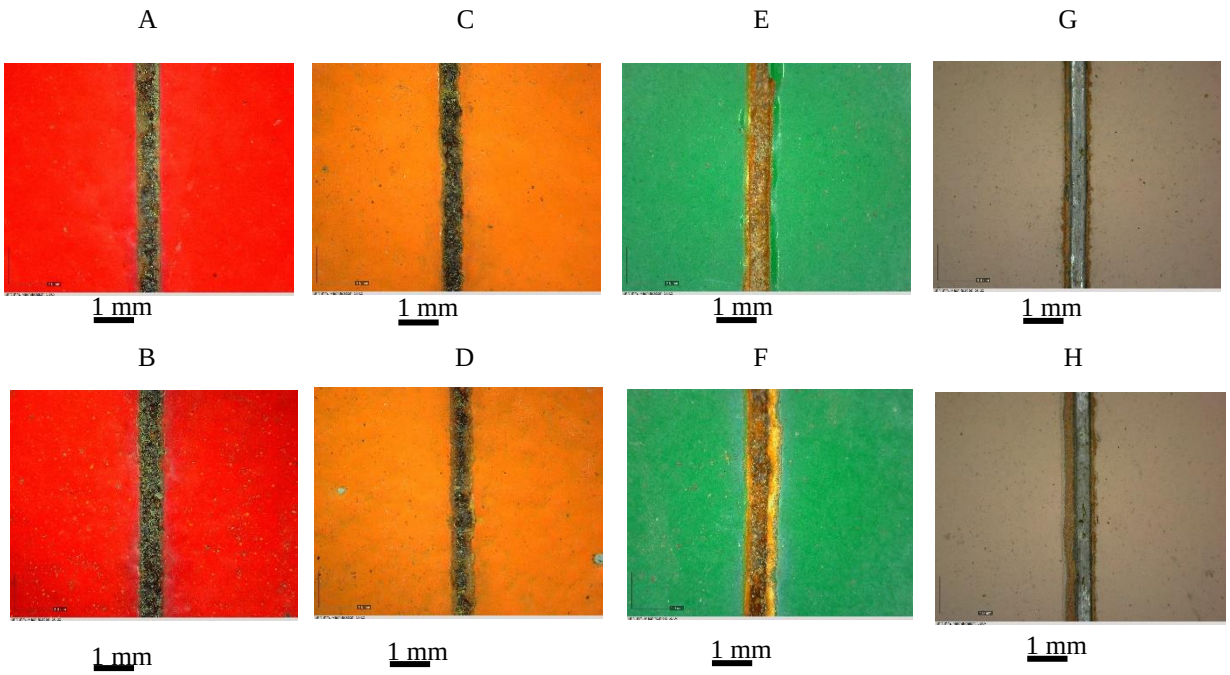

10 Station 10: (Thai Premium Pipe Company Limited)

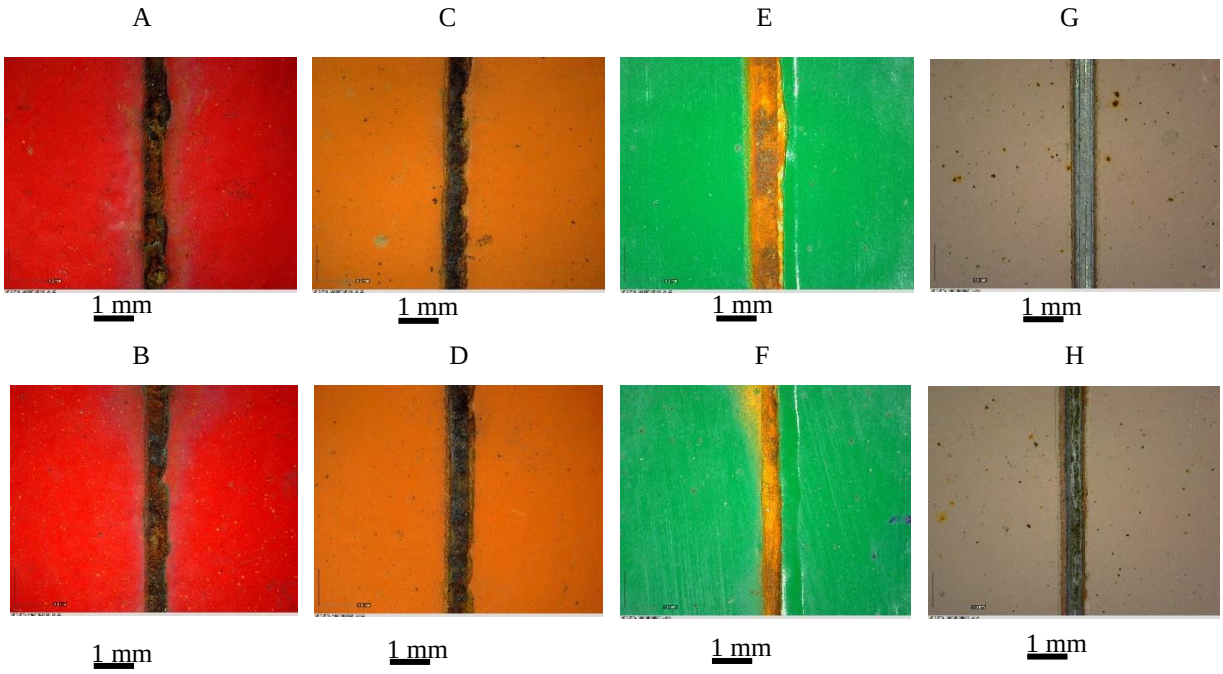

11 Station 11: (Thai Metal Trade Company Limited (Bangkok))

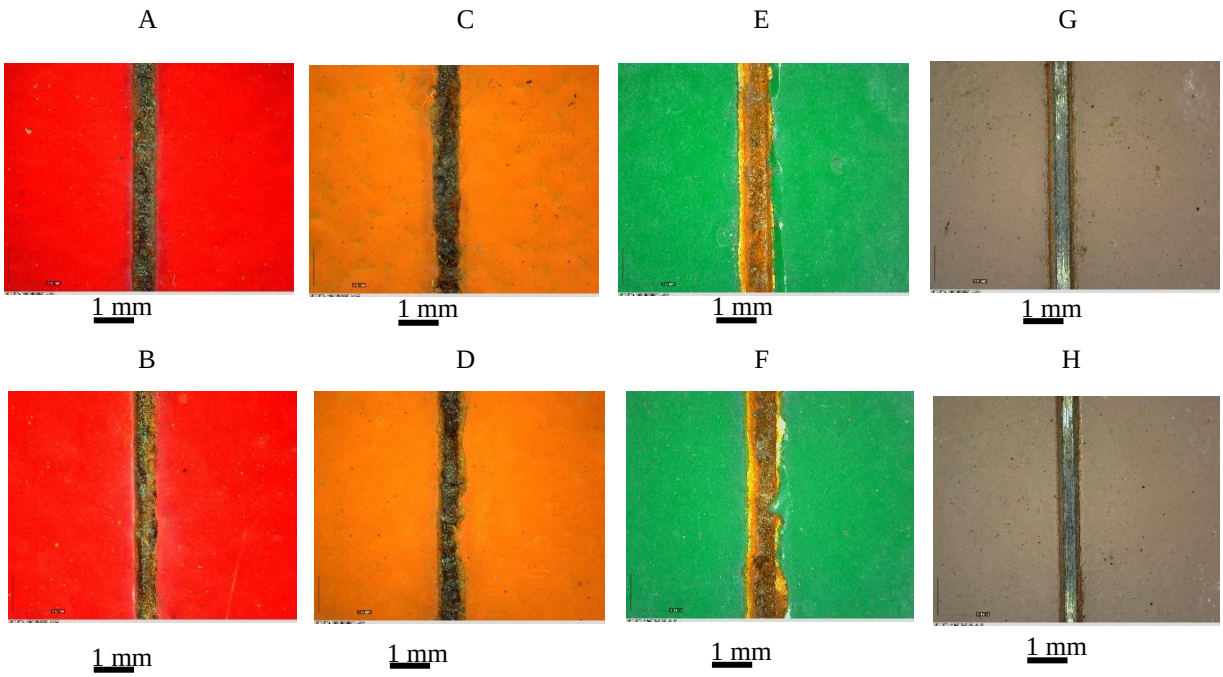

12 Station 12: (Iron and Steel Institute of Thailand)

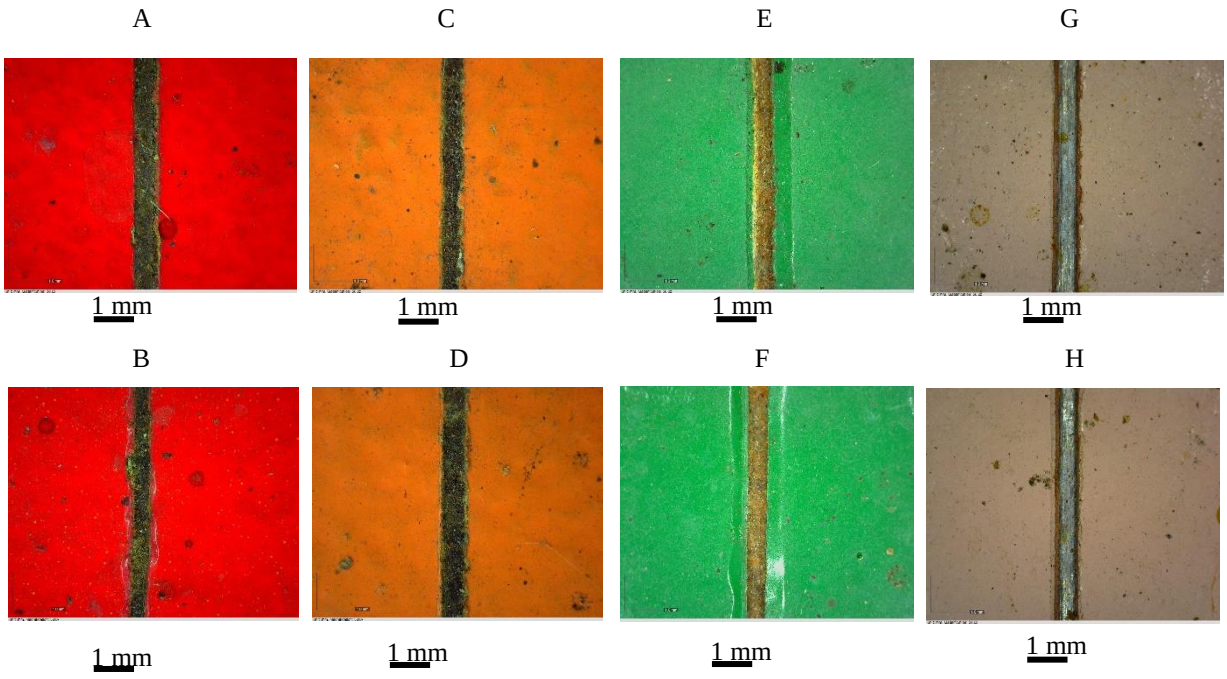

13 Station 13: (Union Galvanizer)

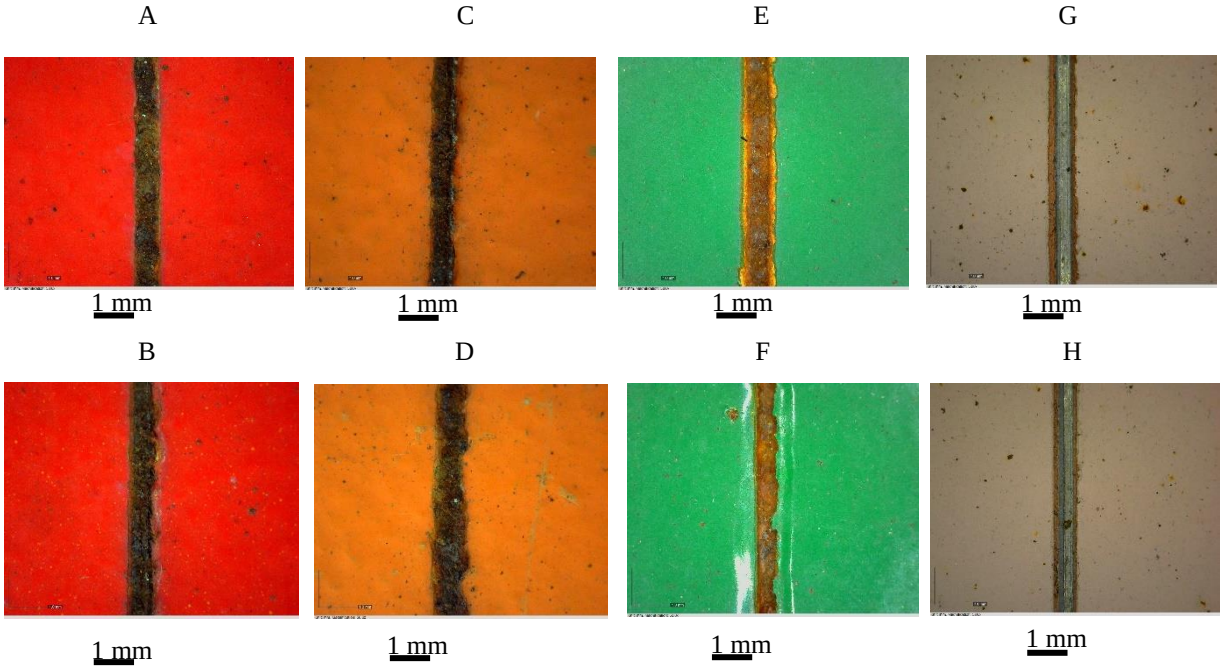

14 Station 14: (Sangchareon Eastern Galvanized)

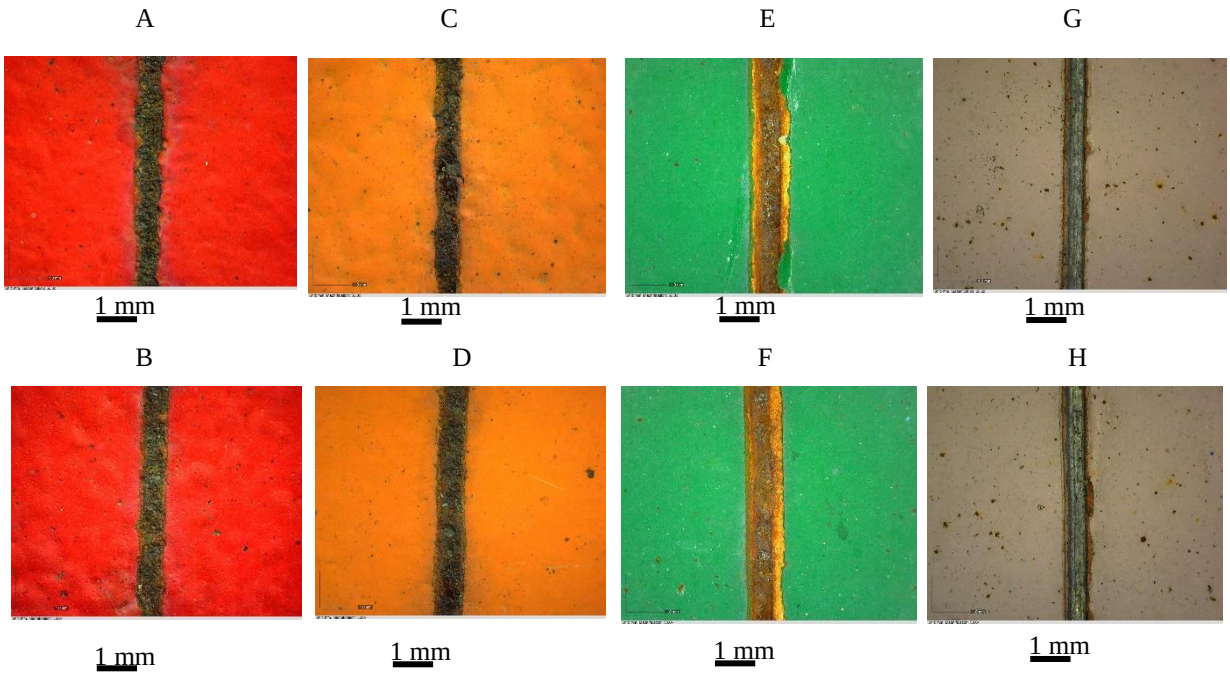

15 Station 1: (Cotco-SV Eastern Steel Pipe LTD)

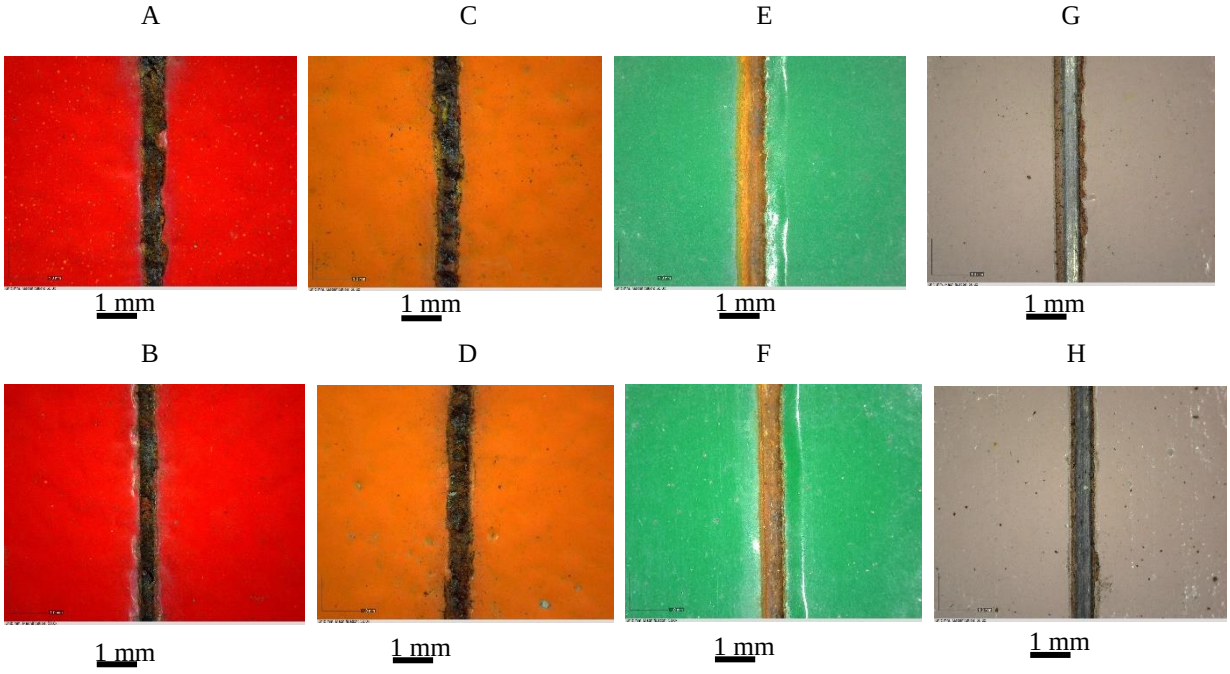

16 Station 16: (Tha Thung Na Dam Power Plant)

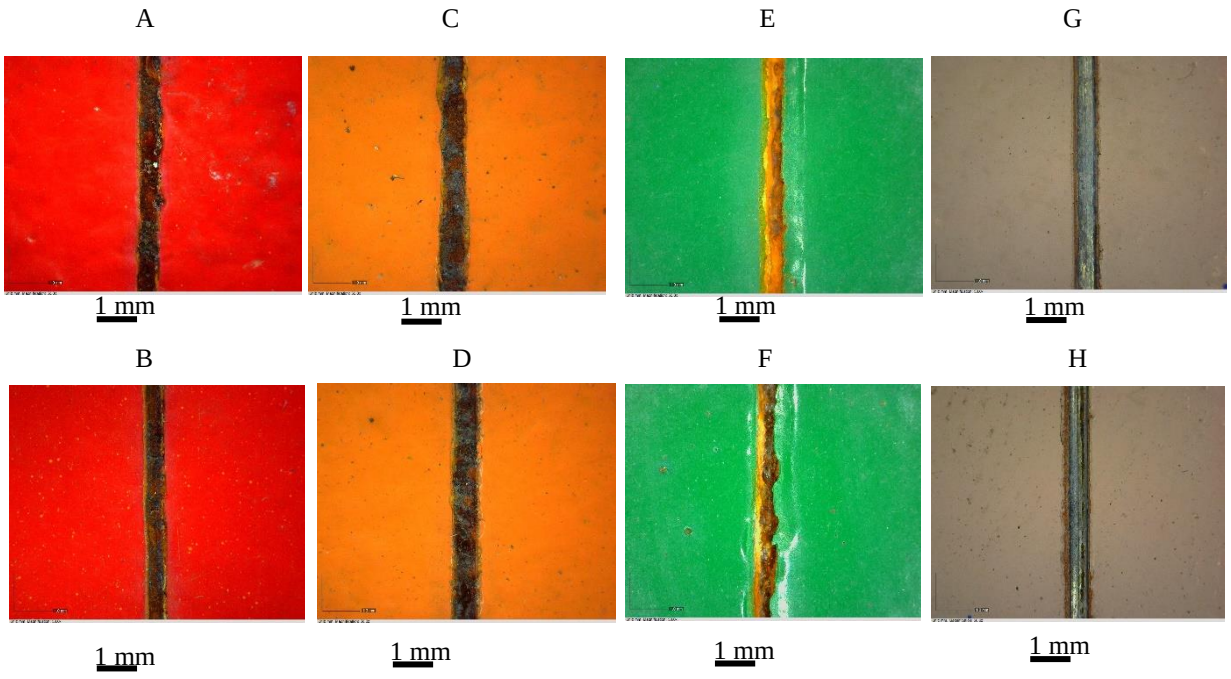

17 Station 17: (Sahaviriya Steel Industries Public Company Limited)

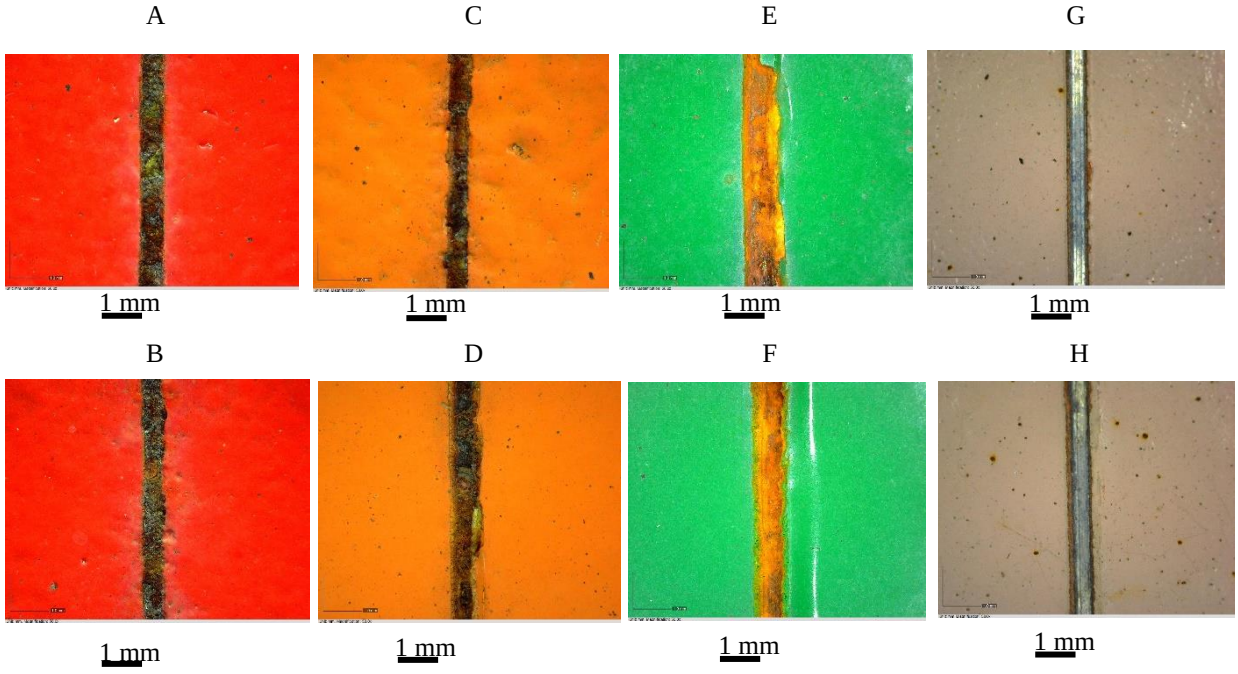

18 Station 18: (Prince of Sonkla University)

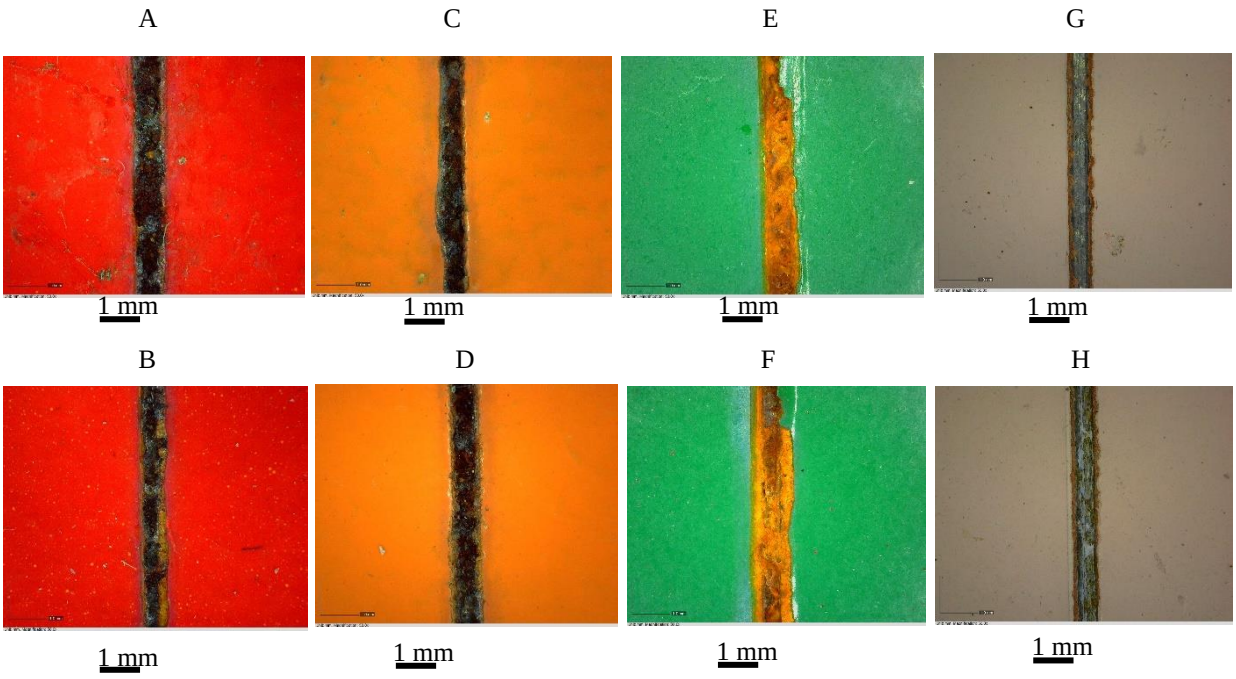

19 Station 19: (Rajamangala University of Technology)

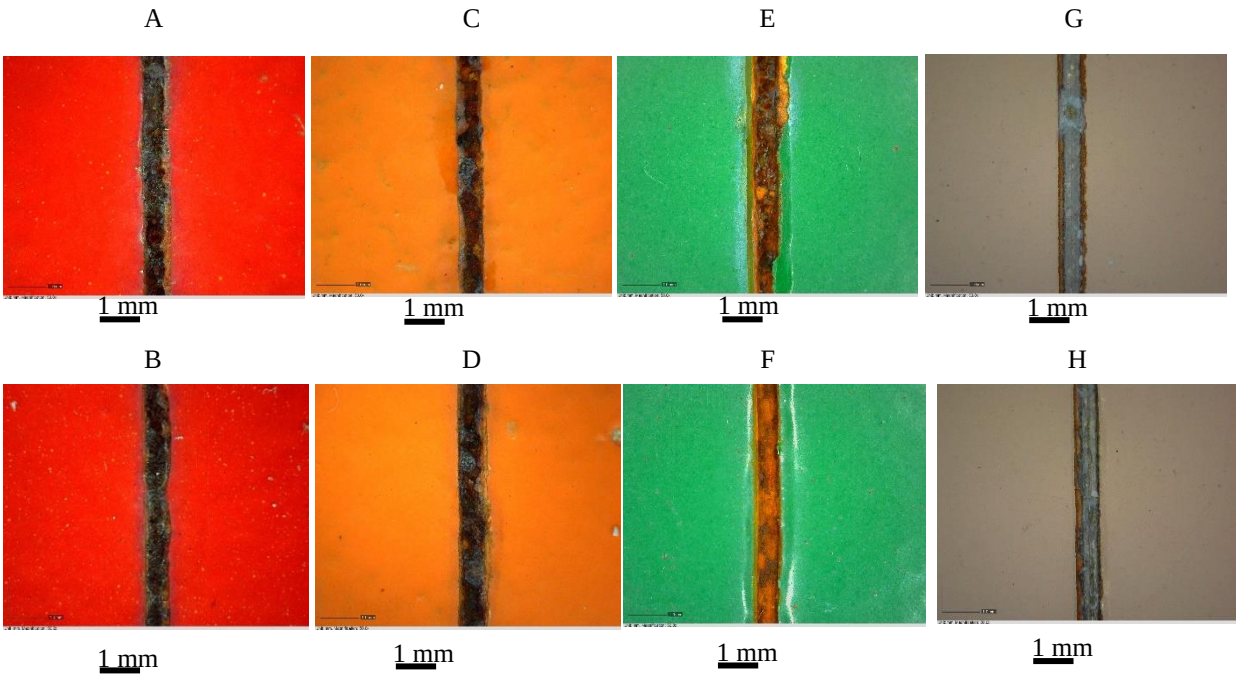

BIOGRAPHY

Name	Bunya Chea
Education	2015: Bachelor of Engineering (Civil Engineering) Institute of Technology of Cambodia
	2017: Master of Science (Engineering and Technology)
	Sirindhorn International Institute of Technology Thammasat University

Publications

Chea, B., Chaisomphob, T., Matsumoto, T. et al. Atmospheric Corrosivity Map of Bare Steel and Hot-Dip Galvanized Steel in Central, Northern, and Northeastern Thailand. Trans Indian Inst Met (2023). https://doi.org/10.1007/s12666-023-03139-1. (Accepted for publication on 02 October 2023).

Chea, B., Chaisomphob, T., Matsumoto, T. (2023). Corrosive Behavior of Structural Steel and Hot Dipped Galvanized Steel in the Central Part of Thailand by Atmospheric Exposure Test. In: Geng, G., Qian, X., Poh, L.H., Pang, S.D. (eds) Proceedings of The 17th East Asian-Pacific Conference on Structural Engineering and Construction, 2022. Lecture Notes in Civil Engineering, vol 302, pp 448–457. Springer, Singapore. https://doi.org/10.1007/978-981-19-7331-4_36

Chea, B., Chaisomphob, T., Matsumoto, T. (2023). Thickness Loss Projection of Bare and Hot-dip Galvanized Steel Based on Atmospheric Exposure Test in the Central Region of Thailand. Japan Society of Civil Engineers, Hokkaido Branch, paper report 79 (A-34) 2023.